Sorption of Naphthenic Acids using β-Cyclodextrin-based Polyurethanes

A Thesis Submitted to the College of

Graduate Studies and Research

in Partial Fulfillment of the Requirements

for the Degree of Doctor of Philosophy

in the Department of Chemistry

University of Saskatchewan

Saskatoon

By

Mohamed Hamid Mohamed

Permission to Use

In presenting this thesis in partial fulfillment of the requirements for a Postgraduate degree from the University of Saskatchewan, I agree that the Libraries of this University may make it freely available for inspection. I further agree that permission for copying of this thesis in any manner, in whole or in part, for scholarly purposes may be granted by the professor or professors who supervised my thesis work or, in their absence, by the Head of the Department or the Dean of the College in which my thesis work was done. It is understood that any copying or publication or use of this thesis or part thereof for financial gain shall not be allowed without my written permission. It is also understood that due recognition shall be given to me and to the University of Saskatchewan in any scholarly use which may be made of any material in my thesis.

Requests for permission to copy or to make other use of material in this thesis in whole or part should be addressed to:

Head of Department of Chemistry

University Of Saskatchewan

Saskatoon, SK (S7N 5C9)

Canada

Acknowledgements

First and foremost, praise to The Almighty Allah for reasons too numerous to mention.

I am heartily grateful to my supervisors, Drs. Lee Wilson and John Headley, whose encouragement, mentorship and support enabled me to develop the success portrayed in this thesis. I wish them more success in their lives.

Not forgetting Drs. Richard Bowles, Ian Burgess, Stephen Urquhart, Gordon Hill, and Paul Jones for their roles as advisors of this project.

My gratitude to the Chemistry Department of the University of Saskatchewan for giving me an opportunity to do research at this reputable institution, Environment Canada for the Science Horizons Program award, University of Saskatchewan for the Graduate Teaching Fellowship and financial assistance from Natural Sciences and Engineering Research Council (NSERC).

I would also like to express thanks the staff from the Saskatchewan Structural Sciences Centre (SSSC), especially Dr. Keith Brown (NMR), Mr. Ken Thomas (CHN analysis, IR spectroscopy and mass spectrometry analysis) and Mr. Jason Maley (Raman spectroscopy), for instrumental training and analysis.

I am grateful to both my previous and current group members; Olu Fadeyi, Jae Kwon, Tarek Mahmud, Rui Guo, Dawn Pratt, Abadalla Karoyo and Louis Poon, for their help in the lab and sharing of knowledge.

I wish all the best to my two best friends in Canada; Josiah Obiero and McDonald Donkuru who made my stay in Canada an enjoyable one especially before I got married. Thank you for being there for me.

Behind every successful man there is a woman; I am indebted to my wonderful loving wife Regeye for her continued love, support, and endurance on the long hours at nights I had to spend in the lab. Thank you for your understanding and prayers you made for my success

MAY ALLAH (S.W.T) BLESS YOU ALL

Dedication

This thesis is dedicated to my parents; Hamid Mohamed Abdulkadir Al-Amoody (Dad) and Sharifa Ahmed Ali Al-Maktary (Mom), my Grandma Zainab Bin Sunkar and my siblings; Zainab, Sukaina, Nuru, Abdul-razak, Aisha and Ahmed. Your love and support has been priceless and I would have never been able to complete this journey without you all.

Allah (S.W.T) said in the Qur'an (Koran):

"Read! In the name of your Lord, Who has created (all that exists). Has created man from a clot. Read! And your Lord is the most Generous, who has taught (the writing) by the pen. Has taught man that which he did not know." Surat Al-'Alaq (The Clot), Chapter 96, Verses 1 to 5.

Prophet Mohamed (P.B.U.H) said the following on knowledge:

"The acquisition of knowledge is obligation on every Muslim, male and female"

"Whoever seeketh knowledge and findeth it, will get two rewards; one of them the reward for desiring it, and the other for attaining it; therefore, even if he do not attain it, for him is one reward."

"Seek knowledge from the cradle to the grave"

"Go in quest of knowledge even as far as China"

Abstract

In general, the research focuses on sequestration of naphthenic acids (NAs) from simulated oil sands process water (OSPW) conditions using engineered copolymers known as β-cyclodextrin-based polyurethanes. The thesis research is divided into two main parts; *i*) synthesis and characterization of β-cyclodextrin-based polyurethanes, and *ii*) sorption studies of the copolymer materials with NAs from aqueous solutions.

In the first part, β-cyclodextrin (β-CD) was crosslinked with five types of linker molecules, respectively, under various synthetic conditions. The various diisocyanates investigated as linkers include the following: 1,6-hexamethylene diisocyanate (HDI), 4,4'-dicyclohexylmethane diisocyanate (CDI), 4,4'-diphenylmethane diisocyanate (MDI), 1,4-phenylene diisocyanate (PDI) and 1,5-naphthalene diisocyanate (NDI). The polyurethanes (PUs) were systematically designed at different mole ratios of monomers by maintaining β-CD and varying the relative mole ratio of diisocyanate monomer from unity to greater values. Diffuse Reflectance Infrared Fourier Transform spectroscopy (DRIFTS), solid state ^{13}C CP-MAS NMR, solution state $^{1}H/^{13}C$ NMR spectroscopy, thermogravimetric analysis (TGA), elemental analysis (CHN), nitrogen porosimetry, and a dye-based (p-nitrophenol; PNP, and phenolphthalein; phth) sorption method were used to characterize the copolymer materials. In general, the β-CD PUs were insoluble in water except for β-CD crosslinked with HDI at the 1:1 mole ratio which was moderately water soluble. All techniques show complementary results about the structural and compositional characterization, particularly for the estimation of the ratios between the co-monomers. The optimal preparation of copolymer materials for sorption-based applications occurs for β-CD/linker monomer mole ratios from 1:1 to 1:3. There is a

maximum limit of the crosslinking density which is ~ 1:7 (β-CD:linker) according to the steric effects of the substituents in the annular region of β-CD. Also, the copolymers were generally found to be mesoporous with relatively low surface area (BET; ~10^1 m^2/g) and they appear to exhibit swelling in aqueous solution due to hydration as observed from the estimation of the dye-based surface areas using PNP. The surface accessibilities of the β-CD inclusion sites ranged between 1-100%, as evidenced by the decolourization of phenolphthalein (phth) due to the formation of 1:1 β-CD/phth inclusion complexes.

In the second part, the inclusion of NAs and its surrogates with three well known types of cyclodextrin (α-, β-, and γ-CD) was confirmed using negative ion mode electrospray ionization (ESI). The CDs were found to form well-defined 1:1 inclusion complexes. The binding constant (K_2) of NAs and its surrogates inclusion with β-CD was determined indirectly using the spectral displacement technique and were found to be 10^3-10^4 M^{-1} (surrogates) and ~ 10^4 M^{-1} (NAs), respectively. Furthermore, the binding constants were found to increase with an increase of the lipophilic surface area (LSA) of the surrogates. The sorption results of NAs with three different types of β-CD materials (i.e. β-CD PU, β-CD crosslinked with epichlorohydrin (EP) and a silica-based mesoporous material containing β-CD), showed β-CD PU had a greater affinity. The sorption capacity (~ 0 – 75.5 mg NAs/g copolymer) and binding affinity (~10^3 – 10^4 M^{-1}) of β-CD PUs varied due to the nature of linker monomer and the mole ratio of the co-monomers. Aromatic-based copolymers showed high sorption binding affinity while aliphatic-based copolymers showed a relatively high sorption capacity at the co-monomer ratio. Finally, Syncrude-Derived NAs showed fluorescent characteristics which contradict the classic definition of NAs. Further studies using UV-Vis and fluorescence emission

spectroscopy showed potential development of an analytical method that can be used to quantify NAs in OSPW for *in-situ* field applications.

Table of Contents

List of Schemes

List of Figures

List of Tables

List of Abbreviations

AC……..Activated Carbon

BET……..Brunauer Emmet Teller

BJH……Barret-Joyner-Halenda

CD…….Cyclodextrin

CDI……..4,4'-dicyclohexylmethane diisocyanate

CD-ICL…….....β-Cyclodextrin Functionalized Triethoxysilane

CD-ICS……..β-Cyclodextrin Functionalized Mesoporous Silica

CL…….Cellobiose

^{13}C NMR……...Carbon 13 Nuclear Magnetic Resonance

CP…….Cross Polarization

DMA……...Dimethylacetamide

DMF…….N,N, Dimethylformamide

DMSO-d_6…….Deuterated Dimethyl Sulfoxide

DRIFT…….....Diffuse Reflectance Infrared Fourier Transform

EA……...Elemental Analysis

ESI-MS…….Electrospray Ionization Mass Spectrometry

EP…….Epichlorohydrin

GAC……Granular Activated Carbon

GL…….Glucose

HDI……1,6-hexamethylene diisocyanate

HLB……...Hydrophile-Lipophile Balance

^{1}H NMR……..Proton Nuclear Magnetic Resonance

hrs…….Hours

K……..Kelvin

KBr…….Potassium Bromide

kHz……Kilo Hertz

LSA…….Lipophilic Surface Area

m……Mass

MAS……..Magic Angle Spinning

MDI……4,4'-diphenylmethane diisocyanate

MEUF……...Micellar-Enhanced Ultrafiltration

MHz……....Mega Hertz

MIP…….Molecular Imprinted Polymer

MO…….Methyl Orange

MW……...Molecular Weight

N_2……Nitrogen

NDI……..1,5-naphthalene diisocyanate

NF……Nanofiltration

NLLS……Nonlinear Least Square

OSPW…….Oil Sands Process Water

P_2O_5……Phosphorus Pentoxide

PD……...Pore Diameter

PDI…….1,4-phenylene diisocyanate

Phth……..Phenolphthalein

PNP……..P-nitrophenol

PU…….Polyurethane

PV…….Pore Volume

RAMEB……Randomly Methylated β-Cyclodextrin

SA…….Surface Area

SPE……Solid Phase Extraction

TEM……...Transmission Electron Microscope

TEOS…….Tetraethoxysilane

TDI……...Toluene diisocyanate

TPW……Tailing Pond Water

UV……Ultraviolet

V……Volume

Vis……..Visible

XRD……...X-ray Diffraction

ZINDO……..Zerner's Intermediate Neglect of Differential Overlap

δ……..Chemical Shift

θ…….Fractional Coverage

CHAPTER 1

1. Introduction

1.1 Research Objectives

The overall objectives of this research work were to design and characterize β-cyclodextrin polyurethanes (β-CD PUs) and to test their utility as sorbents for the sequestration of naphthenic acids (NAs) from aqueous solution. The thesis research is divided into three main parts; *i*) synthesis and characterization of β-CD PUs, *ii*) studies of the inclusion of CDs and its PU copolymers, and *iii*) sorption of NAs with β-CD copolymers.

As mentioned in the first part of the introduction in § 1.4.2, there was no previously published systematic study for these types of copolymers, nor was there extensive work on their characterization and physicochemical properties in the literature. Therefore, there was a precedence to carry out comprehensive systematic studies of such materials by varying the type of linker molecule co-monomer ratio (*cf.* § 1.4.2). The preparation of the materials was followed by characterization using different techniques such as infrared (IR) spectroscopy, NMR spectroscopy, thermogravimetric analysis (TGA), elemental analysis (EA) and nitrogen porosimetry. These materials are anticipated to have variable physicochemical properties such as surface area (SA), and pore structure, variable sorption properties with adsorptives (i.e. NAs and molecular nitrogen). Dye sorption and porosimetry methods were used to determine; *i*) the surface accessible β-CD sites with phenolphthalein (phth) as an optical probe (*cf.* § 1.4.1.3), and *ii*) the surface area and general sorption properties of the copolymers using p-nitrophenol (PNP) as the adsorbate dye as discussed in § 1.4.3.5.

The second part of the research demonstrated that these copolymers have favorable adsorption properties towards NAs and representative examples of component NAs (surrogates). Also, it was determined that NAs are included within the CD cavity, and binding affinity with β-CD. There are no reports in the literature detailing these types of CD inclusion complexes. Three types of CDs (i.e. α-, β-, and γ-CD) with different cavity sizes (*cf.* Table 1.1) were studied along with two types of saccharides, cellobiose and glucose. These compounds differ from CDs since they have no preorganized inclusion cavities and are anticipated to reveal the macrocycle effect by comparative studies with the inclusion complexes between CDs and NAs. As for the determination of the binding constant between β-CD and NAs, the spectral displacement technique was investigated due to the optically transparent UV-Vis properties of NAs. The details on the choice of this technique are given in § 1.3.3.

The remainder of the objectives evaluated the sorption properties of copolymers with NAs in aqueous solution. To achieve this goal, there was a need to design a suitable protocol to further understand the sorption mechanism of these materials towards adsorbates of different sizes at various pH conditions. This was achieved by analyzing the data from the dye sorption method using PNP and phth, respectively, (*cf.* § 1.4.3.5 and 1.4.1.3, respectively). After completion of the dye sorption studies, preliminary sorption tests were conducted for NAs using three different types of β-CD materials (i.e. β-CD crosslinked with epichlorohydrin (EP) copolymer and mesoporous silica materials containing β-CD), and compared with granular activated carbon (GAC) at pH 5 and 9. The results showed the differences in the sorption behavior of these β-CD-based materials and further justify their use as suitable copolymers for sorption-based

applications. GAC was used as a standard sorbent for comparison because of its wide usage and its high surface area. The last step in the research was to conduct systematic sorption studies using the copolymers.

1.2 Research Hypotheses

The thesis research was motivated by various hypotheses that arose at different stages of the work. These hypotheses are summarized below;

1. To determine if β-CD PUs exhibit comparable binding affinity/selectivity (according to molecular size and structure) toward naphthenic acids carboxylates (NAs are complex mixtures of carboxylates) since β-CD forms relatively stable/selective complexes with carboxylic acids and their anions (*cf*. § 1.4.1.1).
2. To determine if β-CD inclusion complexes play a significant role in the sorption mechanism of NAs with β-CD PUs (*cf*. § 1.4.1.2).
3. To determine if "non-inclusion" complexes from the copolymer framework play a significant role during sorption of NAs with β-CD PUs (*cf*. § 1.4.1.2).
4. To determine if phth can be used as a probe to quantitatively determine the surface accessible β-CD sites in the copolymers framework (*cf*. § 1.4.1.2).
5. To determine if the binding affinities reported by Ma and Li[1] apply to particular phenolic dyes (i.e. PNP, phth, etc) or to the nature of the β-CD copolymers (*cf*. § 1.4.1.3).
6. To determine if the synthesis of β-CD with a variety of linkers at different mole ratios of the co-monomers results in products with variable structural features and tunable physicochemical properties (*cf*. § 1.4.2.2).

7. To determine if TGA studies of the copolymers with the variable co-monomer ratios may reveal unique thermal events that enable its application to the composition analyses of the copolymer materials (*cf.* § 1.4.3.2).
8. To determine if increased lipophilicity of the adsorbate will favor its sorption with β-CD PUs, as observed with β-CD inclusion complexes (*cf.* § 1.6.1).
9. To determine if Athabasca-derived NAs are fluorescent (*cf.* § 1.7.2).
10. To determine if UV-Vis absorption and florescence emission spectroscopy can be used as a potential analytical technique for the detection of NAs in oil sands process water (OSPW) (*cf.* § 1.7.2).

1.3 Overview of Naphthenic Acids

1.3.1 Definition

NAs (*cf.* Figure 1.1) are predominantly complex mixtures of saturated cyclic and aliphatic carboxylic acids with the general formula $C_nH_{2n+Z}O_2$, where n is the number of carbons and 2n+Z is number of hydrogen atoms where Z is the hydrogen deficiency; hydrogen loss due to the presence of ring structures.[2-6] Generally, the carboxylic group is attached to a cyclopentane or cylcohexane ring through a $–CH_2-$ group or an alkyl chain containing five or more $–CH_2-$ groups. NAs are found in petroleum due to insufficient catagenesis of petroleum or as a biodegradation product by bacteria. The composition and concentration of NAs depend on the source of oil.[2-6] Although the term NAs may not accurately portray the diverse range of its components, the usage of this term is widespread in the chemical literature. Its origins are attributed to crude oil refining of the naphtha fraction which upon oxidation forms NAs.[7]

NAs are non-volatile, chemically stable, and may act as surfactants. They have acid dissociation constants that range between 10^{-5} M and 10^{-6} M (activities are treated as molar concentrations) which is typical of most carboxylic acids (acetic acid = $10^{-4.7}$ M, propionic acid = $10^{-4.9}$ M, palmitic acid $10^{-8.7}$ M). Sodium salts of naphthenic acids are relatively soluble in water.[6,8-9]

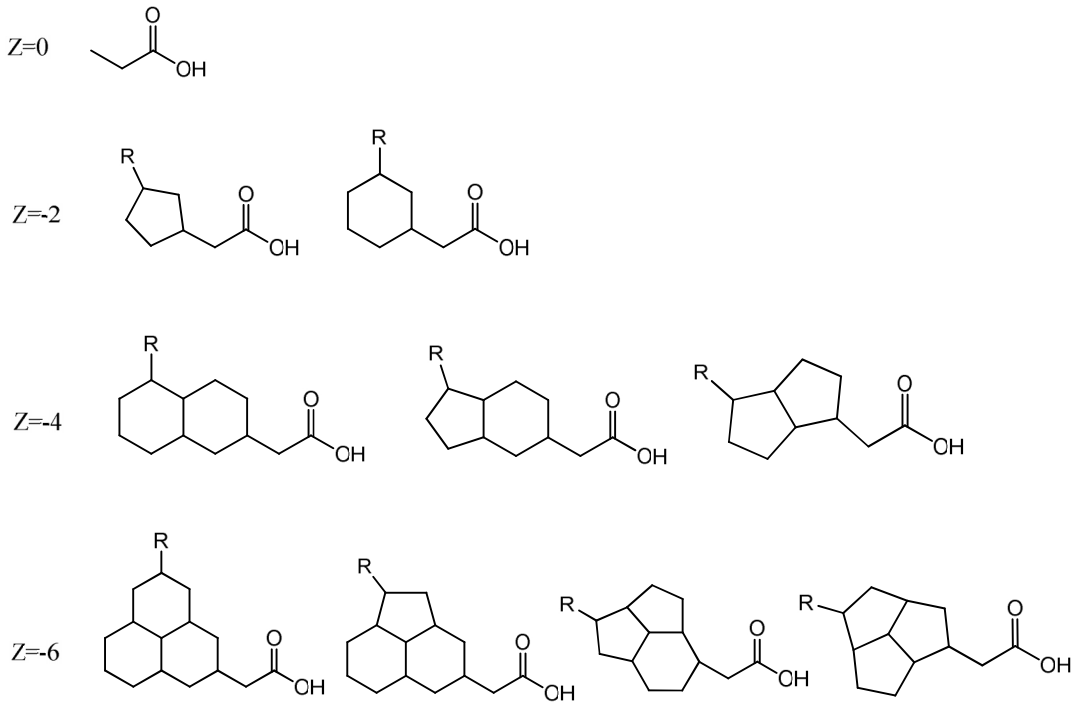

Figure 1.1. Proposed structures for NAs in the Z = 0, -2, -4 and -6 series with both five- and six-member rings present, and n≥1, except for Z= 0 where n≥5. Note: The stereochemistry of the components is omitted.

1.3.2 Problems Posed by Naphthenic Acids

The presence of NAs in petroleum has led to environmental, health and industrial concerns. They are known to be toxic to aquatic organisms, algae, and mammals.[6,10-12] NAs are suspected endocrine-disrupting substances, however; the toxicology of all the various types of NAs is not well understood.[13-14] Consequently, the Government of Canada has issued a zero discharge policy in part, due to the presence of NAs in oil sands

process water (OSPW), also referred to as tailing pond waters (TPWs), from the Athabasca oil sands steam extraction processes. OSPW contain NAs arising from the alkaline hot water used to extract bitumen from oil sands. Given the estimated crude oil reserves (*ca*. 174 billion barrels bitumen) in the Athabasca oil sands and the significant water consumption requirements (*ca*. 2-4 barrels water per 1 barrel bitumen) for the extraction process[15-17], millions of litres of OSPW will be produced and may contain concentration of NAs as high as 110 ppm. [4-5]

In addition, even though OSPW is recycled, high salinity and the presence of NAs eventually limits the degree of recycling due to corrosion problems.[6,18-19] Moreover, the molecular complexity and recalcitrant nature of NAs has made the efficient separation, quantification and identification of individual components in the mixture challenging to date.[6] The aforementioned problems and projected oil sands production activities in the Athabasca region have resulted in an urgent need for new analytical methods to be developed and novel materials for the removal of NAs from OSPW. This in turn emphasizes the overall objectives of this thesis.

1.3.3 Strategies for Removing Naphthenic Acids

Independent studies have examined several different approaches for extracting NAs from synthetic and industrial OSPW with limited success.[20-33] These approaches include sorption, biodegradation, photolysis, ozonation and filtration. The following two sections` will cover these approaches in greater detail, however, the sorption of NAs with β-CD PUs was chosen as the preferred approach for this project as described in § 1.7.

1.3.3.2 Sorption Approach

The sorption of NAs is considered to be a practical approach for removal from wasterwater; however, only a limited variety of materials has been investigated such as zeolites, clay, cellulose and GAC.[21-22,27] Recent studies of sorption of actual NAs from crude oil (not model compounds) date back to 1996 by Gaikar and Maiti[21] and Wong *et al.*[22] Gaikar and Maiti[21] carried out a thorough sorption study of NAs, as compared to Wong. The sorbents studied included zeolites, clay (bentonite), poly (4-vinyl pyridine) and ion-exchange resins (weak and strong). The resins were crosslinked with polystyrene containing tertiary amines as the active functional group. The adsorption capacity increased in the following order: zeolite < clay < poly (4-vinyl pyridine) < ion-exchange resins. Zeolites had the lowest adsorption capacity due to their micropore dimensions which may be smaller than some species of NAs. The ion-exchange resins were concluded to have the highest capacity due to the favourable acid-base interaction between the tertiary amine group and the carboxylic acid groups of the NAs. This was confirmed using a resin with a quaternary instead of tertiary amine which had a lower adsorption capacity. Moreover, weakly ionic resins showed higher sorption capacity for the NAs than that of stronger ion-exchange resins. This was attributed to structural factors and accessibility of the functional groups (tertiary amine) on the polymeric backbone. The goal of the above research was to sequester NAs from non-aqueous petroleum fractions and not from aqueous solutions, as compared to the Ph.D. thesis research described herein.

While interested in showing the toxicity of NAs towards fish, Wong *et al.*[22] reported that GAC adsorbed NAs. Although their work had no extensive sorption studies

(i.e. equilibrium isotherm studies), favourable adsorption was concluded by extracting the NAs from GAC after sorption using supercritical fluid extraction.

Zou *et al.*[24] extended the research done during early 80s on carboxylic acids that mimic NAs[34] and studied these model compounds. The research investigated the enthalpy of adsorption of NAs onto clays using calorimetry and the equilibrium sorption isotherms. Their goal was to study the interaction between clay and NAs in terms of the processibility of oil sands where strong interactions attenuate the extraction efficiency. Thus, the goal was not directly related to remediation of the water phase but to increase the oil sands recovery efficiency. It was shown that clay was an efficient adsorbent for organics; however, the solvent media used was toluene and not water. The adsorption of NAs in aqueous solutions and in OSPW is anticipated to be quite different, and this is the subject of the present work.

In 2004, Saab *et al*.[28] investigated the extraction of NAs using ion-exchange resins. The goal was to extract NAs from crude oil and the resin used was a strong ion-exchange resin with quaternary amine functional groups. Gaikar and Maiti[21] found these materials have reduced adsorption capacities compared to that of weak ion-exchange resins containing tertiary amine functional groups. Their work did not report equilibrium isotherm studies.

Mica and calcite also showed variable selectivity with model NAs during their wettability studies with different long-chain fatty acids.[23] Apart from the demonstrating ionic interaction of the charged hydrophilic surface of mica and calcite with carboxylic group of NAs, no equilibrium isotherm studies were carried out.

The sorption of NAs using organic rich soils as the sorbent was reported by Janfada *et al*.[25] and Peng *et al*.[26] They found that soil with higher organic content (containing greater amounts of carbon compounds) appeared to result in higher levels of sorption. Moreover, the sorption of NAs was not uniform but specific to certain molecular species. Details of their work are given in § 1.7 together with the sorption results of NAs.

1.3.3.3 Other Approaches

Different types of degradation strategies have been employed to remove NAs from OSPW such as biodegradation[10,30-31], UV photolysis[5,35], and ozonation by infusing ozone in OSPW to oxidize NAs[33]. Some NAs are known to be recalcitrant to biodegradation.[36] The production cost in ozonation may be limiting for this type of technology since the cost of generating ozone is quite high.

Filtration is another technique of interest where recent studies have investigated the use of some commercially available nanofiltration (NF) membranes, as characterized according to their rejection efficiency of magnesium sulfate from aqueous solution.[29] The NF membranes were anticipated to produce permeate solutions with low concentrations (< 5 ppm) for NAs and calcium carbonate (< 40 ppm). Another related filtration technique is micellar-enhanced ultrafiltration (MEUF); this method is limited by the presence of residual colloidal materials used to solubilize NAs, along with the trace NAs.[33]

1.3.3.4 Proposed Strategy

Sorption processes are a feasible method of sequestering NAs from aqueous solution provided that a suitable sorbent is available. The use of engineered copolymers with tunable physicochemical properties is considered ideal. Since CDs are known to

form stable complexes with carboxylic acids,[37-43] the use of copolymers containing β-CD are proposed as suitable sorbent materials for this thesis research.

1.4 β-Cyclodextrin-based Polyurethanes

1.4.1 Cyclodextrins and Polymers

1.4.1.1 Background Information

Cyclodextrins (CDs) are cyclic oligosaccharides consisting of six, seven (Figure 1.2), and eight α-D-(+) glucopyranoside units connected by α-(1, 4) linkages commonly referred to as α-, β-, and γ-CDs, respectively.[44-47] Although CD is the common name of these types of compounds; other names have been used since their emergence such as Schardinger dextrins, cycloglucans, cycloamyloses, cyclic oligosaccharides, etc. In 1891, Villiers, was the first to observe an unidentified crystalline substance from the fermentation of starch which he called "cellulosine".[44] In early 1900, while studying the microorganisms which deteriorate food, Franz Schardinger found that *Bacillus macerans* produced two crystalline substances, i.e., α- and β-CD. The chemical structure of α- and β-CD remained unknown until the 1930's when Freudenberg revealed that the molecular structure of CDs was cyclic.[44] It was in the late 1980's when the existence of CDs with more than eight glucopyranoside units was demonstrated.[48-50]

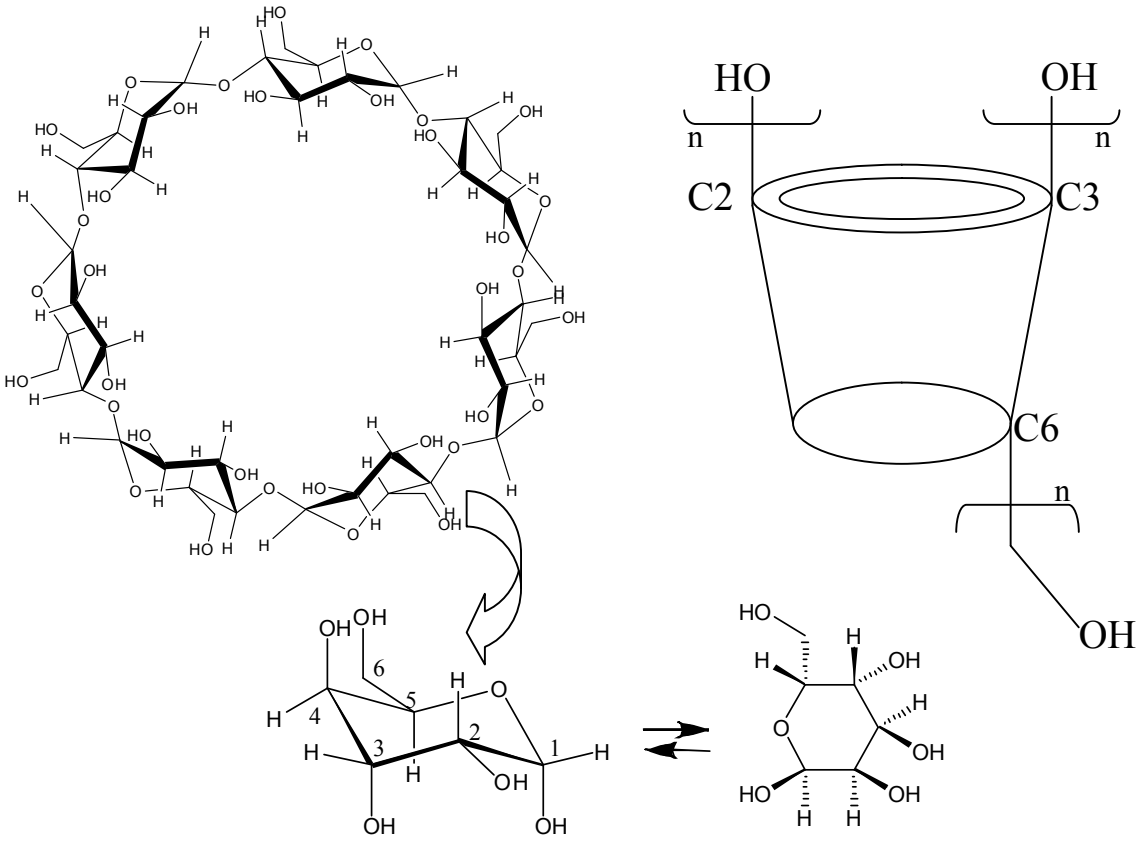

Figure 1.2. Structure of β-CD consisting of seven α-D-(+) glucopyranoside units and a generalized description of its overall toroidal shape where n = 6, 7, or 8 for α-, β-, and γ-CD.

CDs possess a characteristic toroidal shape with a well-defined conical cylinder. This shape is a result of all the secondary hydroxyl groups being situated on one of the two edges of the annular ring while the primary groups on the opposite edge are shown in Figure 1.2. The internal cavity is lipophilic in nature as it is lined with hydrogen atoms and the bridging glucosidic oxygen atoms. The nonbonding electron pairs of the glycosidic-oxygen bridges are directed toward the inside of the cavity, producing a region of high electron density and imparting Lewis base characteristics.[44-45] The presence of a lipophilic cavity and a hydrophilic exterior makes CDs suitable for the inclusion of

appropriate sized guest species (inclusate). The stability of the inclusion complexes varies for the individual CDs due to their cavity size dimensions as a result of the different number of glucopyranoside units. Some of the physical properties and characteristics of the CDs relevant to this research project, are listed in Table 1.1.[45]

Table 1.1. Physical properties and characteristics of α-, β-, and γ-CD. [45]

Property	α-CD	β-CD	γ-CD
Glucopyranoside units	6	7	8
Molecular Weight (g/mol)	972	1135	1297
Internal Diameter (nm)	0.57	0.78	0.95
External Diameter (nm)	1.37	1.53	1.69
Height of Torus (nm)	0.78	0.78	0.78
Cavity Volume ($Å^3$)	174	262	427
Solubility in Water, g/100 mL at room temp	14.5	1.85	23.2

The inclusion of guest molecules within the cavity of CDs has led to useful applications such as chemical separations in chromatography, drug delivery of pharmaceuticals, encapsulation of molecules in the food industry, and other applications in the agro-chemical and petro-chemical industries.[46] The potential industrial applications of CDs led researchers to develop novel synthetic derivatives by linking the CDs covalently or non-covalently.[51-52] Non-covalent self-assembled CD polymers are commonly referred to as supramolecular polymers.[53-54] However, in this work, the interest was focused on the covalently linked CDs due to their inclusion behaviour with organic inclusates. CD polymers are anticipated to display enhanced inclusion properties,

as will be discussed in § 1.4.13. In the late 60's, Sheldon *et al.*,[55] patented the reaction of an aldehyde, diacid, diacid chloride, diester, diepoxide and diisocyanate, respectively, with the hydroxyl groups of CDs to form copolymers. Different approaches have since been applied in polymerizing CDs. Mocanu *et al.*[56] classified these polymerization reactions of CD into three general categories; *i*) crosslinked framework using bi- or multi-functional reagents[51,57-62], *ii*) conventional self-polymerization of acryclic monomers containing pendant CD units[63-64], and *iii*) grafting CDs onto a polymeric template with reactive functional groups through covalent bonding.[65-71]

In this research project, β-CD network (or framework) polymers formation was carried out via crosslinking with diisocyanate (bifunctional agent) crosslinker monomers. The rationale for choosing this type of polymerization route is that it offers the ability to tune the physicochemical properties (*cf.* § 1.4.1.3) of the copolymer by using different types of diisocyanates of different reaction conditions. These types of copolymers are well known as polyurethanes (PUs), and although the patented work on those polymers dates back to 60s[55], it was almost a decade later when research on these materials was observed in different fields.[72-76]

Among the three types of CDs, β-CD was chosen due to its favourable physical properties (*cf.* Table 1.1) and its interesting inclusion chemistry towards different types of aliphatic and aromatic compounds, such as benzene, adamantine, naphthalene, and carboxylic acids.[77-78] Furthermore, α-CD is found to display suitable size-fit compatibility with linear aliphatic chains while γ-CD forms 1:1 and 1:2 complexes with favourable binding with larger guests such as pyrene and two azobenzene moieties.[52] At this point, it is known that β-CD forms relatively stable complexes with carboxylic acids and their

anions.[78] *A working hypothesis was to determine if β-CD PUs may exhibit comparable binding affinity/selectivity (according to molecular size and structure) towards carboxylates in aqueous solution, as compared with β-CD*. This was of interest because NAs represent a complex mixture of carboxylic acids, (*cf.* Figure 1.1) and possess variable molecular structure with different carbon numbers and hydrogen deficiency. One of the objectives of this research is to evaluate the sorption properties of synthetically engineered β-CD polymers (through sorption; this is detailed in Chapter 1.4) with naphthenic acids (NAs) in aqueous solution. The co-monomer β-CD is seen as a suitable choice according to its known binding affinity with carboxylic acids and the known molecular structures of NAs (*cf.* Figure 1.1).

1.4.1.2 Host-Guest Complexation

Interest in the use of CDs in their native or polymeric forms arose from the study of their unique complexation ability with a wide range of apolar guest species within their macrocyclic cavities to form stable host-guest inclusion complexes (Scheme 1.1).[45-47] Inclusion phenomena was first observed by Schardinger[79] when he used the inclusion complexes of CDs with alcohol, chloroform, and ether to selectively precipitate the crystalline dextrins. However, it was Freudenberg[80] who first interpreted these complexes as being formed by guest inclusion inside the macrocyclic cavity of CDs.

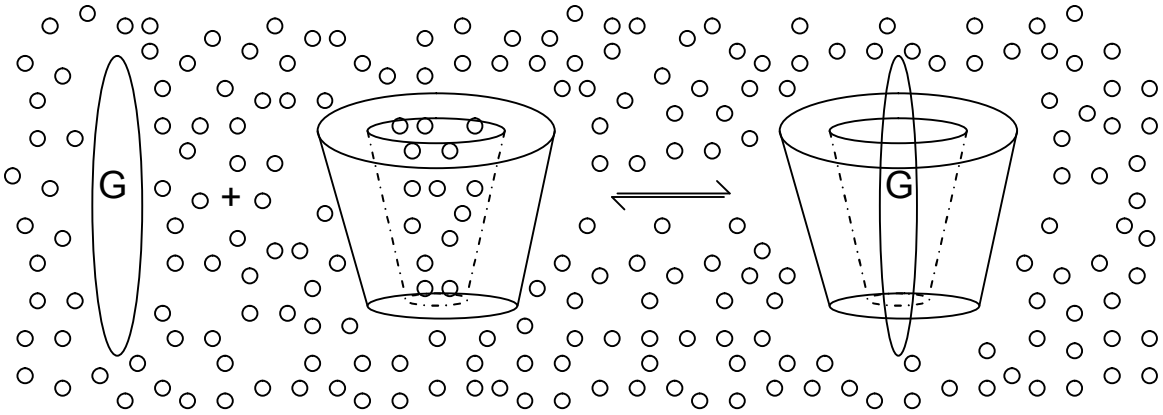

○ = H_20

$$CD + G \underset{}{\overset{K_i}{\rightleftharpoons}} CD.G \qquad K_i = \frac{[CD.G]}{[CD][G]}$$

Scheme 1.1. Formation of a host-guest (inclusion) complex between an apolar guest (G) and a CD host (toroid). K_i represents the 1:1 inclusion binding constant between G and CD where the activity coefficients are assumed to be equal to unity, and solvent is omitted in the equilibrium expression.

Various techniques[78,81] have been used to show evidence of inclusion complexes, for example, Hybl *et al*.[82] determined structure of α-CD/potassium acetate using single crystal X-ray crystallography. The solid state structure supported that the acetate ions were included inside the cavity of α-CD. Also, DeMarco and Thakkar[83] showed the inclusion of benzoic acid derivatives inside the β-CD cavity in the solution state using nuclear magnetic resonance (NMR). They concluded that the host protons situated inside the cavity of β-CD shifted upfield due to shielding effects by the aromatic guest (benzoic acid derivatives) while the hydrogens atoms on the exterior of β-CD showed insignificant complexation induced shifts.

The stability of host-guest inclusion complexes involves different types of factors as follows: *i*) hydrophobic effects, considered as the main driving force for apolar inclusates, *ii*) van der Waals interactions; *iii*) displacement of 'high-energy' water molecules from the CD cavity (Scheme 1.1), *iv*) the relief of conformational strain energy

possessed by the free CD or guest species upon complexation with the inclusate, and *v*) polar and ionic interactions. [47,78,81,84-92] The thermodynamic data for most of these complexation processes follow an enthalpy/entropy linear free energy relationship and illustrates the importance of hydration processes.[81]

The host-guest complex stability of lipophilic (apolar) guest species is generally greater than that for hydrophilic (polar) guests.[93] Connors *et al.*[78] showed a strong correlation between complex stability and the lipophilicity of the inclusate, while no significant correlation has been observed with the polar functional groups of the inclusate.[94] Furthermore, Rekharsky and Inoue[81] reported that; *i*) thermodynamics of the host-guest complexation with CDs should be correlated to the extent in which the inclusate is located inside the cavity, and *ii*) the part of the guest molecule that undergoes any changes in their surroundings upon complexation will contribute significantly to the overall thermodynamic properties.

There is no direct correlation between stability and complexation of a guest with native CD and polymeric CD since the binding stability may result from competitive binding effects at different sorption sites, as shown in Scheme 1.2. This was concluded by Weickenmeier and Wenz[95] when they studied the effect of using a polymer with negatively charged groups with the 1-adamantaammonium cation and 1-adamanatanecarboxylate anion. They concluded that, the presence of opposite electrostatic charges between the cation and the anion increased the binding affinity. Moreover, it has been shown that, some of the adsorbate species that possess hydrogen donor (D) or acceptor (A) groups bind (physisorption) onto the framework domains with compatible (D or A) through hydrogen bonding.[59,96-99] *These findings led to an important*

hypothesis of this work which was to determine if the relative contributions of the β-CD inclusion complexes and "non-inclusion" domains of the copolymer (cf. Scheme 1.2) contribute significantly to the overall mechanism for the sorption process. At present, this is poorly resolved in the literature. In this work, β-CD PUs with a systematic variation of the crosslinker units i.e. aliphatic and aromatic (*cf.* Figure 1.3) will be studied with different adsorbates (variable molecular size) at different pH conditions to further understand where the predominant binding interactions with the adsorbates occur.

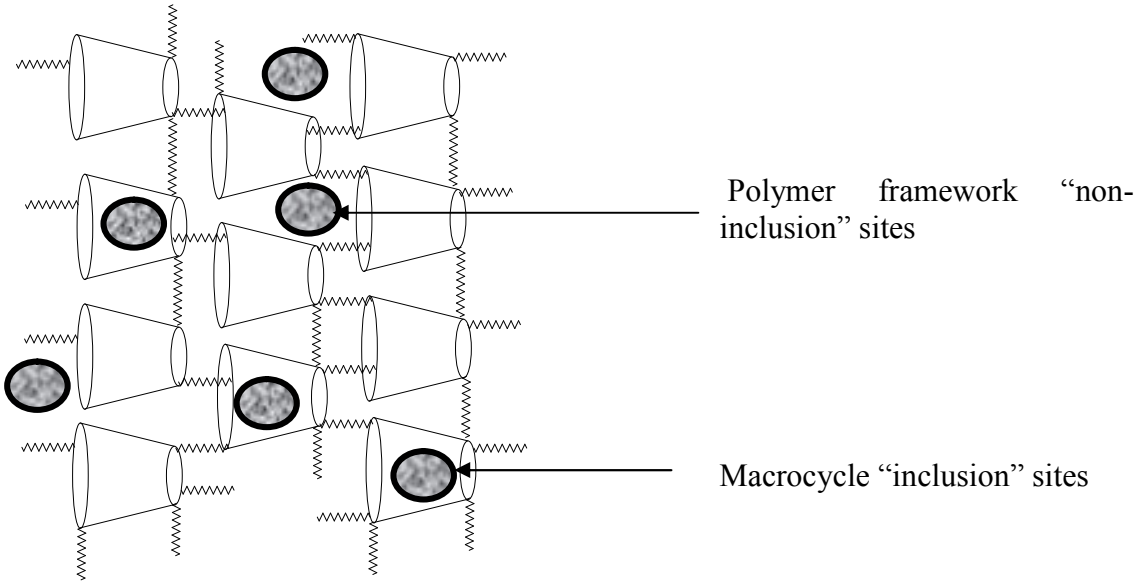

Scheme 1.2. The two potential domains of adsorbate interaction with the CD copolymer; i) "inclusion" binding sites in the CD cavity, and ii) "non-inclusion" binding sites on the copolymer framework.

1.4.1.3 Properties and Applications

The structural and physical properties (such as stability in acidic or basic solutions) of CDs are generally preserved in their polymerized form except for crystallinity.[100] This was shown by Furue *et al*.[101] where they studied a β-CD acrylate copolymer with a molecular weight of ~10^4-10^5 Daltons which showed similar properties

to that of native β-CD. The properties of β-CD PUs may vary according to the type of diisocyanate and the relative mole ratios of the co-monomers. An important property is their solubility in water since the type of applications (i.e. homogeneous vs. heterogeneous) may vary accordingly for the copolymer. In general, when a greater number of CDs are interconnected, the solubility diminishes in many solvents (Scheme 1.3).[102] This is due to lowered solvent accessibility and increased relative molecular weight. This research is focused primarily on the water insoluble copolymers and their properties in solid-solution heterogeneous sorption processes.

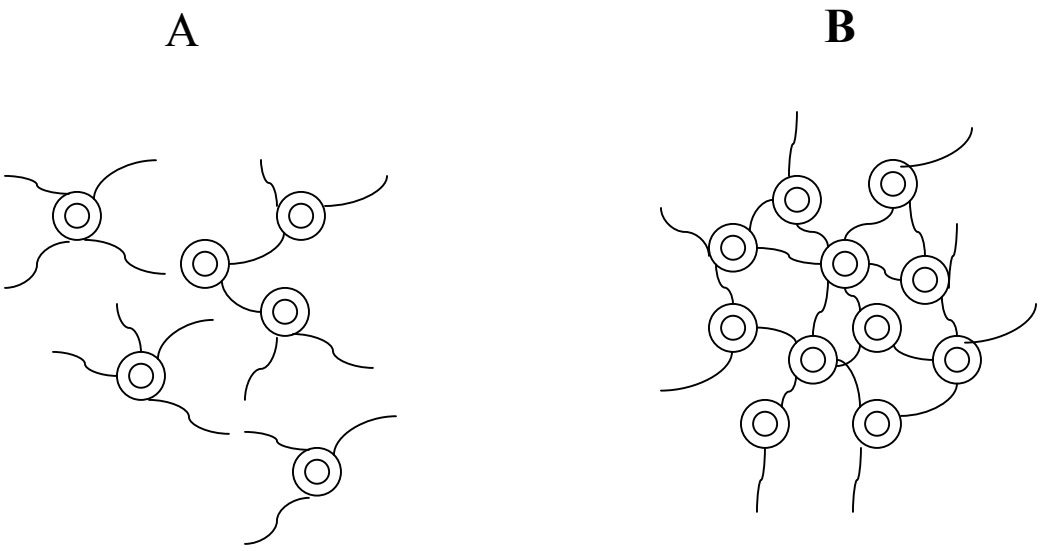

Scheme 1.3. Schematic "end-on" view of CD polymers with different solubility due to the different levels of crosslinking between the co-monomers which directly relates to the relative solvent accessibility and the relative molecular weight. (A) Soluble; low molecular weight oligomers, and (B) Insoluble; highly crosslinked network polymers.

Additional physicochemical properties of such polymers are the surface area, pore structure, thermal and chemical stability of the copolymer sorbents.[76,103-105] In general, these properties will affect the sorption capacities of the copolymers and their applicability to different conditions i.e. variable temperature and pH. These

physicochemical properties are anticipated to play a role in the sorption of NAs from aqueous solution.

The crosslinking co-monomer ratio is another key factor since a highly crosslinked CD polymer will have reduced inclusion accessibility for the inclusion of the adsorbate. This leads to the important issue of the relative availability of the inclusion sites in CD copolymers. An understanding of the relative role of CD and linker domains in the heterogeneous sorption mechanism is an important consideration in the design of copolymers with improved sorption properties.[106-111] The ability to measure the accessibility of the CD inclusion sites is critical for the design of suitable sorbent materials that utilize inclusion binding for specialized applications. Although some studies have shown the qualitative use of phenolphthalein (phth) as a probe for the analysis of polymeric and composite materials containing β-CD groups, there were no reports in the literature of such studies detailing the quantitative determination of the accessible CD inclusion sites.[107,109,112-114] Phenolphthalein (phth) has been shown to exhibit unique molecular recognition with β-CD as evidenced by its specific inclusion geometry[115-117] and its relatively large 1:1 binding constant ($K_1 \sim 10^4$ M^{-1}).[118-123] *Another hypothesis concerning the dye-based method was to determine if phth can be used as a probe to quantify the surface accessible β-CD sites in the urethane copolymers*. This analytical method was successfully developed and it is fully explained in the published work of Chapter 4.

The surface properties of the copolymers are another important consideration. In general, CD polymers are amphiphilic in nature, however, the overall hydrophile-lipophile balance (HLB) is determined by the type of crosslinking agent used and its

relative composition in the copolymer. This is important since polymers which have variable HLB are known to swell in aqueous solutions, hence, affecting the accessibility of the adsorbates and hence the loading efficiency for drug delivery applications.[99,124-125] In the case of the copolymers in this study, they are expected to be more lipophilic in nature due to the type of apolar linkers used in the synthesis (*cf*. Figure 1.3). This is confirmed by recent work on copolymer gels where Thiaparti *et. al.* concluded that swelling decreased as the crosslinking co-monomer ratio increased for β-CD PUs.[124] Moreover, they concluded that the degree of swelling is decreased with decreasing solvent polarity in the following order; DMF < DMF/water < water.

In addition to the aforementioned physicochemical properties, the binding affinity is a critical property in sorption-based applications. However, in the case of β-CD PUs, Ma and Li[1] have reported a pronounced amplification of binding affinity from 10^2 to 10^8-10^9 M^{-1} for complexes formed between PNP and a copolymer comprised of β-CD crosslinked with aliphatic or aromatic diisocyanates (hexamethylene diisocyanate; HDI and toluene diisocyanate; TDI) in aqueous solution.[1,76,126] In order to obtain a further understanding of the binding behaviour of such materials i.e. PU copolymers, it was *hypothesized whether such differences were particular to phenolic dyes (i.e. PNP, phth, etc.) or to the host-guest properties of the copolymer materials*. Furthermore, these types of materials do not leach the organic contaminants once they are bound and this is related to the reported binding affinities of such copolymer materials.[1,76,126]

Since the β-CD PUs have emerged, they have been widely applied in different fields such as chromatographic separations[73-75], molecular recognition of cholesterol through imprinting[60-61,127-128], adsorption of organics from aqueous solution[1,76,126], drug

delivery[124,129-131], adhesive in tapes and wood[132-133], and debittering agents in the food industry[134-135]. In this work, the utility of β-CD PUs as copolymer sorbents for the sequestration of NAs from aqueous solution is investigated.

1.4.1.4 Sorbent Properties

According to the literature, different types of sorbents are proposed for the sequestering of target compounds from aqueous solution; however only suitable sorbents with certain properties are effective or efficient. Usually, a sorbent is deemed efficient if it has a good sorption capacity and binding affinity towards the target sorbates of interest. However, other properties[1,100,134,136-163] that confer suitable sorbent properties are as follows; *i*) regeneration and reusability; this is the ability of sorbent to be recycled after multiple sorption cycles, usually by washing with solvents that dissolve the adsorbate, thereby regenerating the sorbent material, *ii*) chemical stability; this is the ability of the polymer to retain its chemical structure through time, for example, resistance to degradation or biodegradation, *iii*) low cost; this is an important property when comparing adsorbents especially those targeted for large-scale application, *iv*) robustness; application at different pH conditions and temperatures *v*) selectivity; the sorbent should be highly selective for the target adsorbate in cases of complex mixtures in solution, and *vi*) binding affinity; sorbents with greater binding affinity towards target sorbates are non-leaching which is vital during sorption.

1.4.2 Synthesis

Urethanes are esters of carbamic acid and are also known as esters of carbonic acid.[164-165] In general, polyurethane polymers are formed by an addition reaction between polyols with di- or polyfunctional isocyanates. In this research, the polyol used is β-CD

and the formation of the urethane linkage between β-CD and the diisocyanates is shown in Scheme 1.4. The reaction is water sensitive since diisocyanates can react to form carbamic acid. This acid is unstable and decomposes into an amine and carbon dioxide gas. The amine reacts with additional isocyanate to form a substituted urea. Therefore, it is very important to ensure that all starting materials for the synthesis are completely anhydrous.

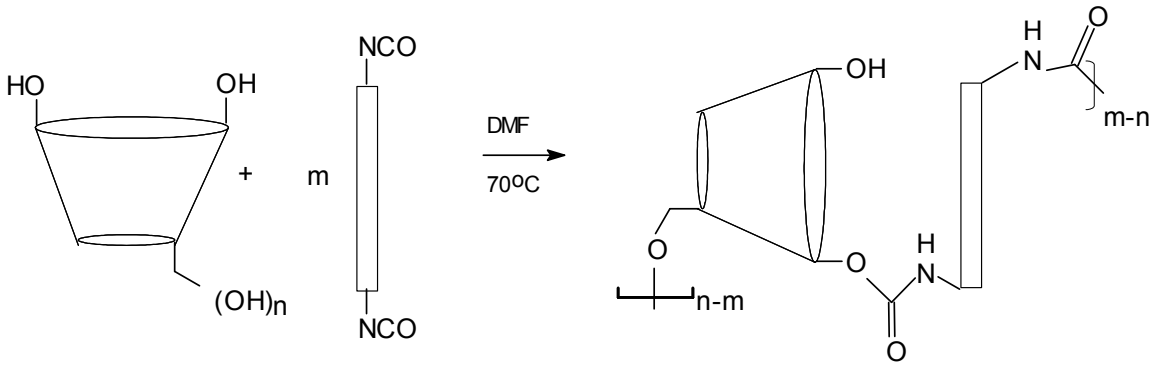

Scheme 1.4. Generalized molecular structure of a β-CD copolymer sorbent material. The extent of reaction between the primary and secondary hydroxyl groups of β-CD and the bifunctional N=C=O groups of the linker depends on the relative mole ratio diisocyanate (m) per mole of β-CD.

1.4.2.1 Procedure

The literature has reported different strategies for the preparation of β-CD PUs. However, the general steps include the following; *i*) drying starting materials, *ii*) synthesis, *iii*) copolymer precipitation, *iv*) washing of the product, *v*) filtering the product and *vi*) drying the final copolymer. More details are given in the forthcoming chapters; however, this section will outline the path towards the development of the protocol developed in this research for synthesis of the β-CD copolymer materials.

The drying of reagents is critical since water will affect the formation and quality of the desired copolymer products. In this work, β-CD was dried under vacuum using a

pistol dryer with phosphorus pentoxide (P_2O_5) which also serves as an indicator of when the β-CD has been completely dried. Typical solvents that have been used for synthesizing β-CD PUs include N,N-dimethylformamide (DMF)[1,73-74,76,97,103-105,124,126,149,166-170], dimethyl sulfoxide (DMSO)[60-61,127] and pyridine[73,171]. In many cases, the literature does not indicate how the solvents were dried but in some cases they were dried with molecular sieves (3 – 4 Å) or calcium hydride for 24-48 hrs, or distilled under nitrogen at reduced pressure.[97,99,127-128,167,172-173] Preliminary results for the synthesis of these types of polymers showed discolored (yellow-brownish) products instead of the expected white colored materials. A trial with dimethylacetamide (DMA) gave better quality products as indicated by the lighter appearance of the materials compared to other solvents. In addition, DMA proved to be easier to dry than other hygroscopic solvents; hence, it was the preferred medium for the synthesis of the copolymers in this study. DMA was dried with molecular sieves (4Å, 8-12 mesh) and the water content was confirmed using ^{1}H NMR spectroscopy. The ideal reaction temperature for β-CD PU synthesis is reported to vary between either 65^{o}C to 70^{o}C, hence, experimental temperatures were chosen over the same range. The reactants were stirred while heating for different durations such as 2 hrs[60-61,127-128,171], 4 hrs[97,105,170], 24 hrs[1,76,104,126,149,166]. To ensure the reaction is complete, duration of 24 hrs was chosen for the strategy described in this thesis. Also, the addition of reagents varied, some were added simultaneously, while others reported the addition of the diisocyanate drop-wise[97,105,149,166,173]. The initial approach taken was the drop-wise addition of the linker; however, the eventual protocol involved the addition of all reactants at the same time. This was due to partial insolubility of some of the aromatic-based linkers in DMA (similar solubility was noted in DMSO,

DMF and pyridine). In order to compare the copolymers, the adopted protocol was done consistently, resulting in more uniform quality of the copolymer products.

Previous reports[60-61,127-128,168] suggest partial solvent removal after the synthesis was performed through evaporation prior to precipitation of the product. In this work, it was noted that the solution (after reaction) turns to a gel state once some of the DMA is removed. Partial removal of DMA was observed to increase the yield by minimizing the loss of copolymer during the precipitation step. Different solvents have been used for precipitating the copolymer such as ethanol[97,173], chloroform[149], methanol[104-105]; however, cold methanol showed good precipitation for the chosen protocol. After precipitation the solid product was filtered using a Büchner funnel with a paper filter. To remove the unreacted starting materials the common method involves washing products with solvents such as water[149] or acetone[60-61,127-128]. Additional protocols used multiple solvents such as, ethanol/acetone[97,173], water/ethanol[170-171], acetonitrile/water/ethanol/acetone[166]. In our case, the starting materials were found to be soluble in methanol hence the precipitated product was washed with hot methanol by Soxhlet extraction for 24 hrs. Traces of DMA were seen in the copolymers using ^{1}H NMR, therefore, an additional Soxhlet extraction for 24 hrs with hot diethyl ether was performed after the hot methanol extraction.

The final step is to dry the copolymer where a commonly used method involved drying under vacuum between 60 – 80 ^{o}C for 24 hrs.[1,60-61,73-74,76,97,105,124,126-127,149,166-167,171-173] In this work, the product was dried after each washing and then crushed into fine particles, with sieving before subsequent washing to ensure complete removal of the unreacted materials.

1.4.2.2 Choice of Linker and Crosslinking Co-monomer Ratio

There are various types of diisocyanate linker molecules; therefore, a great diversity of copolymers can be formed. Nayak *et al.*[174] reported the effectiveness of using different types of diisocyanates as crosslinkers in CD-based macroporous copolymers. In this thesis, five types of diisocyanate molecules were chosen as shown in Figure 1.3. They include 1,6-hexamethylene diisocyanate (HDI), 4,4'-dicyclohexyl diisocyanate (CDI), 4,4'-diphenylmethane diisocyanate (MDI), 1,4-phenylene diisocyanate (PDI), 1,5-naphthalene diisocyanate (NDI). Previously, the most common linkers used were HDI[1,76,97,103-105,124,126,149,170-171,173] and toluene diisocyanate (TDI)[1,60-61,76,126-128,149,166]. A few reports of MDI[97,173] and an ethyl ester of L-Lysine triisocyanate[124] was recently reported. However, the preparation of such copolymers using CDI, PDI and NDI have not been reported. These linkers vary in terms of their relative molecular size and hydrogen deficiency. *An important hypothesis of this research was to determine if a systematic comparison of copolymers prepared with crosslinker units of variable structure described above (cf. Figure 1.3) would afford products with tunable structural features and physicochemical properties (i.e. surface area, pore structure properties, surface area, solubility, cf. § 1.4.1.3)*. This strategy offers a way to compare the effects of the linker framework of the copolymers and their sorption properties. For example, CDI *vs* MDI and PDI *vs* NDI offer a comparison of the structural rigidity and molecular size effects of aromatic vs. aliphatic linkers. A comparison of linkers is reported in Chapter 8 for the sorption of NAs where aromatic-based copolymers showed much higher binding affinity while the aliphatic-based materials showed greater sorption capacity. On the other hand, HDI *vs* CDI linkers offer a perspective into conformational and molecular size effects of

such linkers on the copolymer framework. When there is steric crowding at the narrow end of the β-CD annulus (expected to react preferentially due to their greater reactivity of the primary hydroxyl groups), substituents then react at the wider secondary annular hydroxyl region to compensate for steric crowding. Different modes of substitution may be achieved by using different linkers at similar reactant mole ratios due to their variable molecular size. This is illustrated in Scheme 1.5 which outlines the effect of increasing the degree of substitution in the annular hydroxyl region of β-CD for a diisocyanate linker over the range of co-monomer mole ratios. This concept is elaborated upon further in Chapter 4 in the surface estimation of β-CD inclusion sites using phth. It is concluded that linker molecules with less steric hindrance have a higher degree of accessible β-CD sites.

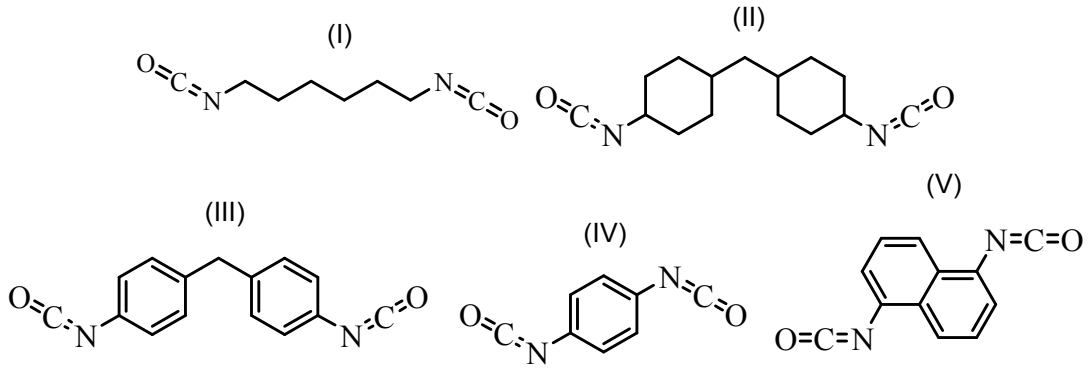

Figure 1.3. Diisocyanates with variable size and degree of unsaturation used in the synthesis of the β-CD PUs; I) HDI, II) CDI), III) MDI, IV) PDI and V) NDI.

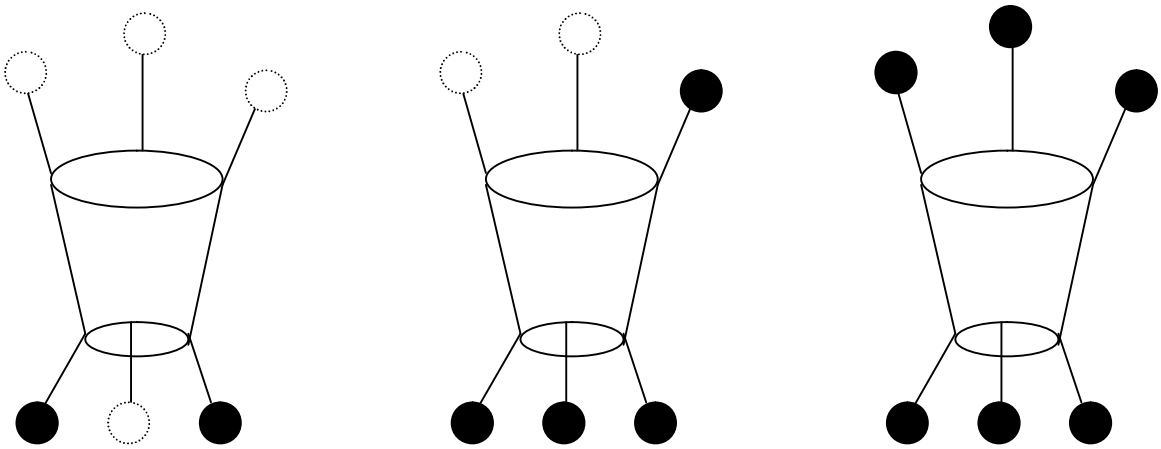

Scheme 1.5. Illustration of the sites of substitution of diisocyanate crosslinker units to the primary (narrow end) and secondary (wide end) hydroxyl groups in the annular regions of β-CD: a) β-CD:linker (1:1), and b) β-CD:linker (1:2), and c) β-CD:linker (1:3) reactant ratios. The solid spheres represent covalently attached sites and open spheres represent available (unreacted) sites

The crosslinking co-monomer ratio described in § 1.4.1.3 is an important property that is controlled by varying the relative mole ratios of the starting materials, i.e., β-CD and diisocyanate. Previous studies have reported the use of higher ratios (between 1:4 – 1:20; β-CD/diisocyanate) without providing a rationale for the chosen co-monomer ratio.[1,60-61,73-74,76,97,104-105,126-127,149,166-173] A sparing number of reports has looked into the effect of the relative mole ratio and its effect on the sorption properties.[124,149] Yamasaki *et al.*[157] proposed the use of copolymers of variable composition (e.g., 1:4, 1:6, 1:8 and 1:10) and concluded that the removal efficiency of phenols was saturated at the β-CD/diisocyanate 1:8.[149] This indicates the possibility of an upper reaction limit between β-CD and diisocyanate (~ 1:8). However, the use of removal efficiency as a metric to conclude the upper limit of crosslinking co-monomer ratio is an indirect approach since sorption may occur on the linker framework sites, as discussed in § 1.4.1.2. Therefore, another alternative approach that uses TGA is described in Chapter 2. In order to further

understand and develop a systematic approach of designing such copolymers with tunable structural and physicochemical properties, the linker type and the crosslinking co-monomer ratio was varied for the five diisocyanates, as shown in Figure 1.3. The approach taken was to synthesize the copolymers at variable ratios (e.g., 1:1, 1:3, 1:6 and 1:9). These copolymers were characterized using the techniques described in § 1.4.3 and the phth adsorption method reported in § 1.4.1.3.

1.4.3 Characterization

At the time of writing this thesis, there were no systematic examples of work in the literature that fully described the extensive characterization of these materials. In this thesis, the techniques used for characterization of the copolymers include spectroscopic (IR and solid state ^{13}C NMR), thermal (TGA and elemental analysis) methods and nitrogen porosimetry.[1,76,97,103-105,126,157,166,170-171,173] A systematic characterization of the copolymers requires a multi-instrumental approach in order to obtain thorough quantitative or semi-quantitative results. For example, the determination of the crosslinking co-monomer ratio of different copolymers at variable co-monomer mole ratios provides a strategy for optimizing the crosslinking co-monomer ratio of β-CD for sorption-based applications.

1.4.3.1 Spectroscopic

The most common method for characterizing these copolymers is IR spectroscopy.[1,76,97,103-105,126,170-171,173] A key observation is the disappearance of the isocyanate group at 2270 cm^{-1}. Other peaks that appear as a result of urethane bond formation are as follows; vibrational band of carbonyl [ν(C=O)] groups in the range of 1701-1715 cm^{-1}, 3310 - 3370 cm^{-1} for ν(N-H) and ν(O-H), 1530-1541 cm^{-1} for δ(N-H)

and ν(NH-CO).[1,76,97,103-105,126,171,173]. This method of characterization was taken a step further by quantifying the relative peak areas for these vibrational bands and comparing copolymers at the different crosslinking co-monomer ratios, as outlined in Chapter 2.

In the case of NMR spectroscopy, one example in the literature was reported that used solid state ^{13}C NMR spectra of an HDI-based copolymer material.[104] This technique is common for these types of copolymers due to relatively very low or no solubility in NMR solvents. However, under the conditions of MAS (magic angle spinning) and CP (cross polarization), structural information analogous to ^{13}C NMR in solution can be obtained. The ^{13}C signatures provide diagnostic support for the presence of β-CD and linker resonance lines in addition to the appearance of carbonyl to support the urethane bond formation. In this work the copolymers were analyzed using both solution (^{1}H and ^{13}C) and solid state ^{13}C NMR. Generally, PUs with aliphatic diisocyanates and low crosslinking ratio (i.e. between 1:1 to 1:3) have relatively good solubility in deteurated NMR solvents such as *d*-DMSO. Chapter 2 provides a detailed analysis of the NMR studies.

1.4.3.2 TGA

TGA has been mainly used to show the thermal stability and composition of the copolymers.[104-105,170] It is a technique where a sample is heated and the weight change is monitored with increasing temperature. The plot between change in weight vs. temperature is known as weight loss curves. The TGA results may be represented as 1st derivative plots and this provides ability to accurately assess the temperature range where the weight loss is most apparent. In cases where the thermal events are overlapping, deconvolution can be applied and quantitative information may be obtained.

In case of the copolymers of interest in this thesis, two-stage degradation profiles have been observed for the HDI-based copolymers by two research groups.[105,170] The first degradation profile of the copolymers occurs in between 315-350 ^{o}C and is relatively high compared to conventional PUs which generally decompose around 200-220 ^{o}C. The second weight loss profile occurs between 410-425 ^{o}C. It was concluded that the first decomposition occurs due to the cleavage of the urethane bonds. No clear explanation was offered for the second decomposition. On the hand, another group saw a third weight loss around 520 ^{o}C.[104] They offered an alternative explanation by concluding that the first weight loss was due to the deamination of the terminal HDI linker, the second weight loss was due to decarbamation of the HDI linker, and the high temperature profile was the decomposition of the glucose units of β-CD. One has to be cautious with the former conclusions because the crosslinking co-monomer ratio used was 1:10 (β-CD/HDI). Such high crosslinking co-monomer ratios may lead to the possibility where the monomers may involve the formation of –A-B-B-A in addition to –A-B-A- copolymers, where A= β-CD and B=diisocyanate. Therefore the third weight loss may be attributed to the urethane oligomer units (-B-B-) of the homopolymer oligomers. Another group reported only two weight losses by using copolymers of variable crosslinking co-monomer ratio 1:4 and 1:10, respectively.[105,170] The interpretation of the weight loss profiles is questionable since native β-CD exhibits a maximum decomposition which has been reported previously to be ~ 312 ^{o}C and is close to the first weight loss profile observed by other groups.[175-176] *It was hypothesized whether TGA could be used to determine quantitative estimates of the co-monomer composition of the copolymer*. The thermal stability of β-CD should increase as the crosslinking co-monomer ratio increases, while

the opposite may be true for the thermal event associated with the linker units. The hypothesis was concluded to be correct and the details of this study are given in Chapter 2.

1.4.3.3 Elemental Analysis

Another characterization technique that has been used for copolymers is CHN elemental microanalysis (EA).[103-104] The technique involves determining the percentage weights of carbon, hydrogen, nitrogen and heteroatoms (such as halogens, sulfur, etc.) of a sample through combustion analysis. The sample is burned in an excess of oxygen, and various traps collect the combustion products i.e. carbon dioxide, water, and nitric oxide. The composition of the sample can be calculated from the weights of these combustion products. In principle, this technique offers a quantitative method to confirm the crosslinking co-monomer ratio while others have used it for determining the content of β-CD. Determination of β-CD content is limited to copolymers which are; *i*) free from the unreacted materials, residual solvent and moisture and *ii*) the mole ratio is similar to the theoretical values. If the copolymer contains impurities, the contaminants have to be identified, quantified and corrected for in the theoretical estimates. As discussed in Chapter 2, EA was considered as a semi-quantitative technique for confirming the level of crosslinking co-monomer ratio for each copolymer because of the presence of residual moisture and trace levels of DMA.

1.4.3.4 Nitrogen Porosimetry

Gas porosimetry measurements have been used to characterize materials where they provide surface and pore structure information. Nitrogen and argon gas are the two commonly used adsorbates gases in the porosimetry technique while organic vapors such

benzene and carbon dioxide can be used too. Nitrogen is the most frequently used gas adsorbate over argon due to the cost and general utility of liquid nitrogen for mesoporous materials. The commonly observed isotherms are Type I, II and III as shown in Figure 1.4.[177]

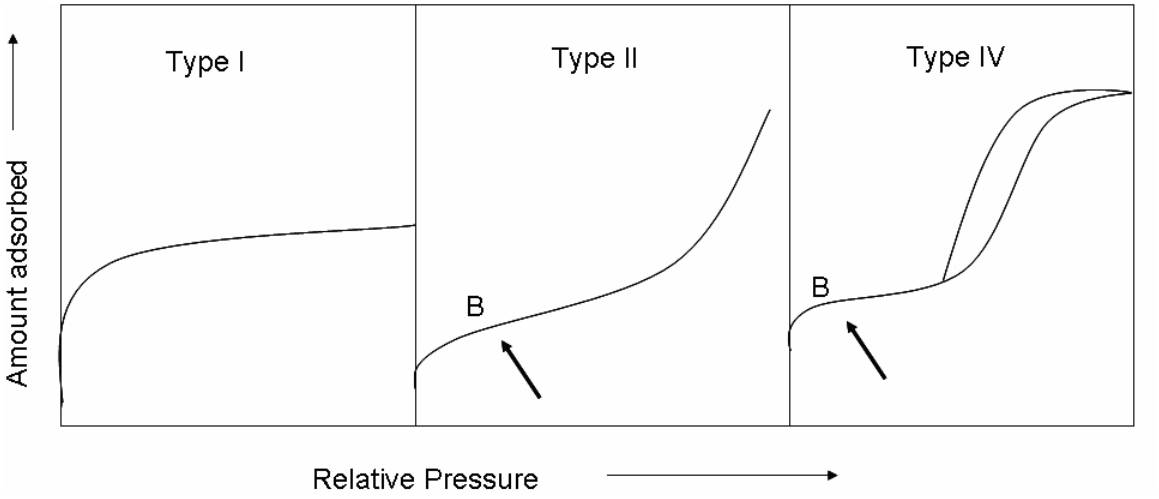

Figure 1.4. Types of adsorption isotherms. B represents the regions where monolayer coverage is complete.

The Type I isotherm depicts a monolayer adsorption and is well described by the Langmuir isotherm (*cf.* § 1.6.2.1).[178] It is usually common for microporous (pore widths not exceeding 2 nm) solid materials having relatively small external surface area. The limiting adsorption is controlled by the accessible micropore pore volume instead of the internal surface area. Materials that depict Type I isotherm are GAC, molecular sieves zeolites, some types of porous oxides, etc.[177]

On the other hand, Type II isotherm shows a large deviation from the Type I case where intermediate region (B region in Figure 1.4) corresponds to the point where monolayer coverage is complete and multilayer adsorption occurs and this type is commonly observed for non-porous or macroporous (pore widths exceeding 50 nm) materials.

As for the Type IV isotherm, it is similar to Type II but it has a characteristic hysteresis loop which results from capillary condensation occurring in the mesopores at intermediate relative pressures. The limiting adsorption occurs over a range of high relative pressure. Usually, the capillary condensation and evaporation occur at different relative pressures, hence, the observation of a hysteresis loop. Hysteresis loops result from either thermodynamic factors or pore connectivity of the porous materials or both.[179] In terms of thermodynamics while using liquid nitrogen, the metastability between the liquid and gas phase behaviour in the pores may be different for capillary condensation or evaporation. While in terms of the pore connectivity effect, if bigger pores have access to the surrounding through constricted pores, the former cannot be described at the relative pressure corresponding to the capillary evaporation in the constricted pores. This has been termed as an "ink-bottle" effect. This isotherm is common for mesoporous (pore widths between 2 – 50 nm) materials. There are additional types of isotherms but the focus of this discussion will be on these three types of isotherms in Figure 1.4.[177]

Analysis of the adsorption and desorption isotherms provide estimates of the surface and pore properties can be calculated using different models. Surface areas can be obtained using Equation 1.1 and Q_m obtained from fitting using the adsorption experimental data with the Langmuir (Type I) or Brunauer-Emmett-Teller (BET; Type II and IV) isotherm models (*cf.* §. 1.6.2.1 and 1.6.2.2.) Pore volume is calculated from the amount of gas adsorbed at a relative pressure close to the saturation vapor pressure i.e. relative pressure close to unity such 0.99. The amount adsorbed is simply converted to volume where it represents the total pore volume of all pores in the material.[179] However,

caution has to be exercised for materials with larger pores where incomplete pore filling will underestimate the pore volume within the material. Pore size distribution is calculated by the Barrett-Joyner-Halenda (BJH) method.[180] This method is based on a model[181] (Equation 1.2) where the adsorbent is treated as a collection of cylindrical pores. BJH accounts for capillary condensation in the pores using the classical Kelvin equation (Equation 1.3) with an assumption that the meniscus is a hemispherical liquid-vapor and has a well-defined surface tension. Therefore, the pore size is calculated from the Kelvin equation and the selected statistical thickness (t-curve) equation. Furthermore, according to the hysteresis phenomenon, the adsorption part (condensation) of the isotherm estimates the size of the larger internal pores while that for desorption part (evaporation) provides the size for the pore openings.[179]

$$SA\ (m^2.g^{-1}) = \frac{n_a \times A_m \times \sigma}{Y} \qquad \text{Equation 1.1}$$

where A_m represents the cross-sectional area occupied by the adsorbate molecule on the surface expressed on a molar basis (m^2/mol), n_a is the monolayer coverage of adsorbate on the surface of the copolymer (mol/g), σ is Avogadro's number (mol^{-1}), and Y is the coverage factor.[182-183]

$$v_{ads}\ (x_k) = \sum_{i=1}^{k} \Delta V_i\ (r_i \le r_c\ (x_k)) + \sum_{i=k+1}^{n} \Delta S_i t_i\ (r_i \rangle\ r_c\ (x_k)) \qquad \text{Equation 1.2}$$

where $v_{ads}(x_k)$ is the volume of liquid adsorbate (cm^3/g) at a relative pressure x_k, V is the pore volume (cm^3/g), S is the surface area (m^2/g) and t is the thickness of adsorbed layer (in appropriate units). This model indicates that the adsorbed amount at k-th point of adsorption isotherm may be divided into two distinct parts: *i*) volume in condensate in all pores smaller than some characteristic size depending on current relative pressure, $r_c(x_k)$,

ii) volume of adsorbed film on all larger pores, is calculated as a sum of terms: Σ (pore surface) (thickness of film in pore).

$$\ln \frac{p}{p^o} = \frac{2\gamma V_m}{rRT} \qquad \text{Equation 1.3}$$

where p is the actual vapour pressure, p_0 is the saturated vapour pressure, γ is the surface tension, V_m is the molar volume, R is the universal gas constant, r is the radius of the droplet, and T is temperature.

Previous reports detailing the analysis of the copolymers using this technique are sparse, and generally, BET surface areas were reported.[103,166] The use of this technique for obtaining surface and pore structure properties of the copolymers provides information about the physicochemical properties which allows optimization of the design of materials for sorption-based applications. The surface areas reported in the literature for these type of copolymers are 5.5 m^2/g for a HDI-based (1:8 β-CD:HDI) copolymer and 0.92 m^2/g for a TDI-based (1:10 β-CD:TDI) copolymer, respectively.[103,166] Solute rejection methods were employed to obtain the surface area and pore structure properties.[1] The latter method involves the use of guest molecules which have linear, rod-like, features which form inclusion complexes with β-CD and is not considered to be very reliable since the framework sites may bind to the guest (adsorbate) as described in § 1.4.1.2. The method is reasonably reliable if there are no sieving effects due to mismatching of size between the adsorptive and the pore dimensions of the framework domains. Furthermore, a dye-based solution method that uses a dye such as p-nitrophenol (PNP) provides estimates of the copolymer surface area, as described in the next section. This technique offers a comparison of how the copolymers differ in their physicochemical properties according to solid-gas to solid-solution adsorption processes.

The results for the copolymers using these techniques reveal that the aromatic-based copolymers had a greater surface area (~10^1 m^2/g) compared to the aliphatic-based copolymers (≤1 m^2/g). The details of this study are described in Chapter 3.

1.4.3.5 Dye Sorption Method

Giles *et al.* have shown the use of PNP in estimating the surface area (SA) of various materials including granular solids, fibers, cellulose, etc.[182,184-187] They showed that the SA (*cf.* Equation 1.4) of the copolymers (m^2/g) can be evaluated from the parameters obtained from the adsorption isotherm models (discussed in § 1.6.2). A_m represents the cross-sectional area occupied by the adsorbate molecule on the surface expressed on a mole basis (m^2/mol), Q_m is the monolayer coverage of adsorbate on the surface of the copolymer (mol/g), σ is Avogadro's number (mol^{-1}), and Y is the coverage factor.[182-183] The A_m value is 52.5 $Å^2$ for PNP when adsorbed in a co-planar geometry (common in aqueous media) and 25 $Å^2$ when adsorbed orthogonal geometry (common in polar inorganic compounds).[182]

$$SA\ \ (m^2.g^{-1}) = \frac{Q_m \times A_m \times \sigma}{Y} \quad \text{Equation 1.4}$$

This method can be used in aqueous media or in organic solvents and is considered suitable for a wide variety of solids, both porous and nonporous, provided the material forms a hydrogen bond with PNP or have aromatic nuclei. It is deemed to be a simpler method than gas adsorption, however, it has its limitations; *i*) variation of the A_m of the adsorbate introduces errors in the SA estimates, *ii*) exclusion of adsorbate from micropores due to size-fit differences, and *iii*) potential micellization of the adsorbate on the surface of the adsorbent. Therefore, this method is reliable when comparing similar materials which are applicable in the case of the present study. This method can also be

used to provide pore structure properties provided that there are no sieving effects due to mismatching of size between the adsorptive and the pore dimensions of the sorbents.

Inel and Tumsek[183] commented that Padday[188] raised concerns about the accuracy of this method since many dye adsorption isotherms show no clearly defined plateau. However, Giles[187] agreed that complete coverage is not always obtained with certain acidic solids and recommends the use of other solvents. Inel and Tumsek[183] concluded that the measurement of the SAs of silicates using various dyes (methylene blue, *o*-phenanthroline and PNP) and nitrogen porosimetry revealed differences in the respective SA estimates. They concluded that the occurrence of swelling of the adsorbent in solution may open up the pores of sorbent. This conclusion provided motivation to compare the results from the dye sorption with the nitrogen adsorption method to see if differences between each method occur. The SA estimates from porosimetry are generally relatively low and require further study. In contrast, the dye sorption method may provide support for the implication of solvent effects on copolymer textural properties. For comparison, GAC was compared since it has no significant swelling in aqueous solution as compared with the copolymers. The details of this work are reported in Chapter 3.

1.5 Inclusion of Naphthenic Acids using Cyclodextrins

1.5.1 Naphthenic Acids complexation with Cyclodextrins

As mentioned in § 1.3.3.3, sorption process is a recommended method of sequestering NAs from aqueous solution provided that a suitable sorbent is available. The use of engineered copolymers that are tunable with variable physicochemical properties are considered ideal. To evaluate the sorption efficiency of NAs, there is a need to

establish that they are efficiently adsorbed and understand the nature of the sorption mechanism.

The formation of complexes between CDs and carboxylic acid compounds have been previously investigated directly using NMR spectroscopy,[37-38] calorimetry,[39] conductivity,[40] spectral displacement methods,[41-42] among other techniques.[43] Non-covalent complexes have recently been studied by electrospray mass spectrometry (ESI-MS).[189-191] In particular, some examples in the literature illustrate ESI-MS methods for the study of the formation of CD-guest inclusion complexes.[192-197] The traditional definition of NAs depicts these compounds as optically transparent in the UV-Vis region; hence, they are not amenable to traditional spectroscopic methods. ESI-MS is essential for the determination of the composition of such complex mixtures of carboxylic acid compounds (NAs).[198-200] To establish proof of the inclusion of NAs within CD cavities, three common types of CDs (i.e., α-, β-, and γ-CD) with variable cavity size (*cf.* Table 1.1), were investigated to obtain an understanding of the type of NAs that are complexed for each host macrocycle. NAs derived from Athabasca (in Alberta) OSPW were extracted using a procedure developed by Janfada.[25] Furthermore it will be valuable to study the formation of these complexes with NA surrogates (specific examples of NAs). Four types of surrogates were chosen in terms of their hydrogen deficiency and variable molecular weight, as shown in Figure 1.5. Moreover, glucose and cellobiose (*cf.* Figure 1.6) are non-porogen carbohydrates were chosen for comparison with CDs. Cellobiose (*cf.* Figure 1.6) is a concave-shaped disaccharide with amphiphilic properties in aqueous solution; hence, it is expected to form noncovalent complexes with apolar molecules such as NAs. In contrast, no complexes are anticipated with glucose because of its greater

hydrophilic character.[201-202] The quantification of NAs was conducted using negative ion ESI-MS. The results of this work are reported in Chapter 5 where NAs and the surrogates were concluded to form inclusion complexes with CDs to varying degrees. Also, the nature of the inclusion complexes varied according to the size-fit between the CD cavity and the guest whereas glucose (nonporogenic saccharide) showed no evidence of complex formation.

.

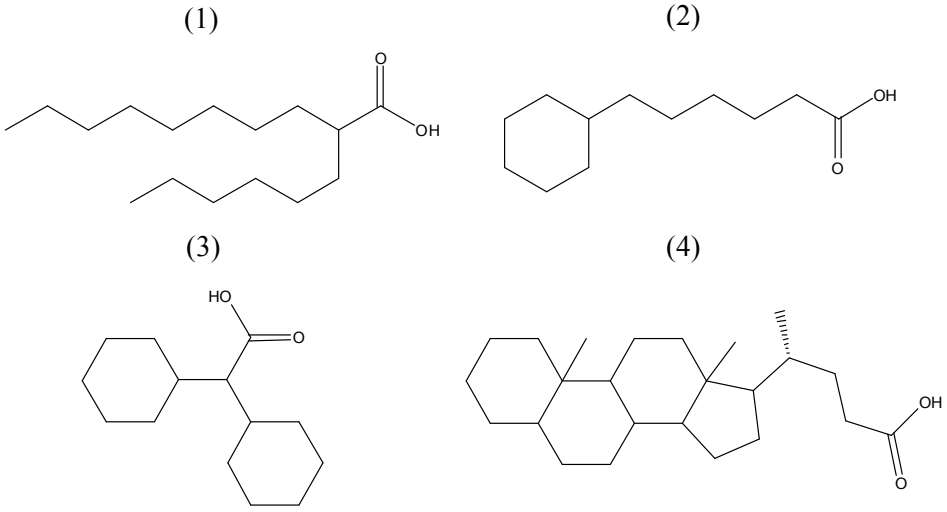

Figure 1.5. Molecular structure of surrogates (1-4): 1) 2-hexyldecanoic acid, 2) pentylcyclohexane carboxylic acid, 3) dicyclohexylacetic acid, and 4) 5β-cholanic acid.

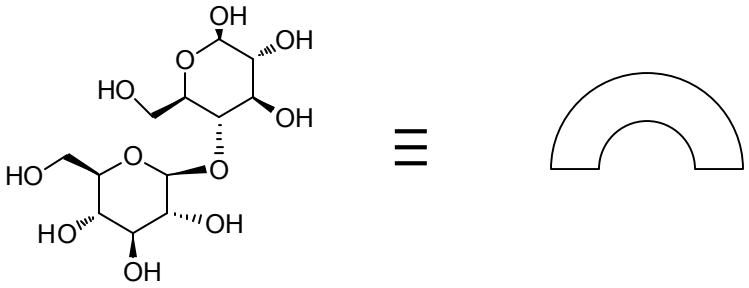

Figure 1.6. Molecular structure of cellobiose which is reported to have a concave shape (hemi-toroid) in solution.

1.5.2 β-CD/Naphthenic Acids Binding Constants

Knowledge of the binding affinity between β-CD and NAs is important for the application of such polymer materials in order to predict isotherm sorption properties and thermodynamic stability. Since NAs, according to the classical definition, are optically transparent in the UV-Vis region, other techniques besides spectroscopy are required. Sound velocity,[203] conductivity,[204] surface tension[205] and electrochemical measurements[206] have been used to examine the inclusion complexes of CDs with carboxylic acids. The former three techniques involve the measurement of a bulk solution property, and represent an average contribution arising from the free and bound fraction of the guest molecule in solution. In contrast, electrochemical methods that use ion-selective electrodes provide direct measurement of the free inclusate concentration. The direct measurement of bound or guest or host is preferred as it yields a more accurate estimate of the binding constant.[207] However, non-spectroscopic techniques are sometimes susceptible to large errors when the binding constant is large ($>10^4$ M^{-1}) because the fraction of unbound species is generally low for this condition. Techniques which involve the measurement of colligative or bulk physical properties in solution do not accurately reflect the relative contributions of bound and unbound species. Consequently, there are greater uncertainties for binding constants derived from such methods. A further complication arises due to the implicit statistical bias in the analysis of the primary data using linearization methods; for example, the inherent assumptions in the Benesi-Hildebrand plots are generally not met for strongly bound host-guest systems and require the use of non-linear fitting methods.[208-209]

Spectroscopic methods which involve the direct measurement of the bound or unbound species using a UV-Vis[210] or fluorescence[211] spectroscopy represent a suitable experimental method. The spectral displacement technique[42,115,118-119,121-123,212-214] has been used to determine the binding constants of spectroscopically transparent compounds such as NAs that form complexes with β-CD. The determination of the binding constants for such complexes involves the measurement of absorbance changes of a suitable chromophore in the presence of β-CD and a competing non-chromophoric inclusate. Examples of such chromophores employed include phth,[77,80-81,83-85,157,212] methyl orange,[213] and *p*-nitrophenol[214]. Scheme 1.5 illustrates the two competitive equilibria involved in the spectral displacement technique. In this project phth was chosen as the chromophore, and similar to the previous section, the binding constants of NAs and surrogates were studied. The spectral displacement technique involves certain assumptions and provides good accuracy for the determination of a CD-inclusate binding constant (K_2) values. The relative change in the absorbance of phth between the bound and unbound states is large, and is directly related to the amount of unbound inclusate. More of this work is covered in Chapter 6 where the binding constant was concluded to be ~10^4 M^{-1} and increased for guests with greater lipophilic surface area (LSA) which form inclusion complexes in the β-CD cavity interior.

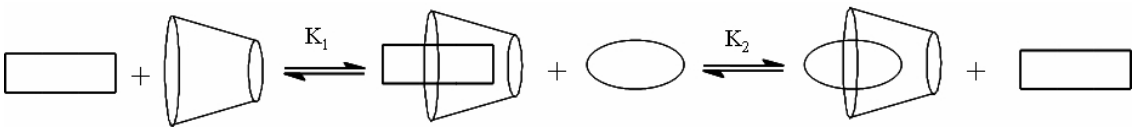

Scheme 1.6. The formation of an host-guest complex is shown for a β-CD (toroid) and a chromophore guest molecule (rectangle) according to an equilibrium process where K_1 is the 1:1 equilibrium binding constant. Addition of a non-chromophore guest molecule

(oval), the chromophore is replaced and the guest molecule is included into the β-CD according to a 1:1 equilibrium constant, K_2.

1.6 Sorption Methodology

1.6.1 General Sorption Overview

Thus far, it has been shown that NAs are included in the cavity of β-CD and they have a relatively large binding affinity ~10^4 M^{-1}. The next step was to evaluate the utility of the copolymers in sequestering NAs from aqueous solution. This is conveniently studied using sorption isotherms in conjunction with an appropriate analytical method. Sorption implies that it is a combination of absorption and adsorption. Absorption is the penetration of the solute within the inner structure of another substance while adsorption is the adherence of the solute onto the surface of another substance. In the case of microporous materials (e.g., CD copolymers), the distinction between adsorption and absorption becomes ill defined and difficult to distinguish. The use of appropriate isotherm models, in this work, will provide strong support in favour of adsorption processes (*vide infra*). Since these two processes (adsorption and absorption) may often occur simultaneously, the term *sorption* is used hereafter. Thus, the terms sorbent and sorbate are used in place of the conventional terms adsorbent and adsorbate, respectively. These terms will be used interchangeably throughout this work.

There are primary driving forces for sorption; *i*) the relative solubility of the sorbate in solution and the sorbent phase; hydrophilic adsorbates will prefer residing in the water phase unlike their lipophilic counterparts which are repulsive in the water phase and show preferential adsorption onto the sorbent, and *ii*) affinity of the sorbate to sorbent, i.e., the type of interaction between the two which consists mainly of either ion-

exchange, physisorption (van der Waal's forces, H-bonding, etc.) and chemisorption (covalent bonding). The anticipated interaction between NAs and the copolymers is physisorption and based on Scheme 1.2. NAs are increasingly lipophilic as the MW increases. Thus, lipophilic NAs are anticipated to partition onto the surface of the solid phase (lipophilic) sorbent. *The hypothesis considered here was to determine if the sorption behaviour of phenolic dyes (PNP and phth) is governed by their variable HLB as evidenced by their respective water solubilities*.

Sorption phenomena are usually analyzed with appropriate isotherms to provide a detailed understanding of the thermodynamics of sorption in a sorbent/sorbate system. The results are represented as a plot of the bound amount of sorbate at equilibrium (Q_e) against the amount of residual (unbound) sorbate remaining in aqueous solution at equilibrium (C_e) at constant temperature. The isotherms are interpreted by using appropriate isotherm models that simulate the sorption behavior. The model that shows the "best fit" overall in terms of lowest sum of square of errors (*cf.* Equation 1.5; where $Q_{e,i}$ = experimental value, $Q_{f,i}$ = fitted value, and N = number of data points) is usually judged as the "best fit" model. The isotherm models chosen for this study include Langmuir,[178] Brunauer−Emmett−Teller (B.E.T),[215] Freundlich,[216] and the Sips[217] isotherm models. Although these models were derived for solid-gas adsorption systems, they have been applied successfully to describe the equilibria for solid-solution isotherms.

$$SSE = \sum \sqrt{\frac{\left(Q_{e,i} - Q_{f,i}\right)^2}{N}} \qquad \text{Equation 1.5}$$

1.6.2 Sorption Isotherm Models

1.6.2.1 Langmuir

This model was named after the founder who won a Nobel Prize in 1932 for his noteworthy research on surface chemistry. This model has three assumptions; *i*) only one monolayer of adsorbate is adsorbed onto the surface, *ii*) all adsorbent surface sites are equivalent and can accommodate, at most, one adsorbed atom, and *iii*) the ability of a molecule to adsorb at a given site is independent of the occupation of the neighbouring sites. This model is described in Equation 1.6 where Q_m is the monolayer surface coverage of the adsorbate on the solid material, and K_L is the equilibrium adsorption constant. Based on the foregoing assumptions, CD copolymers may not fit well with Langmuir since there are at least two potential sorption sites available (Scheme 1.2). Moreover, assumption (*iii*) may not be true in the case of NAs which is a mixture of different types of carboxylic acids, as shown in Figure 1.3 (*cf.* § 1.3.1). As well, the sorption of multi-component adsorbates (dyes) on different adsorbents showed poor agreement with the Langmuir model.[218-219]

$$Q_e = \frac{K_L Q_m C_e}{1 + K_L C_e} \qquad \text{Equation 1.6}$$

1.6.2.2 B.E.T

The most widely used isotherm dealing with multi-layer adsorption processes was derived by Stephen Brunauer, Paul Emmet and Edward Teller, and is called the B.E.T. model.[215] Similar assumptions are proposed as the Langmuir model, i.e. (*ii*) and (*iii*), and the additional criteria that the initial adsorbed layer can act as a substrate for subsequent adsorption. Therefore, the isotherm may rise sharply instead of leveling off at some saturated monolayer capacity at high concentration. This model is described by Equation

1.7 where K_{BET} is the equilibrium adsorption constant and C_s is the saturated concentration of the sorbate at the identical temperature and solution conditions. The B.E.T. model has similar concerns as those mentioned for the Langmuir model, described above.

$$Q_e = \frac{Q_m K_{BET} C_e}{(C_s - C_e)[(1 + (K_{BET} - 1)C_e)]/C_s} \qquad \text{Equation 1.7}$$

1.6.2.3 Freundlich

Freundlich proposed an empirical isotherm model as shown in Equation 1.8. The parameters K_F and n_F, are Freundlich constants related to binding constant and intensity of adsorption, respectively.[216] This isotherm model assumes a heterogeneous sorbent surface with a non-uniform distribution of heats of adsorption. Since NAs are a complex mixture of carboxylic acids and the copolymers may have several potential binding sites, this model is deemed appropriate. However, a limitation of this isotherm model is the inability to obtain direct estimates of Q_m which are required for calculating the surface area of the copolymers. Since the monolayer sorption capacity is a characteristic sorbent property, an alternative model that utilizes similar assumptions but enables the estimation of Q_m is preferred. The Sips isotherm model provides a suitable alternative to the Langmuir, BET, and Freundlich isotherm models.

$$Q_e = K_F C_e^{1/n_f} \qquad \text{Equation 1.8}$$

1.6.2.4 Sips

Sips developed an empirical isotherm while studying the distribution of adsorption energies for the active sites on a catalyst surface. The Sips model is a

derivation based on the form of the Langmuir and Freundlich isotherm models, as shown in Equation 1.9. K_s is the Sips equilibrium constant and n_s is an indicator of the adsorption heterogeneity. Values of n_s that deviate from unity indicate that the sorbent material is heterogeneous. In contrast, $n_s = 1$, indicates the model resembles Langmuir isotherm and infers that the sorbent is homogeneous. Also, when the terms in the denominator equal unity, the model resembles the Freundlich model. Therefore, the Sips model is found to be more versatile and represents a wide range of isotherm behaviour. The generality of the Sips isotherm enables a general description of the Langmuir and Freundlich isotherm models when variable conditions are met.

$$Q_e = \frac{Q_m (K_s C_e)^{n_s}}{1 + (K_s C_e)^{n_s}} \qquad \text{Equation 1.9}$$

1.6.3 Sorption of Model Compounds

Extraction of NAs from OSPW is labor intensive and NAs are generally unavailable in large quantities. Therefore, it is useful to establish a sorption protocol and understand the sorption mechanism of these copolymers. In § 1.4.1.3 and 1.4.3.5 phth and PNP dyes were used as probes in determining the surface accessible sites of β-CD and the surface area estimates of the copolymers, respectively. These phenolic dyes can be used to further understand the diverse sorption behaviour of such copolymers materials. The sorption results for the two dyes are reported Chapter 3 and 4. The isotherms were analyzed to further understand the thermodynamic sorption mechanism of these copolymers. Although phth and PNP are not structural analogues of NAs, they serve as useful model compounds due to the following reasons; *i*) possess ionizable protons like NAs, *ii*) they can be studied at variable pH, *iii*) possess amphiphilic character like NAs,

and iv) the molecular weights fall in the range of the molecular weight distribution of NAs i.e. phth (318 g/mol) and PNP (139 g/mol). The ESI-MS spectrum shown in Figure 1.7 illustrates the distribution of molecular weights of Athabasca-derived NAs. The use of UV-Vis spectrophotometry for phenolic dyes is favored because of its ease of use, simplicity, and relative accuracy. The sorption results for phth and PNP with the copolymers show interesting dual behaviour. It was observed that sorption either occurred in the cavity of β-CD, or in the cavity and the interstitial (non-inclusion) domains, as shown in Scheme 1.2. The occurrence of sorption at multiple sites is consistent with the physicochemical properties of the adsorbate. Further details of the sorption mechanism are reported in Chapter 8.

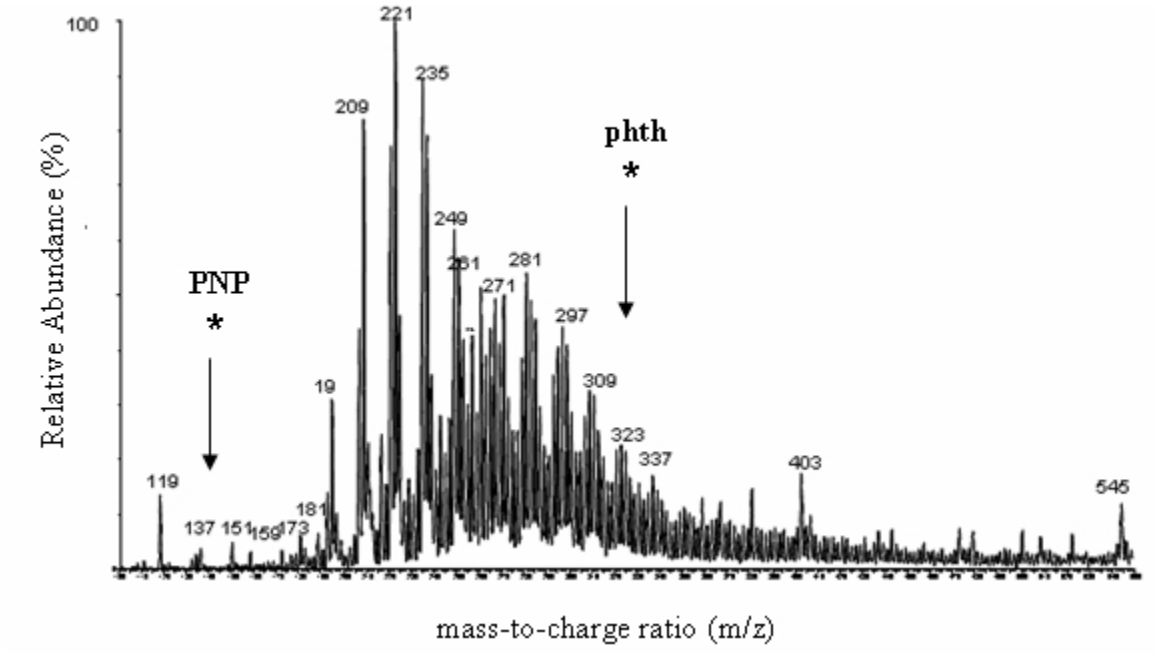

Figure 1.7. ESI-MS spectrum of a 95.8 ppm sample of Athabasca-derived NAs at pH 9.00 30 illustrating the distribution abundance (%) of congeners according to molecular weight. The asterisks and arrows indicate the relative MWs of the phenolic dyes in relation to the values for the NAs.

1.7 Sorption of Naphthenic Acids

1.7.1 Equilibrium Studies

In § 1.3.3.1, it was concluded that comparatively few equilibrium studies are available for the sorption of NAs in the literature, however, some research groups have studied the sorption of NAs and conventional sorbents.[21-22,27] Gaikar and Maiti[21] reported sorption results for various sorbents using n-heptane as the solvent media instead of water. The main reason is that heptane simulates the petroleum fraction in which NAs are distributed in crude oil. The adsorptive recovery of NAs from the petroleum fractions were investigated from equilibrium studies, where the concentrations of adsorbed NAs in the sorbent phase (Q_e) were plotted versus the residual concentration (C_e). The isotherms were modeled with the Langmuir model only and they did not justify why other isotherm models such as B.E.T, Freundlich and Sips were excluded. The fitting of the Langmuir model is not supported by the goodness of fit criteria according to the experimental data. Gaikar and Maiti expressed the amount of adsorbed NAs as moles quantities without stating how the average MW of the NAs was obtained (complex mixture of carboxylic acids). The results obtained are listed in Table 1.2 below where the ion-exchange resin is shown to be the best candidate. The equilibrium constants are relatively low; hence, the sorbents displayed poor affinity towards NAs.

Table 1.2: Adsorption capacities and Langmuir constants at 28°C obtained from Gaikar and Maiti's work[21] using Equation 1.6

Sorbent	Adsorption Capacity (Q_m) (mol/Kg)	Langmuir Equilibrium Constant, K_L, (M^{-1}) x 10^{-3}
Zeolite	0.155	0.105
poly (4-vinyl pyridine)	0.600	0.0447
Clay	0.442	0.0547
Resin	0.920	0.0639

The other two studies that showed isotherm results for NAs are those by Janfada *et al.*[25] and Peng *et al.*[26]. The only detailed isotherm that they studied was the linear isotherm since the mechanism is partitioning of organics from aqueous media to the solid organic material. While Peng *et al.*[26] looked at model compounds of NAs, Janfada *et al.*[25] studied the Syncrude-derived NAs. They both concluded that soils with higher organic content had higher sorption capacity. The results indicate that NAs may be well adsorbed with CD-based copolymers due the organic framework of the sorbent materials. They also observed that the presence of inorganic salts in water enhances sorption due to the decrease (salting out) in the solubility of NAs. The results agreed with the general concept that the degree of sorption of organic compounds is inversely proportional to their water solubility. Peng *et al.*[26] further concluded that an increase of temperature reduced the sorption capacity because the sorption process is generally exothermic and an increase in the temperature reduces the thermodynamic driving force and the sorption capacity. They further studied the effect of pH which had an impact on the distribution coefficient (distribution between solid and aqueous phases). At high pH, NAs partitioned

more favourably in the aqueous phase; this was attributed to ionization and the increase in the polarity of NAs at higher pH, and favourable partitioning into the water phase relative to the soil fraction. They also studied the effect of the size of individual carboxylic acids on the sorption and observed size effects. This conclusion was corroborated by Janfada *et al.*[25] where it was found that NAs with carbon numbers 13-17 had a greater sorption capacity in soil over other species.

There is a need to test the sorption properties of copolymers with NAs and in a systematic fashion in order to provide a better understanding of the sorption mechanism. Initial sorption studies of NAs at pH 5 and 9 were investigated to see if there were any notable differences. A comparison of the sorption behavior of different β-CD sorbent materials; β-CD crosslinked with EP[220-223], β-CD functionalized mesoporous silica[224-227], and GAC were tested. The results of these initial tests are reported in Chapter 7. Sorption studies at pH 5 and 9 for β-CD copolymer materials showed minor differences. The sorption capacity at pH 5 > pH 9 since the solubility of NAs is lower than at pH 9; hence, greater partitioning onto the lipophilic copolymer is favored. Thus, sorption was studied at pH 9 since these conditions are close to that of OSPW (~ pH 8).[4] The sorption of NAs with β-CD copolymers are described in Chapters 7 and 8.

1.7.2 Spectrophotometry of Naphthenic Acids

The classical definition of NAs has been questioned since recent results obtained from mass spectrometry for NAs have revealed a number of other additional components that do not fit the classic conventional definition. The fully saturated molecular structure ($C_nH_{2n+z}O_2$) shown in Figure 1.3 represents the classical definition of NAs. The latter definition is recognized as a generalized but limited description of the diverse types of

organic acids found within crude oil. However, crude oil contains naphthenic acids along with significant levels of other organic acids with N and/or S atoms. These impurities have various levels of unsaturation and aromaticity. Collectively, more than 3000 chemically different elemental compositions that contain O_2, O_3, O_4, O_2S, O_3S, and O_4S were determined recently in a study of South American heavy crude.[198]

There is thus significant levels of impurities reported for oil sands derived NAs, along with mass spectral evidence that suggests various levels of hydrogen deficiency and aromaticity. Indeed Raman spectroscopy has revealed evidence of fluorescence behaviour. *Therefore, it was hypothesized that Syncrude-derived NAs may exhibit fluorescence behavior. Another hypothesis was to determine if UV-Vis absorption and florescence emission spectroscopy are suitable potential analytical techniques for the quantitative detection of NAs in OSPW*. A comparison of the characterization and quantification of Syncrude-derived NAs by conventional direct injection ESI-MS with UV-Vis absorption and fluorescence emission detection methods was investigated. The latter methods are proposed as inexpensive and quick screening tools which use the detection of "impurities" as a surrogate for the analysis of NAs in OSPW. The results of this work are presented in Chapter 10 and have been adopted by Oil Sands Tailing Research Facility (OSTRF) in the project titled "OSTRF Naphthenic acid fluorescence sensor" to build a miniature fluorescence sensor in order to detect and characterize NAs in OSPW.[228]

1.8 Organization and Scope

This Ph.D. thesis is primarily concerned with the design of engineered β-CD PUs and an evaluation of their utility as sorbents for the sequestration of NAs from aqueous solution. It is divided into 11 chapters. Chapter 1 is the introduction, Chapters 2-10 are verbatim copies of articles published in the literature and Chapter 11 is the conclusion. The published articles are outlined below in the order of Chapter 2-10, respectively;

1. **Mohamed, M. H**.; Wilson, L. D. *; Headley, J. V. Design and Characterization of Novel β-Cyclodextrin Based Copolymer Materials. *Carbohydrate Research*. **2011**, *346(2)*, 210-229.
2. Wilson, L. D. *; **Mohamed, M. H**.; Headley, J. V. Surface Area and Pore Structure Properties of Urethane-Based Copolymers Containing β-Cyclodextrin. *Journal of Colloid and Interface Science*. **2011**, *357(1),* 215-222.
3. **Mohamed, M. H**.; Wilson*, L. D.; Headley, J. V. Estimation of the Surface Accessible Inclusion Sites of β-Cyclodextrin Based Copolymer Materials. *Carbohydrate Polymers*. **2010**, *80(1)*, 186-196.
4. **Mohamed, M.H**.; Wilson*, L. D.; Headley, J. V.; Peru, K. M. Electrospray Ionization Mass Spectrometry Studies of Cyclodextrin-Carboxylate Ion Inclusion Complexes. *Rapid Communications in Mass Spectrometry*. **2009,** *23(23)*, 3703.
5. **Mohamed, M. H**.; Wilson*, L. D.; Headley, J. V.; Peru, K. M. A Spectral Displacement Study of Cyclodextrin/Naphthenic Acids Inclusion Complexes. *Canadian Journal of Chemistry*. **2009**, *87(12)*, 1747-1756.
6. **Mohamed, M. H**.; Wilson*, L. D.; Headley, J. V.; Peru, K. M. Novel Materials for Environmental Remediation of Tailing Pond Waters Containing Naphthenic Acids. *Process Safety and Environment Protection*. **2008**, *86(4)*, 237-243.
7. **Mohamed, M. H**.; Wilson*, L. D.; Headley, J. V.; Peru, K. M. Sequestration of Naphthenic Acids from Aqueous Solution Using β-Cyclodextrin-based Polyurethanes. *Physical Chemistry Chemical Physics*. **2011**, *13(3)*, 1112-1122.

8. **Mohamed, M. H**.; Wilson*, L. D.; Headley, J. V. Investigation of the Sorption Properties of β-Cyclodextrin-based Polyurethanes with Phenolic Dyes and Naphthenates. *Journal of Colloid and Interface Science.* **2011**, *356(1)*, 217-226.
9. **Mohamed, M. H**.; Wilson*, L. D.; Headley, J. V.; Peru, K. M. Screening of Oil Sands Naphthenic Acids by UV-Vis Absorption and Fluorescence Emission Spectrophotometry. *Journal of Environmental Science and Health, Part A: Toxic/Hazardous Substances Environmental Engineering.* **2008**, *43(14)*, 1700 - 1705.

**Dr. Lee Wilson was the corresponding author for all of the above publications.*

In each chapter, there is a short summary of the work and a preface denoting the contributions by each author. Furthermore, a description of how each paper relates to the stated objectives of this Ph.D. thesis has been included.

Chapter 1 presents an introduction and overview of the entire Ph.D. thesis. And describes how the overall objectives were tackled in a systematic fashion, and how each hypothesis contributed to the project.

Chapter 2 presents the synthesis and characterization of the copolymers using different methodologies. The copolymers were synthesized by varying the type of linker molecule and its crosslinking co-monomer ratio. This strategy offers a way to tune the materials and examine the effects of the synthetic design on the physicochemical properties of the copolymer materials. The characterization techniques provide supporting proof of the molecular identity of the copolymers and a semi-quantitative analysis of copolymer composition. This work illustrates a first example in the literature of a systematic study for these types of copolymers, especially at such relatively low co-monomer ratios (i.e. 1:1, 1:2, and 1:3).

Chapter 3 presents the characterization of the textural properties of the copolymers using nitrogen porosimetry and a dye sorption method using PNP. The

former gives information about the surface area and pore structure properties while the dye sorption method provides reasonable estimates of the surface area in aqueous solution. This study also shows clear differences in the gas sorption and solution-based methods, respectively. This work represents the first example in the literature of an extensive textural analysis using such techniques.

Chapter 4 presents the use of phth as an adsorptive probe to determine the surface accessible β-CD sites. There was no available quantitative study in the literature for the determination of the accessible CD inclusion sites at the time when this work was published. Hence, this work illustrates the first example of a quantitative study for such β-CD copolymer materials.

Chapter 5 presents the results of an inclusion study between NAs and surrogates with α-, β-, and γ-CDs. Also, non-macrocyclic hosts such as cellobiose and glucose were used to confirm that inclusion complexes are formed within the CD cavity. Cellobiose formed molecular aggregrates with these guests whereas glucose did not show any measurable intermolecular interactions. This work provides the first example in the literature of direct evidence of the formation of such inclusion complexes using ESI-MS.

Chapter 6 presents the results for the determination of the binding constants between NAs and its surrogates with β-CD, using the spectral displacement technique. This technique utilizes the molecular recognition between β-CD and phth and enables the detection of non-chromophoric inclusates. This work is the first example in the literature to estimate the binding constants for the inclusion complexes between β-CD and NAs.

Chapter 7 presents the results for the sorption of NAs with three different types of β-CD materials; i) β-CD crosslinked with PDI, ii) β-CD crosslinked with

epichlorohydrin, and iii) β-CD functionalized mesoporous silica. GAC was also studied as a "standard" sorbent with relatively high surface area to serve as a reference to the β-CD materials. This work is the first example in the literature documenting the sorption of NAs with β-CD-based sorbent materials.

Chapter 8 presents a detailed sorption of NAs with the copolymers (β-CD PUs). Apart from the work in Chapter 7, this research represents the first example in the literature describing a comprehensive and systematic sorption study of such copolymers with NAs in aqueous solutions.

Chapter 9 outlines a generalized sorption mechanism of the copolymers with two types of phenolic dyes of different size (i.e. PNP and phth) at variable pH conditions, and a comparison with the results for NAs. This work provides a detailed understanding of the sorption behavior in aqueous solution. This paper reports the first example of phth sorption isotherms for these materials and clearly illustrates accessible *vs.* inaccessible framework adsorption sites.

Chapter 10 reports the utility of UV-Vis absorption and fluorescence emission spectroscopy as a screening technique for the analytical detection of NAs in OSPW. It also offers a comparison between the characterization and quantification of Syncrude-derived NAs mixtures by conventional direct injection ESI-MS with UV-Vis absorption and fluorescence emission detection. This work represents the first example in the literature illustrating the utility of spectroscopic properties of NAs and raises the question of the accuracy of the classical definition of molecular structure of NAs.

Chapter 11 presents summary, conclusion and proposed future work.

1.9 References

1. Ma, M.; Li, D. *Chem. Mater.* **1999**, *11*, 872-874.
2. Jolly, S. E. In *Kirk-Othmer Encyclopedia of Chemical Technology*; 2nd ed.; Kirk-Othmer, Ed.; Sun Oil Co.: Philadelphia, PA, 1967; Vol. 13, p 727-734.
3. Lo, C. C.; Brownlee, B. G.; Bunce, N. J. *Anal. Chem.* **2003**, *75*, 6394-6400.
4. Headley, J. V.; McMartin, D. W. *J. Environ. Sci. Health, Part A: Toxic/Hazard. Subst. Environ. Eng.* **2004**, *A39*, 1989-2010.
5. McMartin, D. W.; Headley, J. V.; Friesen, D. A.; Peru, K. M.; Gillies, J. A. *J. Environ. Sci. Health, Part A: Toxic/Hazard. Subst. Environ. Eng.* **2004**, *39*, 1361 - 1383.
6. Clemente, J. S.; Fedorak, P. M. *Chemosphere* **2005**, *60*, 585-600.
7. Rudzinski, W. E.; Oehlers, L.; Zhang, Y.; Najera, B. *Energ. Fuel* **2002**, 16, 1178-1185.
8. Brient, J. A.; Wessner, P. J.; Doly, M. N. In *Kirk-Othmer Encyclopedia of Chemical Technology*; 4th ed.; Kroschwitz, J. I., Ed.; John Wiley & Sons, Inc.: New York, NY, 1995; Vol. 16, p 1017-1029.
9. Kanicky, J. R.; Poniatowski, A. F.; Mehta, N. R.; Shah, D. O. *Langmuir* **1999**, *16*, 172-177.
10. Quagraine, E. K.; Peterson, H. G.; Headley, J. V. *J. Environ. Sci. Health, Part A: Toxic/Hazard. Subst. Environ. Eng.* **2005**, *40*, 685-722.
11. Quagraine, E. K.; Headley, J. V.; Peterson, H. G. *J. Environ. Sci. Health, Part A: Toxic/Hazard. Subst. Environ. Eng.* **2005**, *40*, 671-684.
12. Headley, J. V.; Crosley, B.; Conly, F. M.; Quagraine, E. K. *J. Environ. Sci. Health, Part A: Toxic/Hazard. Subst. Environ. Eng.* **2005**, *40*, 1 - 27.
13. Lister, A.; Nero, V.; Farwell, A.; Dixon, D. G.; Van Der Kraak, G. *Aquat. Toxicol.* **2008**, 87, 170-177.
14. Thomas, K. V.; Langford, K.; Petersen, K.; Smith, A. J.; Tollefsen, K. E. *Environ. Sci. Technol.* **2009**, 43, 8066-8071.
15. Department of Energy, Government of Alberta. Edmonton, AB, 2001; 13th March. http://www.energy.gov.ab.ca/1876.asp (accessed 17th January 2006).
16. Schindler, D. W.; Donahue, W. F. *PNAS* **2006**, *103*, 7210-7216.

17. MacKinnon, M. *AOSTRA J. Res.* **1989**, *5*, 109-133.
18. Slavcheva, E.; Shone, B.; Turnbull, A. *Brit. Corros. J.* **1999**, *34*, 125-131.
19. Turnbull, A.; Slavcheva, E.; Shone, B. *Corrosion* **1998**, *54*, 922-930.
20. Rogers, V. V.; Liber, K.; MacKinnon, M. D. *Chemosphere* **2002**, *48*, 519-527.
21. Gaikar, V. G.; Maiti, D. *React. Funct. Polym.* **1996**, *31*, 155-164.
22. Wong, D. C. L.; van Compernolle, R.; Nowlin, J. G.; O'Neal, D. L.; Johnson, G. M. *Chemosphere* **1996**, *32*, 1669-1679.
23. Rezaei Gomari, K. A.; Denoyel, R.; Hamouda, A. A. *J. Colloid Interface Sci.* **2006**, *297*, 470-479.
24. Zou, L.; Han, B.; Yan, H.; Kasperski, K. L.; Xu, Y.; Hepler, L. G. *J. Colloid Interface Sci.* **1997**, *190*, 472-475.
25. Janfada, A.; Headley, J. V.; Peru, K. M.; Barbour, S. L. *J. Environ. Sci. Health, Part A: Toxic/Hazard. Subst. Environ. Eng.* **2006**, *41*, 985-997.
26. Peng, J.; Headley, J. V.; Barbour, S. L. *Can. Geotech. J.* **2002**, *39*, 1419-1426.
27. Frank, R. A.; Kavanagh, R.; Burnison, B. K.; Headley, J. V.; Peru, K. M.; Der Kraak, G. V.; Solomon, K. R. *Chemosphere* **2006**, *64*, 1346-1352.
28. Saab, J.; Mokbel, I.; Razzouk, A. C.; Ainous, N.; Zydowicz, N.; Jose, J. *Energ. Fuel.* **2005**, *19*, 525-531.
29. Peng, H.; Volchek, K.; MacKinnon, M.; Wong, W. P.; Brown, C. E. *Desalination* **2004**, *170*, 137-150.
30. Herman, D.; Fedorak, P. M.; MacKinnon, M. D.; Costerton, J. W. *Can. J. Microbiol.* **1994**, *40*, 467-477.
31. Biryukova, O. V.; Fedorak, P. M.; Quideau, S. A. *Chemosphere* **2007**, *67*, 2058-2064.
32. Scott, A. C.; Zubot, W.; MacKinnon, M. D.; Smith, D. W.; Fedorak, P. M. *Chemosphere* **2008**, *71*, 156-160.
33. Deriszadeh, A.; Harding, T. G.; Husein, M. M. *J. Membr. Sci.* **2009**, *326*, 161-167.
34. Spitzer, J. J.; Heerze, L. D. *Can. J. Chem.* **1983**, *61*, 1067-1070.
35. Headley, J. V.; Du, J.-L.; Peru, K. M.; McMartin, D. W. *J. Environ. Sci. Health, Part A: Toxic/Hazard. Subst. Environ. Eng.* **2009**, *44*, 591 - 597.

36. Scott, A. C.; Mackinnon, M. D.; Fedorak, P. M. *Environ. Sci. Technol.* **2005**, *39*, 8388-8394.
37. Wilson, L. D.; Verrall, R. E. *Langmuir* **1998**, *14*, 4710-4717.
38. Wilson, L. D.; Verrall, R. E. *Can. J. Chem.* **1998**, *76*, 25-34.
39. Siimer, E.; Kurvits, M.; Kostner, A. *Thermochim. Acta* **1987**, *116*, 249-256.
40. Tanaka, K.; Mori, M.; Xu, Q.; Helaleh, M. I. H.; Ikedo, M.; Taoda, H.; Hu, W.; Hasebe, K.; Fritz, J. S.; Haddad, P. R. *J. Chromatogr., A* **2003**, *997*, 127-132.
41. Eftink, M. R.; Andy, M. L.; Bystrom, K.; Perlmutter, H. D.; Kristol, D. S. *J. Am. Chem. Soc.* **1989**, *111*, 6765-6772.
42. Wilson, L. D.; Siddall, S. R.; Verrall, R. E. *Can. J. Chem.* **1997**, *75*, 927-933.
43. Szente, L.; Szejtli, J.; Szeman, J.; Kato, L. *J. Inclusion Phenom.* **1993**, *16*, 339-354.
44. Szejtli, J. *Pure Appl. Chem.* **2004**, *76*, 1825-1845.
45. Szejtli, J. *Chem. Rev.* **1998**, *98*, 1743-1754.
46. Szejtli, J. *Cyclodextrin Technology*; Eds.; Reidel, D.; Nijhoff. M.; Junk. W. Kluwer Academic Publishers: Dordrecht, The Netherlands, 1988.
47. *Cyclodextrin Chemistry*; Bender, M. L.; Komiyama, M., Eds.; Springer-Verlag: Berlin, Germany, 1978.
48. Fujiwara, T.; Tanaka, N.; Hamada, K.; Kobayashi, S. *Chem. Lett.* **1989**, *7*, 1131-1134.
49. Miyazawa, I.; Ueda, H.; Nagase, H.; Endo, T.; Kobayashi, S.; Nagai, T. *Eur. J. Pharm. Sci.* **1995**, *3*, 153-162.
50. Endo, T.; Ueda, H.; Kobayashi, S.; Nagai, T. *Carbohydr. Res.* **1995**, *269*, 369-373.
51. Wenz, G. *Angew. Chem. Int. Ed. Engl* **1994**, *33*, 803-822.
52. Wenz, G. *Recognition of Monomers and Polymers by Cyclodextrins*; Springer: Berlin, Germany, 2009; Vol. 222.
53. Lehn, J.-M. *Supramolecular Chemistry: Concepts and Perspectives.*; VCH: Weinheim, Germany, 1995.
54. Ciferri, A. *Supramolecular Polymers*; Ed.; Marcel Dekker: New York, 2000.

55. Buckler, S. A.; Martel, R. F.; Moshy, R. J.; Insolubilized Schardinger Dextrins, Ed.; American Machine and Foundry Co, 1969; Vol. US 3472835 19691014, pp 3.
56. Mocanu, G. *J. Bioact. Compat. Pol.* **2001**, *16*, 315-342.
57. Kutner, W. *J. Inclusion Phenom.* **1992**, *13*, 257-265.
58. Harada, A.; Hashidzume, A.; Takashima, Y. *Cyclodextrin-based supramolecular polymers*; Springer, 2006; Vol. 201.
59. Crini, G.; Bertini, S.; Torri, G.; Naggi, A.; Sforzini, D.; Vecchi, C.; Janus, L.; Lekchiri, Y.; Morcellet, M. *J. Appl. Polym. Sci.* **1998**, *68*, 1973-1978.
60. Asanuma, H.; Kakazu, M.; Shibata, M.; Hishiya, T.; Komiyama, M. *Supramol. Sci.* **1998**, *5*, 417-421.
61. Asanuma, H.; Kakazu, M.; Shibata, M.; Hishiya, T.; Komiyama, M. *Chem. Commun. (Cambridge, U.K.)* **1997**, *20*, 1971-1972.
62. Shi, X. Y.; Zhang, Y. Q.; Han, J. H.; Fu, R. N. *Chromatographia* **2000**, *52*, 200-204.
63. Harada, A.; Furue, M.; Nozakura, S. *Macromolecules* **1976**, *9*, 701-704.
64. Harada, A.; Furue, M.; Nozakura, S. *Macromolecules* **1976**, *9*, 705-710.
65. Mayr, B.; Sinner, F.; Buchmeiser, M. R. *J. Chromatogr., A* **2001**, *907*, 47-56.
66. David, C.; Millot, M. C.; Sebille, B. *J. Chromatogr., B: Biomed. Life Sci. & Appl.* **2001**, *753*, 93-99.
67. Jingwu, K.; Wistuba, D.; Schurig, V. *Electrophoresis* **2002**, *23*, 1116-1120.
68. Mayr, B.; Schottenberger, H.; Elsner, O.; Buchmeiser, M. R. *J. Chromatogr., A* **2002**, *973*, 115-122.
69. Ramírez, H. L.; Valdivia, A.; Cao, R.; Torres-Labandeira, J. J.; Fragoso, A.; Villalonga, R. *Bioorg. Med. Chem. Lett.* **2006**, *16*, 1499-1501.
70. Sreenivasan, K. *Polym. Int.* **1997**, *42*, 22-24.
71. Fujimura, K.; Ueda, T.; Ando, T. *Anal. Chem.* **1983**, *55*, 446-450.
72. Hayakawa, T.; Yamada, T.; Hidaka, S.; Yamagishi, M.; Takeda, K.; Toda, F. *Polym. Prepr. (Am. Chem. Soc., Div. Polym. Chem.)* **1979**, *20*, 530-531.
73. Mizobuchi, Y. *J. Chromatogr., A* **1980**, *194*, 153-161.
74. Mizobuchi, Y. *J. Chromatogr., A* **1981**, *208*, 35-40.

75. Hirai, H. *J. Inclusion Phenom.* **1984**, *2*, 655-660.
76. Li, D.; Ma, M. *Clean Technol. Environ. Policy* **2000**, *2*, 112-116.
77. Fujimura, K.; Ueda, T.; Kitagawa, M.; Takayanagi, H.; Ando, T. *Anal. Chem.* **1986**, *58*, 2668-2674.
78. Connors, K. A. *Chem. Rev.* **1997**, *97*, 1325-1358.
79. Schardinger, F. *Centr. Bakt. Parasitenk.* **1911**, *29*, 188-197.
80. Freudenberg, K.; Schaaf, E.; Dumpert, G.; Ploetz, T. *Naturwissenschaften* **1939**, *27*, 850-853.
81. Rekharsky, M. V.; Inoue, Y. *Chem. Rev.* **1998**, *98*, 1875-1918.
82. Hybl, A.; Rundle, R. E.; Williams, D. E. *J. Am. Chem. Soc.* **1965**, *87*, 2779-2788.
83. Demarco, P. V.; Thakkar, A. L. *J. Chem. Soc., Chem. Commun.* **1970**, *1*, 2-4.
84. Tabushi, I.; Kuroda, Y.; Mizutani, T. *Tetrahedron* **1984**, *40*, 545-552.
85. Cooper, A.; MacNicol, D. D. *J. Chem. Soc., Perkin Trans. 2* **1978**, *8*, 760-763.
86. Harata, K.; Tsuda, K.; Uekama, K.; Otagiri, M.; Hirayama, F. *J. Inclusion Phenom.* **1988**, *6*, 135-142.
87. Harrison, J.; Eftink, M. R. *Biopolymers* **1982**, *21*, 1153-1166.
88. Liu, L.; Guo, Q.-X. *J. Inclusion Phenom. Macrocyclic Chem.* **2002**, *42*, 1-14.
89. Nakajima, T.; Sunagawa, M.; Hirohashi, T.; Fujioka, K. *Chem. Pharm. Bull.* **1984**, *32*, 383-400.
90. Nishijo, J.; Nagai, M. *J. Pharm. Sci.* **1991**, *80*, 58-62.
91. Tabushi, I.; Kiyosuke, Y.; Sugimoto, T.; Yamamura, K. *J. Am. Chem. Soc.* **1978**, *100*, 916-919.
92. Takagi, S.; Maeda, M. *J. Inclusion Phenom.* **1984**, *2*, 775-780.
93. Li, S.; Purdy, W. C. *Chem. Rev.* **1992**, *92*, 1457-1470.
94. Saenger, W. *Angew. Chem. Int. Ed. Engl* **1980**, *19*, 344-362.
95. Weickenmeier, M.; Wenz, G. *Macromol. Rapid Commun.* **1996**, *17*, 731-736.
96. Crini, G. *Bioresour. Technol.* **2003**, *90*, 193-198.
97. Ozmen, E. Y.; Sezgin, M.; Yilmaz, A.; Yilmaz, M. *Bioresour. Technol.* **2008**, *99*, 526-531.
98. Shao, Y.; Martel, B.; Morcellet, M.; Weltrowski, M.; Crini, G. *J. Inclusion Phenom. Macrocyclic Chem.* **1996**, *25*, 209-212.

99. García-Zubiri, Í. X.; González-Gaitano, G.; Isasi, J. R. *J. Colloid Interface Sci.* **2007**, *307*, 64-70.
100. Crini, G. *Prog. Polym. Sci.* **2005**, *30*, 38-70.
101. Furue, M.; Harada, A.; Nozakura, S. *J. Polym. Sci. Polym. Lett.* **1975**, *13*, 357-360.
102. Fenyvesi, E. *J. Inclusion Phenom.* **1988**, *6*, 537-545.
103. Sun, Z.-Y.; Cao, G.-P.; Lv, H.; Zhao, L.; Liu, T.; Montastruc, L.; Iordan, N. *J. Appl. Polym. Sci.* **2009**, *114*, 3882-3888.
104. Lee, K.-P.; Choi, S.-H.; Ryu, E.-N.; Ryoo, J. J.; Park, J. H.; Kim, Y.; Hyun, M. H. *Anal. Sci.* **2002**, *18*, 31-34.
105. Bhaskar, M.; Aruna, P.; Ganesh Jeevan, R. J.; Radhakrishnan, G. *Anal. Chim. Acta* **2004**, *509*, 39-45.
106. Janus, L.; Crini, G.; El-Rezzi, V.; Morcellet, M.; Cambiaghi, A.; Torri, G.; Naggi, A.; Vecchi, C. *React. Funct. Polym.* **1999**, *42*, 173-180.
107. Topchieva, I. N.; Kalashnikov, F. A.; Spiridonov, V. V.; Mel'nikov, A. B.; Polushina, G. E.; Lezov, A. V. *Dokl. Chem.* **2003**, *390*, 115-118.
108. Wintgens, V.; Amiel, C. *Langmuir* **2005**, *21*, 11455-11461.
109. Vélaz, I.; Isasi, J.; Sánchez, M.; Uzqueda, M.; Ponchel, G. *J. Inclusion Phenom. Macrocyclic Chem.* **2007**, *57*, 65-68.
110. Burckbuchler, V.; Wintgens, V. r.; Leborgne, C.; Lecomte, S.; Leygue, N.; Scherman, D.; Kichler, A.; Amiel, C. *Bioconjugate Chem.* **2008**, *19*, 2311-2320.
111. de Rossi, R. H.; Silva, O. F.; Vico, R. V.; Gonzalez, C. J. *Pure Appl. Chem.* **2009**, *81*, 755-765.
112. de Bergamasco, R.; Zanin, G.; de Moraes, F. *J. Inclusion Phenom. Macrocyclic Chem.* **2007**, *57*, 75-78.
113. Fontananova, E.; Di Profio, G.; Curcio, E.; Giorno, L.; Drioli, E. *J. Inclusion Phenom. Macrocyclic Chem.* **2007**, *57*, 537-543.
114. Uyar, T.; Havelund, R.; Nur, Y.; Hacaloglu, J.; Besenbacher, F.; Kingshott, P. *J. Membr. Sci.* **2009**, *332*, 129-137.
115. Buvari, A. *J. Inclusion Phenom.* **1983**, *1*, 151-157.
116. Taguchi, K. *J. Am. Chem. Soc.* **1986**, *108*, 2705-2709.

117. Georgiou, M. E.; Georgiou, C. A.; Koupparis, M. A. *Anal. Chem.* **1995**, *67*, 114-123.
118. Buvari, A.; Barcza, L. *Inorg. Chim. Acta* **1979**, *33*, L179-L180.
119. Selvidge, L.; Eftink, M. R. *Anal. Biochem.* **1986**, *154*, 400-408.
120. Buvari, A.; Barcza, L.; Kajtar, M. *J. Chem. Soc., Perkin Trans. 2* **1988**, *1972-1999*, 1687-1690.
121. Sasaki, K. J.; Christian, S. D.; Tucker, E. E. *Fluid Phase Equilib.* **1989**, *49*, 281-289.
122. Gray, J. E.; MacLean, S. A.; Reinsborough, V. C. *Aust. J. Chem.* **1995**, *48*, 551-556.
123. Tutaj, B.; Kasprzyk, A.; Czapkiewicz, J. *J. Inclusion Phenom. Macrocyclic Chem.* **2003**, *47*, 133-136.
124. Thatiparti, T. R.; Recum, H. A. v. *Macromol. Biosci.* **2010**, *10*, 82-90.
125. Romo, A.; Peñas, F. J.; Isasi, J. R.; García-Zubiri, I. X.; González-Gaitano, G. *React. Funct. Polym.* **2008**, *68*, 406-413.
126. Li, D.; Ma, M. *Chemtech* **1999**, *29*, 31-37.
127. Hishiya, T.; Shibata, M.; Kakazu, M.; Asanuma, H.; Komiyama, M. *Macromolecules* **1999**, *32*, 2265-2269.
128. Hishiya, T.; Asanuma, H.; Komiyama, M. *J. Am. Chem. Soc.* **2002**, *124*, 570-575.
129. Chen, L.; Zhu, X.; Yan, D.; He, X. *Polym. Prepr. (Am. Chem. Soc., Div. Polym. Chem.)* **2003**, *44*, 669-670.
130. Yang, C.; Ni, X.; Li, J. *J. Mater. Chem.* **2009**, *19*, 3755-3763.
131. Tan, Y.; Hu, A.; Xia, L.; You, T.; Cao, J. *J. Appl. Polym. Sci.* **2009**, *113*, 1811-1815.
132. Shibanai, I.; Horikoshi, K.; Kato, T.; Crosslinking Agents and Process for their Preparation, Ed. World Intellectual Property Organization, 1985; Patent No. WO/1985/003303.
133. Boeglin, N.; Pizzi, A.; Masson, D. *Holz als Roh- und Werkstoff* **1995**, *53*, 354.
134. Shaw, P. E.; Buslig, B. S. *J. Agric. Food Chem.* **1986**, *34*, 837-840.
135. Binello, A.; Robaldo, B.; Barge, A.; Cavalli, R.; Cravotto, G. *J. Appl. Polym. Sci.* **2008**, *107*, 2549-2557.

136. Sciban, M.; Klasnja, M.; Skrbic, B. *Wood Sci. Technol.* **2006**, *40*, 217-227.
137. Shaw, P. E.; Wilson, C. W. *J. Food Sci.* **1983**, *48*, 646-647.
138. Ujhazy, A.; J, S. *Gordian* **1989**, *89*, 43-45.
139. Warner-Schmid, D.; Tang, Y.; Armstrong, D. W. *J. Liq. Chromatogr.* **1994**, *17*, 1721-1735.
140. Murai, S.; Imajo, S.; Maki, Y.; Takahashi, K.; Hattori, K. *J. Colloid Interface Sci.* **1996**, *183*, 118-123.
141. Martel, B.; Thuaut, P. L.; Bertini, S.; Crini, G.; Bacquet, M.; Torri, G.; Morcellet, M. *J. Appl. Polym. Sci.* **2002**, *85*, 1771-1778.
142. Vienken, J. *Int. J. Artif. Organs* **2002**, *25*, 470-479.
143. Janos, P. *Environ. Sci. Technol.* **2003**, *37*, 5792-5798.
144. Chiu, S.-H.; Chung, T.-W.; Giridhar, R.; Wu, W.-T. *Food Res. Int.* **2004**, *37*, 217-223.
145. Sciban, M.; Klašnja, M. *Eur. J. Wood Wood Prod.* **2004**, *62*, 69-73.
146. Jing, C.; Liu, S.; Patel, M.; Meng, X. *Environ. Sci. Technol.* **2005**, *39*, 5481-5487.
147. Sim Bean, L.; Yook Heng, L.; Yamin, B. M.; Ahmad, M. *Thin Solid Films* **2005**, *477*, 104-110.
148. Crini, G. *Biores. Tech.* **2006**, *97*, 1061-1085.
149. Yamasaki, H.; Makihata, Y.; Fukunaga, K. *J. Chem. Technol. Biotechnol.* **2006**, *81*, 1271-1276.
150. Chen, C.-Y.; Chen, C.-C.; Chung, Y.-C. *Biores. Tech.* **2007**, *98*, 2578-2583.
151. Kida, T.; Nakano, T.; Fujino, Y.; Matsumura, C.; Miyawaki, K.; Kato, E.; Akashi, M. *Anal. Chem.* **2007**, *80*, 317-320.
152. Mhlanga, S. D.; Mamba, B. B.; Krause, R. W.; Malefetse, T. J. *J. Chem. Technol. Biotechnol.* **2007**, *82*, 382-388.
153. Vamvakaki, V.; Chaniotakis, N. A. *Biosens. Bioelectron.* **2007**, *22*, 2650-2655.
154. Crini, G.; Badot, P.-M. *Prog. Polym. Sci.* **2008**, *33*, 399-447.
155. Hicks, J. C.; Drese, J. H.; Fauth, D. J.; Gray, M. L.; Qi, G.; Jones, C. W. *J. Am. Chem. Soc.* **2008**, *130*, 2902-2903.
156. Sciban, M.; Klasnja, M.; Skrbic, B. *Desalination* **2008**, *229*, 170-180.

157. Yamasaki, H.; Makihata, Y.; Fukunaga, K. *J. Chem. Technol. Biotechnol.* **2008**, *83*, 991-997.
158. Yang, Y.; Long, Y.; Cao, Q.; Li, K.; Liu, F. *Anal. Chim. Acta* **2008**, *606*, 92-97.
159. Asouhidou, D. D.; Triantafyllidis, K. S.; Lazaridis, N. K.; Matis, K. A. *Colloids Surf., A* **2009**, *346*, 83-90.
160. Li, J.-M.; Meng, X.-G.; Hu, C.-W.; Du, J. *Biores. Tech.* **2009**, *100*, 1168-1173.
161. Li, N.; Mei, Z.; Chen, S.-M. *Fresenius Environ. Bull.* **2009**, *18*, 2249-2253.
162. Krause, R. W. M.; Mamba, B. B.; Dlamini, L. N.; Durbach, S. H. *J Nanopart Res* **2010**, *12*, 449-456.
163. Ujhazy, A.; Szejtli, J. *Gordian* **1989**, *89*, 43-45.
164. Dombrow, B. A. *Polyurethanes*; Reinhold Pub. Corp: New York; pp 157.
165. Saunders, J. H.; Frisch, K. C. *Polyurethanes: Chemistry and Technology. Pt. 1: Chemistry.*; Interscience Pubs: New York, 1962; pp 157.
166. Appell, M.; Jackson, M. *J. Inclusion Phenom. Macrocyclic Chem.* **2010**; In Press.
167. Mamba, B.; Krause, R.; Malefetse, T.; Nxumalo, E. *Environ. Chem. Lett.* **2007**, 5, 79-84.
168. Mamba, B. B.; Krause, R. W.; Matsebula, B.; Haarhoff, *J. Water SA*. **2009**, 35, 121-127.
169. Ng, S. M.; Narayanaswamy, R. *Sensor. Actuat. B: Chem.* **2009**, 139, 156-165.
170. Yilmaz, A.; Yilmaz, E.; Yilmaz, M.; Bartsch, R. A. *Dyes & Pigm.* **2007**, 74, 54-59.
171. Tang, S.; Kong, L.; Ou, J.; Liu, Y.; Li, X.; Zou, H. *J. Mol. Recognit.* **2006**, 19, 39-48.
172. Jessie Lue, S.; Peng, S. H. *J. Membr. Sci.* **2003**, *222*, 203-217.
173. Ozmen, E. Y.; Sirit, A.; Yilmaz, M. *Journal of Macromolecular Science, Part A: Pure and Applied Chemistry* **2007**, *44*, 167 - 173.
174. Nayak, D. P.; Kotha, A. M.; Yemul, O. S.; Ponrathnam, S.; Raman, R. C. *Biomacromolecules* **2001**, *2*, 1116-1123.
175. Harada, A.; Takahashi, S. *J. Inclusion Phenom.* **1984**, *2*, 791-798.
176. Sakuraba, H.; Ishizaki, H.; Tanaka, Y.; Shimizu, T. *J. Inclusion Phenom.* **1987**, *5*, 449-458.

177. Sing, K. S. W. *Pure Appl. Chem.* **1985**, 57, 603-619.
178. Langmuir, I. *J. Am. Chem. Soc.* **1918**, 40, 1361-1402.
179. Kruk, M.; Jaroniec, M. *Chem. Mater.* **2001**, 13, 3169-3183.
180. Barrett, E. P.; Joyner, L. G.; Halenda, P. P. *J. Am. Chem. Soc.* **1951**, 73, 373-380.
181. Marczewski, A. W. A Practical Guide to Isotherms of Adsorption on Heterogeneous Surfaces. http://adsorption.org/awm/ads/meso/BJH.htm. 2002 (accessed 20th October 2010).
182. Giles, C. H.; MacEwan, T. H.; Nakhwa, S. N.; Smith, D. *J. Chem. Soc.* **1960**, 3973-3993.
183. Giles, C. H.; D'Silva, A. P.; Trivedi, A. S. *J. Appl. Chem.* **1970**, *20*, 37-41.
184. Inel, O.; Tumsek, F. *Turk. J. Chem.* **2000**, *24*, 9-19.
185. Giles, C. H.; Nakhwa, S. N. *J. Appl. Chem.* **1962**, *12*, 266-273.
186. Giles, C. H.; Tolia, A. H. *J. Appl. Chem.* **1964**, *14*, 186-195.
187. Giles, C. H.; D'Silva, A. P.; Easton, I. A. *J. Colloid Interface Sci.* **1974**, *47*, 766-778.
188. Padday, J. F. In *Surface Area Determination, Proc. Int. Symp.*; Everett, D. H., Ed.; Butterworth: Wealdstone/Middlesex, UK, 1970, p 331-340.
189. Ganem, B.; Li, Y. T.; Henion, J. D. *J. Am. Chem. Soc.* **1991**, *113*, 6294-6296.
190. Smith, R. D.; Light-Wahl, K. J. *Biol. Mass Spectrom.* **1993**, *22*, 493-501.
191. Cunniff, J. B.; Vouros, P. *J. Am. Soc. Mass Spectrom.* **1995**, *6*, 437-447.
192. Danikiewicz, W. *Mass spectrometry of CyDs and their complexes*; Wiley-VCH Verlag GmbH & Co. KGaA: Weinheim, Germany, 2008; Vol. 257.
193. Barbara, J. E.; Eyler, J. R.; Powell, D. H. *Rapid Commun. Mass Spectrom.* **2008**, *22*, 4121-4128.
194. Kralj, B.; Scaronmidovnik, A.; Jo; zcaron; Kobe, e. *Rapid Commun. Mass Spectrom.* **2009**, *23*, 171-180.
195. Galaverna, G.; Corradini, R.; Dossena, A.; Marchelli, R. *Electrophoresis* **1999**, *20*, 2619-2629.
196. Cai, Y.; Tarr, M. A.; Xu, G.; Yalcin, T.; Cole, R. B. *J. Am. Soc. Mass Spectrom.* **2003**, *14*, 449-459.

197. Gabelica, V.; Galic, N.; Rosu, F.; Houssier, C.; Pauw, E. D. *J. Mass Spectrom.* **2003**, *38*, 491-501.

198. Headley, J. V.; Peru, K. M.; Barrow, M. P. *Mass Spectrom. Rev.* **2009**, *28*, 121-134.

199. Martin, J. W.; Han, X.; Peru, K. M.; Headley, J. V. *Rapid Commun. Mass Spectrom.* **2008**, *22*, 1919-1924.

200. Richardson, S. D. *Anal. Chem.* **2008**, *80*, 4373-4402.

201. Coteron, J. M.; Vicent, C.; Bosso, C.; Penades, S. *J. Am. Chem. Soc.* **1993**, *115*, 10066-10076.

202. Kalenius, E.; Koivukorpi, J.; Kolehmainen, E.; Vainiotalo, P. *Eur. J. Org. Chem.* **2010**, *2010*, 1052-1058.

203. Junquera, E.; Tardajos, G.; Aicart, E. *Langmuir* **1993**, *9*, 1213-1219.

204. Saint Aman, E.; Serve, D. *J. Colloid Interface Sci.* **1990**, *138*, 365-375.

205. Dharmawardana, U. R.; Christian, S. D.; Tucker, E. E.; Taylor, R. W.; Scamehorn, J. F. *Langmuir* **1993**, *9*, 2258-2263.

206. Wan Yunus, W. M. Z.; Taylor, J.; Bloor, D. M.; Hall, D. G.; Wyn-Jones, E. *J. Phys. Chem.* **1992**, *96*, 8979-8982.

207. Mwakibete, H.; Cristantino, R.; Bloor, D. M.; Wyn-Jones, E.; Holzwarth, J. F. *Langmuir* **1995**, *11*, 57-60.

208. Selvidge, L. A.; Eftink, M. R. *Anal. Biochem.* **1986**, *154*, 400-408.

209. Funasaki, N.; Yodo, H.; Hada, S.; Neya, S. *Bull. Chem. Soc. Jap.* **1992**, *65*, 1323-1330.

210. Gelb, R. I.; Schwartz, L. M.; Cardelino, B.; Laufer, D. A. *Anal. Biochem.* **1980**, *103*, 362-368.

211. Fourmentin, S.; Surpateanu, G.; Blach, P.; Landy, D.; Decock, P.; Surpateanu, G. *J. Inclusion Phenom. Macrocyclic Chem.* **2006**, *55*, 263-269.

212. Meier, M. M.; Bordignon Luiz, M. T.; Farmer, P. J.; Szpoganicz, B. *J. Inclusion Phenom. Macrocyclic Chem.* **2001**, *40*, 291-295.

213. Landy, D.; Fourmentin, S.; Salome, M.; Surpateanu, G. *J. Inclusion Phenom. Macrocyclic Chem.* **2000**, *38*, 187-198.

214. Suzuki, I.; Yamauchi, A. *J. Inclusion Phenom. Macrocyclic Chem.* **2006**, *54*, 193-200.
215. Brunauer, S.; Emmett, P. H.; Teller, E. *J. Am. Chem. Soc.* **1938**, *60*, 309-319.
216. Freundlich, H. M. F. *J. Phys. Chem.* **1906**, *57A*, 385-470.
217. Sips, R. *J. Chem. Phys.* **1948**, *16*, 490-495.
218. Jandera, P.; Komers, D. *J. Chromatogr., A* **1997**, *762*, 3-13.
219. Choy, K. K. H.; Porter, J. F.; McKay, G. *J. Chem. Eng. Data* **2000**, *45*, 575-584.
220. He, B.; Zhao, X. *React. Polym.* **1992**, *18*, 229-235.
221. Wiedenhof, N.; Trieling, R. G. *Starch* **1971**, *23*, 129-132.
222. Shao, Y.; Martel, B.; Morcellet, M.; Weltrowski, M.; Crini, G. *J. Inclusion Phenom.* **1996**, 25, 209-212.
223. Szente, L.; Fenyvesi, É.; Szejtli, J. *Environ. Sci. Technol.* **1999**, *33*, 4495-4498.
224. Huq, R.; Mercier, L.; Kooyman, P. J. *Chem. Mater.* **2001**, *13*, 4512-4519.
225. Bibby, A.; Mercier, L. *Green Chem.* **2003**, *5*, 15-19.
226. Liu, C.; Lambert, J. B.; Fu, L. *J. Org. Chem.* **2004**, *69*, 2213-2216.
227. Liu, C.; Naismith, N.; Economy, J. *J. Chromatogr., A* **2004**, *1036*, 113-118.
228. OSTRF; Oil Sands Tailing Research Facility Edmonton, AB, 2009; http://www.ostrf.com/research (accessed 13th March 2010).

CHAPTER 2

PUBLICATION 1

Description

The following is a verbatim copy of an article that was published in November of 2010 in the Carbohydrate Research (*Carbohydr. Res.:* **2011**, *346(2)*, 210-229). This paper describes the systematic synthesis of β-CD PUs and its characterization.

Authors' Contribution

I carried out all the experimental work (i.e. synthesis and characterization of the copolymers) except for the solid state ^{13}C NMR analysis which was conducted by Abdalla Karoyo. This work was supervised by Dr. Wilson and Dr. Headley. I wrote the first draft of the manuscript with extensive editing by each supervisor prior to submission for publication. Written permission was obtained from all contributing authors to include this material in this thesis.

Relation of Chapter 2 (Publication 1) to the Overall Objectives of this Project

As mentioned in the introduction, the first research objective was to design and characterize β-CD PUs. This chapter covers the systematic design of these materials through variation of the linker types and co-monomer ratios (crosslinking density). This strategy is anticipated to affect the physicochemical properties of these copolymers in a controlled fashion. The manuscript describes the characterization of the materials with various techniques such as IR, NMR, EA and TGA. A noteworthy contribution is the

illustration of TGA as a potential analytical method for determination of the relative co-monomer composition.

Graphical Abstract

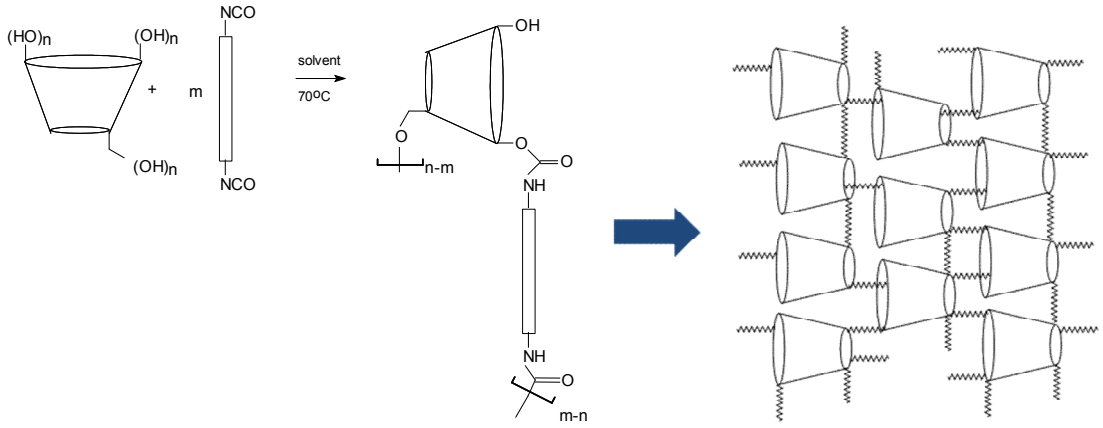

Research Highlights

A series of novel macrocycle-based polyurethanes were designed from β-CD and diisocyanate cross linkers with variable molecular structure and tunable physicochemical properties. Characterization of the co-monomer composition was achieved using ^{13}C solids and $^{13}C/^{1}H$ solution NMR spectroscopy, FT-IR spectroscopy, TGA, and CHN elemental analyses. Optimal copolymer design was achieved based on an estimated upper limit of the β-CD:linker mole ratio (~1:6) whereas an independent determination of the optimal sorption properties for the co-monomer mole ratio in the range 1:1 - 1:3 was concluded. The results reported herein are anticipated to contribute to the further development of copolymers with improved sorption capacity and molecular recognition properties for a range of sorption-based applications.

2. Design and Characterization of Novel β-Cyclodextrin Based Copolymer Materials

Mohamed H. Mohamed,[§] Lee D. Wilson,[§] John V. Headley[¥]*

[§]Department of Chemistry, University of Saskatchewan, 110 Science Place, Saskatoon, Saskatchewan, S7N 5C9

[¥]Water Science and Technology Directorate, 11 Innovation Boulevard, Saskatoon, Saskatchewan, S7N 3H5

*Corresponding Author

Received 16 October 2010

2.1 Abstract

Reported herein are the systematic design and characterization of several novel polyurethane (PU) copolymers containing a macrocyclic porogen (β-Cyclodextrin; β-CD). These copolymers were synthesized from the reaction between β-CD with different types of diisocyanate linker molecules (*e.g.*, 1,6-hexamethylene diisocyanate (HDI), 4,4'-dicyclohexylmethane diisocyanate (CDI), 4,4'-diphenylmethane diisocyanate (MDI), 1,4-phenylene diisocyanate (PDI) and 1,5-naphthalene diisocyanate (NDI)) at variable synthetic conditions. The copolymers were characterized using: diffuse reflectance infrared Fourier transform spectroscopy (DRIFTS), solid state ^{13}C CP-MAS NMR, $^{1}H/^{13}C$ solution NMR spectroscopy, thermogravimetric analysis (TGA) and elemental analyses (CHN). The PU copolymers were generally insoluble in water and the optimal preparation of copolymer materials for sorption-based applications is for β-CD/linker

synthetic mole ratios from 1:1 to 1:3. The practical upper limit of the crosslink density (~ 1:7, β-CD/linker) depends on the steric bulk of the cross linker units.

2.2 Introduction

Cyclodextrin (CD) copolymer materials have a wide range of industrial applications because of their unique sorption properties.[1-4] The sustained interest in the research and application of CD-based copolymer materials is attributed, in part, to the ability of such copolymer materials to form host-guest complexes comparable to native CDs.[3,5-9] Technologies that that rely on the formation of inclusion complexes are wide ranging; and include for example, chemical separations, catalysis, molecular sieves, food processing, pharmaceutical excipients and cosmetics.[1,10-17] In particular, the ability to tune the inclusion properties of CD-based copolymers is an important parameter in materials research and design.

Previous reports have shown that polymeric β-CD materials may function as sorbents for the inclusion of organic molecules from aqueous solutions.[7-8] More recently[18], it was shown that the systematic variation of the copolymer structure enables tuning of the inclusion site accessibility. The ability to tune the copolymers is critical in cases where the copolymer sorption and molecular recognition involve the formation of CD/guest inclusion complexes.[19] Although, CD-based PU copolymers have been prepared previously,[7,18,20] the range of synthetic conditions was limited, as was the selection of diisocyanate crosslinkers investigated. The importance of co-monomer composition has been overlooked as evidenced by numerous studies which have employed arbitrary co-monomer ratios for the synthesis of β-CD copolymers.[7,21-23] For example, a common approach utilizes β-CD/co-monomer mole ratios ~ 1:7. Presumably,

this is based on the presence of seven primary hydroxyl groups with moderate reactivity. The use of bulky diisocyanate linkers with mole ratios that exceed 1:7 is considered problematic because of extensively crosslinked materials which have limited inclusion site accessibility of β-CD. The optimal design of CD-based copolymer sorbents takes into account the nature of the crosslink unit and the relative co-monomer ratios since these parameters will strongly affect the structure copolymer framework and its adsorption properties.

In this study, we report the synthesis and characterization of a novel series of β-CD-based copolymer PU materials. The β-CD copolymers contain diisocyanate co-monomers with variable aliphatic and aromatic molecular structure which vary according to their molecular size and conformational motility (*cf*. Figure 1.3 in Chapter 1). The copolymer sorbent frameworks have tunable adsorption properties since changes to the co-monomer ratios affect the surface areas, pore size distribution, mechanical properties and surface chemistry of the sorbent. The results of this research will contribute to the development of improved solid phase extraction materials with enhanced sorption and molecular recognition properties.[2,4,24]

2.3 Experimental

2.3.1 Materials

β-CD was purchased from VWR. 1,6-hexamethylene diisocyanate (HDI), 4,4'-dicyclohexylmethane diisocyanate (CDI), 4,4'-diphenylmethane diisocyanate (MDI), 1,4-phenylene diisocyanate (PDI), 1,5-naphthalene diisocyanate (NDI), dimethyl acetamide (DMA), anhydrous ethyl ether, potassium bromide, 4 Å (8-12 mesh) molecular sieves,

were purchased from Sigma Aldrich, except for NDI, which was obtained from TCI America. Deuterated dimethyl sulfoxide was obtained from Cambridge Isotope Laboratories, Inc. All materials were used as received unless specified otherwise.

2.3.2 Methods

2.3.2. 1 Synthesis of copolymer materials

The synthesis of CD-based polyurethane materials was adapted from previous work,[18,20] as outlined in the following procedure. DMA was dried with 4 Å (8-12 mesh) molecular sieves, (Aldrich). The ^{1}H NMR spectrum of DMA was recorded before and after the addition of molecular sieves, and the water content was estimated to be ~ 0.5%. 1:1 β-CD/diisocyanate copolymer was prepared with 3 mmol of dried β-CD by addition to a round bottom flask with stirring until dissolved in 10 mL of DMA, and followed by the addition of 9 mmol diisocyanate solution in 30 mL of DMA. The stirred mixture was heated at 68^{o}C for 24 hrs under argon. The final reaction mixture was cooled to room temperature and excess residual solvent removed through a rotoevaporator under vacuum (pressure = 1mbar). The addition of cold methanol (~ 0°C) to the gelled copolymer product was followed by filtration through Whatman no. 2 filters. The crude product was thoroughly washed in a Soxhlet extractor with refluxing methanol for 24 h to remove unreacted starting materials and low molecular weight oligomers. The final product was dried in a pistol dryer for 24 h, subsequently ground and then passed through a 40 mesh sieve to ensure a uniform particle size. A second cycle of washing in the Soxhlet extractor with refluxing anhydrous diethyl ether for 24 h was performed to ensure the removal of residual solvents and reagents. Prior to characterization, the copolymer was repeatedly dried, ground, and sieved, as outlined above.

2.3.2.2 Copolymer Characterization

IR spectra were obtained with a Bio-RAD FTS-40 instrument and samples were analyzed in reflectance mode. Copolymers were prepared by mixing ~5 mg with pure spectroscopic grade KBr (~150 mg) by grinding in a small mortar and pestle. DRIFT (Diffuse Reflectance Infrared Fourier Transform) spectra were recorded at room temperature with a resolution of 4 cm^{-1} over the range of 400-4000 cm^{-1}. Fifty scans were recorded and corrected against a background spectrum of pure KBr. The DRIFT spectra are reported as Kubelka-Munk units, while the IR spectra of neat HDI and CDI were obtained in transmittance mode using a sodium chloride liquid cell configuration.

The elemental content (w/w, %) of carbon (C), hydrogen (H), and nitrogen (N) was measured by a Perkin-Elmer 2400 CHN Elemental Analyzer with a detection limit of ±0.3%. The CHN results were uncorrected relative to the estimated water/solvent content.

^{1}H and ^{13}C solution state NMR was performed on a 500 MHz Brüker Avance NMR Spectrometer with an inverse triple resonance probe (TXI, 5mm). The solid state ^{13}C MAS (magic angle spinning) NMR spectra were obtained on a Varian Inova-500 operating at 125 MHz for ^{13}C. Samples were obtained with a MAS frequency of 16 kHz in 3.2 mm vespel rotors. All ^{13}C spectra were acquired under $^{1}H \rightarrow {}^{13}C$ CP (cross polarization) conditions with proton decoupling $\{^{1}H\}$, and were referenced externally to adamantane (δ 38.5 ppm) at 295 K.

Thermal decomposition of the copolymers was performed using a thermogravimetric analyzer, TGA (Q50 TA Instruments). Samples were heated in open

aluminum pans to 30^{o}C and allowed to equilibrate for 5 min before further heating to 500^{o}C at a scan rate of 5^{o}C per min.

2.4 Results and Discussion

2.4.1 Synthesis

The nomenclature of the copolymers is described according to the type of diisocyanate and the co-monomer mole ratio (β-CD:diisocyanate linker). The diisocyanates investigated include the following: 1,6-hexamethylene diisocyanate (HDI), 4,4'-dicyclohexylmethane diisocyanate (CDI), 4,4'-diphenylmethane diisocyanate (MDI), 1,4-phenylene diisocyanate (PDI) and 1,5-naphthalene diisocyanate (NDI). For example, the 1:3 β-CD:HDI copolymer designation used herein is denoted as HDI-X (X=3) where the molar quantity of β-CD is assumed to be unity relative to 3 moles of HDI.

The copolymers were prepared by the addition reaction between the primary or secondary hydroxyl groups of β-CD with a bifunctional diisocyanate crosslinker, as shown in Scheme 1.4 in Chapter 1. There are numerous hydroxyl groups in β-CD; seven primary and fourteen secondary hydroxyl groups, at the narrow and wide ends of the CD torus, respectively. The yield of the copolymer was observed to increase with greater diisocyanate mole ratio (X>1) relative to β-CD. In the case of the HDI-X copolymers, the product formed a gel phase at the 1:3, 1:6 and 1:9 mole ratios. The gellation time decreased with an increased crosslink density (X ≥ 3). The yields are 37 and 62 % for HDI-1 and HDI-2 copolymers, respectively, and the greater mole ratios afforded quantitative (~98-100 %) yields. Similar trends were observed for the CDI-X copolymers; however, the gellation time occurred more rapidly at lower mole ratios (i.e.

X=1). The yield of CDI-1 was 88%, whereas, CDI-2 and -3 were nearly quantitative. At the 1:9 mole ratio, the reaction was complete, as evidenced by rapid gel formation within an hour. During the solvent removal step, DMA was more difficult to remove at the higher crosslink densities. This observation may indicate the trapping of solvent within the mesopore copolymer framework. For the aromatic-based copolymers, the yield of MDI-based copolymer materials exceeded that for PDI than NDI. The yields for the copolymers with aromatic linkers are given as follows; MDI-1 (76%), MDI-2 (86%), MDI-3 (97%); PDI-1 (62%), PDI-2 (74%), PDI-3 (83%); and NDI-1 (31%), NDI-2 (46%) and NDI-3 (77%). The HDI and CDI-based copolymers were white in color, whereas, MDI- and PDI-based copolymers were a lightly cream colored, and NDI copolymers were light brown in appearance.

2.4.2 Characterization

2.4.2.1 IR

DRIFT spectroscopy was used to assess the spectral signatures of the functional groups in the products prepared according to Scheme 1.4 in Chapter 1. Figure 2.1a-e illustrate the DRIFT spectra for the starting materials; β-CD hydrate and the diisocyanate linkers (HDI, CDI, MDI, PDI and NDI), along with the corresponding copolymers. The IR spectra confirmed the identity of the copolymers and a noteworthy feature is the disappearance of the isocyanato group between 2500 and 2080 cm^{-1} and the co-appearance of the amide and carbonyl vibrational bands. The vibrational band of ν(N-H) appears ~ 3376 cm^{-1} and overlaps with the broad –OH band from β-CD hydrate.[25] The vibrational band for ν(C=O) is observed to vary between 1702-1666 cm^{-1}, as shown in

Table 2.1. The rotational/vibrational bands δ(N-H) + ν(C-N) range between 1549-1521 cm^{-1} for the aliphatic and aromatic diisocyanate linker units.[25] The relative peak area increases as X increases (*cf*. Table 2.1) and these results offer a semi-quantitative approach for assessing the relative copolymer composition which contain similar diisocyanate units. A comparison of the relative β-CD/diisocyanate mole ratio in the reaction mixture indicates that the IR results further support the formation of urethane bonds as X increases, as described by Scheme 1.4 in Chapter 1.

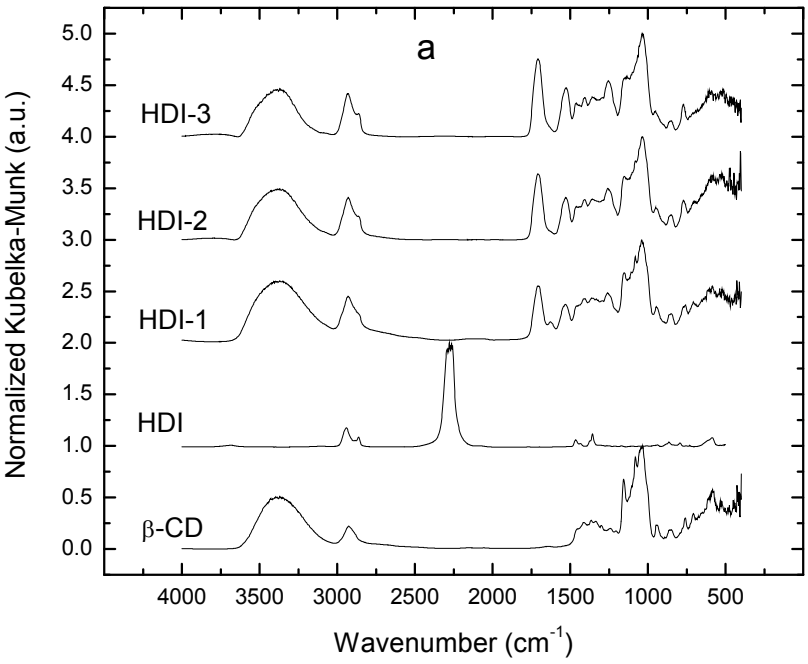

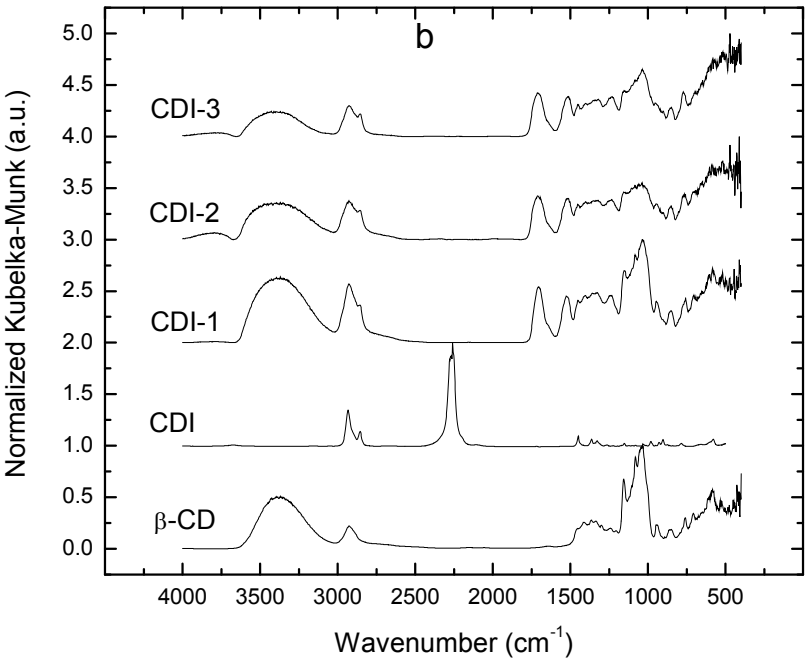
b
CDI-3
CDI-2
CDI-1
CDI
β-CD
Normalized Kubelka-Munk (a.u.)
Wavenumber (cm-1)
5.0
4.5
4.0
3.5
3.0
2.5
2.0
1.5
1.0
0.5
0.0
4000
3500
3000
2500
2000
1500
1000
500

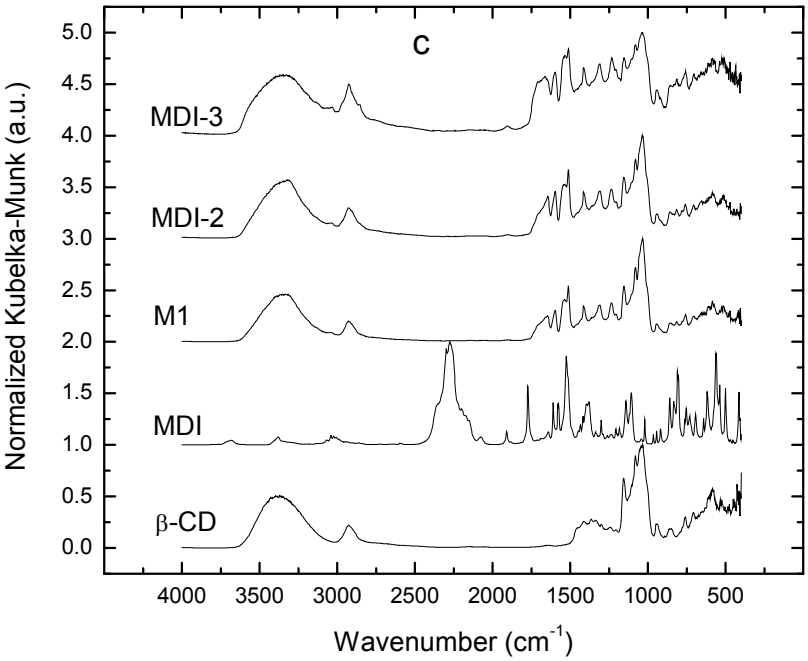
c
MDI-3
MDI-2
M1
MDI
β-CD
Normalized Kubelka-Munk (a.u.)
Wavenumber (cm-1)
5.0
4.5
4.0
3.5
3.0
2.5
2.0
1.5
1.0
0.5
0.0
4000
3500
3000
2500
2000
1500
1000
500

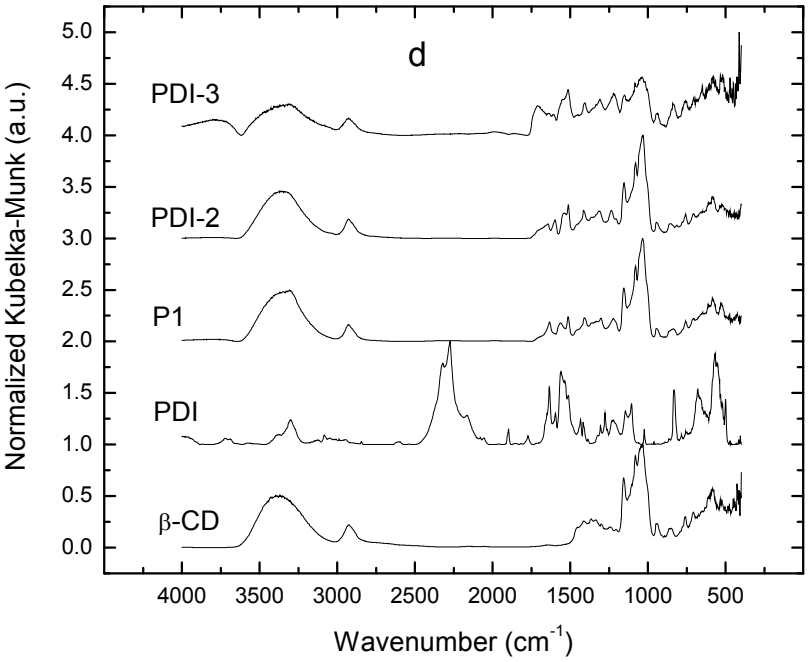
d
PDI-3
PDI-2
P1
PDI
β-CD
Normalized Kubelka-Munk (a.u.)
Wavenumber (cm-1)
5.0
4.5
4.0
3.5
3.0
2.5
2.0
1.5
1.0
0.5
0.0
4000
3500
3000
2500
2000
1500
1000
500

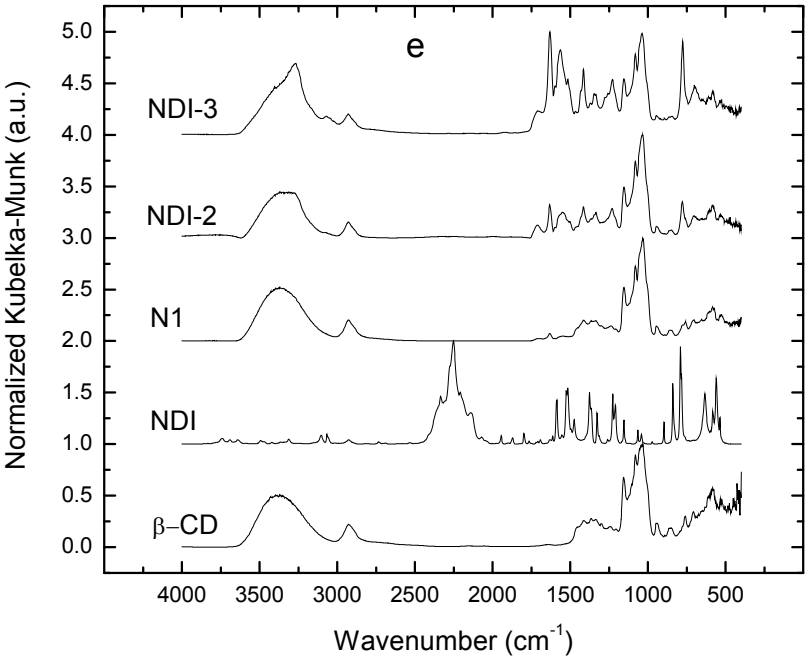
e
NDI-3
NDI-2
N1
NDI
β–CD
Normalized Kubelka-Munk (a.u.)
Wavenumber (cm-1)
5.0
4.5
4.0
3.5
3.0
2.5
2.0
1.5
1.0
0.5
0.0
4000
3500
3000
2500
2000
1500
1000
500

Figure 2.1a-e: IR of β-CD, diisocyanate linkers (HDI, CDI, MDI, PDI and NDI, respectively.) and their corresponding copolymers. The number designations (X=1-3) for the copolymers denote the synthetic mole ratio of each diisocyanate per 1 mole of β-CD.

Table 2.1. FT-IR C=O and C-N band assignments for each copolymer and their relative percent peak areas as bracketed terms. HDI-X, CDI-X, MDI-X, PDI-X and NDI-X where X= 1, 2, 3 for 1:1, 1:2, and 1:3 β-CD/diisocyanate monomer mole ratios, respectively.

Copolymer	Wavenumber (cm^{-1}), (% Peak Area)[α]	
	ν(C=O)	δ(N-H)+ν(C-N)[β]
HDI-1	1702 (7.1)	1543 (4.8)
HDI-2	1704 (8.2)	1542 (5.2)
HDI-3	1705 (13)	1539 (7.0)
CDI-1	1700 (5.9)	1521 (4.5)
CDI-2	1704 (6.9)	1522 (6.2)
CDI-3	1703 (7.6)	1524 (6.5)
MDI-1	1667 (4.8)	1538 (8.9)
MDI-2	1666 (5.7)	1538 (9.2)
MDI-3	1675 (6.8)	1537 (9.5)
PDI-1	1667 (1.7)	1549 (3.9)
PDI-2	1670 (2.7)	1539 (6.2)
PDI-3	1692 (5.7)	1533 (7.6)
NDI-1	1704 (0.30)	1549 (1.2)
NDI-2	1711 (0.39)	1549 (6.6)
NDI-3	1710 (1.8)	1554 (12)

[α]Area of total integrated peaks of the whole spectrum
[β]Yen & Cheng[25]

2.4.2.2 Elemental Analyses

CHN elemental microanalyses provided estimates of the linker composition since the N content originates solely from the diisocyanate co-monomers or residual solvent (*e.g.*, DMA) and generally increases as the relative mole ratio (X) increases (*cf.* Table 2.2). The increasing N content of copolymer materials with increasing X provides further support for the molecular identity of the copolymer products. Corrections due to residual water and/or solvent mixtures remaining within the copolymer framework were not applied because the relative amounts of residual solvents were not assessed. The overall total contribution of solvent varied from 0.1–6%, and in good agreement with the ^{1}H

NMR results where solvent signatures (i.e. DMA, methanol and water) were observed in the spectra (*cf*. section 2.4.2.3). Residual solvents are attributed to the occlusion of solvent within the copolymer framework during the crosslinking and/or purification stages. The presence of residual solvents were previously concluded[26] for an HDI-3 copolymer which showed a markedly different (i.e. 1:1.5) co-monomer ratio using a similar methodology. The calculated values for the elemental analyses in Table 2.2 for β-CD hydrate were corrected by accounting for its water content but those for the copolymers are uncorrected. In general, the content of C and N increase as expected; however, the content of H does not scale quantitatively as predicted by the theoretical copolymer stoichiometry. The slight differences between calculated and experimental values (CHN) can be related to the non-stoichiometric reaction efficiency as X increases, and the potentiality of homo- vs. hetero-polymerization of diisocyanates, as described analogously for β-CD/epichlorohydrin polymers.[27] According to Table 2.1, the overall increase in N content of the products provides reasonable agreement with the anticipated copolymer composition.

Table 2.2. Elemental Analyses (C, H, N) results for β-CD and copolymer materials; HDI-X, CDI-X, MDI-X, PDI-X and NDI-X where X= 1, 2, 3 for 1:1, 1:2, and 1:3 β-CD:diisocyanate co-monomer ratios, respectively.

Material	Theoretical (%)			Experimental (%)		
	C	H	N	C	H	N
β-CD	38.4	6.90	0.00	38.2	6.81	0.00
HDI-1	46.1	6.34	6.89	41.8	6.99	2.68
HDI-1	47.4	6.44	3.81	43.0	6.68	3.73
HDI-3	48.4	6.52	5.13	44.0	6.89	5.00
CDI-1	49.0	6.64	2.00	47.0	6.52	2.30
CDI-2	52.1	6.92	3.38	47.1	7.25	2.34
CDI-3	54.4	7.13	4.37	51.3	7.72	3.75
MDI-1	49.4	5.82	2.02	43.4	6.21	3.70
MDI-2	52.9	5.55	3.43	51.1	5.73	4.21
MDI-3	55.4	5.34	4.46	52.6	5.90	4.50
PDI-1	46.4	5.76	2.16	41.4	6.20	2.37
PDI-2	47.9	5.40	3.85	45.5	5.75	2.90
PDI-3	49.1	5.12	5.20	44.6	5.43	4.90
NDI-1	48.2	5.69	2.08	40.5	6.01	0.76
NDI-2	51.0	5.31	3.6	46.5	5.60	3.68
NDI-3	53.1	5.02	4.76	54.4	5.64	7.47

2.4.2.3 NMR

The integrated ^{1}H NMR line intensities in solution provide accurate quantitative information on the relative co-monomer composition for HDI-, CDI-, and MDI-based copolymers. The 1:1, 1:2 and 1:3 co-monomer ratios yielded products that were soluble in DMSO-d_6 at room temperature. In contrast, HDI-X and CDI-X (X= 6 and 9) copolymers, as well as the PDI-X and NDI-X copolymers, were relatively insoluble in DMSO-d_6. Figures 2.2 and 2.3 depict the solution ^{1}H NMR spectra for the HDI- and CDI-based copolymers, respectively. The key features are the broadening of the resonance lines. The NMR chemical shifts indicate the polymeric nature of the products relative to the pure co-monomers. The increased line broadening occurs as the linker content (X) of the copolymer increases. Furthermore, the δ values of the methylene

protons of the HDI linker were shifted upfield, as shown in Figure 2.2. Specifically, the α-CH_2 (adjacent to the isocyanato group) was shifted upfield from δ=3.36 to δ=1.40; the β-CH_2 was shifted upfield from δ=1.57 to δ=1.26 ppm, and the γ-CH_2 was shifted from δ=1.36 to δ=1.10 ppm. These upfield δ values are consistent with the formation of polyurethane copolymer framework, as described previously.[28-34] The integrated line intensity of the primary hydroxyl groups of β-CD at δ=5.6-5.8 ppm and the secondary hydroxyl groups at δ=4.4-4.5 ppm decrease as the linker mole content (X) increases. The chemical shift (δ~6.5-7.2 ppm) is assigned to NH, as described previously.[34] The DMA solvent was observed to have the following chemical shifts in the HDI-based copolymer; CH_3CO (δ=1.97 ppm), NCH_3 (δ=2.79 ppm) and NCH_3 (δ=2.95 ppm) whereas the reported δ values for the neat solvent are δ=1.96, 2.78 and 2.94 ppm, respectively.[35] Therefore, the DMA is occluded within the copolymer framework since the chemical shifts are largely unaffected by DMSO-d_6 and closely resemble values observed in neat DMA. The relative co-monomer content was estimated from the integration of the ^{1}H NMR lines of β-CD and the linker, respectively. The NMR lines were integrated by calibrating the H1 resonance line of β-CD (δ=4.7-4.8 ppm) to an area of 7 protons. The relative areas of the HDI protons in the copolymers were 23, 43 and 119 for HDI-1, HDI-2 and HDI-3, respectively. This gave a crosslinking mole ratio of 1:2, 1:4 and 1:10, β-CD/linker respectively, and corresponds to an attenuated mole composition of β-CD.

The ^{1}H solution NMR of CDI-based copolymer materials are illustrated in Figure 2.3. DMA was not occluded in the copolymer framework for the various synthetic preparations, unlike the HDI-based copolymer materials. The NMR lines for the CDI-based copolymers are similarly broadened as X increases (*cf.* Figure 2.3 c-e; δ 2.00 - 0.80

pm). The CDI linker is an isomeric mixture and the chemical shift (δ=3.87 and δ=3.37 ppm) of the α-CH (methine) groups (adjacent to the urethane linkage) was independently confirmed with an ^{1}H NMR COSY spectrum. However, these chemical shifts were not observed in the other copolymers. The absence of an observed change in chemical shift of the α-CH group may be due to coincident upfield shifts of the resonance lines and possible overlap with β-CD and/or water (HOD) chemical shifts in the region δ=3.3-3.7 ppm. The α-CH (methine) groups were concluded previously for CDI-based copolymers at δ~3-4 ppm.[25,36-38] Additionally, the appearance of a signature for the methylene group (δ=4.09 ppm) of β-CD (-C_6H_2-) adjacent to the urethane bond agrees with previous NMR studies.[25] Crosslink ratios were estimated by integration of NMR lines, as described above, and the relative area of -C_6H_2- (β-CD) adjacent to urethane bond was 2, 4 and 10 protons for CDI-1, CDI-2 and CDI-3, respectively. The corresponding crosslink ratio is 1:2, 1:4 and 1:8, respectively. Furthermore, a chemical shift δ=3.17 ppm was observed and assigned to that of the CH_3 group of methanol (δ=3.16 ppm) in DMSO-*d*$_6$.[35] In contrast to the above results, this chemical shift was not observed for the HDI-X copolymers. The absence of the chemical shift in question may be due to differences in the adsorption behaviour arising from the mesopore framework structure. CDI-X copolymers can retain residual methanol within the copolymer framework despite exhaustive Soxhlet extraction with diethyl ether.

The ^{1}H NMR spectra (results not shown) in solution for MDI-based copolymers do not show occlusion of DMA or methanol and the resonance lines are in agreement with previous NMR results.[28,39] To obtain the crosslink ratio, the corresponding ^{1}H NMR spectral signatures were integrated, as described above. The aromatic protons adjacent to

the urethane bond (δ=7.1-7.4), relative to one mole equivalent of β-CD, were estimated as 2, 3 and 4 for MDI-1, MDI-2 and MDI-3, respectively. The corresponding co-monomer ratios were 1:2, 1:3 and 1:4, respectively. These offset calculated ratios are lower than those reported for HDI-X and CDI-X (X=2 and 3) copolymers and are likely due to steric hindrance and rigidity of MDI, as compared with the flexible aliphatic (i.e. HDI and CDI) linkers, respectively.

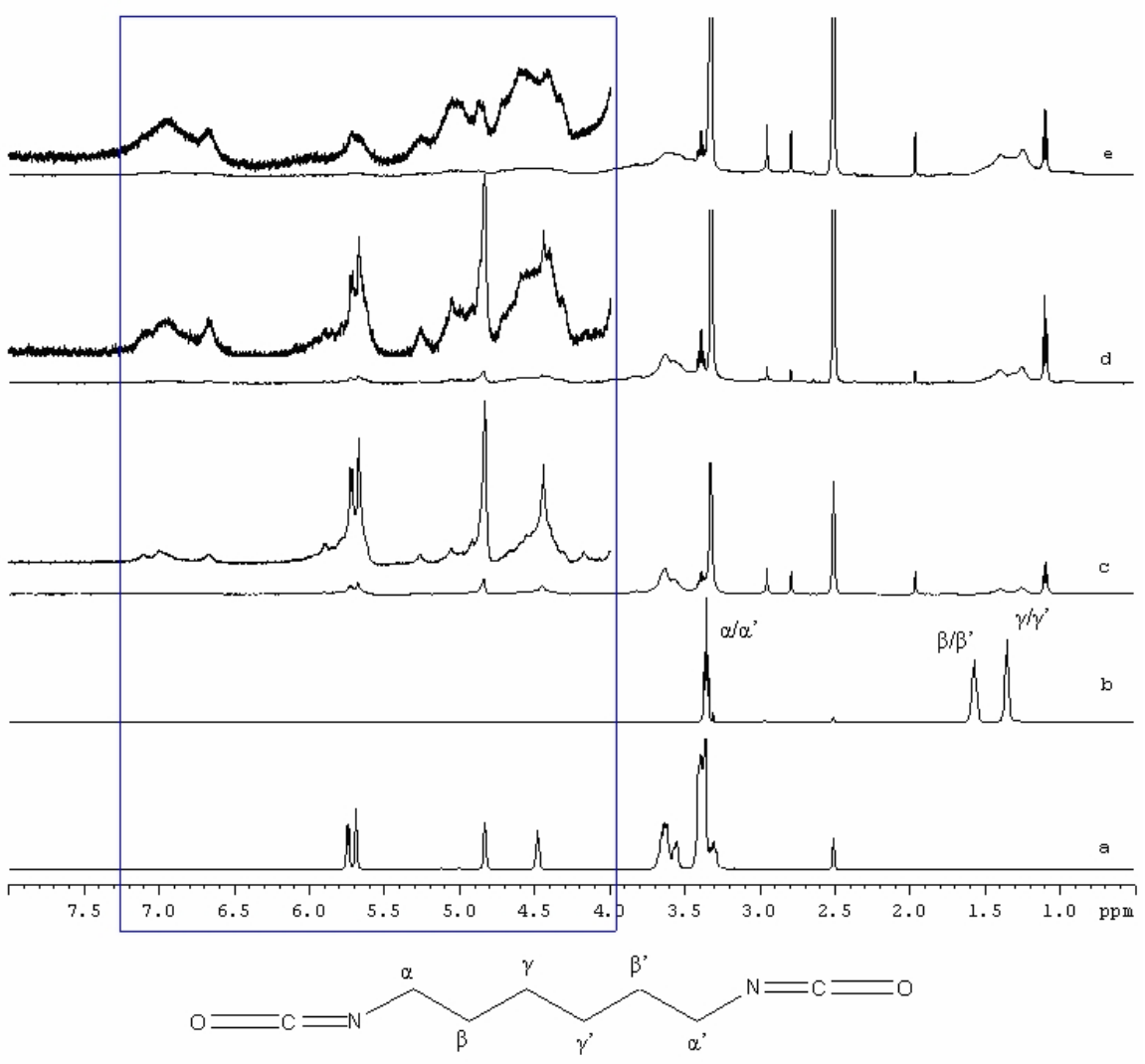

Figure 2.2. [1]H NMR spectra recorded at 295 K and 500 MHz: a) β-CD, b) HDI, c) HDI-1, d) HDI-2, and e) HDI-3 in DMSO-d_6. Chemical shifts are reference to tetramethylsilane (δ=0.0 ppm). The insets represent expanded regions of interest in the [1]H NMR spectra.

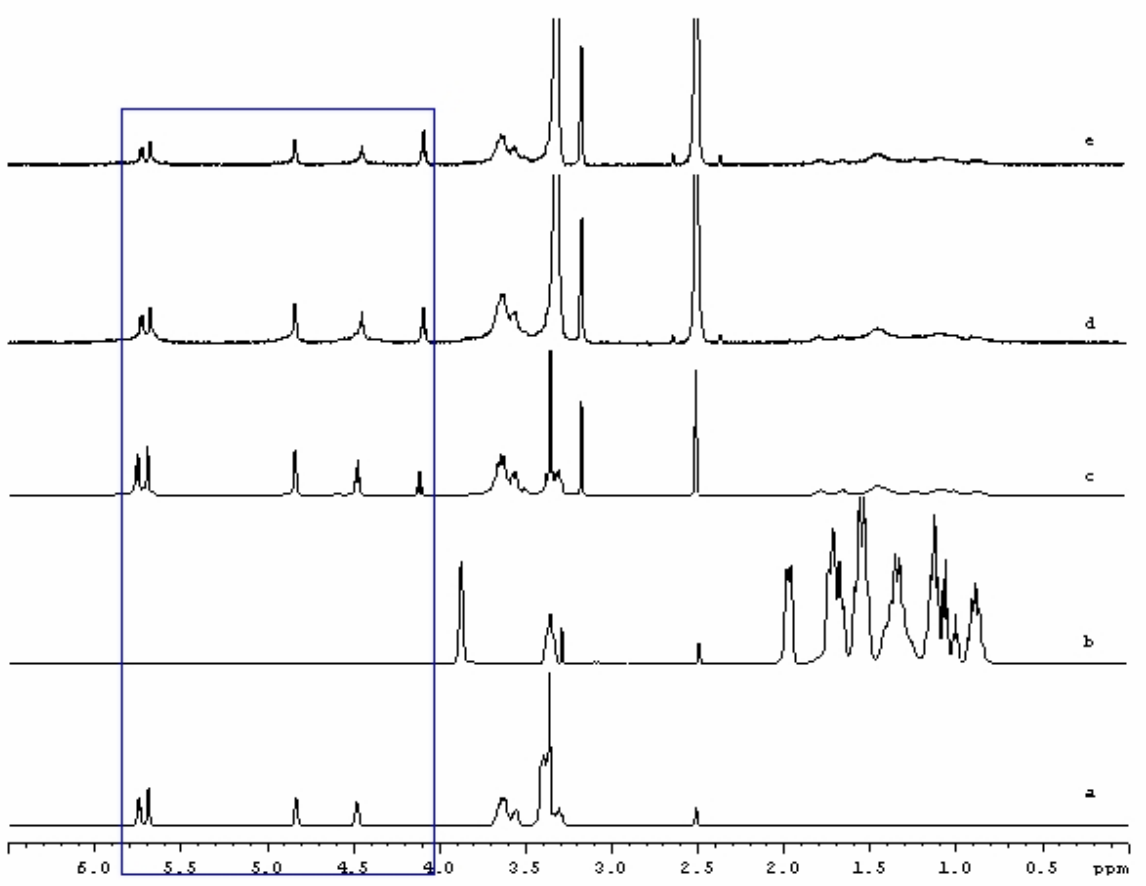

Figure 2.3. ^{1}H NMR spectra recorded at 295 K and 500 MHz: a) β-CD, b) CDI, c) CDI-1, d) CDI-2, and e) CDI-3 in DMSO-d_6. Chemical shifts are internally referenced to tetramethylsilane (δ=0.0 ppm).

Solid state ^{13}C NMR provides complementary structural information to the solution ^{1}H NMR results for the polymers with limited solubility in DMSO-d_6. The solid state ^{13}C CP-MAS NMR and IR spectra were previously reported for limited examples of copolymer materials prepared at the 1:3 mole ratios.[18] Figure 2.4 illustrates the ^{13}C solids NMR results for the urethane copolymer materials over the entire co-monomer composition range. The spectra shown are for the CD-based polymers composed of HDI-, CDI- and PDI-based linkers at X = 1-3. Solid state NMR spectra were not obtained for

the diisocyanate linkers to avoid potential melting during acquisition with magic angle spinning. The solution ^{13}C NMR spectra of β-CD, CDI, HDI and HDI-1 (dissolved in DMSO-d_6) were obtained (*cf*. Figure 2.5) for comparison with the solid state results in Figure 2.4. Although each glucose unit of β-CD contains six unique ^{13}C atoms per glucose residue, the spectra for the copolymers in Figure 2.4 reveal approximately four unique ^{13}C NMR lines between 60 and 110 ppm due to the spectral overlap of certain ^{13}C signatures. Similarly, the individual ^{13}C resonance lines for each pyranose carbon atom are not individually observed for the copolymer materials (*cf*. Figure 2.4). In contrast, the resonance lines for each of the six carbons (C1-C6) are observed in the ^{13}C NMR spectrum for β-CD hydrate in solution, as shown in Figure 2.5a. The spectral assignment reported here agrees with previous results.[32,40] In Figure 2.4, ^{13}C signatures are observed for β-CD and the spectral lines for the aliphatic (*i.e*. HDI and CDI; *cf*. 20-70 ppm) and aromatic (~110-170 ppm) diisocyanate linker molecules, respectively. The spectral lines of the co-monomer, HDI and CDI, are shown in Figure 2.5 and agree with the anticipated CP-MAS spectra observed for the copolymers in Figure 2.4. The urethane copolymers exhibit broader resonance lines that are often observed for such amorphous materials. The increased line widths are evident for HDI-1 from a comparison of the solid state and solution state spectra given in Figures 2.4 and 2.5, respectively. The appearance of a carbonyl signature (~165-170 ppm) provides additional support for the copolymer products. The corresponding increased line intensity as X increases provides further evidence of the urethane copolymer framework. The amorphous character observed in the ^{13}C NMR spectra is attributed to the random attachment of the diisocyanate linker molecules to the available hydroxyl group sites (C_2, C_3, and C_6) of β-CD. Likewise, the

amorphous character is also attributes to the differences in the cross polarization dynamics of the copolymer materials, as compared with native β-CD hydrate. Furthermore, the high resolution ^{13}C spectrum in solution for HDI-1 indicates that DMA is occluded within the copolymer framework despite exhaustive Soxhlet extraction and vacuum drying of the products. The lines labeled S1, S2, S3 and S4 correspond to CH_3, NCH_3, NCH_3 and CO, respectively and are in agreement with the spectrum reported for ^{13}C NMR of DMA in DMSO-d_6.[35]

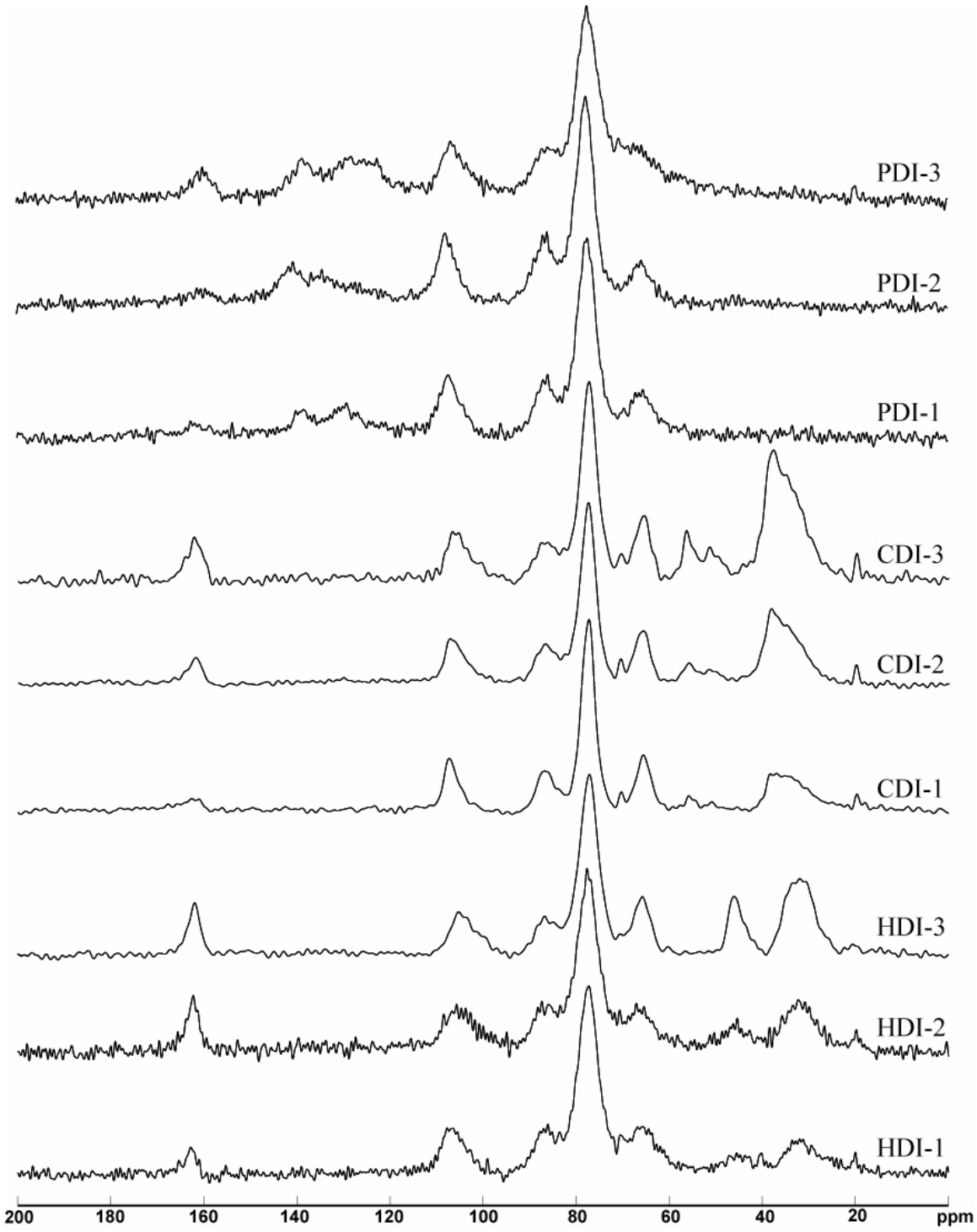

Figure 2.4. Solid state ^{13}C HC→CP-MAS NMR spectra of CD copolymer materials recorded at ambient temperature, 16 kHz spinning speed, and 125 MHz at 293 K.

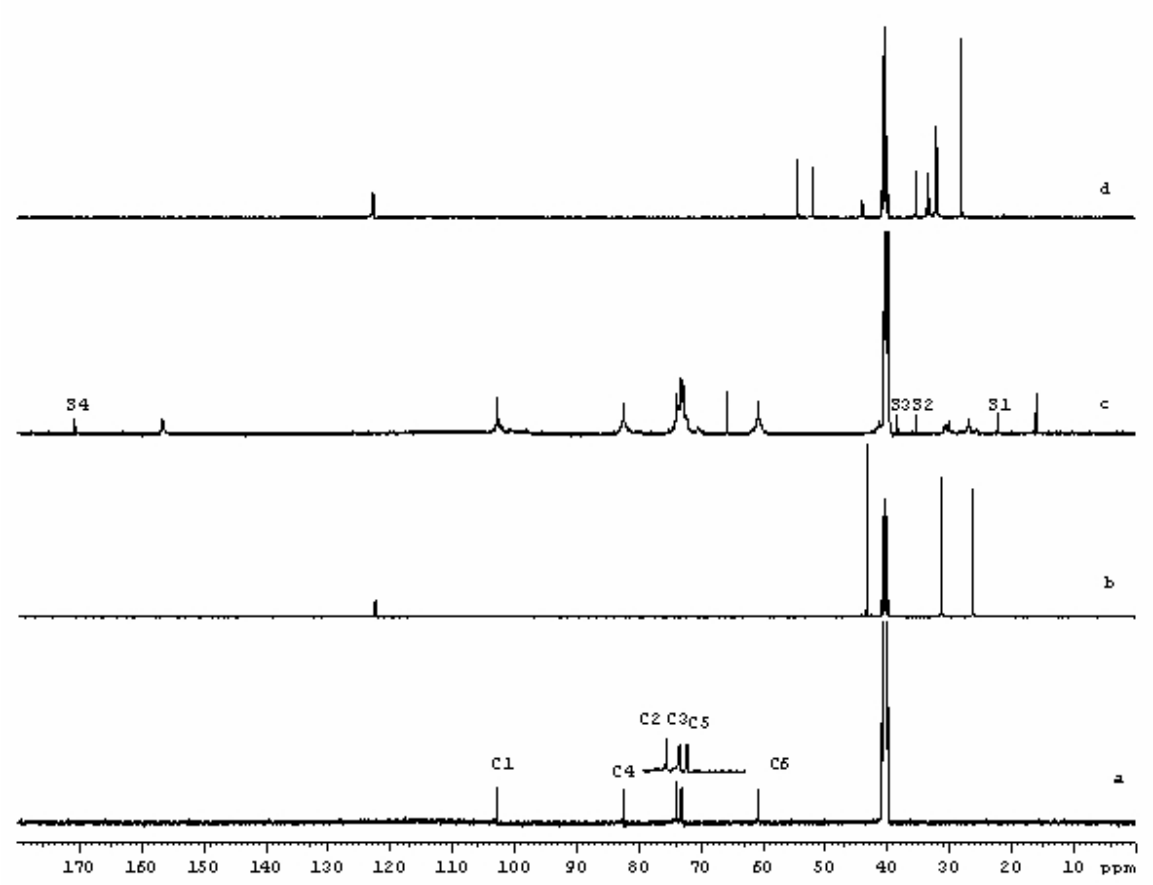

Figure 2.5. Solution state ^{13}C NMR spectra of CD copolymer materials recorded in DMSO-d_6 at 295 K and 125 MHz: a) β-CD hydrate, b) HDI, c) HDI-1 copolymer and d) CDI.

2.4.2.3 TGA

TGA is a novel thermoanalytical technique that may provide quantitative estimates of the relative co-monomer composition.[27] Figure 2.6a-d shows the first derivative TGA plots (% weight loss/^{o}C) for HDI-, CDI-, MDI- and PDI-based copolymers, respectively. Several thermal events characterized by weight losses were observed upon heating the copolymers. In the case of HDI- and CDI-based copolymers, the transitions occurring between 30-100 ^{o}C and are attributed to the desorption of water. In contrast, copolymers with aromatic-based linkers appear to be less hygroscopic

because the corresponding thermal events are not evident. Each copolymer exhibits a transition ~ 250-375 ^{o}C and is attributed to the cleavage of the urethane linkages between β-CD and the linker unit. The thermogram for native β-CD (not shown) reveals a maximum decomposition at ~312^{o}C, in good agreement with the observed values of 300-320 ^{o}C reported previously.[41-42] As illustrated in Figure 2.6a-b, , another thermal event of importance occurs between 375-500 ^{o}C for HDI-X and CDI-X copolymers. The observed weight loss for this region is consistent with independent TGA results and is attributed to the cleavage of the urethane linkage and/or volatilization of the decomposition products.[22,43] The observed onset temperature for cleavage of the urethane framework increases as the linker content (X) of the copolymer increases (*cf.* Table 2.4 supplementary data).

The first derivative TGA plots were further analyzed with deconvolution analysis using PeakFit v4.12 to obtain quantitative estimates of the respective peak areas. Multiple peaks appear in the region between 375-500 ^{o}C for HDI-X (X = 6 and 9) copolymers and for CDI-X copolymers (X=2, 3, 6 and 9). The deconvolution of the TGA results for CDI-6 is illustrated in Figure 2.7 where three thermal processes are observed (*i.e.* 377, 414 and 454 ^{o}C) as well as the thermal decomposition of β-CD. These results indicate that the framework of the polyurethane is relatively complex. This may be understood according to possible reaction of linkers with multiple hydroxyl groups (both primary and secondary) of β-CD, as evidenced by the differing thermal stability profiles for each copolymer. The absence of multi-thermal events in the region 375-500 ^{o}C for HDI-X (X=1-3) and CDI-1 copolymers suggest that the linkers are attached at the relatively reactive primary hydroxyl groups of β-CD. At greater mole ratios (X>1),

crosslinking may occur at the secondary hydroxyl groups to alleviate steric crowding in the annular region of β-CD. This interpretation is supported by the fact that CDI is bulkier than HDI; hence, the earlier onset of multiple thermal events for CDI-X (X≥2) copolymers. The co-monomer content was estimated for each copolymer, assuming that the step-wise weight loss occurs between 375-500 ^{o}C, and is attributed to the linker unit. The calculated weight loss from the peak areas of the deconvoluted TGA data (*cf*. Figures 2.6 and 2.7) provides estimates of the relative co-monomer composition, as outlined in Table 2.3. The crosslink ratio reaches a plateau at X=6 for HDI-X and CDI-X copolymers. Likewise, an upper crosslink ratio was independently concluded from the sorption properties of such copolymers, according to observed steric effects in the annular hydroxyl region of β-CD.[18] Since the yield of the HDI-X and CDI-X (X=9) copolymers was ~ 100%, the crosslinking of the co-monomers may involve a combination of both –A-B-B-A and –A-B-A- copolymers; where A= β-CD and B=diisocyanate.[27] Independent estimates of the co-monomer mole ratios obtained from TGA and ^{1}H NMR spectroscopy are in disagreement. For example, copolymers with greater co-monomer mole ratios (1:2 and 1:3) were not in agreement; however, better convergence is observed for the 1:1 products. ^{1}H NMR is considered to provide the most reliable quantitative estimates of copolymer composition; whereas, TGA may be more prone to artifacts. The divergence between TGA and ^{1}H NMR is attributed to the variable dependence of the thermophysical properties of copolymers with variable co-monomer ratios. Nevertheless, TGA is well suited for the characterization of highly crosslinked, insoluble copolymers in the solid state and provides values in agreement with ^{13}C CP-MAS NMR.

The aromatic-based copolymers (MDI, PDI and NDI) were characterized by thermal events corresponding to the loss of β-CD. The overall total weight loss is lower than that measured for the HDI and CDI copolymers, in agreement with the lower ash content from the mass loss *vs*. temperature curves. Comparable thermal stability of the aromatic-based copolymers was reported for MDI-based polyurethanes with diols.[44-45] Moreover, the increased thermal stability was associated with cleavage of urethane bonds, as shown by greater peak broadening with increasing crosslink density. The peak broadening observed in TGA plots (*cf*. Figure 2.6c-e) indicates an overlap of additional thermal events as the number of urethane bonds increase, as evidenced by greater thermal stability of the framework. Thus, β-CD copolymers containing aromatic linkers may require a wider range of temperatures (> 500 ^{o}C) to fully characterize their thermal properties because increased crosslinking density imparts greater thermal stability for these types of materials.

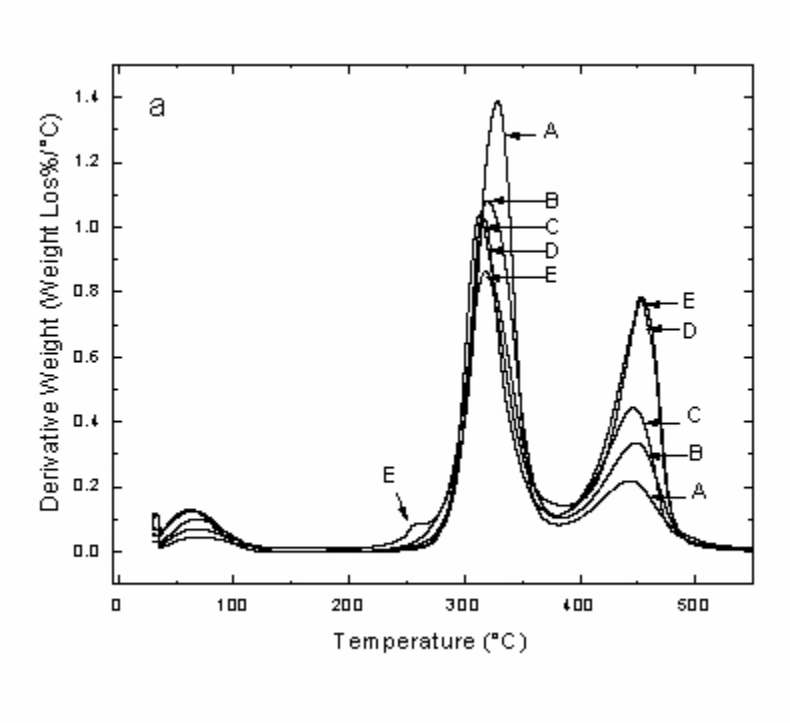

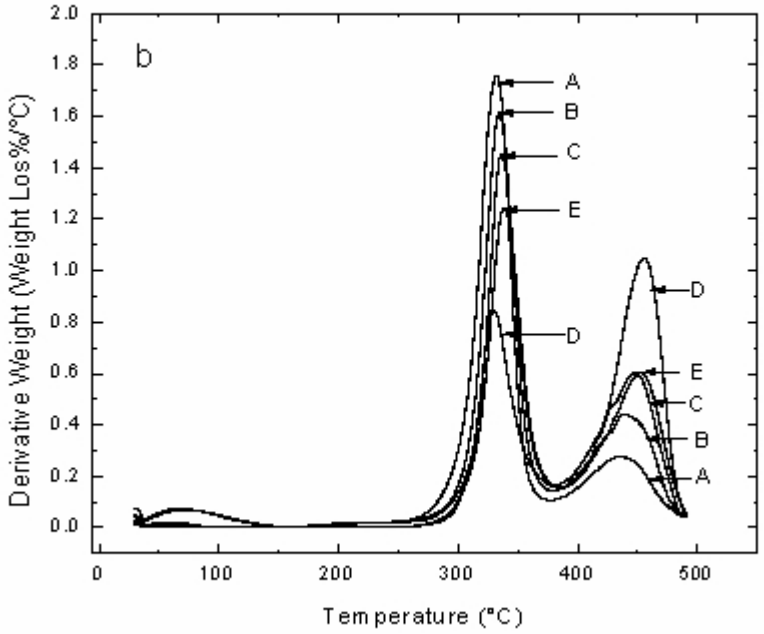
b
A
B
C
E
D
D
E
C
B
A
Derivative Weight (Weight Los%/°C)
Temperature (°C)
0.0
0.2
0.4
0.6
0.8
1.0
1.2
1.4
1.6
1.8
2.0
0
100
200
300
400
500

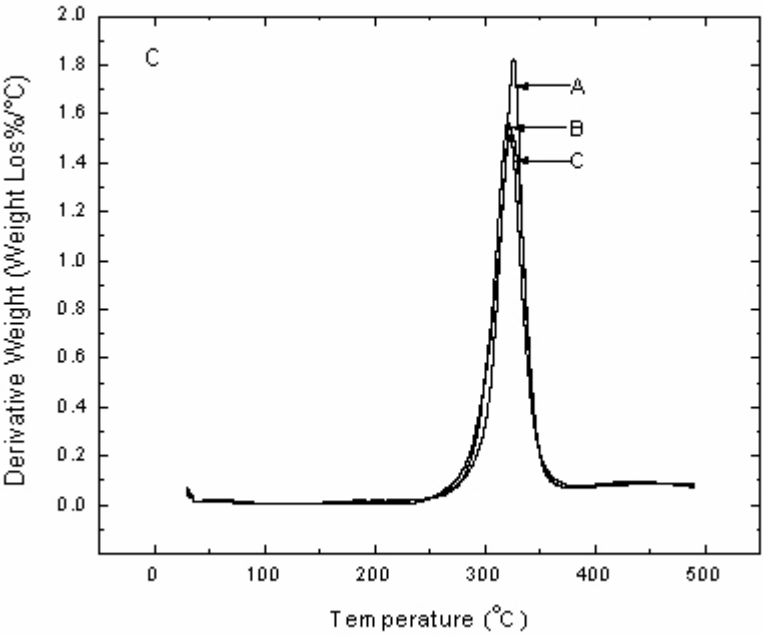
C
A
B
C
Derivative Weight (Weight Los%/°C)
Temperature (°C)
0.0
0.2
0.4
0.6
0.8
1.0
1.2
1.4
1.6
1.8
2.0
0
100
200
300
400
500

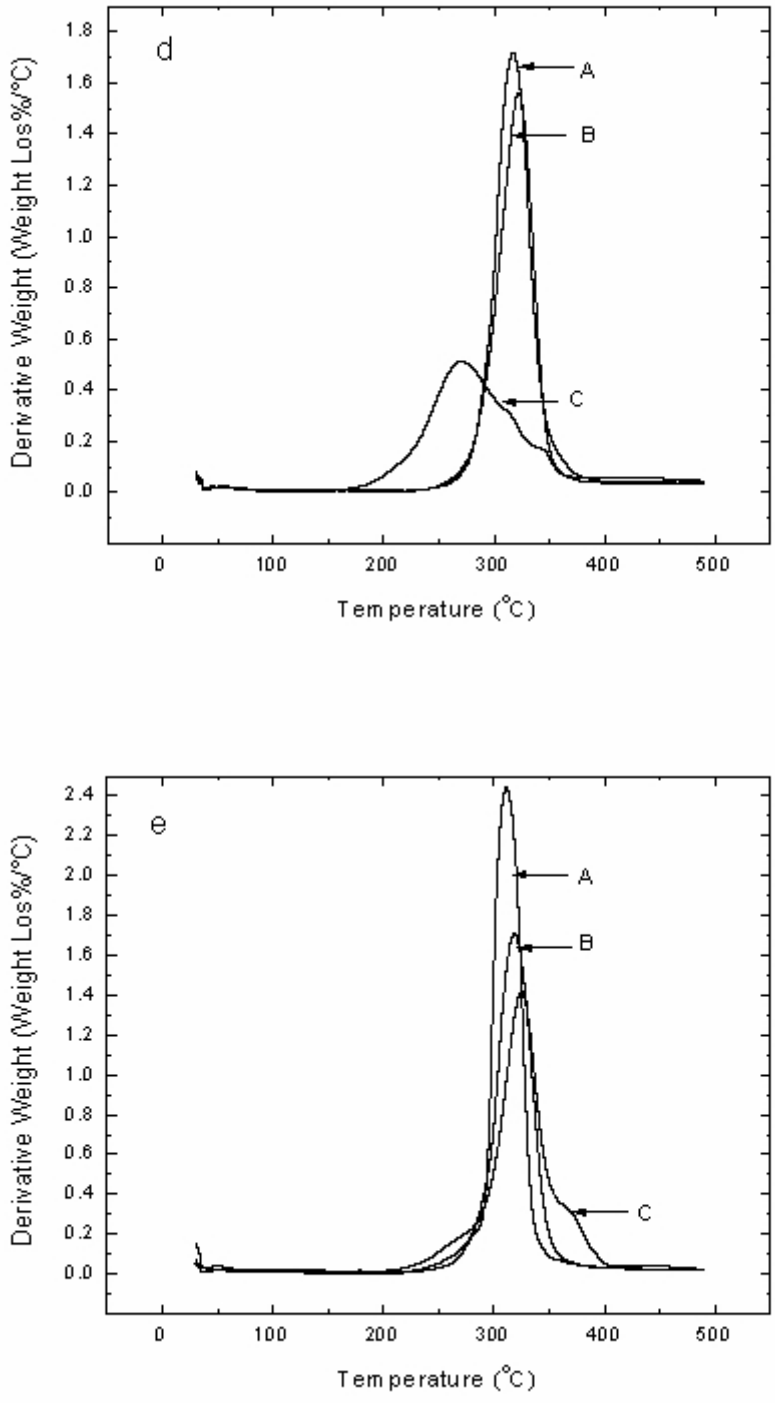

Figure 2.6a-e. First derivative plots (weight loss/˚C vs. temperature) of TGA data for the copolymers with the following linkers: a)HDI , b) CDI, c) MDI, d) PDI, and e) NDI, respectively. The letters a-e represents increasing β-CD/diisocyanate mole ratios at 1:1, 1:2, 1:3, 1:6 and 1:9, respectively.

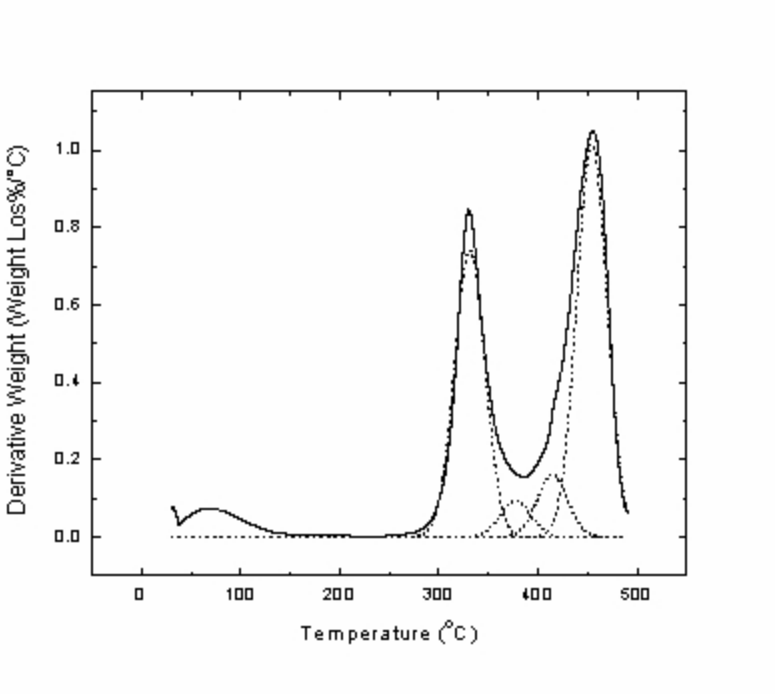

Figure 2.7. Deconvolution of CDI-6 TGA derivative plots using PeakFit v4.12 Model: Gaussian. $R^2 = 0.972$. Standard Error = 0.0463values were > 0.9. The solid line is the experimental derivative plot while the dotted lines are the deconvoluted fitted curves.

Table 2.3. Synthetic β-CD:diisocyanate co-monomer ratios and those estimated by TGA for HDI-X, CDI-X, MDI-X and PDI-X copolymers, respectively.

Copolymer	β-CD/diisocyanate Synthetic Feed Ratio	β-CD/diisocyanate Mole Ratio Estimated by Deconvolution Analysis*
HDI-1	1:1	1:2
HDI-2	1:2	1:3
HDI-3	1:3	1:4
HDI-6	1:6	1:7
HDI-9	1:9	1:5
CDI-1	1:1	1:2
CDI-2	1:2	1:3
CDI-3	1:3	1:4
CDI-6	1:6	1:7
CDI-9	1:9	1:4

* Gaussian deconvolution function performed using PeakFit v4.12 Model: All of the R^2 values were > 0.9.

2.5 Conclusions

A series of novel water insoluble macrocycle-based polyurethanes were successfully synthesized from β-CD and diisocyanate cross linkers with variable molecular structure. The yield of the copolymers was variable (~30-100%), whereas, greater yields were observed for diisocyanate rich (X>1) copolymer materials. Different methods were used to characterize the copolymers such as; FT-IR, elemental analysis, NMR and TGA. FT-IR spectroscopy confirms the product identity and semi-quantitative co-monomer composition, whereas, quantitative results were obtained with ^{1}H NMR spectroscopy in DMSO for HDI-X, CDI-X and MDI-X (X=1-3). Copolymers with poor solubility in DMSO-d_6 (X>3) were generally observed for copolymers with aromatic linkers except MDI, whereas, HDI-1 and CDI-1 were sparingly soluble in water. Solid state ^{13}C NMR spectroscopy, TGA, and CHN elemental analysis provided reasonable semi-quantitative estimates of the co-monomer composition, particularly for insoluble copolymer materials. In contrast to ^{13}C CP-MAS NMR spectroscopy, TGA is relatively cost effective, requires relatively small sample sizes, short analysis times, and provides good estimates of the co-monomer content of such copolymer materials.

An improved understanding of copolymer design and characterization was achieved based on: (*i*) an upper limit of β-CD:linker mole ratio (~ 1:7) for the copolymer materials, and (*ii*) determination of the optimal adsorption properties for co-monomer ratios in the range X=1-3. This study illustrates the importance of understanding the inclusion accessibility of β-CD, and the utility of multi-instrumental characterization methods for the systematic design and characterization of insoluble copolymers. The results reported herein are anticipated to contribute to the further development of

copolymers with improved sorption capacity and molecular recognition properties for a range of sorption-based applications.[46-48]

2.6 Acknowledgments

The authors gratefully acknowledge the Natural Sciences and Engineering Research Council and the Program of Energy Research and Development for support of this research. M.H.M acknowledges the University of Saskatchewan for the award of a Graduate Teaching Fellowship and Environment Canada for the Science Horizons Program award.

2.7 References

1. Szejtli, J. *Chem. Rev.* **1998**, *98*, 1743-1754.
2. Choi, S.; Amajjahe, S.; Ritter, H. *Polymerization of included monomers and behavior of resulting polymers-Inclusion Polymers*, 2009; Vol. 222.
3. Wenz, G. *Recognition of Monomers and Polymers by Cyclodextrins*; Springer: Berlin, Germany, 2009; Vol. 222.
4. Yhaya, F.; Gregory, A. M.; Stenzel, M. H. *Aust. J. Chem.* **2010**, *63*, 195-210.
5. *Cyclodextrin Chemistry*; Bender, M. L.; Komiyama, M., Eds.; Springer-Verlag: Berlin, Germany, 1978.
6. He, B.; Zhao, X. *React. Polym.* **1992**, *18*, 229-235.
7. Ma, M.; Li, D. *Chem. Mater.* **1999**, *11*, 872-874.
8. Crini, G. *Prog. Polym. Sci.* **2005**, *30*, 38-70.
9. Song, L. X.; Bai, L.; Xu, X. M.; He, J.; Pan, S. Z. *Coord. Chem. Rev.* **2009**, *253*, 1276-1284.
10. Wiedenhof, N. *Staerke* **1969**, *21*, 119-123.
11. Hoffman, J. L. *J. Macromol. Sci., Part A* **1973**, *7*, 1147-1157.
12. Mizobuchi, Y. *J. Chromatogr., A* **1980**, *194*, 153-161.

13. Sreenivasan, K. *J. Appl. Polym. Sci.* **1998**, *68*, 1857-1861.
14. Szejtli, J. *Pure Appl. Chem.* **2004**, *76*, 1825-1845.
15. Buschmann, H.-J. *J. Cosmet. Sci.* **2002**, *53*, 185-191.
16. Del Valle, E. M. M. *Process Biochem.* **2004**, *39*, 1033-1046.
17. Astray, G.; Gonzalez-Barreiro, C.; Mejuto, J. C.; Rial-Otero, R.; Simal-Gándara, J. *Food Hydrocolloids* **2009**, *23*, 1631-1640.
18. Mohamed, M. H.; Wilson, L. D.; Headley, J. V. *Carbohydr. Polym.* **2010**, *80*, 186-196.
19. Steed, J. W.; Atwood, J. L. *Supramolecular Chemistry*; 2nd ed.; John Wiley & Sons, Ltd: West Sussex, UK, 2009.
20. Mohamed, M. H.; Wilson, L. D.; Headley, J. V.; Peru, K. M. *Process Saf. Environ. Prot.* **2008**, *86*, 237-243.
21. Asanuma, H.; Kakazu, M.; Shibata, M.; Hishiya, T.; Komiyama, M. *Supramol. Sci.* **1998**, *5*, 417-421.
22. Bhaskar, M.; Aruna, P.; Ganesh Jeevan, R. J.; Radhakrishnan, G. *Anal. Chim. Acta* **2004**, *509*, 39-45.
23. Ozmen, E. Y.; Sezgin, M.; Yilmaz, A.; Yilmaz, M. *Bioresour. Technol.* **2008**, *99*, 526-531.
24. Pan, B.; Pan, B.; Zhang, W.; Lv, L.; Zhang, Q.; Zheng, S. *Chem. Eng. J.* **2009**, *151*, 19-29.
25. Yen, M.-S.; Cheng, K.-L. *J. Polym. Res.* **1996**, *3*, 115-123.
26. Hirai, H. *J. Inclusion Phenom.* **1984**, *2*, 655-660.
27. Pratt, D. Y.; Wilson, L. D.; Kozinski, J. A.; Mohart, A. M. *J. Appl. Polym. Sci.* **2010**, *116*, 2982-2989.
28. Nakamura, H.; Takata, T.; Endo, T. *Macromolecules* **1990**, *23*, 3032-3035.
29. Kim, S. T.; Moon, H. S.; Gong, M. S. *Macromolecules* **1992**, *25*, 7392-7394.
30. Wilbullucksanakul, S.; Hashimoto, K.; Okada, M. *Macromol. Chem. Physic.* **1996**, *197*, 135-146.
31. Dez, I.; De Jaeger, R. *Phosphorus, Sulfur Silicon Relat. Elem.* **1997**, *130*, 1-14.
32. Lee, K.; Jung, H.; Kim, S. Y.; Lee, B. H.; Choe, S. *Polymer* **2006**, *47*, 1830-1836.

33. Salmaso, S.; Semenzato, A.; Bersani, S.; Matricardi, P.; Rossi, F.; Caliceti, P. *Int. J. Pharm.* **2007**, *345*, 42-50.
34. Mishra, A. K.; Allauddin, S.; Radhika, K. R.; Narayan, R.; Raju, K. V. S. N. *Polym. Adv. Technol.* **2009**, In Print.
35. Gottlieb, H. E.; Kotlyar, V.; Nudelman, A. *J. Org. Chem.* **1997**, *62*, 7512-7515.
36. Mehdipour-Ataei, S.; Sarrafi, Y.; Hatami, M. *Eur. Polym. J.* **2004**, *40*, 2009-2015.
37. Maruyama, K.; Kudo, H.; Ikehara, T.; Nishikubo, T.; Nishimura, I.; Shishido, A.; Ikeda, T. *Macromolecules* **2007**, *40*, 4895-4900.
38. Mehdipour-Ataei, S.; Bahri-Laleh, N.; Rabei, A.; Saidi, S. *High Perform. Polym.* **2007**, *19*, 283-295.
39. Tharanikkarasu, K.; Radhakrishnan, G. *Eur. Polym. J.*, *33*, 1779-1786.
40. Jiao, H.; Goh, S. H.; Valiyaveettil, S.; Zheng, J. *Macromolecules* **2003**, *36*, 4241-4243.
41. Harada, A.; Takahashi, S. *J. Inclusion Phenom.* **1984**, *2*, 791-798. (42)
42. Sakuraba, H.; Ishizaki, H.; Tanaka, Y.; Shimizu, T. *J. Inclusion Phenom.* **1987**, *5*, 449-458.
43. Lee, K.-P.; Choi, S.-H.; Ryu, E.-N.; Ryoo, J. J.; Park, J. H.; Kim, Y.; Hyun, M. H. *Anal. Sci.* **2002**, *18*, 31-34.
44. Oprea, S. *J. Mater. Sci.* **2008**, *43*, 5274-5281.
45. Oprea, S. *Adv. Polym. Tech.* **2009**, *28*, 165-172.
46. Mohamed, M.H.; Wilson, L. D.; Headley, J. V.; Peru, K. M. *J. Colloid Interface Sci.* **2010**, *in press***.**
47. Mohamed, M. H.; Wilson, L. D.; Headley, J. V.; Peru, K. M. *Phys. Chem. Chem. Phys*. **2010**, DOI: 10.1039/c0cp00421a.
48. Mohamed, M.H.; Wilson, L. D.; Headley, J. V.; Peru, K. M. *Rapid Commun. Mass Spectrom*. **2009,** 23, 3703.

2.8 Supplementary Information

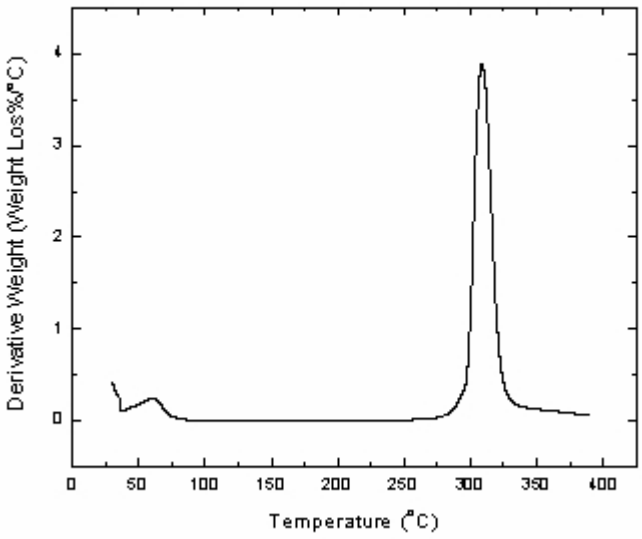

Figure 2.8. First derivative plots (weight loss/˚C vs. temperature) of TGA data for β-CD.

Table 2.4. Onset temperatures[1] for thermal events of copolymer materials depicted in Figure 2.6a-e.

Copolymer	Onset Temperatures (^{o}C)
HDI-1	328, 447
HDI-2	319, 451
HDI-3	312, 448
HDI-6	317, 453
HDI-9	318, 455
CDI-1	332, 439
CDI-2	334, 443
CDI-3	336, 449
CDI-6	329, 456
CDI-9	338, 454
MDI-1	325
MDI-2	321
MDI-3	324
PDI-1	317
PDI-2	322
PDI-3	269
NDI-1	311
NDI-2	318
NDI-3	325

[1]The values were obtained from the peak maxima of the first derivate plot.

CHAPTER 3

PUBLICATION 2

Description

The following is a verbatim copy of an article that was published in February of 2011 in the Journal of Colloid and Interface Science (*J. Colloid Interface Sci..:* **2011**, *357(1),* 215-222). This paper describes surface area and pore structure properties of the β-CD PUs using nitrogen adsorption at 77 K and a dye-based method in aqueous solution at 295 K.

Authors' Contribution

I carried out all the experimental work (i.e. synthesis and characterization of the copolymers). This work was supervised by Dr. Wilson and Dr. Headley. The first draft was written and extensively edited by Dr. Wilson, and for this reason I appear as second author. Written permission was obtained from all contributing authors to include this material in this thesis.

Relation of Chapter 3 (Publication 2) to the Overall Objectives of this Project

As mentioned in Chapter 1, the surface and pore structure properties are important physicochemical properties for the optimal design of the copolymers. This chapter covers the measurement of these properties using a common solid-gas adsorption method applied in the literature. In contrast, a dye-based solution adsorption techniques was

investigated and significant differences between these two methods were shown and their applicability for characterization of physicochemical properties.

Graphical Abstract

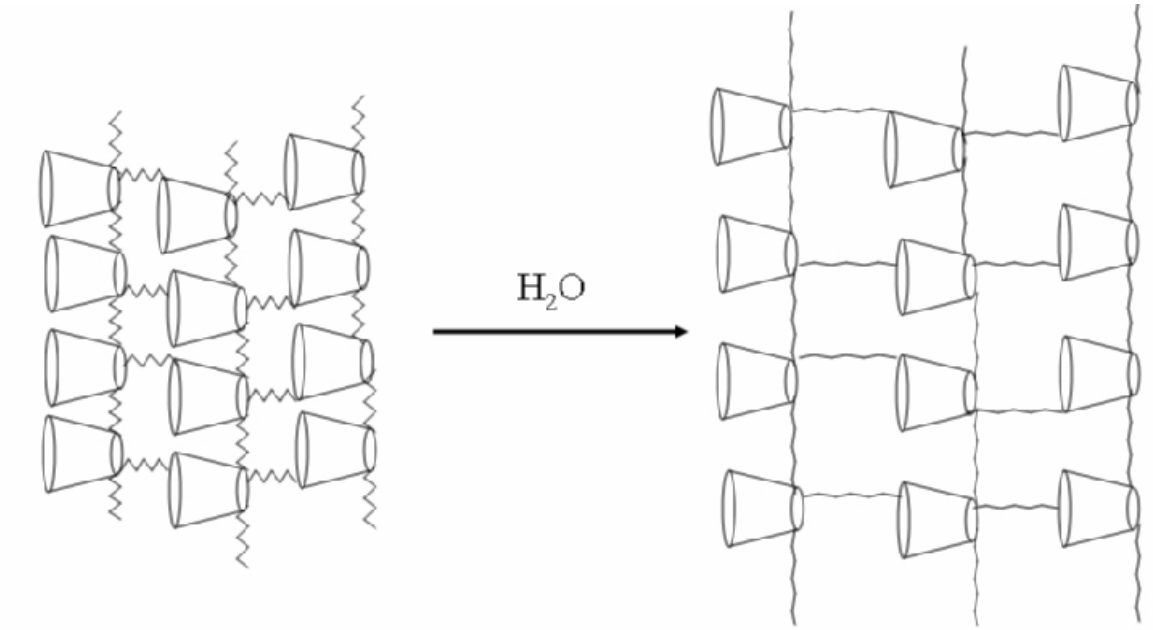

Research Highlight

Copolymer containing β-CD possesses tunable surface area and pore structure (textural) properties. Sorbents with variable co-monomer composition were studied using N_2 and PNP adsorptives. Remarkable differences in solid-gas and solid-solution adsorption properties were observed. Solvent-induced swelling and morphological changes occurs are observed for such copolymers. Hydration phenomena affect the textural properties of "*soft*" carbohydrate-based materials.

3. Surface Area and Pore Structure Properties of Nanosponge Copolymers

Lee D. Wilson,[§*] *Mohamed H. Mohamed,*[§] *John V. Headley,*[¥]

[§]Department of Chemistry, University of Saskatchewan, 110 Science Place, Saskatoon, Saskatchewan, S7N 5C9

[¥]Water Science and Technology Directorate, 11 Innovation Boulevard, Saskatoon, Saskatchewan, S7N 3H5

*Corresponding Author

Received 9 November 2010

3.1 Abstract

The surface area and pore structure characteristics were investigated for a series of aliphatic- and aromatic-based polyurethane (PU) copolymers containing a macromolecular porogen (β-cyclodextrin). The bi-functional diisocyanates used as crosslinker units were: 1,6-hexamethylene diisocyanate, 4,4'-dicyclohexylmethane diisocyanate, 4,4'-diphenylmethane diisocyanate, 1,4-phenylene diisocyanate and 1,5-naphthalene diisocyanate. The macromolecular porogen content was controlled by fixing the composition of β-CD and varying the co-monomer mole ratio from unity to larger integer values. Nitrogen adsorption results reveal that copolymer materials with variable mole ratios (β-CD: crosslinker) from 1:1 to 1:3 displayed relatively low BET surface areas (SA ~ 10^1 m^2/g) and mesopore diameters (~ 16-29 nm). In contrast, a dye adsorption method in aqueous solution with *p*-nitrophenol (PNP) at pH = 4.60 and 295 K provided estimates of the surface area (1.5 - 6.2 $\times 10^2$ m^2/g) for the corresponding

copolymer materials. Variation of the copolymer SA was attributed to the type of diisocyanate crosslinker and its relative mole ratio. The differences in the estimated SA values from porosimetry and UV-Vis dye adsorption method for these nanoporous copolymers were attributed to the role of solvent as evidenced by swelling of the copolymer framework in aqueous solution and respective temperature conditions.

3.2 Introduction

The use of polymers, colloids, and supramolecular tectons as porogens in nanocasting strategies yield a wide variety of novel imprinted porous materials.[1] By analogy, the development of porous materials with unique morphometric properties and parameters is possible by the incorporation of porogens within a polymer framework. Physical mixtures of soil containing randomly methylated β-cyclodextrin (RAMEB) or thin films of methyl silsesquioxane containing triacetyl-β-cyclodextrin illustrate that covalent attachment of porogens can significantly alter the physicochemical and textural properties of sorbent materials[2-3]. Covalent incorporation of porogens offers certain advantages, as compared with conventional molecular imprinted polymers, since the textural properties depend on the porogen content and framework accessibility.[4] The incorporation of β-cyclodextrin (β-CD) porogens within the framework structure, represents a novel materials design approach with significant potential for controlled tuning of the textural mesoporosity of supramolecular frameworks.[5] β-CD copolymers represent an innovative design strategy for development of "*smart*" or "*functional*" porous materials with improved solid phase extraction (SPE) and molecular recognition properties because of the porogen characteristics and their unique host-guest properties.[6-8]

Carbohydrate-based copolymers containing cyclodextrins (CDs) are of interest, in part, because of their ability to form inclusion complexes in aqueous solution.[8] The inclusion properties of β-CD copolymers are determined by the surface area, pore structure, and site accessibility of β-CD within the copolymer framework. In the context of sorption-based applications for these types of materials, the adsorption parameters (*e.g.*, Q_m) are arguably the most important physicochemical property.[7,9-10] Therefore, the the surface area and pore structure properties provide useful physicochemical parameters for achieving the optimal design of materials for sorption-based applications. The systematic variation of the framework structure of the cyclodextrin-based copolymers facilitates the tuning of the textural properties and inclusion site accessibility since the latter is critical in cases where the copolymer sorption involves molecular recognition through the formation of well-defined host-guest inclusion complexes.[11]

In this paper, we compare the results of a systematic nitrogen adsorption study at 77 K along with a dye-based adsorption study in aqueous solution at 295 K and pH = 4.6 for a series of β-CD-based urethane copolymer materials. The polyurethane-based β-CD copolymers are comprised of diisocyanate co-monomers with either aliphatic or aromatic bi-functional crosslinker units (*cf*. Figure 1.3 in Chapter 1). The study of such copolymers with an adjustable framework architecture and macrocyclic porogen (β-CD) content will contribute to the development of SPE materials with improved molecular recognition properties, variable surface area, and tunable pore structure characteristics.[1,6,12-13]

3.3 Experimental

3.3.1 Materials

β-CD was purchased from VWR. 1,6-hexamethylene diisocyanate (HDI), 4,4'-dicyclohexylmethane diisocyanate (CDI), 4,4'-diphenylmethane diisocyanate (MDI), 1,4-phenylene diisocyanate (PDI), dimethyl acetamide (DMA), cellobiose (CL), p-nitrophenol (PNP), methanol, anhydrous ethyl ether, potassium bromide, 4 Å (8-12 mesh) molecular sieves, were purchased from Sigma Aldrich. 1,5-naphthalene diisocyanate (NDI), was obtained from TCI America. Potassium phosphate monobasic and D(+)-glucose monohydrate (GL) were purchased from EMD Chemicals. Medical grade nitrogen gas (Praxair) and all materials were used as received unless specified otherwise.

3.3.2 Synthesis and Characterization of Copolymer Materials

The synthesis of CD-based polyurethane materials was adapted from previous work[10-11] and the products were fully characterized using spectroscopy, thermoanalytical methods, and elemental analyses. The nomenclature of the copolymers is defined in accordance with the diisocyanate acronym, and the co-monomer mole ratio (β-CD:diisocyanate). For example, in the case of 1:3 β-CD:HDI copolymer, the designation is referred to as HDI-3. The molar quantity of β-CD is taken to be unity for all copolymers.

3.3.3 Porosimetry

Nitrogen adsorption measurements were made using a Micromeritics ASAP 2020 (Norcross, GA) to obtain the surface area and pore structure properties with an accuracy of ± 5 % for β-CD and its copolymers. A 1.0 g sample was degassed at an evacuation rate

of 5 mmHg/s in the sample chamber until the outgas rate became stabilized (<10 μmHg/min). The degassing temperature for the samples was maintained ~ 120 °C for 24 hrs. Alumina, and silica-alumina standards (Micromeretics) were used to check the calibration of the instrumental parameters for low and high surface areas, respectively. The BET surface area was calculated from the adsorption isotherm using 0.162 nm^2 as the surface area for nitrogen gas.[14-15] The micropore surface area was obtained using a t-plot (de Boer method).[16] The Barret-Joyner-Halenda (BJH) method was used to estimate the pore volume and pore diameter from the adsorption isotherm.[17] The BJH method used the Kelvin equation and the assumption of slit-shaped pores.[14-15]

3.3.4 Dye Sorption Method

The equilibrium concentration of PNP was determined using a double beam spectrophotometer (Varian CARY 100) at room temperature (295 ± 0.5 K) by monitoring the absorbance changes at λ_{max} = 317 nm (pH 4.60) where the molar absorptivity was estimated to be 10, 026 L mol^{-1} cm^{-1}.[14,18]

The experimental dye sorption results were studied in aqueous solution with equilibrium isotherms represented as plots of the adsorbed amount of PNP from solution per unit mass of copolymer (Q_e) versus the unbound equilibrium concentration (C_e) of PNP. Equation 3.1 defines Q_e in terms of the experimental variables, C_o is the initial stock concentration (M) of PNP, V is volume of solution (L), and m is the mass of sorbent (g).

$$Q_e = \frac{(C_o - C_e) \times V}{m} \qquad \text{Equation 3.1}$$

The Sips isotherm[19] (*cf.* Equation 3.2) provides an assessment of the heterogeneity of the sorption process and is preferred because it represents a generalized isotherm which can

be interpreted in context of the Langmuir or Freundlich isotherms,[20-21] in accordance with the adjustable parameters (Q_m, n_s, and K_s).

$$Q_e = \frac{Q_m (K_s C_e)^{n_s}}{1 + (K_s C_e)^{n_s}} \qquad \text{Equation 3.2}$$

The binding affinity between the adsorbate (PNP) and the sorbent can be related to the equilibrium constant (K_s). The adjustable parameters were obtained from the "best fit" of the data to the Sips isotherm (*cf.* Equation 3.2) using a nonlinear least squares fitting procedure. Equation 3.2 assumes a distribution of adsorption energies at the sorbent surface and the exponent parameter (n_s) confers the properties of a homogenous sorbent when n_s=1.

Equation 3.3 provides an estimate of the surface area (SA) of copolymer materials, where Q_m is the maximum adsorption for monolayer coverage at equilibrium (mol/g), N is Avogadro's number (6.02×10^{23}/mol), σ is the cross-sectional molecular area of the adsorbate (m^2), and Y is the coverage factor (Y = 1 for *p*-nitrophenol).[22-23]

$$SA(m^2/g) = \frac{Q_m \times N \times \sigma}{Y} \qquad \text{Equation 3.3}$$

The coverage factor is determined according to the number of adsorbed layers of dye species at the surface of a solid adsorbent. The relatively low apolar surface area of PNP limits its aggregation behaviour, as compared with surfactants with moderate cmc values, and this is evidenced by the surface coverage factor (Y) of unity for this dye. The molecular area (σ) is 52.5 $Å^2$ for PNP when it orients in a co-planar orientation and 25.0 $Å^2$ when it adsorbs orthogonally with respect to a planar surface.[14]

Equation 3.4 provides an estimate of the accessible surface volume (SV) of the sorbent from the quantity of dye adsorbed (V_{ads}); where V_{PNP} is the molecular volume of PNP, and Q_m, N, and Y are defined in Equation 3.3.

$$SA(m^2/g) = \frac{Q_m \times N \times V_{PNP}}{Y} \quad \text{Equation 3.4}$$

3.4 Results and Discussion

3.4.1 Nitrogen Adsorption

Gas adsorption is typically carried out using suitable volatile (*e.g.*, N_2, CH_2Cl_2, and NH_3) adsorptives with solid adsorbents at various temperature and pressure conditions, as described by Equation 3.5.

$$n^a = f(p/p^o)_{T,\ gas,\ solid} \quad \text{Equation 3.5}$$

where n^a is the number of moles of gas adsorbed according to the relative equilibrium pressure conditions for the solid-gas adsorption experiment.

Figure 3.1 illustrates the nitrogen adsorption-desorption isotherms for an aliphatic-based (CDI-3) copolymer material. The behaviour portrayed by CDI-3 is representative of a Type IV isotherm characteristic of a non-porous material, according to IUPAC.[24-25] The SA (BET) estimate for CDI-3 is 0.332 m^2/g and is consistent in magnitude with an estimate (1.7-2.5 m^2/g) obtained in a recent study by Mahlambi *et al.*[26] for an HDI-based and a toluidine diisocyanate (TDI) urethane copolymer.[26] Other groups have reported greater SA estimates (~5.5 m^2/g) for HDI-8 copolymer (1:8 β-CD:HDI) and 0.92 m^2/g for TDI-10 copolymers (1:10 β-CD:TDI), respectively.[27-28] Comparable results to those shown in Figure 3.1 were reported for 1:22 β-CD-epichlorohydrin copolymers, and it was concluded that the latter is non-porous in nature with a very low

SA (BET, ~ 0.2 m^2/g).[6] The non-porous nature of CDI-3 is consistent with the low adsorbed volume of nitrogen (~ 0.3 m^2/g). The porosimetry results for the other CDI-X and HDI-X copolymers are not shown because the overall uptake characteristics with nitrogen are similarly low, as evidenced by their low surface areas (< 1 m^2/g).

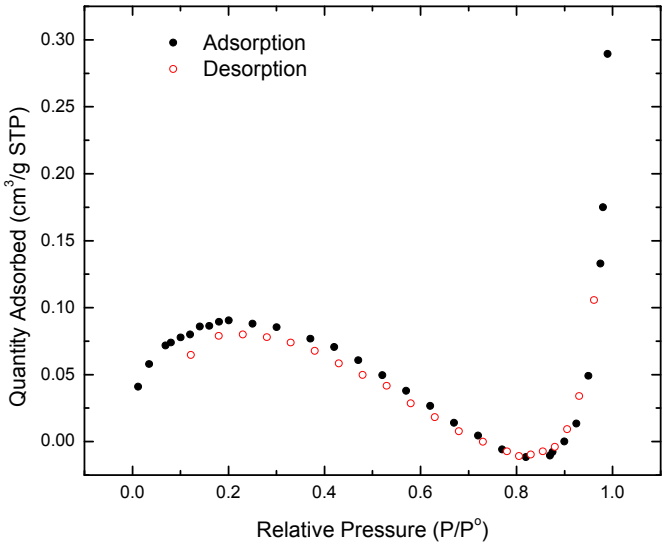

Figure 3.1. Nitrogen adsorption-desorption isotherm for the CDI-3 copolymer material at 77 K.

Figures 3.2-3.4 illustrate the nitrogen adsorption-desorption isotherms for the copolymer materials with variable types of aromatic linker units (PDI-X, MDI-X, and NDI-1) at different co-monomer mole ratios (X=1-3). The magnitude of the adsorbed volume of nitrogen varies according to the type of aromatic linker and the co-monomer mole ratio. PDI-X copolymers show similar mesopore characteristics and exhibit incremental adsorption capacity for nitrogen as –X increases. MDI-X copolymers show variable adsorption behaviour which does not appear to correlate with the relative co-monomer mole ratios. However, MDI-2 exhibits the largest SA (BET) among the

copolymers studied. The adsorption behaviour of NDI-1 (Figure 3.4) is very similar to that observed for PDI-1 (Figure 3.2a). In all cases, there is a sharp rise in adsorption for $p/p^o > 0.9$. This feature is attributed to interparticle condensation, and such domains represent substantial adsorption of nitrogen for such low SA mesopore materials.[24,29] In general, the greater SA of aromatic- *vs*. aliphatic-based copolymers is attributed to the more rigid scaffold framework of the former. At sufficiently high co-monomer ratios (~1:10) for the aliphatic-based copolymers,[27-28] the structural integrity of the framework is sufficiently dense to produce low surface area mesopore materials, as compared to the relatively non-porous material at low co-monomer ratios (*cf*. Figure 3.1).

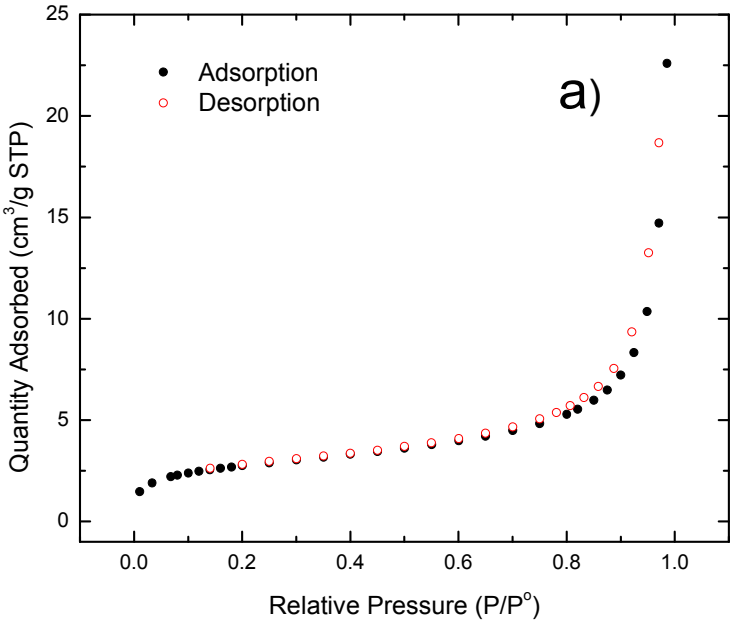

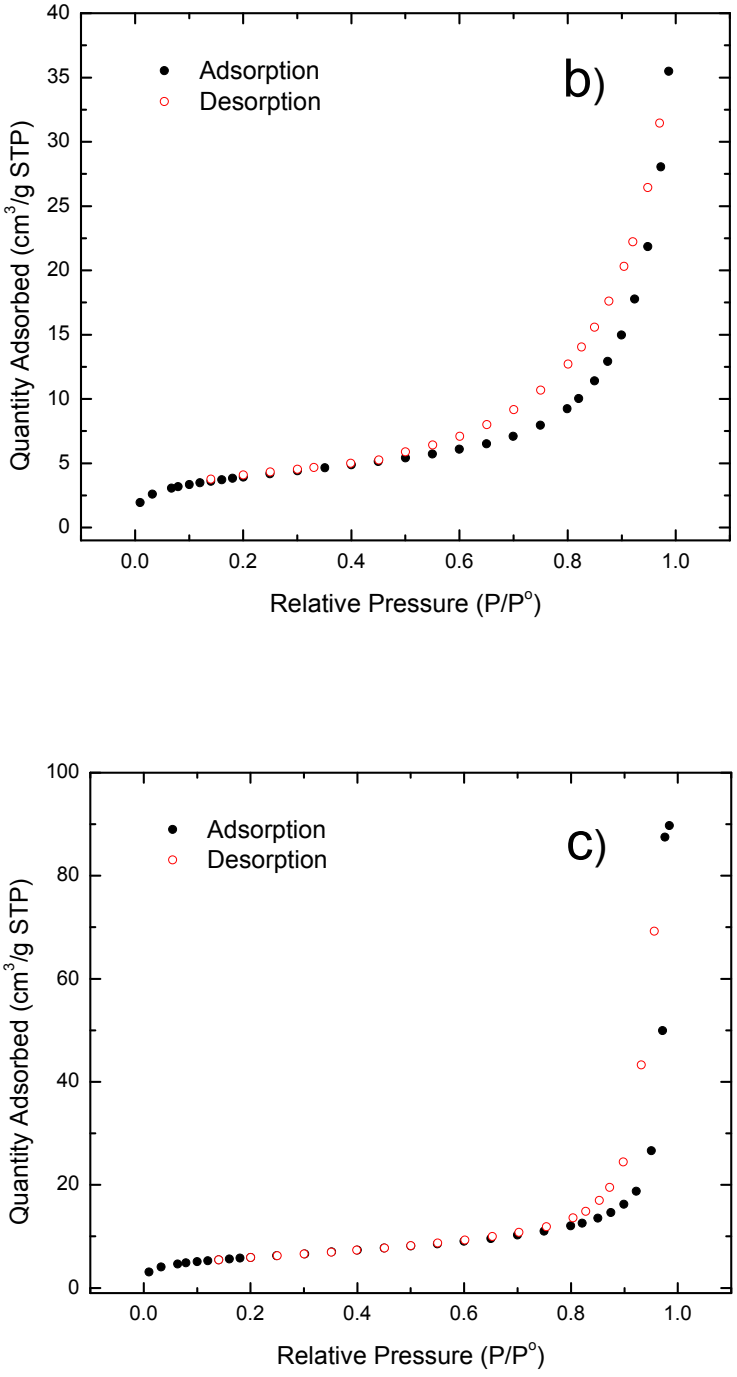

Figure 3.2. Nitrogen adsorption-desorption isotherm for β-CD copolymer materials; a) PDI-1, b) PDI-2, and c) PDI-3 at 77 K.

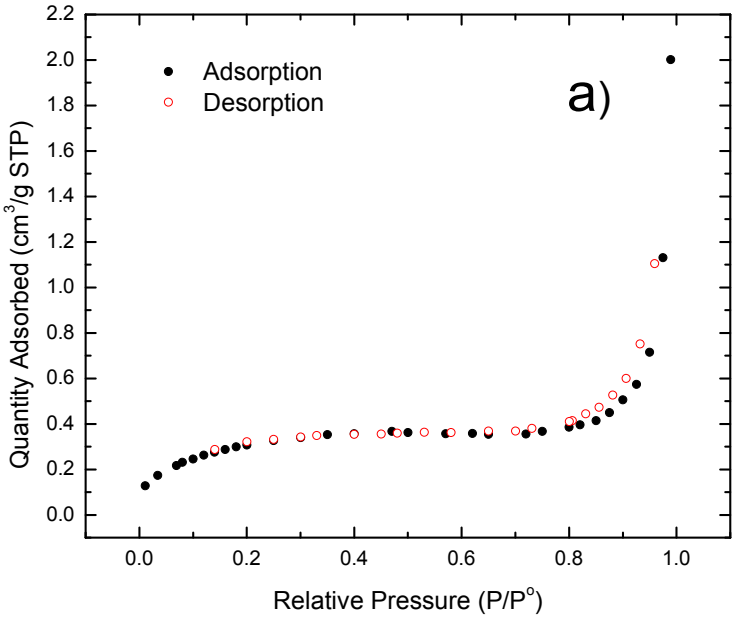
Adsorption
Desorption
a)
Quantity Adsorbed (cm3/g STP)
Relative Pressure (P/Po)
0.0
0.2
0.4
0.6
0.8
1.0
1.2
1.4
1.6
1.8
2.0
2.2

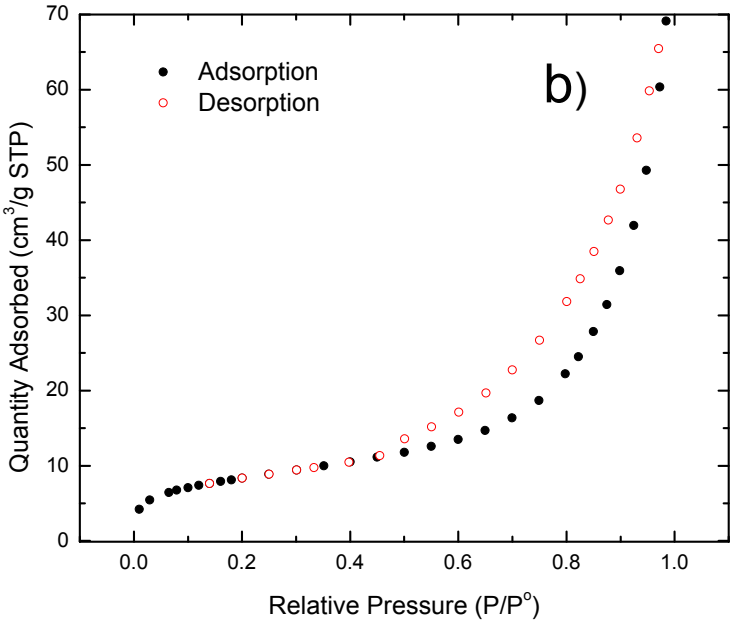
Adsorption
Desorption
b)
Quantity Adsorbed (cm3/g STP)
Relative Pressure (P/Po)
0
10
20
30
40
50
60
70
0.0
0.2
0.4
0.6
0.8
1.0

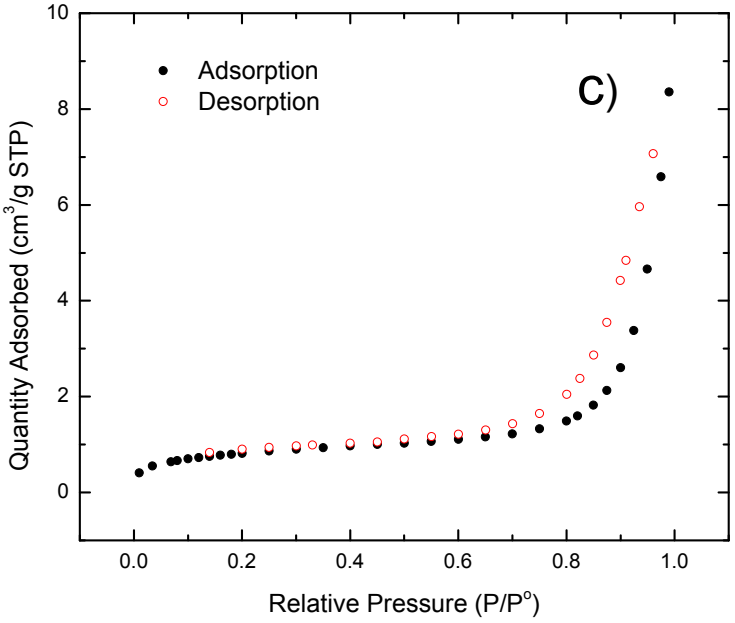

Figure 3.3. Nitrogen adsorption-desorption isotherm for β-CD copolymer materials; a) MDI-1, b) MDI-2, and c) MDI-3 at 77 K.

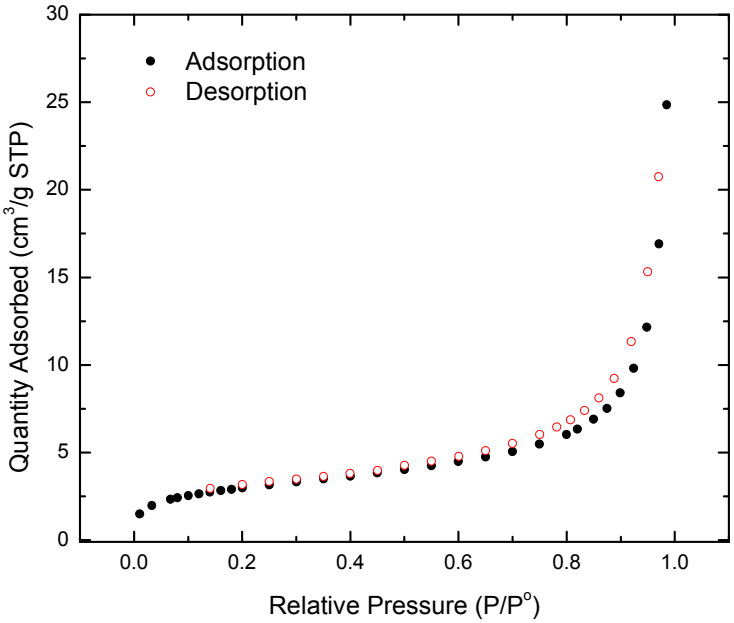

Figure 3.4. Nitrogen adsorption-desorption isotherm for the NDI-1 copolymer material at 77 K.

The qualitative features in Figures 3.1-3.4 describing the hysteresis loops enable prediction of the different categories of adsorption-desorption isotherms known to occur for copolymer materials.[25] In general, Type IV isotherms are observed with hysteresis loops arising from mesopore adsorption-desorption characteristics.[25] Type IV hysteresis loops also feature parallel and nearly horizontal branches which have been attributed to adsorption-desorption in narrow slit-like pores associated with narrow mesopore characteristics.[25]

As illustrated in Figures 3.1-3.4, the mesoporous copolymer materials display limited nitrogen adsorption according to their attenuated textural and framework mesoporosity characteristics, as compared with mesoporous silica materials and molecular imprinted polymers (MIPs).[4-5] Templated silica materials generally possess SA (BET) values in the range 10^2 – 10^3 m^2/g with substantive pore volume and good mechanical stability.[12] Framework mesopores originate from the inclusion and interstitial sites embedded within the copolymer network, as shown in Scheme 1.2 in Chapter 1.[30] The framework confined micropores are comparable to the diameter of the porogen (β-CD ~7-8 Å);[8] whereas, the interstitial mesopores can vary according to the size and the structural rigidity of the diisocyanate scaffold and the relative co-monomer mole ratios. A significant component of the textural porosity arises from the interparticle voids within the powdered sample. At 77 K, there may be potential shrinkage of the copolymer framework which affects the packing density and attenuates the adsorption capacity of the framework. Independent support of framework shrinkage in aerogel materials was previously reported and estimates indicate that ~50% of the pore volume may remain undetected.[31] The sinusoidal behaviour observed in Figure 3.1 for CDI-3 is consistent

with such shrinkage effects. These effects are anticipated to be less important as the co-monomer (-X) content increases. The presence of framework confined porosity is indicated by an adsorption over the relative pressure range from 0.4 to 0.9. From the height and slope of the sorption step in this region, a qualitative indication of the nature of the mesopore framework may be concluded. For materials with greater linker content (X>1), adsorption of nitrogen in this region generally increases, as evidenced by a steeper slope (*cf*. Figures 3.2-3.4). This general trend indicates that the framework confined porosity increases as –X increases for such copolymers. The results are consistent with the general observation that smaller mesopores result in materials with greater surface area and improved nitrogen adsorption.[15]

Regions with a reduced slope indicate that the mesopore framework is evidently less accessible. Similar observations were reported for calixarene-*co*-styrene polymer resins because of their amorphous, aperiodic, and limited pore structure characteristics.[32] The predominant pore structure was attributed to the "*inclusion sites*" of the calixarene macrocycle, as concluded by the low BET surface areas (0.15–1.7 m^2/g). In Figures 3.1-3.4, the textural mesoporosity (2-50 nm) is evidenced by a well-defined hysteresis loop for relative pressures between 0.4 - 0.8. A comparison of the adsorption isotherms for the copolymers reveal that the characteristics of the hysteresis loop depends on the relative co-monomer mole ratio and the type (*i.e*. aliphatic *vs*. aromatic) of the diisocyanate. In the case of PDI-X copolymers, the hysteresis loops are observed between the relative pressures between p/p^o = 0.4 to 0.7, MID-X ranges from 0.4 to 0.6, and the hysteresis loop for NDI-1 is observed at $p/p^o \sim 0.4$. The occurrence of hysteresis is a function of the porosity as well as the packing efficiency of the powder grains in the copolymer

sample.[29] The aliphatic and aromatic diisocyanates may vary according to their molecular volume according to their conformational motility, particularly for the flexible aliphatic co-monomers. In view of the variable molecular volume of the diisocyanate linkers, there is no unequivocal trend that exemplifies increasing SA for the aromatic-based copolymers materials. However, copolymers which contain aromatic-based linkers are generally more rigid than aliphatic-based copolymer materials. The greater conformational lability of aliphatic-based diisocyanates results in a collapsed mesopore structure in order to offset the unfavourable interfacial energy of an open framework. Independent estimates of the non-porous characteristics of HDI- and TDI-based copolymers was previously reported and the results are in accordance with the low SA (BET) values (1.7-2.5 m^2/g) obtained herein.[26] Table 3.1 lists the parameters for the textural properties of β-CD copolymer materials estimated from the nitrogen adsorption results at 77 K. The textural properties of polyamines and silica materials grafted with cyclodextrins were similarly investigated.[33-35] In most cases, relatively small changes in the SA (BET) was observed upon incorporation of CD onto the sorbent framework, and this is consistent with the results provided in Table 3.1.

Table 3.1. Textural parameters of nanoporous copolymer materials derived from nitrogen adsorption isotherms at 77K.

Sorbent Material	SA (BET) (m^2/g)[a]	Micropore SA(m^2/g)[b]	Mesopore PV[c] $10^3(cm^3/g)$	Total PV[d] (cm^3/g)	PD[e] (nm)
HDI-3	< 1	NR	NR	NR	NR
CDI-3	0.332	NR	NR	NR	NR
PDI-1	9.88	1.83	0.726	0.0343	18.2
PDI-2	14.3	1.15	0.329	0.0554	16.3
PDI-3	21.3	2.98	1.13	0.140	29.1
MDI-1	1.18	~ 0	~ 0	0.00297	16.3
MDI-2	30.4	2.30	0.632	0.108	14.0
MDI-3	2.96	0.363	0.125	0.0128	22.4
NDI-1	10.8	1.13	0.369	0.0382	16.7
GAC	951	641	310	0.307	5.71

NR – not reported due to the limited nitrogen adsorption
The SA (BET) for crystalline β-CD = 0.635 m^2/g
[a]BET Surface area, as determined from multi-point BET analysis
[b]Micropore SA obtained using the t-plot
[c]Micropore volume obtained using the t-plot
[d]Total pore volume (PV) obtained using BJH adsorption isotherm
[e]Average pore diameter (PD) using BJH adsorption isotherm

Figures 3.5a-b illustrates the pore size distribution as depicted by the dependence between the BJH pore volume and the pore diameter (PD) for MDI-2 and MDI-3 copolymers, respectively. The PD results reported here are representative of the copolymers investigated, and were obtained from an analysis of the adsorption branch depicted in Figures. 3b-c. The well-defined mesopore characteristics for MDI-2 are more evident than those for PDI-3. The narrow pore size distribution for MDI-2 and its greater intensity compared with MDI-3 parallels the relative differences for he SA (BET) values; MDI-2 > MDI-3 (*cf.* Table 3.1).

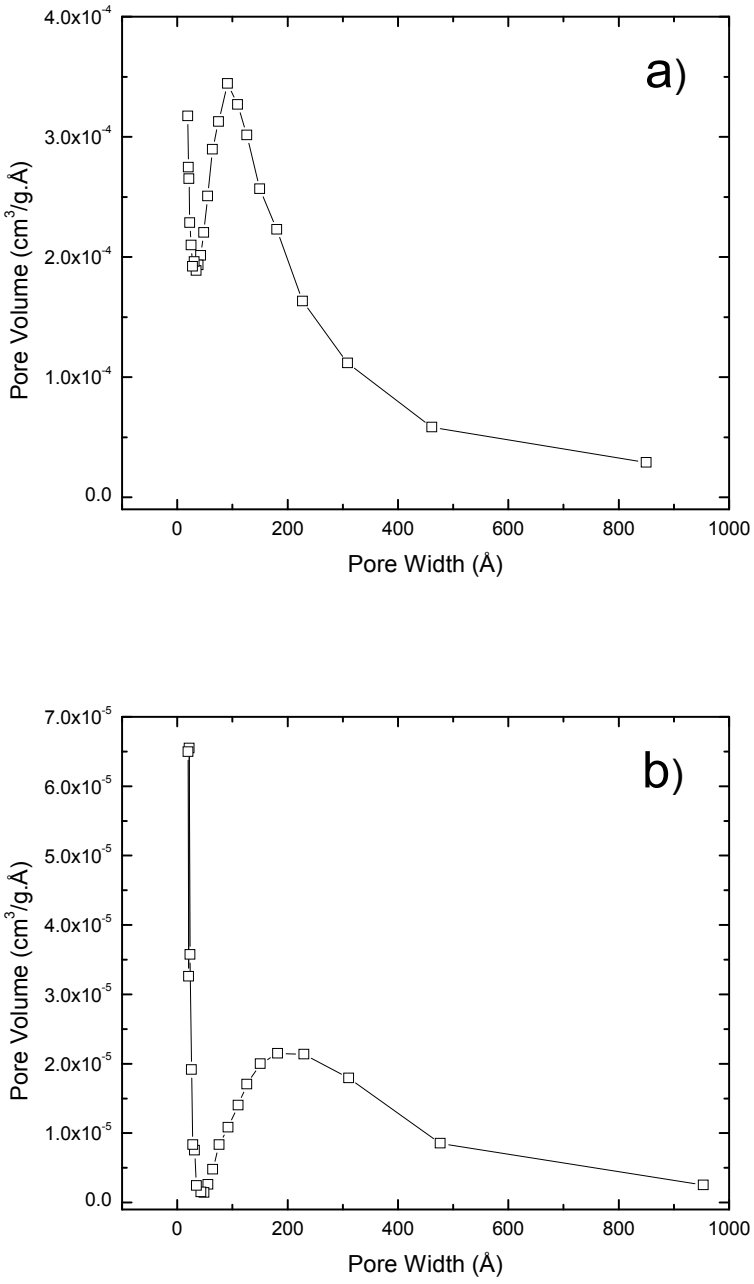

Figure 3.5. BJH Pore volume vs. pore diameter (Å) for MDI-X copolymer materials determined from the nitrogen adsorption branch of the nitrogen isotherm profile: a) MDI-2 and b) MDI-3 at 77 K.

In general, the BJH pore diameter (PD) for the copolymer materials ranges between 16.3 to 29.1 nm. Given that the inner diameter of β-CD ~ 0.7-0.8 nm, a major

contribution to the pore structure likely originates from the "non-inclusion sites" and/or the textural mesoporosity (*cf*. Scheme 1.2 in Chapter 1). Despite the variable molecular volume of the aromatic diisocyanates (*i.e*. PDI, NDI, and MDI), relatively invariant pore widths are observed. Likewise, a similar range of pore diameters (11.1 - 21.1 nm) was observed in siloxane-based films templated with (2,3,6-tri-O-methyl)-β-CD that varied according to the level of porogen loading of the film.[34]

3.4.2. Dye Sorption Results

In the case of solid-solution isotherms, adsorption into the sorbent phase (Q_e) can be investigated by measuring the equilibrium concentration (C_e) of the unbound dye relative to the total dye concentration (C_o),

$$Q_e = f\,(C_e / C_o)_{T,\ solution,\ solid} \qquad \text{Equation 3.6}$$

In contrast to gas adsorption methods at 77 K (*cf*. Equation 3.5), the temperature conditions are generally greater (~295 K) for solid-solution adsorption processes. The equilibrium isotherms provide a detailed understanding of the thermodynamics of adsorption for a given sorbent-sorbate system. The isotherm is represented as a plot of Q_e versus C_e (*cf*. Equation 3.1) and the Sips (*cf*. Equation 3.2) adsorption parameters (*e.g*., Q_m) is arguably the most important physicochemical property, as suggested in recent reviews.[7,9]

At pH = 4.6, PNP is adsorbed uniformly onto the linker domains and within the β-CD inclusion sites of the entire framework. Therefore, dye-based SA estimates are considered to be more reliable for PNP in its protonated form (pH=4.6) since the dye adsorbs to the entire framework at these conditions.[35] At elevated pH (pH = 9.0) above the pK_a of PNP, the dye is bound predominantly within the inclusion sites of β-CD.[35]

Table 3.2 summarizes the monolayer adsorption capacity (Q_m) of the copolymer materials along with the SA estimates of the copolymers in the presence of PNP. A comparison of these results (Table 3.2) with the SA (BET) estimates obtained from nitrogen adsorption (*cf*. Table 3.1) reveals significant differences. The porosimetry derived SA (BET) values in Table 3.1 range from 1 to 30 m^2/g and are an order of magnitude lower than the dye-based values in Table 3.2. The differences are attributed to the diverse nature of the experimental conditions (*cf*. Equation 3.5 and 3.6) for each technique. The greater SA estimates derived from the dye-based method are attributed to framework structural changes of the copolymer in water. In a previous study, the occurrence of swelling for CD-based copolymers was reported.[6-7,30,36-37] Quantitative estimates of the swelling were determined from the water uptake measurements for a urethane-methacrylate β-CD copolymer that ranged from 34.2-50.2%.[38] Preliminary results obtained for the swelling of CDI-X copolymers in water at ambient conditions indicate uptake values that range from ~30% to ~20% for X = 1 to X = 3. In view of the substantial hydration and volumetric changes between an anhydrous copolymer and its hydrated state, the changes in hydration are anticipated to contribute significantly to their textural properties. Pronounced changes in the textural properties were observed in a recent structural study of dextran-based hydrogels by Ferreira *et al.*.[39] The observed differences in the pore diameter of anhydrous gels were concluded from nitrogen adsorption and mercury intrusion porosimetry. The hydrated hydrogels were cryofixed and examined using TEM and the observed swelling and increased pore diameters agreed with the equilibrium swelling theory of Flory-Rehner.[40]

Table 3.2. Dye-based estimates of the monolayer adsorption capacity (Q_m)[a], surface area (SA)[b], and adsorbed volume (V_{ads})[c] for the copolymer materials at 295 K and pH 4.60 in aqueous solution with p-nitrophenol (PNP).

Copolymer	SA (m^2/g)	V_{ads} (m^3/g)	Q_m (mmol/g)
HDI-1	~0	~0	~0
HDI-2	364	19.9	1.15
HDI-3	364	19.9	1.15
CDI-1	156	8.51	0.492
CDI-2	598	32.7	1.89
CDI-3	620	33.9	1.96
MDI-1	180	9.82	0.568
MDI-2	300	16.4	0.950
MDI-3	449	24.6	1.42
PDI-1	149	8.14	0.471
PDI-2	395	21.6	1.25
GAC	641	35.1	2.03
GL-CDI (1:3)	31.0	1.70	0.0981
CL-CDI (1:3)	348	19.0	1.10

CL = cellobiose and GL = glucose

[a]Obtained using the Sips isotherm model (*cf*. Equation 3.2)

[b]SA (m^2/g) = ($Q_m \times N \times \sigma$) / Y; where Y=1 and σ= 52.5 Å^2

[c] $\mathbf{V_{ads}}$ (m^3/g) as in Equation 3.4 where Y=1 and

V_{PNP} = 0.64 nm × 0.43 nm × 0.33 nm = 9.08×10^{-26} nm^3 (*cf*. ref. 47)

The values of Q_m listed in Table 3.2 for PNP adsorption were determined using the Sips isotherm model (Equation 3.2). The apparent surface area (SA) for each copolymer was calculated according to the known value for PNP in its protonated form (*cf*. Equation 3.3), as listed in Table 3.2. The surface area estimates are dependent on an assumed orientation (planar) of PNP with respect to the sorbent surface,[14] in accordance with the parameter (σ) in Equation 3.3.[18,36] Webster *et al*.[41] reported a quantum mechanical approach that uses ZINDO (Zerner's Intermediate Neglect of Differential Overlap) molecular orbital theory in conjunction with a multiple equilibrium analysis for the calculation of sorbent surface areas. This approach is beyond the scope of this study

but it does reveal that surface areas of sorbents are probe dependent, and parameters (i.e. σ) that are generally obtained from bulk density measurements may not be representative of conditions used in dye-based experiments. However, the utility of the dye-based approach using PNP is fairly well established for low surface area sorbents and the method has been extended to other dye-adsorbate systems.[22,42] The reliability of the dye-based method for the determination of sorbent textural properties is evidenced by the relative similarity of the SA values for activated carbon (AC) in Tables 3.1 and 3.2, respectively. Previous reports on the surface area properties of carbon black AC using nitrogen- and dye-based (i.e. PNP) adsorption showed very good agreement.[23,43] Inel and Tumsek[18] have reported consistent surface area estimates of silicate materials using the above methods. Similarly, good agreement was observed for calcined or sulfated MCM-41 materials [44] and phthalocyanine network polymers[45]. The comparable values obtained from porosimetry and dye-based methods are attributed to the limited swelling and rigid framework characteristics of such materials in the solid state and aqueous solution, respectively.

According to the dye-based estimates in Table 3.2, the SA and V_{ads} generally increase as X increases for a particular crosslinker unit. The textural results for two non-porogen copolymers are included for cellobiose (CL) and glucose (GL), and these materials provide a comparison with the CD-based (*i.e.* porogen-based) copolymer materials. The SA values for CL-CDI (1:3) are greater than GL-CDI (1:3). This difference in SA values for GL-CDI and CL-CDI copolymers are related to the difference in molecular volume of the monosaccharide (GL) and disaccharide (CL) crosslinker units respectively. The relative similarity of the SA for the cellobiose-based copolymer

compared to the CDI-X copolymers merit further support that dye sorption occurs at "*non-inclusion*" as well as the β-CD "*inclusion*" sites of the copolymer (*cf*. Scheme 2).[35]

Previous sorption studies have hypothesized the occurrence of inclusion binding and non-inclusion adsorption of dyes onto the copolymer framework.[30,46] Therefore, SA estimates of CD-based polymers using the dye-based method are subject to error when an inappropriate isotherm (e.g. Langmuir) is applied to the heterogeneous sorption (i.e. multi-site binding) phenomena. The Sips isotherm represents a versatile and general model which accounts for a broad range of homogeneous and heterogeneous sorption phenomena, according to the exponent parameter (n_s) in Equation 3.2.[17,47] Ma and Li previously reported[48] that PNP solely forms inclusion complexes with urethane copolymer materials with a substantially higher binding affinity (K_{eq} ~10^9 M^{-1}), as compared with the 1:1 β-CD/PNP complex (K_{eq} ~ 197 M^{-1}).[49] We conclude that the binding affinity reported in the latter study[49] is an artifact arising from an inadequate assessment of the bound concentrations of PNP in relation to the two types of potential binding sites, as outlined in Scheme 1.2 in Chapter 1. The published results[49] do not adequately account for the presence of multiple binding sites (i.e. inclusion *vs.* non-inclusion) in the urethane copolymer framework (*cf*. Scheme 1.2 in Chapter 1), as outlined previously.[30,35] Based on a comprehensive sorption study (*cf*. Chapter 9)[35] of related urethane copolymers with PNP, the binding affinities (K_{eq} ~ 10^1 -10^2 M^{-1}) for the copolymers are similar to those for the 1:1 native β-CD/PNP complex in aqueous solution at 295 K. We conclude that the slightly attenuated binding affinity observed for urethane copolymer materials is attributed to steric effects of the inclusion sites and contributions arising from competitive binding equilibria at the different adsorption sites (*cf*. Scheme

1.2) on the copolymer framework. It is worthwhile noting that the binding affinity derived from Equation 3.3 represents an average value of the multiple adsorption sites (*cf*. Scheme 1.2) for the copolymer materials.[35] Experimental support in favour of the presence of multiple binding sites is further supported by the heterogeneity parameter (n_s), and its magnitude is observed to deviate from unity (n_s = 0.56 – 1.2) deviate from unity. The latter corresponds to a homogeneous sorbent material with one type of adsorption site (i.e. Langmuir model). Such deviations from n_s are more pronounced for aromatic-based copolymer materials (*e.g*., PDI-, MDI-, and NDI-X) as compared with the aliphatic-based sorbents. Aromatic-based copolymers are expected to exhibit favourable π-π stacking and lipophilic interactions with PNP and the diisocyanate crosslinker sites in the interstitial domains of the copolymer framework.[8,35,47]

3.5. Conclusions

The nitrogen adsorption-desorption isotherms of porogen-based urethane copolymers provided estimates of the surface area and pore structure properties. \in general, aromatic-based copolymers displayed greater BET surface areas (~10^1 m^2/g), as compared with aliphatic-based materials (≤ 1 m^2/g), according to nitrogen adsorption. Nitrogen adsorption surface area estimates (BET) were systematically lower than results obtained using the dye-based method (SA = 1.5-6.2×10^2 m^2/g) where PNP was used as the adsorptive probe at pH = 4.6.

The results illustrate the importance of framework rigidity, swelling, and surface accessibility of the adsorptive onto the sorbent surface. Differences in the adsorption parameters from the solid-gas and solid-solution isotherms were attributed to differences

arising because of hydration and swelling of the anhydrous *vs*. hydrated states of the copolymer framework. The surface area and pore structure properties of the copolymers were found to vary according to the type of diisocyanate crosslinker, co-monomer mole ratios, and the hydration state of the copolymer framework. In general, the disparity of SA values between solid-gas and solid-solution adsorption techniques is apparent for these types of "*soft*" carbohydrate-based materials. In contrast, good agreement is obtained for "*rigid*" frameworks such as silicates and graphene-based carbon materials were previously reported.[18,23,43] The results obtained in this work are anticipated to contribute to the systematic design of "*soft*" copolymer sorbents with improved sorption capacity and molecular recognition properties for a range of sorption-based applications. Additional work in our laboratory is underway to obtain a deeper understanding of the swelling and hydration properties of these types of nanoporous copolymer materials.

3.6 Acknowledgments

The authors are grateful for the support provided by the Natural Sciences and Engineering Research Council (NSERC), the Program of Energy Research and Development (PERD), and the Canada Foundation for Innovation (CFI). M.H.M acknowledges the University of Saskatchewan for the award of a Graduate Teaching Fellowship and Environment Canada for the Science Horizons Program award.

3.7 References

1. Polarz, S.; Antonietti, M. *Chem. Commun. (Cambridge, U.K.)* **2002**, 2593-2604.
2. Lin-Gibson, S.; Cooper, J. A.; Landis, F. A.; Cicerone, M. T. *Biomacromolecules* **2007**, *8*, 1511-1518.

3. Jozefaciuk, G.; Muranyi, A.; Fenyvesi, E. *Environ. Sci. Technol.* **2003**, *37*, 3012-3017.
4. Urraca, J. L.; Carbajo, M. C.; Torralvo, M. J.; González-Vázquez, J.; Orellana, G.; Moreno-Bondi, M. C. *Biosens. Bioelectron.* **2008**, *24*, 155-161.
5. Asouhidou, D. D.; Triantafyllidis, K. S.; Lazaridis, N. K.; Matis, K. A. *Colloids Surf., A,* **2009**, *346*, 83-90.
6. Yu, J. C.; Jiang, Z.-T.; Liu, H.-Y.; Yu, J.; Zhang, L. *Anal. Chim. Acta* **2003**, *477*, 93-101.
7. Crini, G. *Prog. Polym. Sci.* **2005**, *30*, 38-70.
8. Steed, J. W.; Atwood, J. L. *Supramolecular Chemistry*; 2nd ed.; John Wiley & Sons, Ltd: West Sussex, UK, 2009.
9. Pan, B.; Pan, B.; Zhang, W.; Lv, L.; Zhang, Q.; Zheng, S. *Chem. Eng. J.* **2009**, *151*, 19-29.
10. Mohamed, M. H.; Wilson, L. D.; Headley, J. V.; Peru, K. M. *Process Saf. Environ. Prot.* **2008**, *86*, 237-243.
11. Mohamed, M. H.; Wilson, L. D.; Headley, J. V. *Carbohydr. Polym.* **2010**, *80*, 186-196.
12. Carbonnier, B.; Janus, L.; Lekchiri, Y.; Morcellet, M. *J. Appl. Polym. Sci.* **2004**, *91*, 1419-1426.
13. Zhang, W.; Qin, L.; He, X.-W.; Li, W.-Y.; Zhang, Y.-K. *J. Chromatogr., A* **2009**, *1216*, 4560-4567.
14. Allen, T. *Particle Size Measurement:: Surface Area and Pore Size Determination*; 5th ed.; Chapman & Hall, 2-6 Boundary Row: London, UK, 1997; Vol. 2.
15. Sing, K. *Colloids Surf., A,* **2001**, *187-188*, 3-9.
16. Broekhoff, J. C. P.; De Boer, J. H. *J. Catal.* **1968**, *10*, 153-165.
17. Barrett, E. P.; Joyner, L. G.; Halenda, P. P. *J. Am. Chem. Soc.* **1951**, *73*, 373-380.
18. Inel, O.; Tumsek, F. *Turk. J. Chem.* **2000**, *24*, 9-19.
19. Sips, R. *J. Chem. Phys.* **1948**, *16*, 490-495.
20. Langmuir, I. *J. Am. Chem. Soc.* **1918**, *40*, 1361-1402.
21. Freundlich, H. M. F. *J. Phys. Chem.* **1906**, *57A*, 385-470.

22. Giles, C. H.; Macewan, T. H.; Nakhwa, S. N.; Smith, D. *J. Chem. Soc.* **1960**, *3*, 3973-3993.
23. Lynam, M. M.; Kilduff, J. E.; Weber, W. J. *J. Chem. Educ.* **1995**, *72*, 80-84.
24. Sing, K. S. W. *J.Porous Mat,* **1995**, *2*, 5-8.
25. Sing, K. S. W. *Pure Appl. Chem.* **1985**, *57*, 603-619.
26. Mahlambi, M.; Malefetse, T.; Mamba, B.; Krause, R. *J. Polym. Res.* **2010**, *17*, 589-600.
27. Sun, Z. Y.; Cao, G. P.; Lv, H.; Zhao, L.; Liu, T.; Montastruc, L.; Iordan, N. *J. Appl. Polym. Sci.* **2009**, *114*, 3882-3888.
28. Appell, M.; Jackson, M. *J. Inclusion Phenom. Macrocyclic Chem.* **2010**, 1-6.
29. Conner, W. C.; Blanco, C.; Coyne, K.; Neil, J.; Pajares, J. *J. Catal.* **1987**, *106*, 202-209.
30. Pratt, D. Y.; Wilson, L. D.; Kozinski, J. A.; Mohart, A. M. *J. Appl. Polym. Sci.* **2010**, *116*, 2982-2989.
31. *Aerogels, Springer Proceedings in Physics 6*; Schuck, G.; Dietrich, W.; Fricke, J., Eds.; Springer-Verlag: Berlin, 1986.
32. Baudry, R.; Graillat, C.; Felix, C.; Lamartine, R. *J. Mater. Chem.* **2005**, *15*, 759-763.
33. a) Crini, G.; Janus, L.; Morcellet, M.; Torri, G.; Naggi, A.; Bertini, S.; Vecchi, C. *J. Appl. Polym. Sci.* **1998**, *69*, 1419-1427. b) Phan, T. N. T.; Bacquet, M.; Morcellet, M. *J. Inclusion Phenom. Macrocyclic Chem.* **2000**, *38*, 345-359.
34. Yim, J. H.; Lyu, Y. Y.; Jeong, H. D.; Song, S.; Hwang, I. S.; Hyeon-Lee, J.; Mah, S.; Chang, S.; Park, J. G.; Hu, Y.; Sun, J.; Gidley, D. *Adv. Funct. Mater.* **2003**, *13*, 382-386.
35. Mohamed, M. H.; Wilson, L. D.; Headley, J. V. *J. Colloid Interface Sci.* **2011**, *356*, 217-226.
36. Thatiparti, T. R.; Recum, H. A. v. *Macromol. Biosci.* **2010**, *10*, 82-90.
37. Mele, A.; Castiglione, F.; Malpezzi, L.; Ganazzoli, F.; Raffaini, G.; Trotta, F.; Rossi, B.; Fontana, A.; Giunchi, G. *J. Inclusion Phenom. Macrocyclic Chem.* **2010**, 1-7.

38. Demir, S.; Kahraman, M. V.; Bora, N.; Apohan, N. K.; Ogan, A. *J. Appl. Polym. Sci.* **2008**, *109*, 1360-1368.
39. Ferreira, L.; Figueiredo, M. M.; Gil, M. H.; Ramos, M. A. *J. Biomed. Mater. Res., Part B* **2006**, *77B*, 55-64.
40. Flory, P. J.; Rehner, J. *J. Chem. Phys.* **1943**, *11*, 521-526.
41. Webster, C. E.; Drago, R. S.; Zerner, M. C. *J. Am. Chem. Soc.* **1998**, *120*, 5509-5516.
42. a) Kuhn, P.; Kruger, K.; A, T.; Antonietti, M. *Chem. Commun* **2008**, 5815-5817. b) Giles, C. H.; D'Silva, A. P.; Trivedi, A. S. *J. Appl. Chem.* **1970**, 20, 37-41.
43. Gonzalez-Martin, M. L.; Valenzuela-Calahorro, C.; Gomez-Serrano, V. *Langmuir* **1994**, *10*, 844-854.
44. Monash, P.; Pugazhenthi, G. *Adsorption* **2009**, *15*, 390-405.
45. Maffei, A. V.; Budd, P. M.; McKeown, N. B. *Langmuir* **2006**, *22*, 4225-4229.
46. García-Zubiri, Í. X.; González-Gaitano, G.; Isasi, J. R. *J. Colloid Interface Sci.* **2007**, *307*, 64-70.
47. Mohamed, M. H.; Wilson, L. D.; Headley, J. V.; Peru, K. M. *Phys. Chem. Chem. Phys*.: **2011**, *13*, 1112-1122.
48. Ma, M.; Li, D. *Chem. Mater.* **1999**, *11*, 872-874.
49. Eftink, M. R.; Harrison, J. C. *Bioorg. Chem.* **1981**, *10*, 388-398.

3.8 Supplementary Information

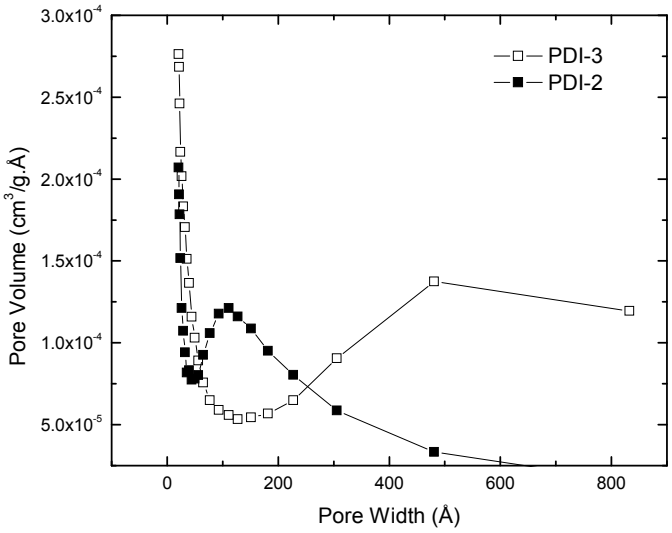

Figure 3.6. BJH Pore volume vs. pore diameter (Å) for PDI-X copolymer materials determined from the nitrogen adsorption branch of the nitrogen isotherm profile: a) PDI-2 and b) PDI-3 at 77 K

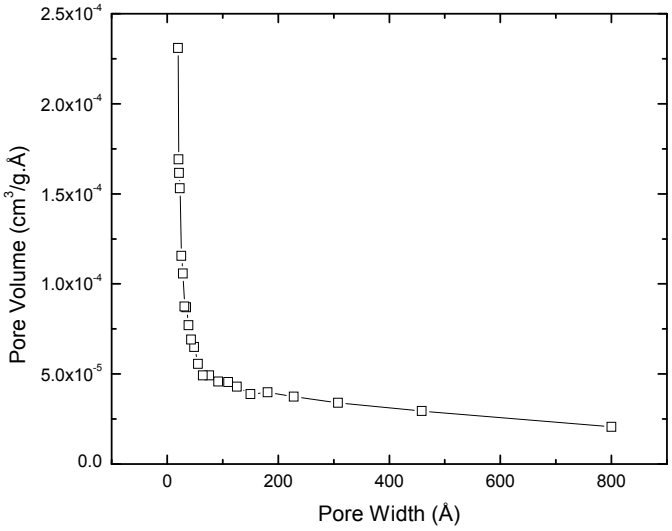

Figure 3.7. BJH Pore volume vs. pore diameter (Å) for NDI-X1copolymer material determined from the nitrogen adsorption branch of the nitrogen isotherm profile.

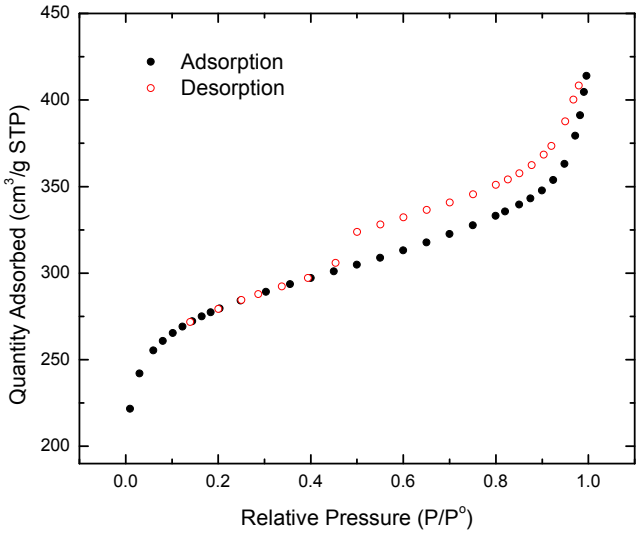

Figure 3.8. Nitrogen adsorption-desorption isotherm for GAC at 77 K

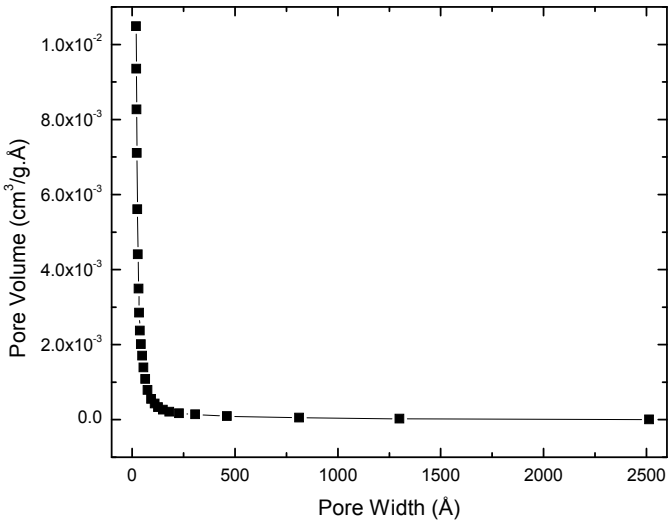

Figure 3.9. BJH Pore volume vs. pore diameter (Å) for GAC determined from the nitrogen adsorption branch of the nitrogen isotherm profile

CHAPTER 4

PUBLICATION 3

Description

The following is a verbatim copy of an article that was published in December of 2008 in the journal Carbohydrate Polymers (*Carbohydr. Polym.:* **2010**, *80(1)*, 186-196) and describes the estimation of surface accessible β-CD sites in the copolymers studied in this project. Phth was used as a probe to determine the inclusion accessibility of β-CD under heterogeneous solid-solution adsorption conditions.

Authors' Contribution

I performed all of the experimental work with some technical assistance from Mr. Joel Hardes who collected UV-Vis data. I wrote the first draft of the manuscript with extensive editing by each supervisor prior to submission for publication. This work was supervised by Dr. Wilson and Dr. Headley. Written permission was obtained from all contributing authors and the publishers to include this material in this thesis.

Relation of Chapter 4 (Publication 3) to the Overall Objectives of this Project

As mentioned in the introduction (Chapter 1), there is a significant interest in determining the surface accessible β-CD sites. The target of this project was to use β-CD in polymeric form to include NAs in its cavity. Therefore, it was important to determine the percentage of accessible sites of the β-CD cavities. At the time of this publication,

there was no literature that has shown the use of this method for the quantification as outlined in this publication.

4. Estimation of the Surface Accessible Inclusion Sites of β-Cyclodextrin Based Copolymer Materials

Mohamed H. Mohamed,[§] Lee D. Wilson, [§] John V. Headley[¥]*

[§]Department of Chemistry, University of Saskatchewan, 110 Science Place, Saskatoon, Saskatchewan, S7N 5C9

[¥]Water Science and Technology Directorate, 11 Innovation Boulevard, Saskatoon, Saskatchewan, S7N 3H5

*Corresponding Author

Received 25 September 2009

4.1 Abstract

Aqueous solutions containing insoluble β-cyclodextrin (β-CD) based urethane copolymers were studied in aqueous solutions by measuring the absorbance changes (decolourization) of phenolphthalein (phth) at pH 10.5. The various copolymers were comprised of β-CD and five diisocyanate linkers (1,6-hexamethylene diisocyanate (HDI), 4,4'-dicyclohexyl diisocyanate (CDI), 4,4'-diphenylmethane diisocyanate (MDI), 1,4-phenylene diisocyanate (PDI), and 1,5-naphthalene diisocyanate (NDI)). The copolymers studied were prepared at the β-CD: linker reactant ratios 1:1, 1:2, and 1:3, respectively. The decolourization studies provided estimates of the 1:1 binding constants (K_1) for the monomer β-CD/phth inclusion complex. It was concluded that the values of K_1 for copolymer/phth systems for highly accessible β-CD inclusion sites in copolymer materials closely resembles the K_1 value for the 1:1 β-CD/phth complex. The surface accessibility of the β-CD inclusion binding sites for the copolymers ranged from 1-100%.

The observed variability was attributed to steric effects in the annular hydroxyl region of β-CD and the relative accessibility of the micropore sites within the polymer framework as a consequence of the variable cross linking. The Gibbs free energy of complex formation (ΔG^o) and site occupancy (θ) of phth adsorbed to the copolymer materials was estimated independently using the Sips isotherm model. The ΔG^o values ranged between -27 to -30 kJ mol^{-1} and are in agreement with the Gibbs free energy for the 1:1 β-CD/phth complexes (~ -27 kJ mol^{-1}). The phth decolourization technique provides a simple, low cost and versatile method for the estimation of the surface accessible inclusion sites of β-CD in CD based urethane copolymer materials. This method is anticipated to have extensive analytical applications in materials research and for the design of functional β-CD based sorbent materials.

4.2 Introduction

Cyclodextrins (CDs) are cyclic compounds consisting of six, seven, or eight α-D-glucopyranose units connected by α-(1→4) linkages commonly referred to as α-, β-, and γ-CDs, respectively.[1] CDs possess a characteristic toroidal shape with a well-defined lipophilic cavity and a hydrophilic exterior that is suitable for the inclusion binding of appropriate sized guest compounds (*cf*. Scheme 4.1). CDs are of interest, in part, because of their ability to form stable inclusion complexes in aqueous.[2-7]

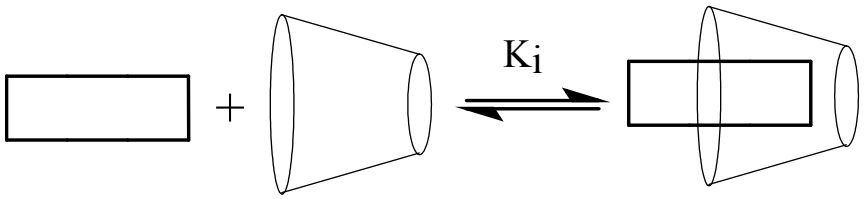

Scheme 4.1: The formation of a host-guest complex is shown for a β-CD (toroid) and a guest molecule (rectangle) according to an equilibrium process where K_i is the 1:1 equilibrium binding constant and the solvent has been omitted for clarity.

Recently, β-CD has been incorporated into cross linked polymeric forms using a variety of linker molecules (e.g., epichlorohydrin, glutaraldehye, succinyl chloride, diisocyanates, diacid chlorides, dicarboxylic acids, cyanuric chloride).[8-11] These types of copolymer materials have been utilized for the sequestration of organic compounds from the gas and condensed phases. The determination of the number of availability of inclusion sites is an important parameter for the characterization of the sorption properties β-CD based copolymer materials. The surface area and pore structure characteristics are important physiochemical properties known to affect the sorption properties of porous polymeric materials; particularly for amorphous and non-templated materials.[12] Estimation of the available inclusion sites is anticipated to provide an understanding of the relative role of β-CD inclusion sites and the linker domains in the sorption mechanism, particularly for heterogeneous polymer sorption in aqueous solution. Porosimetry provides estimates of all the surface accessible regions (micropores to macropores), however; backfill gases (e.g., nitrogen or argon) are not selectively bound to different adsorption sites. In contrast, techniques such as X-ray diffraction (XRD) are less discriminatory and provide estimates of the total surface accessible and inaccessible pores. Solution based dye sorption methods provide complementary information about the surface accessible regions (e.g., inclusion and linker domains) of β-CD based copolymer materials.

Binding constants of β-CD inclusion complexes have been previously estimated using direct and indirect methods. Direct methods typically involve the measurement of the concentration of bound or unbound guest molecules and include methods such as ^{1}H NMR[13], sound velocity[14], conductivity[15], surface tension[16], electrochemical

measurements[17], UV-Vis[18], and fluorescence[19] spectrophotometry. Spectrophotometric methods[19-26] employ the measurement of absorbance changes of suitable organic dyes such as phenolphthalein (phth), methyl orange (MO) and *p*-nitrophenol (PNP) in the presence of a host molecule.[20-29] Phenolphthalein is a preferred chromophoric dye in UV-Vis spectrophotometry because it exhibits molecular recognition with β-CD as evidenced by its specific inclusion geometry,[2-3,5] and a relatively large 1:1 binding constant ($K_1 \sim 10^4$ M^{-1}).[20,22-24,26-27]

Characterization of the sorption properties of microporous copolymer materials containing β-CD involves an estimation of the surface accessible binding sites.[30-34] The ability to measure the accessible β-CD inclusion sites is necessary when designing suitable sorbent materials that require inclusion binding for specialized applications. Recent studies have examined the interaction between phenolphthalein (phth) and β-CD copolymer materials; however, no detailed quantitative studies were reported at the time of this publication.[32,35-38] Studies that utilize phth as a probe for the analysis of polymeric materials containing β-CD groups have been reported.[32,35-38] Topchieva *et al.*[35] estimated the number of binding sites for β-CD based nanotubes; however, the use of a non-zero molar absorptivity (ε) for the bound form of phth (*i.e.* β-CD/phth) in the equilibrium binding model is inconsistent with the parameter estimates ($\varepsilon \approx 0$) reported by other researchers, *vide infra*. Velaz *et al.*[32] concluded that the changes in the absorbance of phth provided evidence of the limited accessibility of the β-CD inclusion sites in their polymer materials. Fontanova *et al.*[37] indicated that the accessibility and binding sites of the β-CD polymers may be estimated using the decolourization of phth[37] while Uyar *et*

al.[38] recently reported the degree of decolourization of β-CD based composite polystryrene fibers.

In this paper, we report a detailed quantitative study of the estimation of the surface accessible β-CD inclusion sites for a systematic series of urethane based copolymer materials. As well, we conclude that the 1:1 binding constants for the β-CD inclusion sites in copolymer/phth systems with relatively high accessibility are similar to those of native β-CD. The 1:1 binding constants decrease as the relative accessibility of β-CD decreases. The copolymers investigated are urethanes comprised of β-CD and five types of diisocyanate cross linker molecules at 1:1, 1:2, and 1:3 reactant (β-CD:linker) mole ratios, respectively. The diisocyanates are as follows: 1,6-hexamethylene diisocyanate (HDI), 4,4'-dicyclohexyl diiscoyanate (CDI), 4,4'-diphenylmethane diisocyanate (MDI), 1,4-phenylene diisocyanate (PDI), and 1,5-naphthalene diisocyanate (NDI). Finally, the importance and application of this dye based method will be discussed.

4.3 Experimental

4.3.1 Materials

Dimethylacetamide (DMA) DriSolv 99.8%min (EMD), methanol, chromasolv for HPLC, ≥ 99.9% (Sigma-Aldrich) and ethyl ether anhydrous (EMD) were used at different stages of polymer preparation. Phosphorous pentoxide, P_2O_5 (BDH Chemicals Ltd) was used for drying β-CD. Phenolphthalein, phth (BDH Chemicals Ltd), sodium hydrogen carbonate (BDH Chemicals Ltd) and sodium hydroxide (Alfa Aesar) was used to prepare aqueous phth dye solutions.

4.3.2 Polymer Preparation

A procedure for the synthesis of urethane based β-CD materials was adopted from our previous work with an additional Soxhlet extraction step after methanol with ethyl ether.[10] Polymers of β-CD (VWR) and D(+)-glucose monohydrate (EMD) were synthesized via cross linking reactions with diisocyanate cross linker molecules. These linkers include the following; HDI (Fluka), CDI (Aldrich), MDI (Aldrich), PDI (Aldrich) and NDI (TCI).

4.3.3 Polymer Characterization

Solid-state ^{13}C NMR spectroscopy was performed using cross polarization (CP; ^{13}C $\{^{1}H\}$) with magic angle spinning (MAS). ^{13}C NMR spectra were run at 150.8 MHz on a Varian Inova-600 NMR spectrometer with a 3.2 mm rotor, spinning rate 16 kHz with a cp (^{13}C $\{^{1}H\}$) ramp pulse program. The chemical shifts were externally referenced to hexamethyl benzene at 16.9 ppm at ambient temperature. Data were processed with a 100 Hz line broadening with left shifting of the FID (1–2 data points) to correct the spectral baseline. IR reflection spectra were obtained with a BIO-RAD FTS-40 spectrophotometer. Spectroscopic grade KBr was used as both the background and matrix over the range of 400–4000cm^{-1}. Samples were prepared by mixing with pure spectroscopic grade KBr in appropriate amounts and ground in a small mortar and the powders were subsequently analyzed. The spectra were recorded in a diffuse reflectance mode (with Fourier Transform processing) at room temperature with a 4 cm^{-1} resolution and multiple scans. The content (w/w, %) of carbon (C), hydrogen (H), and nitrogen (N) was measured by Perkin Elmer 2400 CHN Elemental Analyzer with a detection limit ± 0.3%. The results were uncorrected according to the estimated water/solvent content. The

presence of water/solvent mixtures in the polymers was confirmed by ^{1}H NMR (500 MHz Bruker), and ^{13}C NMR for water soluble and insoluble materials, respectively. The residual solvent content (e.g., water and DMA) was estimated using a thermogravimetric analyzer, TGA (Q50 TA Instruments).

4.3.4 Solution Preparation

All solutions were prepared by volume in a 0.1 M sodium hydrogen carbonate buffer adjusted to pH 10.5 with 6 M sodium hydroxide. The concentration of phth (C_{phth}) was maintained at ~ 3.6 x 10^{-5} M in all experiments. A stock solution of phth in ethanol was made and aliquots were utilized to prepare aqueous solutions of phth in buffer. The ethanol/water (0.04%; v/v), solution was used to increase the solubility of phth.[6] All aqueous solutions were freshly prepared and run within 24 hrs to ensure that absorbance changes due to any instability of phth did not contribute to experimental artefacts. All absorption measurements were carried out at λ=552 nm and no change in the shape of the visible absorption band with increasing concentration of β-CD ($C_{\beta\text{-CD}}$) was observed at this wavelength.

4.3.5 Polymer Sorption

7 mL of aqueous solution containing phth (~3.6 x 10^{-5} M) were added to vials containing variable mass amounts of sorbent (e.g., β-CD, glucose, glucose copolymer and CD copolymers). The mixtures were shaken for 24 hrs, centrifuged (Precision Micro-Semi Micro Centricone, Precision Scientific Co.) at 1550 rpm, and the absorbance of the supernatant was measured using a double beam spectrophotometer (Varian CARY 100) at room temperature (295 ± 0.5 K) to monitor the absorbance changes at λ_{max} of 552 nm.

4.3.6 Data Analysis

A previously described,[6] non-linear least squares (NLLS) fitting procedure was used to determine the 1:1 equilibrium binding constants (K_1) between β-CD and phth. The method utilizes the Beer-Lambert law and the assumption that the molar absorptivity of the β-CD/phth complex is zero.[2-4] The formation of the 1:1 complex for β-CD and phth at equilibrium, and the mass-balance relations are given below

$$\beta\text{-CD} + \text{phth} \overset{K_1}{\rightleftharpoons} \beta\text{-CD/phth} \qquad \text{Equation 4.1}$$

$$[\text{phth}]_o = [\text{phth}] + [\text{CD-phth}] = [\text{phth}](1+K_1[\text{CD}]) \qquad \text{Equation 4.2}$$

$$[\text{CD}]_o = [\text{CD}] + [\text{CD-phth}] \qquad \text{Equation 4.3}$$

The terms $[CD]_0$, [CD], and [CD-phth] refer to the total, unbound, and 1:1 complexed forms of β-CD, respectively. The 1:1 equilibrium binding constant (K_1) for β-CD and phth is expressed as follows

$$[CD - phth] = [phth]_o\left(1 + \frac{1}{K_1[CD]}\right)^{-1} \qquad \text{Equation 4.4}$$

The values for [CD-phth] and [phth] were obtained using the Beer-Lambert law for phth and Equations (4.1-4.3). The estimates of K_1 using Equation 4.4 employ the Beer-Lambert law for the unbound fraction of phth and the assumption that the molar absorptivity of the β-CD/phth complex is zero.[2-4] The criterion utilized for the best fit in the NLLS procedure involved the minimisation of the sums of the squares of the residuals (SSR) according to the relation, $SSR = \sum_i [(A_{calc})_i - (A_{expt})_i]^2$, where A_{calc} and A_{expt} are the calculated and experimental absorbance values, respectively.

The site occupancy (θ) for phth onto the polymer framework and ΔG^o values for sorption (complex formation) were determined independently as fitting parameters, Q_m and K_{eq}, from the Sips equilibrium isotherm, according to Equation 4.5.[39-40] The Sips model accounts for the heterogeneity of the adsorbents and the interactions with the adsorbed layer. This model provides a better fit over the Langmuir model and reaffirms that other sorption sites and modes of interaction for phth may contribute apart from the β-CD inclusion sites. The contribution of non-inclusion polymer/phth interactions is not anticipated to be significant; however, they are taken into account with the Sips isotherm model.

$$Q_e = Q_m \frac{K_{eq} C_e^{\,n_s}}{1 + K_{eq} C_e^{\,n_s}} \qquad \text{Equation 4.5}$$

Q_e is the amount of phth adsorbed by the polymer (mol phth/g copolymer), Q_m is the maximum amount of phth adsorbed by the polymer, C_e is the equilibrium amount of phth in aqueous solution (M), K_{eq} is the 1:1 equilibrium binding constant (M^{-1}), and n_s is the Sips constant (where $n_s>1$) . It is worth to note that the Sips model converges with the Langmuir model when n_s is equal to unity for homogenous sorption processes. The fractional site occupancy of the adsorbate and the corresponding ΔG^o of complex formation are defined as follows

$$\theta = \frac{Q_e}{Q_m} \qquad \text{Equation 4.6}$$

$$\Delta G^o = -RT \ln K_{eq} \qquad \text{Equation 4.7}$$

R is the gas constant ($Jmol^{-1}K^{-1}$), T is temperature in K, and K_{eq} is defined as in Equation 4.5. The Sips parameters are forthwith interpreted in terms of the formation of 1:1 β-CD/phth inclusion complexes (*cf*. Equation 4.1); where $K_{eq} \approx K_1$.

4.4 Results and Discussion

4.4.1 Characterization of the CD polymers

^{13}C solid state NMR and IR have been reported previously where the copolymer materials (e.g., CD-PDI copolymer**)** were fully characterized.[10] In this work, additional urethane copolymer materials were investigated and the corresponding ^{13}C CP-MAS spectra are included in Figure 4.1. Figure 4.1a-f illustrates typical ^{13}C solids NMR spectra observed for the CD-based polymers with variable diisocyanate linker units at a fixed mole ratio (*i.e.*, NDI, PDI, MDI, CDI and HDI) along with the native β-CD precursor. Although each glucose unit of β-CD contains six unique C atoms, the spectrum for β-CD in Figure 4.1a reveals four ^{13}C NMR lines between 60-110 ppm due to overlap of some of the carbon signatures. The assignment and spectrum reported here agrees with previous reports. As observed in Figure 4.1b-f, ^{13}C signatures are observed for β-CD and the various types of aliphatic (*cf*. 20-70 ppm) and aromatic (*cf*. 110-170 ppm) linker molecules, respectively. In comparison to the ^{13}C NMR signals of native β-CD and the diisocyanates (results not shown), the urethane copolymers exhibit broader line widths, as is often observed in such amorphous CD based copolymer materials. The decreased crystallinity observed in the ^{13}C NMR spectra is related to the random attachment of the diisocyanate linker molecules to the various hydroxyl group positions (C_2, C_3, and C_6) of β-CD (*vide infra*) and the differences in cross polarization dynamics of the copolymer urethane materials.

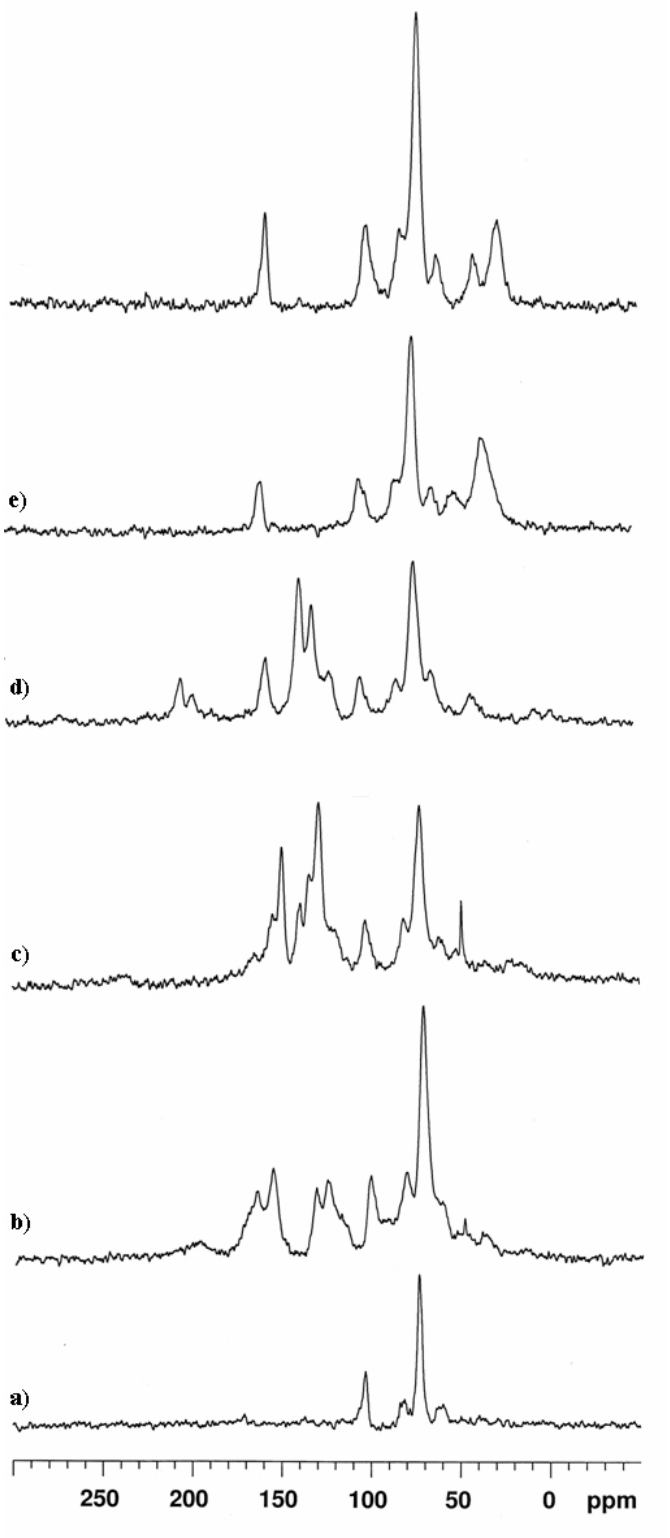

Figure 4.1. ^{13}C CP-MAS NMR spectra of CD copolymer materials recorded at ambient temperature, 16 kHz spinning speed, and 150.8 MHz: The spectra are listed as follows: a) β-CD, b) NDI-3, c) PDI-3, d) MDI-3, e) CDI-3, and f) HDI-3.

Elemental analyses provided estimates of the linker composition since the N content increased as the linker ratio increased, as shown in Table 2.2 in Chapter 2. Corrections due to water and/or solvent mixtures within the copolymers after extensive drying under vacuum were not applied due to a lack of quantitative estimates of the relative amounts of residual solvent in the products. However, the total contribution of solvent varied from ~0.3-2% as indicated by TGA. The presence of water/solvent contributions was confirmed with ^{1}H NMR spectra where DMA and water signatures were observed (results not shown). The occurrence of trace solvent residues was attributed to the occlusion of solvent within the polymer framework during copolymer formation. The elemental analyses in Table 2.2 in Chapter 2 for the theoretical composition of β-CD and glucose were corrected by varying the hydrate water content. Whilst the percentages of C and N increase as expected, H does not decrease as predicted and corrections due to presence of hydrate water result in better agreement between experimental and the calculated values.

4.4.2 Sorption of Phenolphthalein

A low ethanol composition (0.04%(v/v)) was chosen to eliminate possible interferences due to competitive binding by ethanol and to limit undue solvent effects.[6,41-43] The solution pH at 10.5 was chosen in order to optimize ε_{phth}, to provide greater sensitivity for absorption measurements, and to minimize the potential for deprotonation of the hydroxyl groups of β-CD ($pK_a \cong 12$). The equilibrium structures of the phth dianions in aqueous solution are shown in Scheme 4.2.

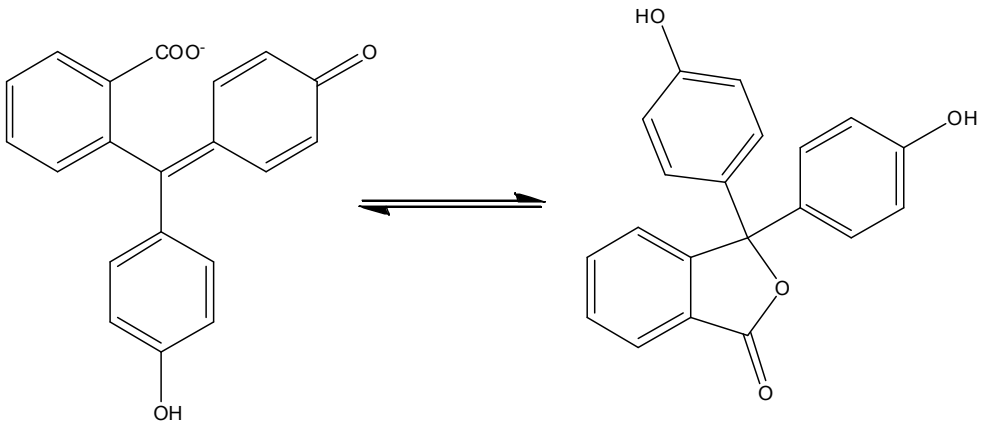

Scheme 4.2. The molecular structure of the two equilibrium forms of the red colored phenolphthalein dianion in aqueous solution at pH 10.5. The left hand structure represents the quinoid form and the right hand structure is the benzenoid dianion form of phenolphthalein.

Bertau & Jorg[44] previously studied the interaction of low molecular weight saccharides with phth and it was concluded that decolourization of phth was induced. Decolourization was attributed to non-specific enclathration and H-bonding interactions between the saccharides and phth suggests that the potential of phth as an inclusion specific probe may be limited. To evaluate any potential interferences, a glucose based urethane copolymer was synthesized (*i.e.* glucose:CDI (1:3)) and the nature of the polymer interactions with phth were studied. Figure 4.2 illustrates the change in absorbance (Abs) of phth against the mole concentration of glucose for a glucose:CDI (1:3) copolymer. There is a minor but gradual decolourization of phth (~ 0.1 absorbance units) over a 10 mM concentration range. The weak interaction of phth with glucose:CDI (1:3), as compared with β-CD, is evidenced by the lower magnitude of the 1:1 binding constant ($K = 19.6\ M^{-1}$; *cf.* Table 4.1) and is consistent with the decolourization effects concluded by Bertau & Jorg.

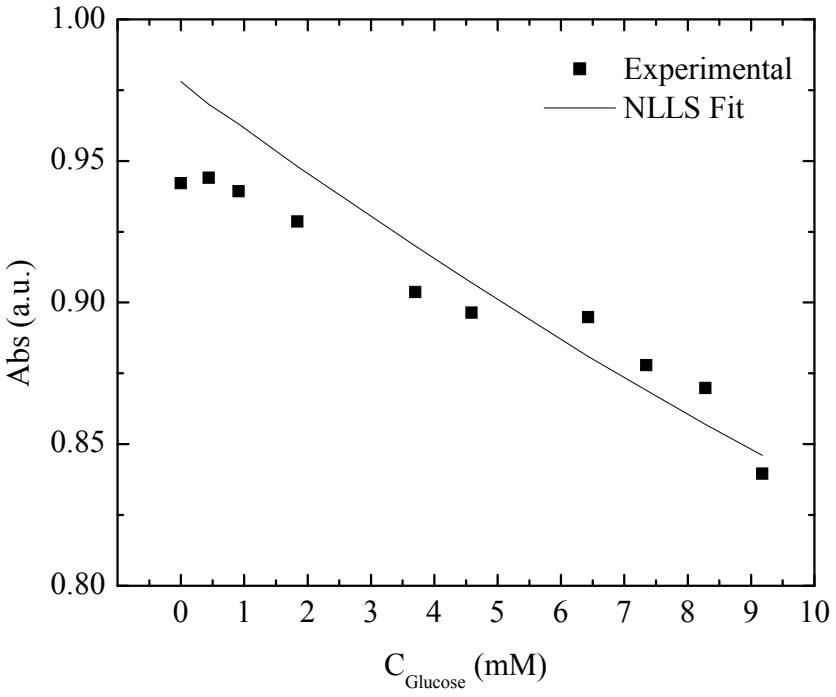

Figure 4.2. Phenolphthalein sorption with variable amount of insoluble Glucose:CDI (1:3) polymer at 295 K and pH 10.5 in 0.1 M $NaHCO_3$ buffer solution. The solid line refers to the NLLS best-fit according to Equation 4.4.

Figure 4.3 outlines the amount of phth removed (%) from solution by glucose and glucose:CDI (1:3) copolymer. The decolourization of phth by each adsorbent material is very similar and the attenuation of the absorbance of phth is attributed to the presence of glucose; however, the linker is concluded to contribute negligibly. The mole content of pure glucose exceeds that of glucose:CDI (1:3), and therefore, shows an apparently greater decolourization effect. Thus, the results in Figures 2-3 support that the interaction between glucose and phth results in an attenuation of the dye absorbance through a non-inclusion interaction, whereas; the linker (CDI) molecule does not contribute to any significant decolourization.

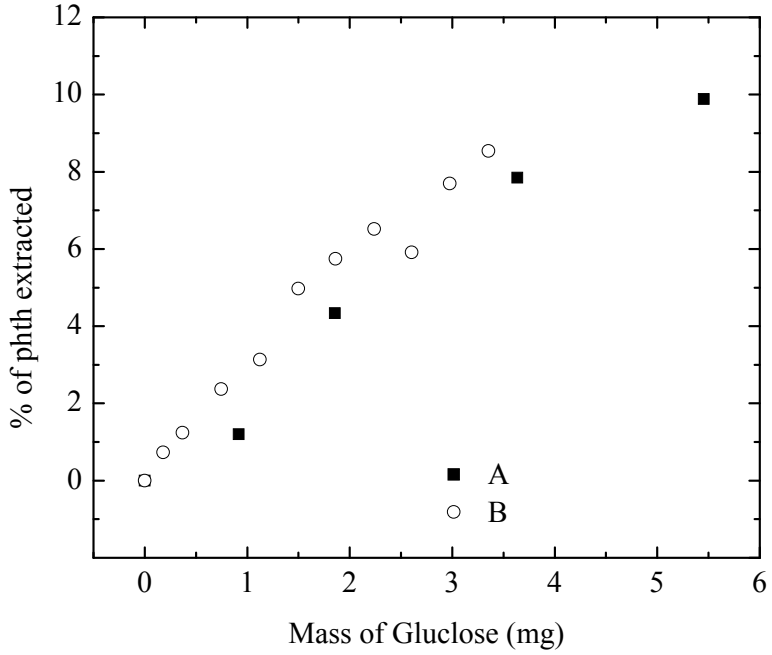

Figure 4.3. Phenolphthalein removal (decolourization) from solution using with variable amount of material at 295 K and pH 10.5 in 0.1 M $NaHCO_3$ buffer solution at fixed concentration of phth (3×10^{-5} M); A) D-(+)-Glucose, and B) Glucose:CDI((1:3) copolymer.

4.4.3 Calculation of the β-CD/phth 1:1 Binding Constant ($K_{1:1}$)

Figure 4.4 illustrates a typical plot of absorbance *vs* $C_{\beta\text{-CD}}$ for a fixed concentration of phth. The line through the data points represents the calculated absorbance values obtained from the NLLS fitting procedure (*cf*. Equation 4.4). The sharp decrease in absorbance as the $C_{\beta\text{-CD}}$ increases represents the formation of the β-CD/phth complex since the molar absorptivity of the latter is regarded as zero.[2-4] The calculated curves through the experimental data represent the best-fit NLLS curve corresponding to a 1:1 equilibrium binding model. The average 1:1 equilibrium binding constant (K_1) for the β-CD/phth complex binding is estimated as $K_1=2.66\pm0.3 \times 10^4$ M^{-1} with a standard error of

7.0% from four independent experimental trials. The latter result is in good agreement with independent estimates.[1-2,4,24,27] The conditions employed, here, utilized lower ethanol compositions than those of Selvidge & Eftink[22] and the value of K_1 obtained is correspondingly higher.

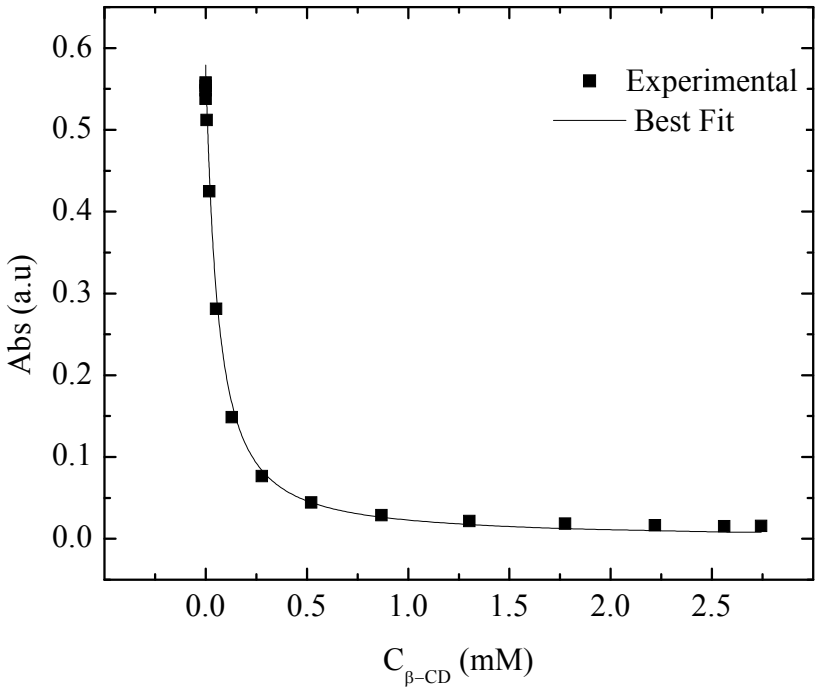

Figure 4.4. Absorbance (Abs) of phenolphthalein with variable concentration of β-CD ($C_{\beta\text{-CD}}$) in its native form in aqueous 0.1 M $NaHCO_3$ buffer solution at pH 10.5 and 295 K. The solid line refers to the NLLS best-fit according to Equation 4.4.

Figure 4.5 represents a plot of Abs vs $C_{Glucose}$ at a fixed concentration of phth. In contrast to the results obtained for β-CD, Figure 4.5 shows a more gradual decrease in absorbance for glucose and indicates that it has an attenuated binding constant, as compared with β-CD. The maximum absorbance change for glucose was ~15% and the estimated 1:1 binding constant value from NLLS fitting procedure was 15.7 M^{-1}. This relatively weak non-inclusion binding is attributed to H-bonding between glucose and phth, as described above.[44]

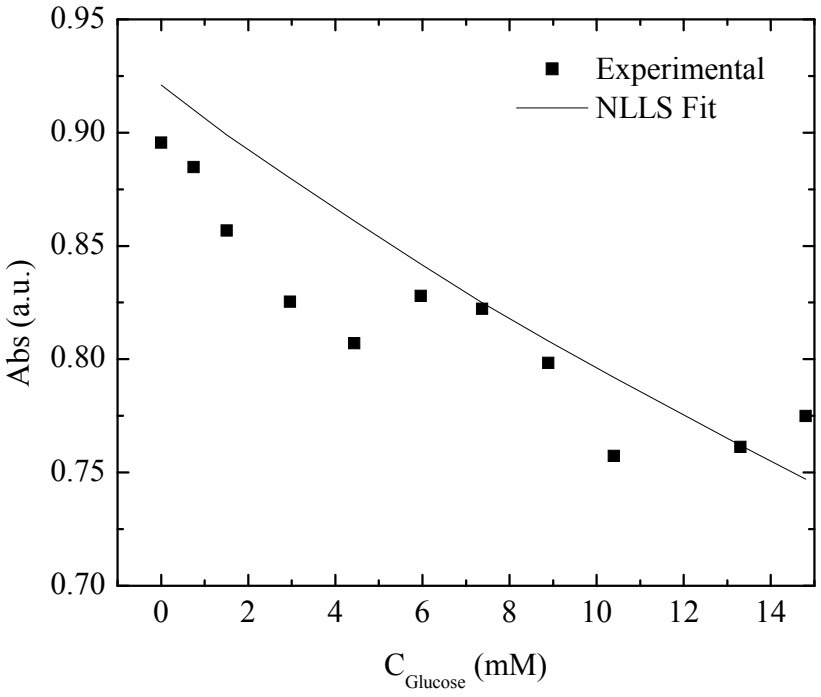

Figure 4.5. Phenolphthalein sorption with variable amount of glucose at 295 K and pH 10.5. The solid line refers to the NLLS best-fit according to Equation 4.4.

4.4.4 Sorption of Phenolphthalein with CD polymers

The decolourization of phth increased as the relative amount of CD polymer was increased for a constant value of C_{phth}. The decolourization results provide support that phth forms 1:1 inclusion complexes between phth and β-CD within the polymer framework. The results from Figure 4.3 indicate that non-inclusion and H-bonding interactions with glucose contribute to some decolourization of phth[44]; however, the effect is small in comparison with the observed inclusion effect for β-CD (*cf*. Figure 4.4).

Figure 4.6a-e illustrates the removal of unbound phth *vs*. the mass of β-CD copolymer materials. In Figure 4.6a, the β-CD:HDI copolymer (1:1) shows substantial removal of phth, as shown by the sharp asymptotic increase in bound phth, whereas; the

1:2 and 1:3 materials are incrementally less effective in removing phth from aqueous solution. The attenuation of phth removal is evident according to the estimates of the accessible β-CD (%) for the 1:1 (~100%), 1:2 (66.7%), and 1:3 (4.78%) copolymer materials, in accordance with the reduced accessibility of the β-CD inclusion sites. The greater removal of phth implies that phth forms 1:1 complexes with the β-CD inclusion sites in the polymer framework and results in decolourization of the dye. Increasing the cross link density may reduce the sorption properties of the polymeric materials for two possible reasons; *i*) steric crowding of the hydroxyl annular region of β-CD, and *ii*) attenuated access to the pore framework and β-CD inclusion sites due to an increased cross link density. According to the space filling models of Taguchi[3], inclusion of the benzenoid form of phth (*cf*. Scheme 4.2) as well as the H-bonding between the phenolate ions and the hydroxyl groups of β-CD are required to form the transparent 1:1 β-CD/phth dianion inclusion complex (*cf*. Scheme 2; Taguchi, 1986). Increased substitution at the β-CD annular region inhibits favourable H-bonding and inclusion binding between β-CD and phth. Thus, the anticipated steric effects are consistent with the attenuated decolourization of phth in highly cross linked materials, as observed in Figure 4.6a-e. In addition, copolymers with greater cross link density result in reduced access of phth to the microporous domains of the copolymer framework and result in reduced phth removal because of steric restrictions to the β-CD inclusion sites.

In Figure 4.6b, the β-CD:CDI (1:1) copolymer displayed the greatest removal of phth and the 1:2 and 1:3 materials show a reduced effect. A comparison of CDI and HDI linkers indicates that the former is a bulkier linker molecule, and the anticipated steric effects of CDI are more pronounced compared to the results for HDI (Figure 4.6a).

Figure 4.6c-e depicts the removal efficiency for three polymeric materials containing aromatic linker molecules (MDI, PDI, and NDI) at variable reactant mole ratios. In each case, similar sorption of phth is observed for the 1:1 and 1:2 materials; however, complex formation is severely attenuated for the 1:3 copolymers. Steric effects are anticipated between phth and the annular hydroxyl groups of β-CD and domains containing the β-CD inclusion sites of at greater cross link ratios. In general, an increase in the linker composition of the copolymers results in significant reduction to the inclusion binding of β-CD and phth, as shown by the different profiles shown in Figure 4.6a-e.

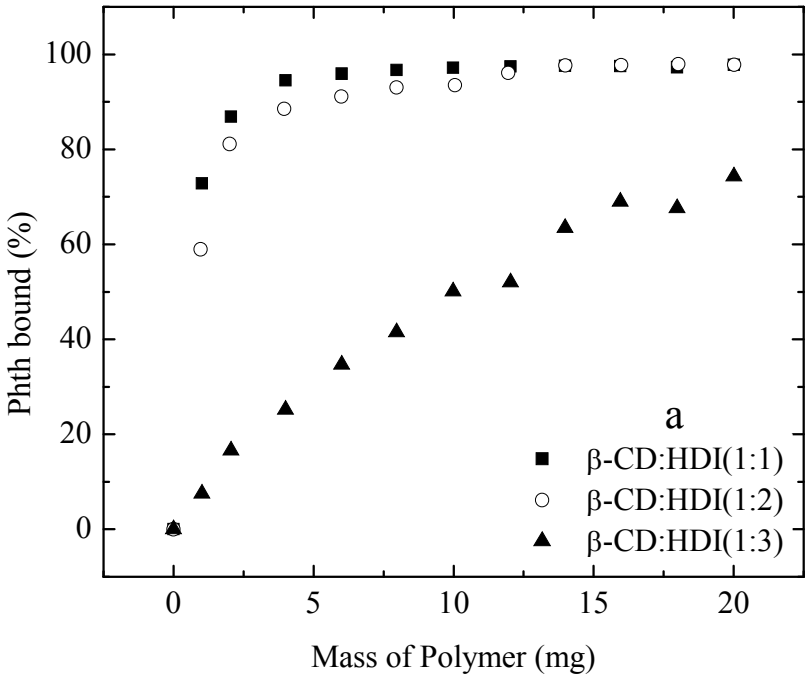

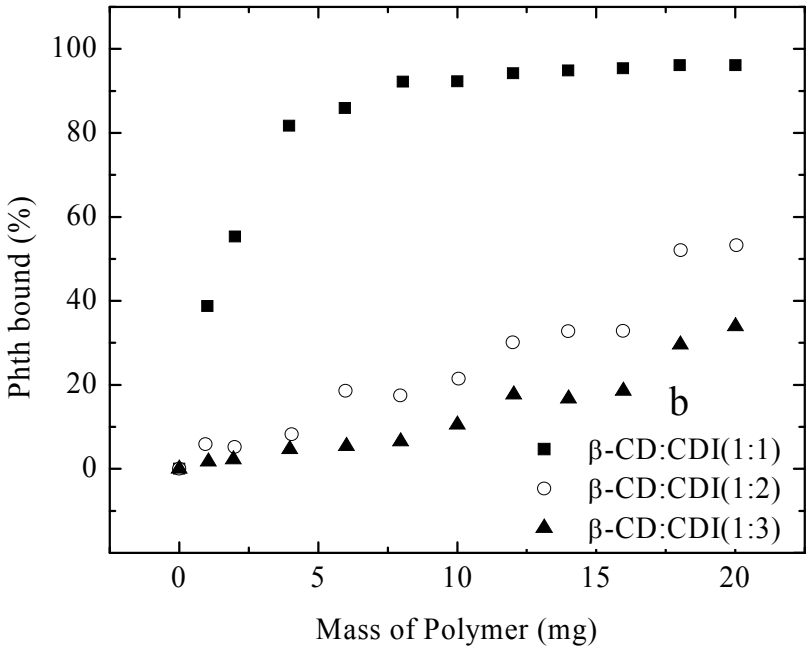
Phth bound (%)
Mass of Polymer (mg)
b
β-CD:CDI(1:1)
β-CD:CDI(1:2)
β-CD:CDI(1:3)

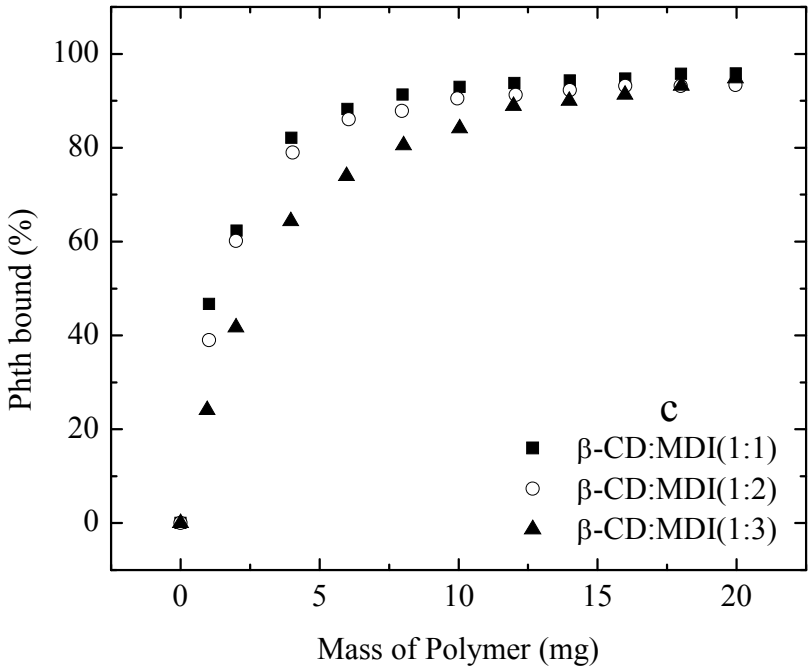
Phth bound (%)
Mass of Polymer (mg)
c
β-CD:MDI(1:1)
β-CD:MDI(1:2)
β-CD:MDI(1:3)

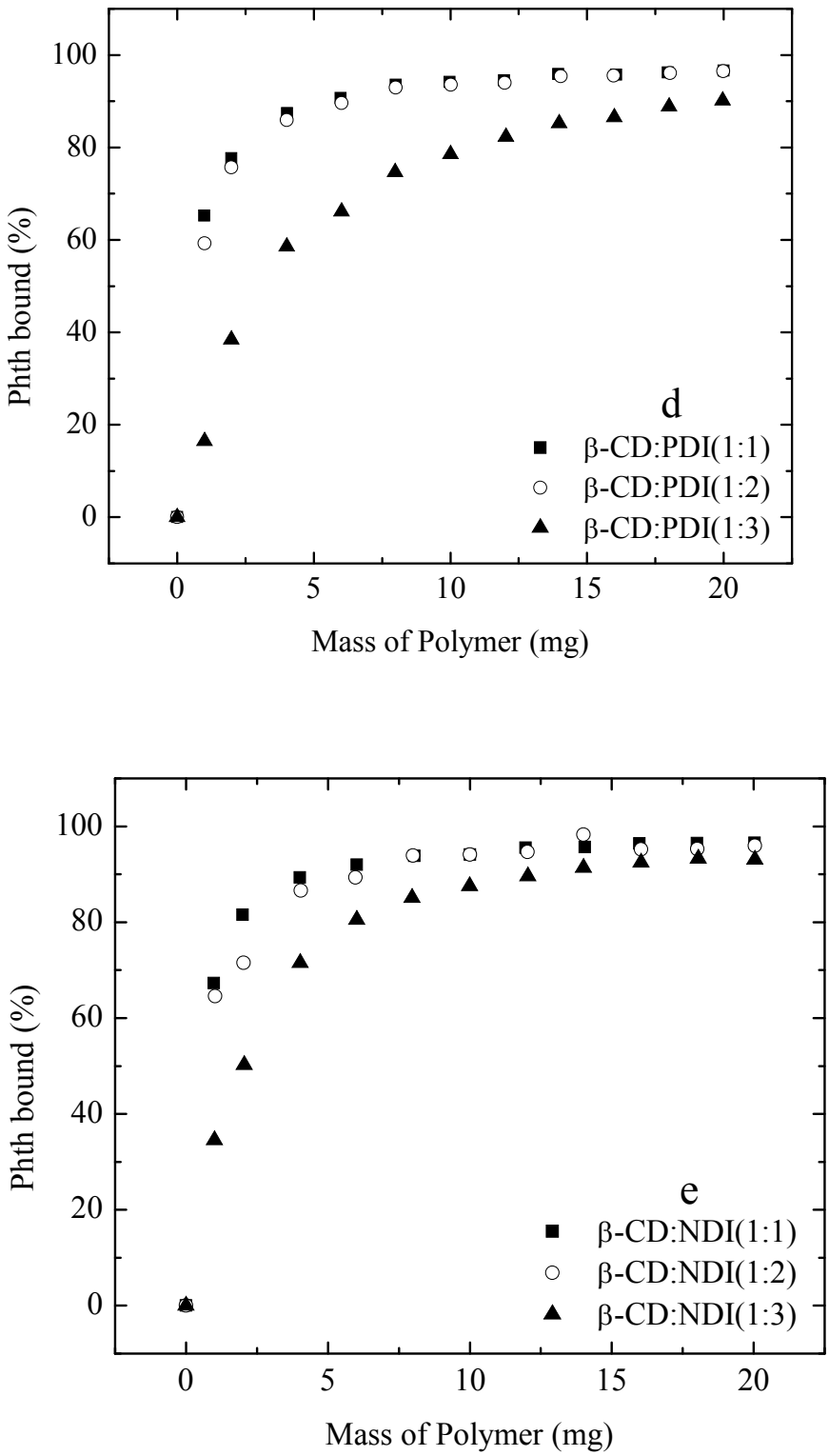

Figure 4.6a-e. Percentage of phenolphthalein bound from aqueous solution with β-CD based copolymers *vs*. polymer mass (mg) in 0.1 M $NaHCO_3$ buffer at pH 10.5 and 295K: a) β-CD:HDI, b) β-CD:CDI, c) β-CD:MDI, d) β-CD:PDI, and e) β-CD:NDI at 1:1, 1:2, and 1:3 reactant mole ratios, respectively.

Figure 4.7a-e illustrates the change in absorbance (Abs) of phth vs $C_{\beta\text{-CD}}$ in β-CD copolymers at a fixed concentration of phth (C_{phth}). The solid lines through the experimental data represent the calculated Abs values according to the NLLS fitting routine, according to Equation 4.4. The decrease in Abs as $C_{\beta\text{-CD}}$ increases is more gradual as the linker ratio content increases for all copolymers studied. In the case of CDI (Figure 4.7b), the rapid falloff is less evident and indicates that inclusion binding of phth is reduced even at intermediate (1:2) linker ratios. The greatest attenuation of phth binding is observed at the highest (1:3) linker content for both the aliphatic (*i.e.* HDI and CDI) and aromatic (NDI, PDI, and MDI) linkers. The steric effect appears to correlate with the approximate size of the linker. The decolourization of phth by the 1:1 copolymer materials is listed in descending order as follows: HDI>NDI>PDI>MDI≈CDI. This observation suggests that the relative size of the linker plays a steric role in affording accessibility to the β-CD inclusion sites within the polymeric framework. Figure 4.7a-b illustrates the behaviour for polymers with aliphatic linkers while Figure 4.7c-e shows results for polymers with aromatic linkers. It is important to note that the aliphatic and aromatic linkers are anticipated to exhibit differences in their conformational rigidity. Thus, aromatic linkers such as NDI and MDI may form more open pore structures within the polymer framework. Flexible aliphatic linkers such as HDI and CDI may form compact frameworks because their variable conformations may result in a collapsed framework structure. This hypothesis is supported by the attenuated access to the inclusion sites for phth, as evidenced by the results shown in Figure 4.6 and 4.7. There appears to be a compromise between steric crowding in the annular hydroxyl region of β-

CD *vs* the creation of accessible pore structures within the framework as the relative size and rigidity of the linker increases.

Scheme 1.5 in Chapter 1 outlines the effect of increasing the degree of substitution in the annular hydroxyl region of β-CD for a diisocyanate linker over the range of β-CD:linker mole ratios (1:1, 1:2, and 1:3). In this work, synthetic ratios were studied. At the 1:1 ratio, the primary hydroxyl groups of the β-CD are more reactive as compared with the secondary hydroxyl groups. In the case of bulky diisocyanates, the estimated number of substituents in the annular hydroxyl region is estimated *ca*. three substituents per annular face (*cf*. Scheme 1.5 in Chapter 1) and this has been independently supported elsewhere.[45-48] Once steric crowding occurs at the narrow end of the β-CD annulus, linkers react at the wider secondary annular region until the degree of substitution approaches ~3. Scheme 1.5 in Chapter 1 illustrates the distribution of substituents from left to right (a-c) in accordance with the β-CD:linker reactant ratio from 1:1 to 1:3, respectively. The accessibility of inclusion sites presented in Table 4.1 support this hypothesis since relatively high accessibility is observed at the 1:1 reactant ratio. According to Taguchi, the formation of the 1:1 β-CD/phth inclusion complex occurs by inclusion of the benzenoid form of phth (*cf*. Scheme 4.2) and H-bonding between the two phenoxide anions and the secondary annular hydroxyl groups located at the wide end of the β-CD annulus (*cf*. Scheme 4.2).[2] According to Glazyrin *et al.*,[47] a study of various modified forms of β-CD indicated that a four- to fourty-fold decrease in the 1:1 binding constant was observed for acetylated and hydroxypropyl substituted β-CD where the average degree of substitution reaches ~ 3.8 and 3.6, respectively. They concluded that the binding of β-CD and some of its water-soluble derivatives may form complexes with

phth depending on the structure, substitution position, and degree of substitution at the 2-, 3-, and 6-hydroxyl positions, respectively.

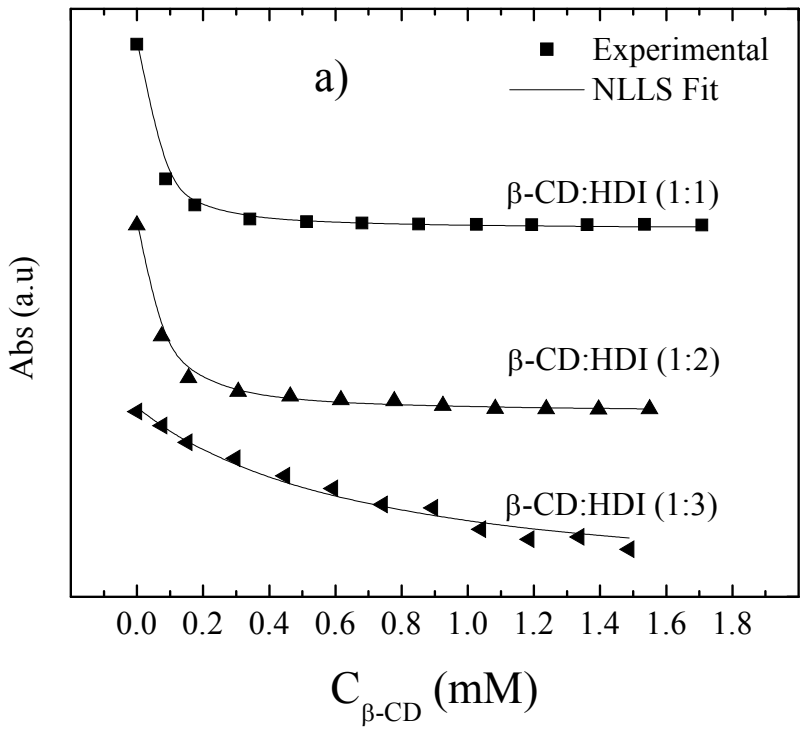

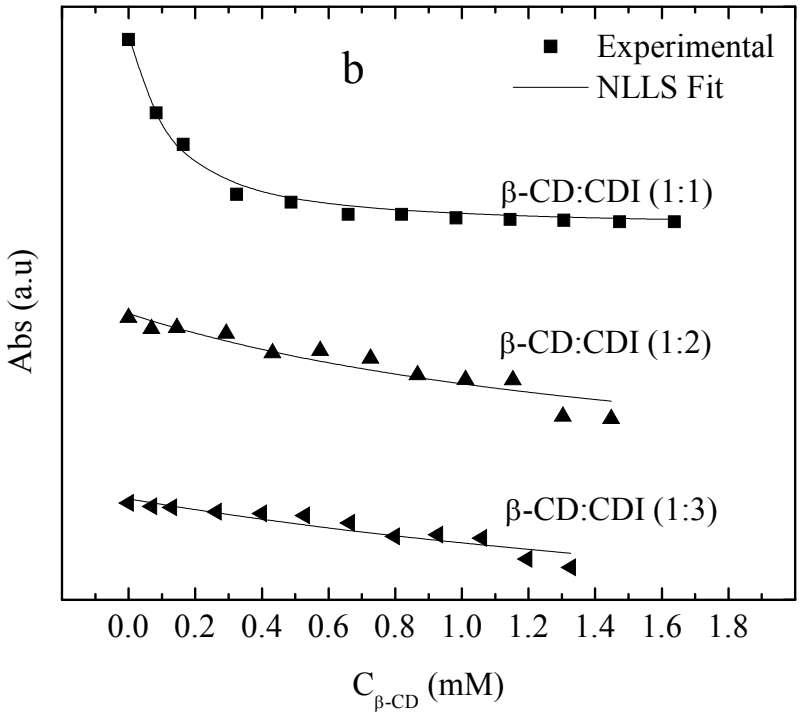
b
Experimental
NLLS Fit
β-CD:CDI (1:1)
β-CD:CDI (1:2)
β-CD:CDI (1:3)
Abs (a.u)
0.0 0.2 0.4 0.6 0.8 1.0 1.2 1.4 1.6 1.8
C β-CD (mM)

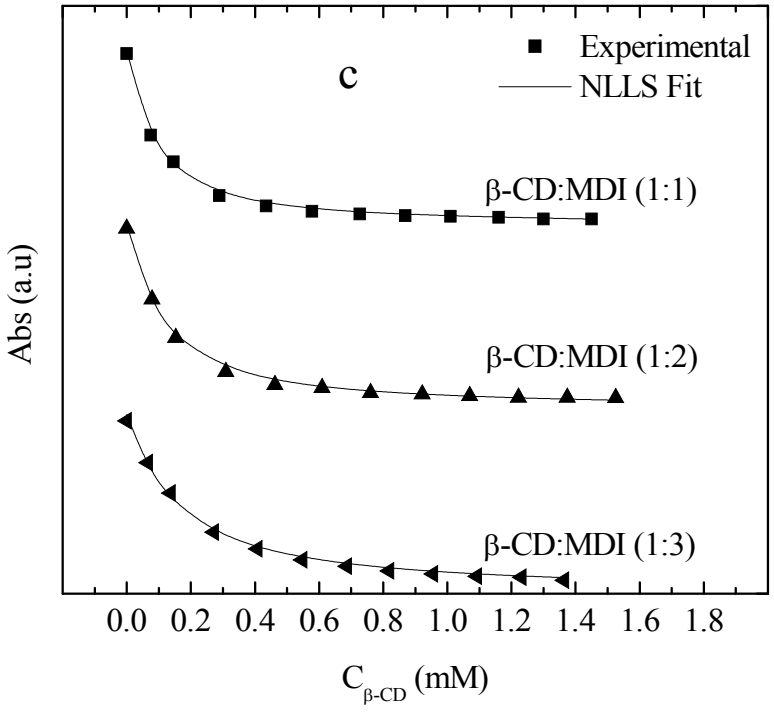
c
Experimental
NLLS Fit
β-CD:MDI (1:1)
β-CD:MDI (1:2)
β-CD:MDI (1:3)
Abs (a.u)
0.0 0.2 0.4 0.6 0.8 1.0 1.2 1.4 1.6 1.8
C β-CD (mM)

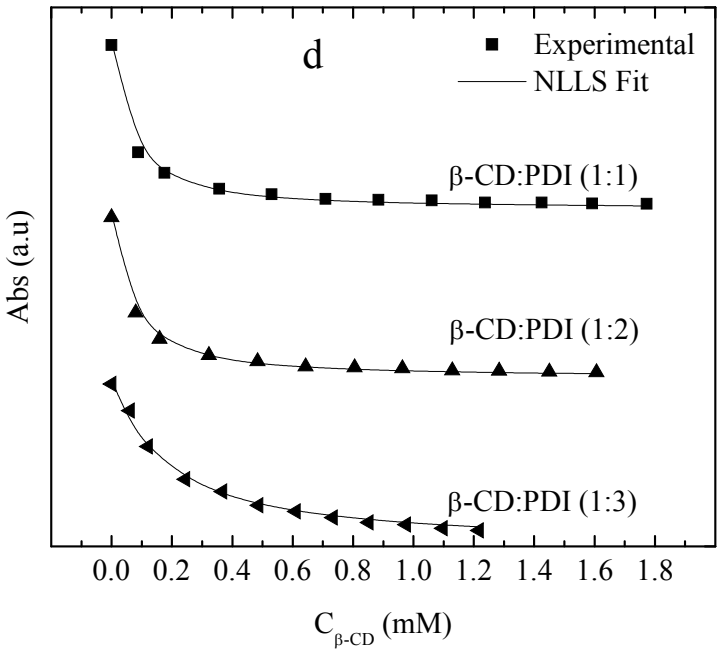

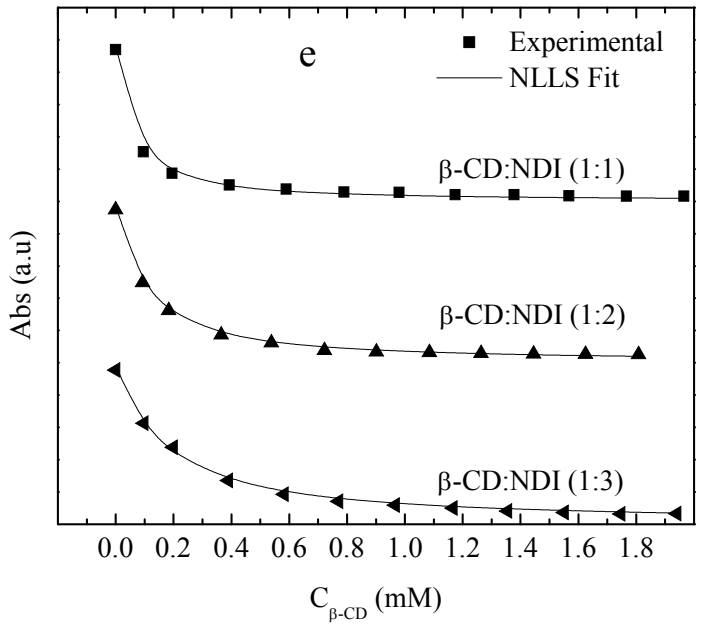

Figure 4.7a-e. Absorbance changes for phenolphthalein as a function of increased mole content of β-CD ($C_{β\text{-}CD)}$ for various insoluble copolymers at variable synthetic feed ratios at pH 10.5 in 0.1 M $NaHCO_3$ and 295K: a) β-CD:HDI, b) β-CD:CDI, c) β-CD:MDI, d) β-CD:PDI, and e) β-CD:NDI. The solid line refers to the NLLS best-fit according to Equation 4.4 where $K_1 = 2.66 \times 10^4$ M^{-1} and the fraction bound of β-CD (CD-phth) is an adjustable parameter between 0 to 100 mol%.

4.4.5 Accessibility of β-CD Inclusion Binding Sites in the Copolymers

The estimation of accessible inclusion binding sites of β-CD requires certain assumptions: *i*) polymers possess variable accessibility due to differences in the cross link density, *ii*) phth binds exclusively to β-CD as a 1:1 inclusion complex where the molar absorptivity of bound phth is zero, and *iii*) the 1:1 binding constant is assumed to be similar to that of native β-CD in the absence of steric effects. The third assumption is supported from experiments that compare the binding between glucose and glucose based polymers. It was concluded that the urethane linkage does not affect the magnitude of the 1:1 binding constant for glucose-CDI copolymers. The presence of available hydroxyl groups affects the decolourization of phth as observed in aqueous solutions containing glucose and the results obtained here are also supported by the conclusions of Bertau & Jorg.[44]

The percentage of the accessible β-CD was calculated by varying the percentage of bound β-CD (varying [CD-phth] in Equation (4.2-4.4)) for copolymers containing β-CD. The best-fit between the calculated Abs and experimental values (*cf*. Figure 7 a-e) provided estimates of the accessible inclusion sites. Equation 4 was used with a fixed value for K_1 for the polymeric materials, similar to that obtained for the 1:1 β-CD/phth complex. Table 4.1 shows the estimates of the surface accessible β-CD for each copolymer at different cross link density. The accessibility of the inclusion sites decreases as the cross link density increases. The relative ordering of the steric effects at high cross link density correlates inversely with the size of the linker as follows: HDI> CDI> PDI > MDI ≈ NDI. Steric crowding and the reduction of the pore volume within the framework are anticipated to retard the 1:1 inclusion complex formation between β-

CD and phth. Polymers with low cross link density such as the β-CD:HDI (1:1) copolymer possesses the greatest inclusion accessibility whereas the β-CD:CDI (1:3) copolymer has the lowest accessibility values. The linker domains within the framework do not contribute to complex formation with phth to any appreciable extent (*cf.* Figure 4.3) as shown by the minor decolourization effect of the glucose-CDI polymer is less than 0.1% (*cf*. Table 4.1).

Table 4.2 lists the Gibbs free energy change of complex formation (ΔG^o) and provides independent support for the comparable 1:1 binding constants of the native β-CD/phth complex and β-CD copolymer/phth complexes. The reasonable fit obtained using the Sips model instead of the Langmuir ($n_s = 1$) model suggests that the linkers may affect the decolourization of phth, albeit limited. However, the formation of the 1:1 inclusion complexes between β-CD based copolymers and phth is the predominant mechanism responsible for the observed decolourization. In Table 4.2, the site occupancy decreased as the cross linking density increases, and correlates with the decreased accessibility of the inclusion sites. The Gibbs free energy change depends on the site occupancy of the sorption sites where they are directly proportional to the amount of accessible β-CD. Moreover, the magnitude of ΔG^o for the copolymers is slightly greater than the ΔG^o of the 1:1 β-CD/phth complexes (~ -25 kJ/mol).[6,49] The slight differences in ΔG^o may be due to differences in hydration and steric effects because of cross linking in the β-CD copolymers, as suggested by Glazyrin *et al.*[47]

Table 4.1. Phenolphthalein based estimates (%) of the surface accessible β-CD site in β-cyclodextrin urethane copolymer materials

Material	β-CD:linker Synthetic Ratio	β-CD$_{total}$ (mol %)	K_1 (M^{-1})	Accessible β-CD (%)[a]
B-CD	-	100	$2.66(0.3)\times10^4$	100
Glucose	-	0	15.7	$5.91x10^{-2}$
Glucose:CDI	1:3	0	17.0	$6.39x10^{-2}$
β-CD:HDI	1:1	87.1	$2.66(0.3)\times10^4$	106
	1:2	77.1	$2.66(0.3)\times10^4$	66.7
	1:3	69.2	$2.66(0.3)\times10^4$	4.78
β-CD:CDI	1:1	81.2	$2.66(0.3)\times10^4$	33.2
	1:2	68.4	$2.66(0.3)\times10^4$	2.03
	1:3	59.1	$2.66(0.3)\times10^4$	1.04
β-CD:MDI	1:1	81.4	$2.66(0.3)\times10^4$	38.0
	1:2	69.4	$2.66(0.3)\times10^4$	31.6
	1:3	60.2	$2.66(0.3)\times10^4$	18.6
β-CD:PDI	1:1	87.6	$2.66(0.3)\times10^4$	68.3
	1:2	78.0	$2.66(0.3)\times10^4$	57.4
	1:3	70.3	$2.66(0.3)\times10^4$	14.1
β-CD:NDI	1:1	84.4	$2.66(0.3)\times10^4$	77.6
	1:2	73.0	$2.66(0.3)\times10^4$	39.2
	1:3	68.4	$2.66(0.3)\times10^4$	24.2

[a]Accessible β-CD (%)= (β-CD/phth / β-CD$_{total}$)×100%

Table 4.2. Fractional coverage, θ[a], at 1mg of the polymer and Gibbs free energy change[b], ΔG^o of complex formation with phth in aqueous solution at pH 10.5 and 295K.

Polymer	Ratio β-CD:Linker	
	1:1 (θ, ΔG^o kJ/mol)	1:2 (θ, ΔG^o kJ/mol)
HDI	0.773, -29.7	0.741, -28.7
CDI	0.619, -27.0	NR[c]
MDI	0.838, -28.3	0.818, -28.3
PDI	0.633, -27.9	0.501, -27.3
NDI	0.598, -28.4	0.500, -26.7

θ[a] – refer to Equation (6), ΔG^{ob} –refer to Equation (7), and NR[c] – not reported because the surface accessibility was too low resulting in poor fits according to the Sips isotherm model (*cf.* Equation (4.5))

4.5 Conclusions

In this research we report the results of a dye-based study of water insoluble β-CD based copolymer sorbents in aqueous solution at pH 10.5 and 295 K. In contrast to other design strategies that employ relatively high β-CD:linker reactant ratios, the copolymers in this study utilized relatively low ratios (1:1 to 1:3), and yet, the surface accessibility was remarkably different for the five sets of copolymer sorbent materials. The copolymer surface accessibility of the β-CD inclusion sites ranged between 1-100%, as evidenced by the formation of 1:1 β-CD/phth inclusion complexes. The Gibbs free energy change for the formation of 1:1 complexes between phth and β-CD copolymer materials ranged between -27 to -30 kJ mol^{-1}, according to the Sips isotherm model.

This paper represents the first systematic and quantitative analysis of β-CD inclusion sites in urethane copolymer materials. The dye based sorption method presented herein represents a facile and relatively low cost analytical method for β-CD based copolymer materials. This method relies on the specific molecular recognition between β-CD and phenolphthalein, and it provides useful results about the sorption properties of β-CD based sorbent materials. We propose the use of phth as an inclusion selective guest and versatile optical probe for β-CD based copolymer sorbent materials. The molecular selectivity of this dye based method will contribute to the design of novel types of β-CD based materials for sorption based applications involving the inclusion binding of adsorbates from solution and gas phase media, respectively.

4.6 Acknowledgments

Financial assistance was provided by the Natural Sciences and Engineering Research Council and the Program of Energy Research and Development. M.H.M acknowledges the University of Saskatchewan for the award of a Graduate Teaching Fellowship and Environment Canada for the Science Horizons Program award. Mr. Joel Hardes is acknowledged for his helpful technical assistance.

4.7 References

1. *Cyclodextrin Chemistry*; Bender, M. L.; Komiyama, M., Eds.; Springer-Verlag: Berlin, Germany, 1978.
2. Buvari, A. *J. Inclusion Phenom.* **1983**, *1*, 151-157.
3. Taguchi, K. *J. Am. Chem. Soc.* **1986**, *108*, 2705-2709.
4. Eftink, M. R.; Andy, M. L.; Bystrom, K.; Perlmutter, H. D.; Kristol, D. S. *J. Am. Chem. Soc.* **1989**, *111*, 6765-6772.
5. Georgiou, M. E.; Georgiou, C. A.; Koupparis, M. A. *Anal. Chem.* **1995**, *67*, 114-123.
6. Wilson, L. D.; Siddall, S. R.; Verrall, R. E. *Can. J. Chem.* **1997**, *75*, 927-933.
7. Mohamed, M. H.; Wilson, L. D.; Headley, J. V.; Peru, K. M. *Rapid Commun. Mass Spectrom.* **2009**, *23*, 3703-3712.
8. Wenz, G. *Angew. Chem. Int. Ed. Engl* **1994**, *33*, 803-822.
9. Harada, A.; Hashidzume, A.; Takashima, Y. *Cyclodextrin-based supramolecular polymers*; Springer, 2006; Vol. 201.
10. Mohamed, M. H.; Wilson, L. D.; Headley, J. V.; Peru, K. M. *Process Saf. Environ. Prot.* **2008**, *86*, 237-243.
11. Mohamed, M. H.; Wilson, L. D.; Headley, J. V. *Carbohydr. Polym.* **2010**, *80*, 186-196.
12. Crini, G. *Prog. Polym. Sci.* **2005**, *30*, 38-70.
13. Wood, D. J.; Hruska, F. E.; Saenger, W. *J. Am. Chem. Soc.* **1977**, *99*, 1735-1740.

14. Junquera, E.; Tardajos, G.; Aicart, E. *Langmuir* **1993**, *9*, 1213-1219.
15. Saint Aman, E.; Serve, D. *J. Colloid Interface Sci.* **1990**, *138*, 365-375.
16. Dharmawardana, U. R.; Christian, S. D.; Tucker, E. E.; Taylor, R. W.; Scamehorn, J. F. *Langmuir* **1993**, *9*, 2258-2263.
17. Wan Yunus, W. M. Z.; Taylor, J.; Bloor, D. M.; Hall, D. G.; Wyn-Jones, E. *J. Phys. Chem.* **1992**, *96*, 8979-8982.
18. Gelb, R. I.; Schwartz, L. M.; Cardelino, B.; Laufer, D. A. *Anal. Biochem.* **1980**, *103*, 362-368.
19. Fourmentin, S.; Surpateanu, G.; Blach, P.; Landy, D.; Decock, P.; Surpateanu, G. *J. Inclusion Phenom. Macrocyclic Chem.* **2006**, *55*, 263-269.
20. Buvari, A.; Barcza, L. *Inorg. Chim. Acta* **1979**, *33*, L179-L180.
21. Harrison, J.; Eftink, M. R. *Biopolymers* **1982**, *21*, 1153-1166.
22. Selvidge, L.; Eftink, M. R. *Anal. Biochem.* **1986**, *154*, 400-408.
23. Buvari, A.; Barcza, L.; Kajtar, M. *J. Chem. Soc., Perkin Trans. 2* **1988**, *1972-1999*, 1687-1690.
24. Gray, J. E.; MacLean, S. A.; Reinsborough, V. C. *Aust. J. Chem.* **1995**, *48*, 551-556.
25. Meier, M. M.; Bordignon Luiz, M. T.; Farmer, P. J.; Szpoganicz, B. *J. Inclusion Phenom. Macrocyclic Chem.* **2001**, *40*, 291-295.
26. Tutaj, B.; Kasprzyk, A.; Czapkiewicz, J. *J. Inclusion Phenom. Macrocyclic Chem.* **2003**, *47*, 133-136.
27. Sasaki, K. J.; Christian, S. D.; Tucker, E. E. *Fluid Phase Equilib.* **1989**, *49*, 281-289.
28. Landy, D.; Fourmentin, S.; Salome, M.; Surpateanu, G. *J. Inclusion Phenom. Macrocyclic Chem.* **2000**, *38*, 187-198.
29. Suzuki, I.; Yamauchi, A. *J. Inclusion Phenom. Macrocyclic Chem.* **2006**, *54*, 193-200.
30. Janus, L.; Crini, G.; El-Rezzi, V.; Morcellet, M.; Cambiaghi, A.; Torri, G.; Naggi, A.; Vecchi, C. *React. Funct. Polym.* **1999**, *42*, 173-180.
31. Wintgens, V.; Amiel, C. *Langmuir* **2005**, *21*, 11455-11461.

32. Vélaz, I.; Isasi, J.; Sánchez, M.; Uzqueda, M.; Ponchel, G. *J. Inclusion Phenom. Macrocyclic Chem.* **2007**, *57*, 65-68.
33. Burckbuchler, V.; Wintgens, V. r.; Leborgne, C.; Lecomte, S.; Leygue, N.; Scherman, D.; Kichler, A.; Amiel, C. *Bioconjugate Chem.* **2008**, *19*, 2311-2320.
34. Rossi, R. H.; Silva, O. F.; Vico, R. V.; Gonzalez, C. J. *Pure Appl. Chem.* **2009**, *81*, 755-765.
35. Topchieva, I. N.; Kalashnikov, F. A.; Spiridonov, V. V.; Mel'nikov, A. B.; Polushina, G. E.; Lezov, A. V. *Dokl. Chem.* **2003**, *390*, 115-118.
36. de Bergamasco, R.; Zanin, G.; de Moraes, F. *J. Inclusion Phenom. Macrocyclic Chem.* **2007**, *57*, 75-78.
37. Fontananova, E.; Di Profio, G.; Curcio, E.; Giorno, L.; Drioli, E. *J. Inclusion Phenom. Macrocyclic Chem.* **2007**, *57*, 537-543.
38. Uyar, T.; Havelund, R.; Nur, Y.; Hacaloglu, J.; Besenbacher, F.; Kingshott, P. *J. Membr. Sci.* **2009**, *332*, 129-137.
39. Sips, R. *J. Chem. Phys.* **1948**, *16*, 490-495.
40. Liu, Y.; Liu, Y.-J. *Separ. Sci. Technol.* **2008**, *61*, 229-242.
41. Donze, C.; Chatjigakis, A.; Coleman, A. W. *J. Inclusion Phenom.* **1992**, *13*, 155-161.
42. Warner-Schmid, D.; Tang, Y.; Armstrong, D. W. *J. Liq. Chromatogr.* **1994**, *17*, 1721-1735.
43. Schuette, J. M.; Warner, I. M. *Anal. Lett.* **1994**, *27*, 1175 - 1182.
44. Bertau, M.; Jorg, G. *Bioorg. Med. Chem.* **2004**, *12*, 2973-2983.
45. Martel, B.; Leckchiri, Y.; Pollet, A.; Morcellet, M. *Eur. Polym. J.* **1995**, *31*, 1083-1088.
46. Weickenmeier, M.; Wenz, G. *Macromol. Rapid Commun.* **1996**, *17*, 731-736.
47. Glazyrin, A. E.; Grachev, M. K.; Kurochkina, G. I.; Nifant'ev, E. E. *Russ. J. Gen. Chem.* **2004**, *74*, 1922-1925.
48. Yuan, C.; Jin, Z.; Li, X. *Food Chemistry* **2008**, *106*, 50-55.
49. Mohamed, M. H.; Wilson, L. D.; Headley, J. V.; Peru, K. M. *Can. J. Chem.* **2009**, *87*, 1747-1756.

CHAPTER 5

PUBLICATION 4

Description

The following is a verbatim copy of an article that was published in September of 2009 in the Rapid Communications in Mass Spectrometry journal (*Rapid Commun. Mass Spectrom.:* **2009**, *23(23)*, 3703-3712) and describes binding studies of CDs/NAs and CDs/NAs-surrogates inclusion complexes studies using ESI-MS.

Authors' Contribution

I conducted all of the experimental work while the ESI-MS measurements were done by Mr. Kerry Peru. This work was supervised by Dr. Wilson and Dr. Headley. I wrote the first draft of the manuscript with extensive editing by each supervisor prior to submission for publication. Written permission was obtained from all contributing authors and the publishers to include this material in this thesis.

Relation of Chapter 5 (Publication 4) to the Overall Objectives of this Project

As mentioned in Chapter 1, there was a need to provide direct proof of inclusion of NAs within the cavities of CDs. Four surrogates were chosen in terms of their hydrogen deficiency and variable molecular weight to further confirm the formation of inclusion complexes of the specific examples of NAs. Glucose and cellobiose are non-porogen saccharides that were chosen for comparison with CDs since they do not possess a pre-organized binding site as in the case of CD macrocyclic hosts.

5. Electrospray Ionization Mass Spectrometry Studies of Cyclodextrin-Carboxylate Ion Inclusion Complexes

Mohamed H. Mohamed,[§] Lee D. Wilson, [§] John V. Headley[¥] Kerr M. Peru[¥]*

[§]Department of Chemistry, University of Saskatchewan, 110 Science Place, Saskatoon, Saskatchewan, S7N 5C9

[¥]Water Science and Technology Directorate, 11 Innovation Boulevard, Saskatoon, Saskatchewan, S7N 3H5

*Corresponding Author

Received 25 June 2009

5.1 Abstract

Aqueous solutions containing simple model aliphatic and alicyclic carboxylic acids (surrogates 1-4) were studied using negative ion electrospray ionization mass spectrometry (ESI-MS) in the presence and absence of α-, β-, and γ-cyclodextrins, respectively. Molecular ions were detected corresponding to the parent carboxylic acids and complexed forms of the carboxylic acids; the latter corresponding to noncovalent inclusion complexes formed between carboxylic acid and cyclodextrin compounds (e.g. α-CD, β-CD, and γ-CD). The formation of 1:1 noncovalent inclusion cyclodextrin-carboxylic complexes and non-inclusion forms of the cellobiose-carboxylic acid compounds were also observed.

Aqueous solutions of Syncrude-derived mixtures of aliphatic and alicyclic carboxylic acids (i.e. naphthenic acids; NAs) were similarly studied using ESI-MS, as

outlined above. Molecular ions corresponding to the formation of CD-NAs inclusion complexes were observed whereas 1:1 non-inclusion forms of the cellobiose-NAs complexes were not detected. The ESI-MS results provide evidence indicating some measure of inclusion selectivity according to the "size-fit" of the host and guest molecules (according to carbon number) and the hydrogen deficiency (Z-series) of the naphthenic acid compounds. The relative abundance of the molecular ions of the CD-carboxylate anion adducts provides support for differing complex stability in aqueous solution. In general, the 1:1 complex stability according to hydrogen deficiency (Z-series) of NAs can be attributed to the nature of the cavity size of the cyclodextrin host compounds and the relative lipophilicity of the guest.

5.2 Introduction

Cyclodextrins (CDs) are cyclic compounds consisting of six, seven, or eight α-D-glucopyranoside units connected by α-(1, 4) linkages commonly referred to as α-, β-, and γ-CDs, respectively.[1] CDs typically possess a characteristic toroidal shape with a well-defined lipophilic cavity and a hydrophilic exterior that is suitable for the inclusion binding of appropriate sized guest compounds (*cf.* Scheme 4.1 in Chapter 4). CDs are of interest, in part, because of their ability to form inclusion complexes in aqueous solution.[2-4] CDs are well known to form relatively stable inclusion complexes with aliphatic and alicyclic carboxylic acids.[5-8] The formation and stability of CD-apolar guest complexes in aqueous solution are strongly governed by the hydrophobic effect, as evidenced from thermodynamic studies in aqueous solution.[9-12]

Naphthenic acids (NAs), according to classical definition are a class of aliphatic and alicyclic carboxylic acids of the following generic molecular formula, $C_nH_{2n+Z}O_2$, where n is the number of carbons and Z is "hydrogen deficiency"; hydrogen loss due to the formation of ring structures (*cf*. Figure 1.1 in Chapter 1).[13-16] NAs are part of the constituents of petroleum and have generated much recent interest because they are found as a by-product in the oil sands process water (OSPW) produced from the steam treatment and extraction of oil sands production. In their acidic form, NAs are found in OSPW *ca*. 100-150 ppm and are present predominantly in their anionic form at elevated pH conditions.[15] The occurrence of NAs in OSPW is an environmental and toxicological concern according to their known toxicity profiles.[14-16]

Recently, cyclodextrin (CD)-based polymeric materials have been utilized for the sequestration of organic compounds from gas and condensed phases.[17-21] In a previous report on the sorption between CD-based polymeric materials and NAs, favourable sorption was observed and evidence of molecular selectivity towards certain cogeners was concluded.[22] The strong binding affinity between CD-based copolymers and NAs was attributed to cooperative binding and hydrophobic effects. However, a more detailed understanding of the role of the polymer linker units and the cyclodextrin moieties in sorption processes is not established. The thermodynamic properties and sorption selectivity of the polymer framework may be understood by systematically investigating the nature of the complexes formed between native cyclodextrins and carboxylic acid compounds in aqueous solution.

The formation of complexes between CDs and carboxylic acid compounds have been investigated directly using NMR,[23] calorimetry,[24] conductivity,[25] among other

methods.[9] In the cases of non-chromophoric carboxylic acid compounds, the spectral displacement method[6,26] has been utilized to estimate binding constants, however; the technique is limited to situations for 1:1 inclusion complexes. Non-covalent complexes have recently been studied by ESI-MS,[27-29] and there are some recent examples of the utility of ESI-MS for the study of cyclodextrin-guest complexes.[30-34] In the case of non-chromophoric guests that are not amenable to spectroscopic methods, ESI-MS is useful for the determination of the composition of complex mixtures of carboxylic acid compounds (NAs).[35-37] In this work, we report a study of the complexes formed between carbohydrate host molecules (α-, β-, and γ-cyclodextrins, cellobiose) with carboxylic acid guest compounds (four types of aliphatic/alicyclic carboxylic acids and NAs) in aqueous solution using negative ion ESI-MS. The objectives of this work were to verify the formation of complexes and characterize their nature (e.g., inclusion *vs*. non-inclusion) and stoichiometry for the anionic forms of the surrogate carboxylic acids and Syncrude-derived NAs with α-, β-, and γ-CDs in aqueous solution.

5.3 Experimental

5.3.1 Materials

2-Hexyldecanoic acid (*Surrogate 1*; 256.43 g/mol), Pentylcyclohexane carboxylic acid (*Surrogate 2*; 198.3 g/mol), Dicyclohexylacetic acid (*Surrogate 3*; 224.35 g/mol), and 5β-Cholanic acid (*Surrogate 4*; 360.6 g/mol) were obtained from Sigma-Aldrich Canada Ltd. (Oakville, ON), and used as received (*cf*. Scheme 5.1). α-, β-, and γ-CD and cellobiose were obtained from Sigma-Aldrich Canada Ltd. (Oakville, ON), and used as

received. All reagents were of the highest commercial quality available unless noted otherwise.

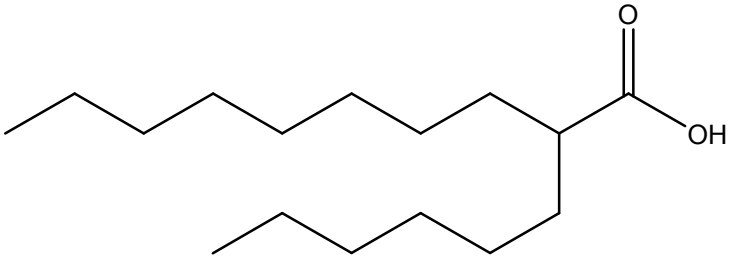

A) Surrogate 1; M_r = 256.43

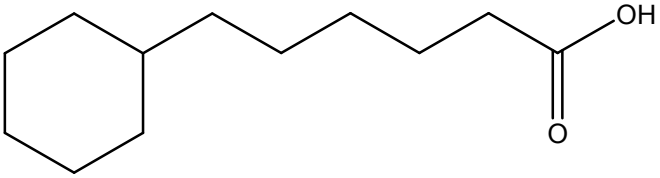

B) Surrogate 2; M_r = 198.3

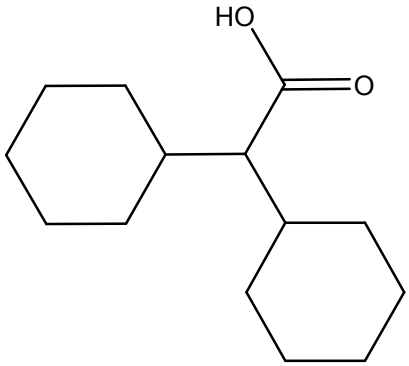

C) Surrogate 3 ;M_r = 224.35

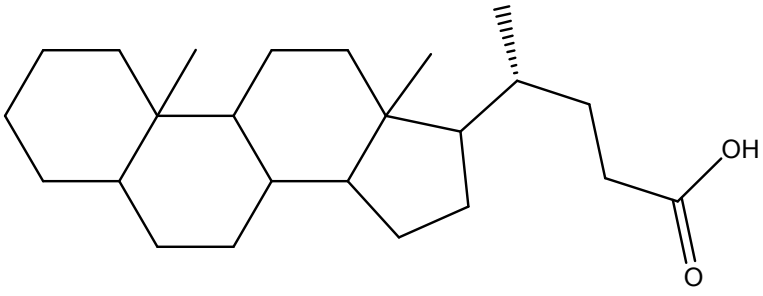

D) Surrogate 4 ; M_r = 360.6

Scheme 5.1. Molecular structure of surrogates (1-4): A) 2-hexyldecanoic acid, B) pentylcyclohexane carboxylic acid, C) dicyclohexylacetic acid, and D) 5β-cholanic acid.

Syncrude derived NAs were obtained from Athabasca oil sands tailings pond waters (OSPW) according to an established general procedure.[38] A volume of 6 L of OSPW was

allowed to settle in a 20 L carboy after the mixture was acidified with 0.4 ml of 18.76 M H_2SO_4 per 2 L of OSPW. The supernatant was then transferred to 3 × 2 L separatory funnels. Approximately 400 mL of dichloromethane was added to each 2 L separatory funnel and the organic phase was collected. The emulsion phase in the aqueous mixture was allowed to separate and the organic fractions were combined together and transferred to a round bottom flask. The solvent was removed using a rotovaporator at 60°C until a tar-like material remained. The mixture was reconstituted in 600 mL of water and brought to pH = 13 using 1.0 N NaOH. Upon reconstitution, the pH was lowered to 10 using concentrated H_2SO_4 and subsequently filtered through 0.45 μm and 0.1μm glass fibre micro filters, respectively. The filtrate was subjected to ultra filtration membranes with a 1000 molecular weight cutoff which was subsequently used as a stock solution for sorption experiments.

5.3.2 Preparation of Solutions

Two separate stock solutions of NAs were made at 2 different pH values (i.e. pH 9.00 and 5.00) from a 6990 mg/L aqueous stock solution extracted from Syncrude derived OSPW (pH 7.60). The stock solution was raised to pH 9.00 using 10^{-3} M ammonium hydroxide while the stock was lowered to pH 5.00 using 10^{-3} M acetic acid. The two pH values were chosen for this study because industrial OSPW have a pH of ~ 8, hence, the NAs exist in their ionized forms. In the case of surrogates, 100 ppm of each surrogate was prepared by measuring 10 mg of each in a 100 mL volumetric flask then diluting to a volume of 100 mL with Millipore water containing methanol (5%v/v) and ammonium hydroxide to adjust the pH. Stock solutions of host compounds (CDs and cellobiose) ~2,000 ppm of each were separately prepared by dissolving 200mg in a

100mL volumetric flask then diluting with Millipore water. Solutions of CD/guests (guests = surrogates 1-4, and Syncrude NAs) were made with 2000ppm of CD/cellobiose with 100 ppm guest. The pH was adjusted using 10^{-3} M ammonium hydroxide or acetic acid.

5.3.3. Electrospray Ionization Mass Spectrometry (ESI-MS)

The equilibrium concentrations of NAs were determined using negative ion ESI-MS. Samples (5.0μL) were introduced into the eluent stream (200 μL/minute, 50:50 CH_3CN:H_2O containing 0.1% NH_4OH) using a Waters 2695 advanced separation system (Milford, MA). Mass spectrometry analysis was conducted using a Quattro Ultima mass spectrometer (Micromass, UK). MS conditions were as follows: source temperature 90 °C, desolvation temperature 220 °C, cone voltage setting 62 V, capillary voltage setting 2.63 kV, cone gas (N_2) 147 L/hr, desolvation gas (N_2) 474 L/hr. The low and high mass resolutions were set at 14.0 (arbitrary units) and ion energy was 1.7 eV. Entrance voltage was 96 V, collision energy 13 eV and exit voltage 56 V. The multiplier was set at 410 V. Full scan MS (m/z 100-550) was employed. MassLynx version 4.1 software was utilized for all instrumental control and data acquisition/manipulation.

5.4 Results and Discussion

Figures 5.1 a-d depict the ESI-MS spectra for binary solutions containing each of the four different host compounds (CDs and cellobiose) with surrogate 1, respectively. In all cases, the concentration of the host exceeds that of the guest ([host]≈20×[guest]) and such conditions favour the formation of bound guest molecule for noncovalent host-guest complexes. The stock solutions were prepared at pH 5 and 9; however, the ESI-MS

results for alkaline conditions (pH 9) showed mass spectra with improved signal-to-noise as compared to pH 5. Therefore, the results shown in this work represent ESI-MS results for solutions at pH 9.While the formation of adducts in the gas phase may occur during the electrospray ionization process, the formation of 1:1 host-guest complexes in the solution phase are favoured. This is supported by increasing the relative concentrations of host and guest concentrations (not shown) and the increasing intensity of the adduct ions corresponding to the 1:1 inclusion complexes. Consequently the discussion that follows will assume that the adducts observed in the ESI-MS spectra were formed predominantly in solution, the relative abundances of which reflect their relative binding constants. In Figure 5.1a, the ESI-MS results for α-CD/surrogate 1 are shown. The molecular ions corresponding to the free guest (m/z = 225.2) and host (m/z = 971.6) are observed and the molecular ion for the 1:1 inclusion complex (m/z = 1228.2). Evidence of the formation of 1:1 complexes are similarly observed for binary solutions containing surrogate 1 and both β- and γ-CD, respectively (*cf*. Figures 5.1b-c). Cellobiose is a disaccharide with amphiphilic properties that is known to form non-covalent complexes with lipophilic compounds.[39-40] As can be seen in Figure 5.1d, a low abundance molecular ion (m/z=939.5) is observed corresponding to the 1:1 complex. The relative abundance for the CD-surrogate 1 adducts are as follows in descending order: β-CD-surrogate 1 > α-CD-surrogate 1 > γ-CD, and is consistent with the relative ordering of binding constants for medium to long chain fatty acid anions.[1,26] The ESI-MS of a solution containing glucose and surrogate 1 was examined and no apparent molecular ions corresponding to a 1:1 adduct was directly observed (results not shown). The observation is in accordance

with the highly solvated character of glucose[41] and its weak propensity to form noncovalent complexes with apolar solutes, as compared with cellobiose or CDs.

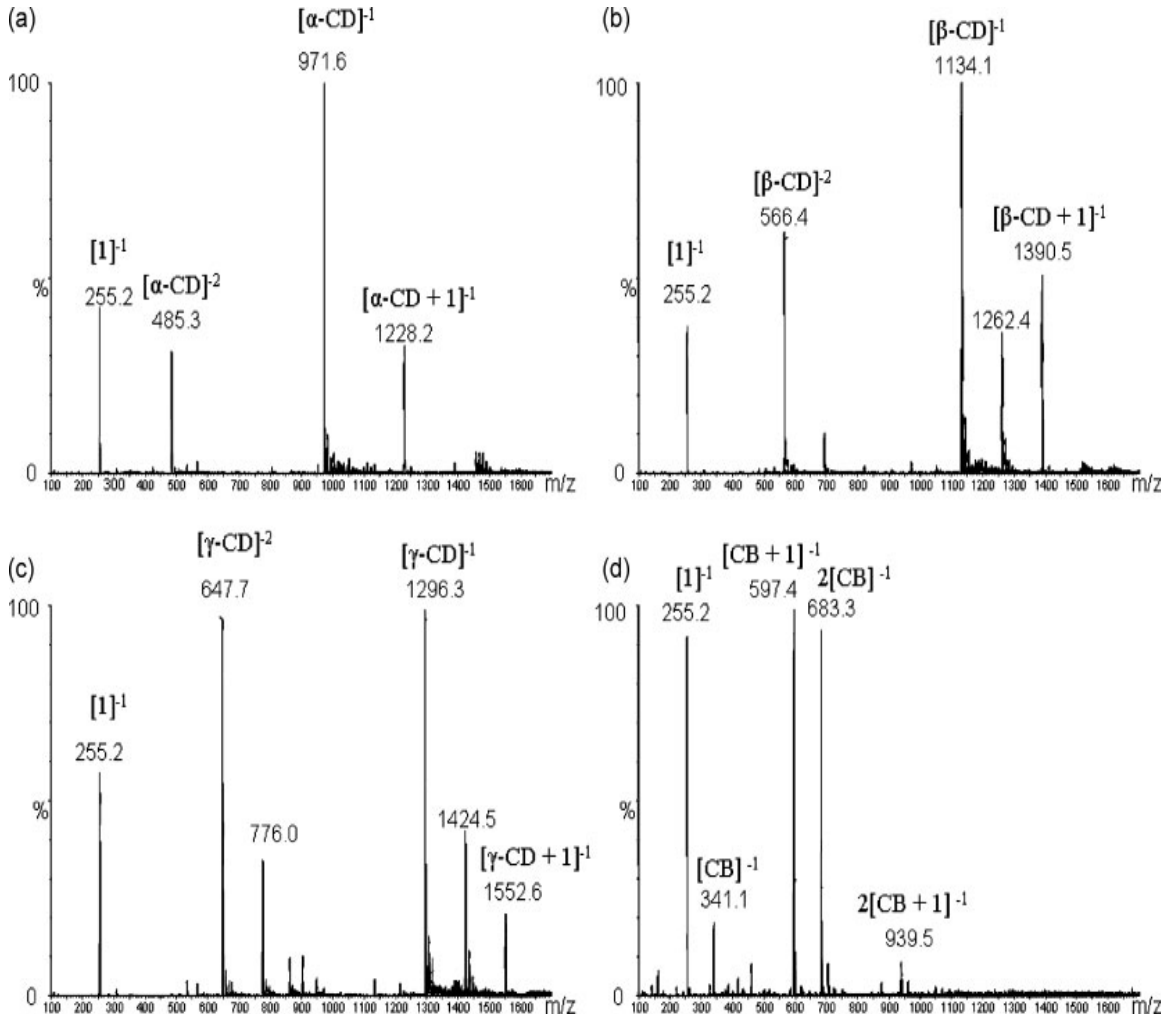

Figure 5.1. Electrospray ionization mass spectra of surrogate 1 (2-hexyldecanoic acid) in the presence of carbohydrate host molecules: a) α-CD, b) β-CD, c) γ-CD, and d) cellobiose at pH= 9.

Figures 5.2a-d depicts the ESI-MS spectra for binary solutions containing each of the four different host compounds (CDs and cellobiose) with surrogate 2, respectively. The results for surrogate 2 parallel those for surrogate 1 in the case of α- and β-CD (*cf.* Figures 5.2a and b), however, γ-CD and cellobiose does not indicate the formation of a

1:1 adduct (*cf*. Figures 2c and d). Although γ-CD is capable of forming a 1:1 inclusion complex, 1:2 complex may form since 2 guests can be co-included within this larger host molecule.[1,42] As seen in Figure 5.2c, there is evidence of molecular ions ~ m/z=850-900, and are attributed to the formation of a 1:2 γ-CD-surrogate 2 complex. The apparent lack of a molecular ion for cellobiose-surrogate 2 complex may be due to its low binding affinity for this host-guest system. The ESI-MS of a solution containing glucose and surrogate 2 was also examined and no molecular ions corresponding to a 1:1 adduct was observed (results not shown).

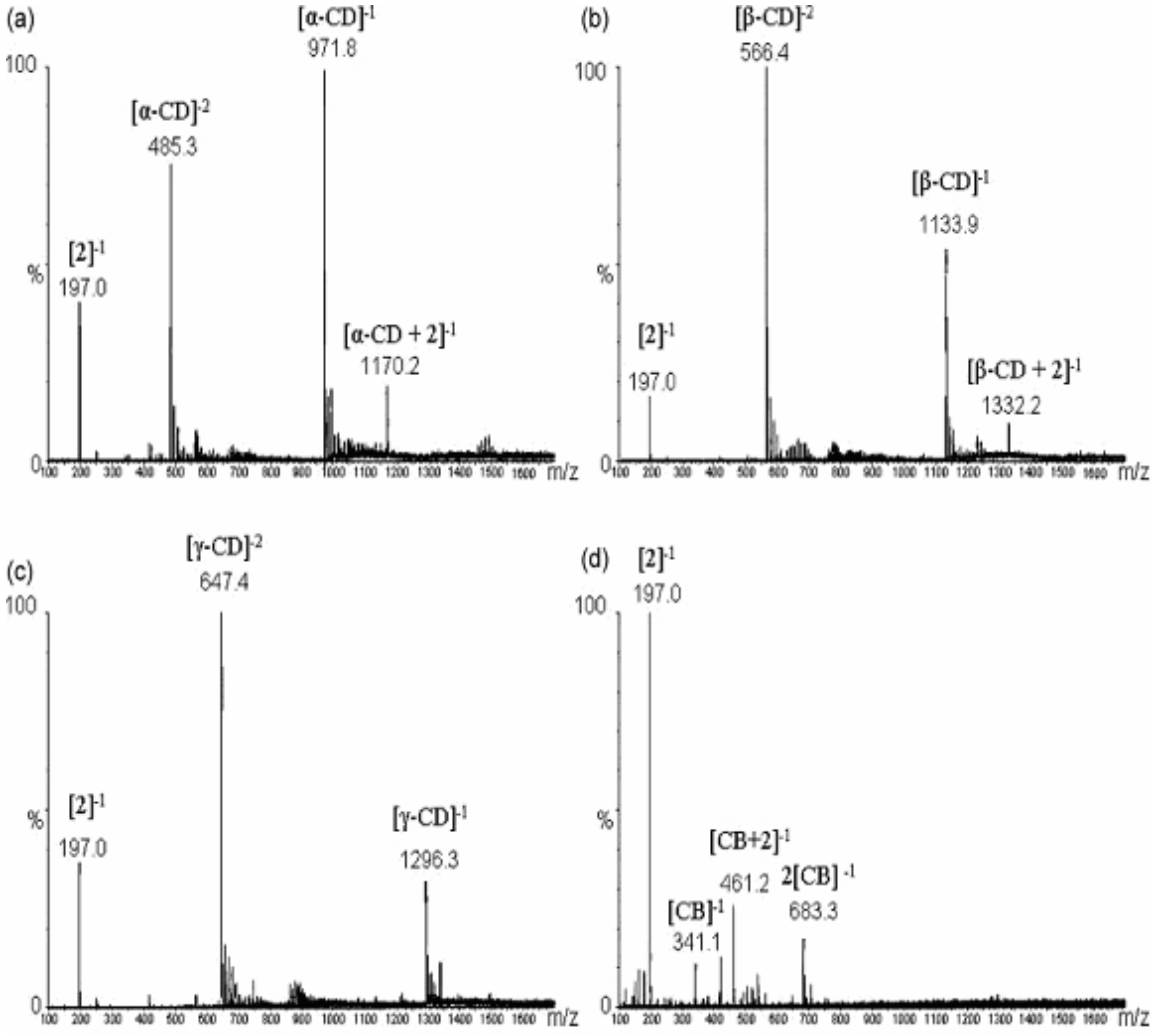

Figure 5.2. Electrospray ionization mass spectra of surrogate 2 (pentylcyclohexane carboxylic acid) in the presence of carbohydrate host molecules: a) α-CD, b) β-CD, c) γ-CD, and d) cellobiose at pH= 9.

Figures 5.3a-d depicts the ESI-MS spectra for binary solutions containing each of the four different host compounds (CDs and cellobiose) with surrogate 3, respectively. The results for surrogate 3 parallel those for surrogate 1 with α-, β- and γ-CD (*cf*. Figures 5.3a-c), however, a weak intensity molecular ion corresponding to the formation of a 1:1 cellobiose-surrogate 3 adduct was observed (*cf*. Figure 5.3d). The abundance of the 1:1 complexes for surrogate 3 are as follows: β-CD > α-CD > γ-CD > cellobiose. No molecular ions were observed corresponding to a 1:1 adduct for the ESI-MS solution containing glucose and surrogate 3 (results not shown).

Figures 5.4a-d depicts the ESI-MS spectra for binary solutions containing each of the four different host compounds (CDs and cellobiose) with surrogate 4, respectively. The results for surrogate 4 parallel those for surrogate 1 with α-, β- and γ-CD (*cf*. Figures 5.4a-c), however, the relative ordering of the 1:1 adducts for surrogate 4 are as follows: γ-CD > β-CD ≈ α-CD. The formation of favourable 1:1 molecular adducts for γ-CD is consistent with its suitable "size-fit"[43-44] for larger guest molecules, as compared to β-CD and α-CD. A weak intensity ion (m/z = 1043.9) corresponding to the 1:1 cellobiose-surrogate 4 complex is observed and is consistent with the lipophilic behaviour of the larger carboxylic acid guests. The ESI-MS of a solution containing glucose and surrogate 4 was examined and no molecular ion corresponding to a 1:1 adduct was observed (not shown).

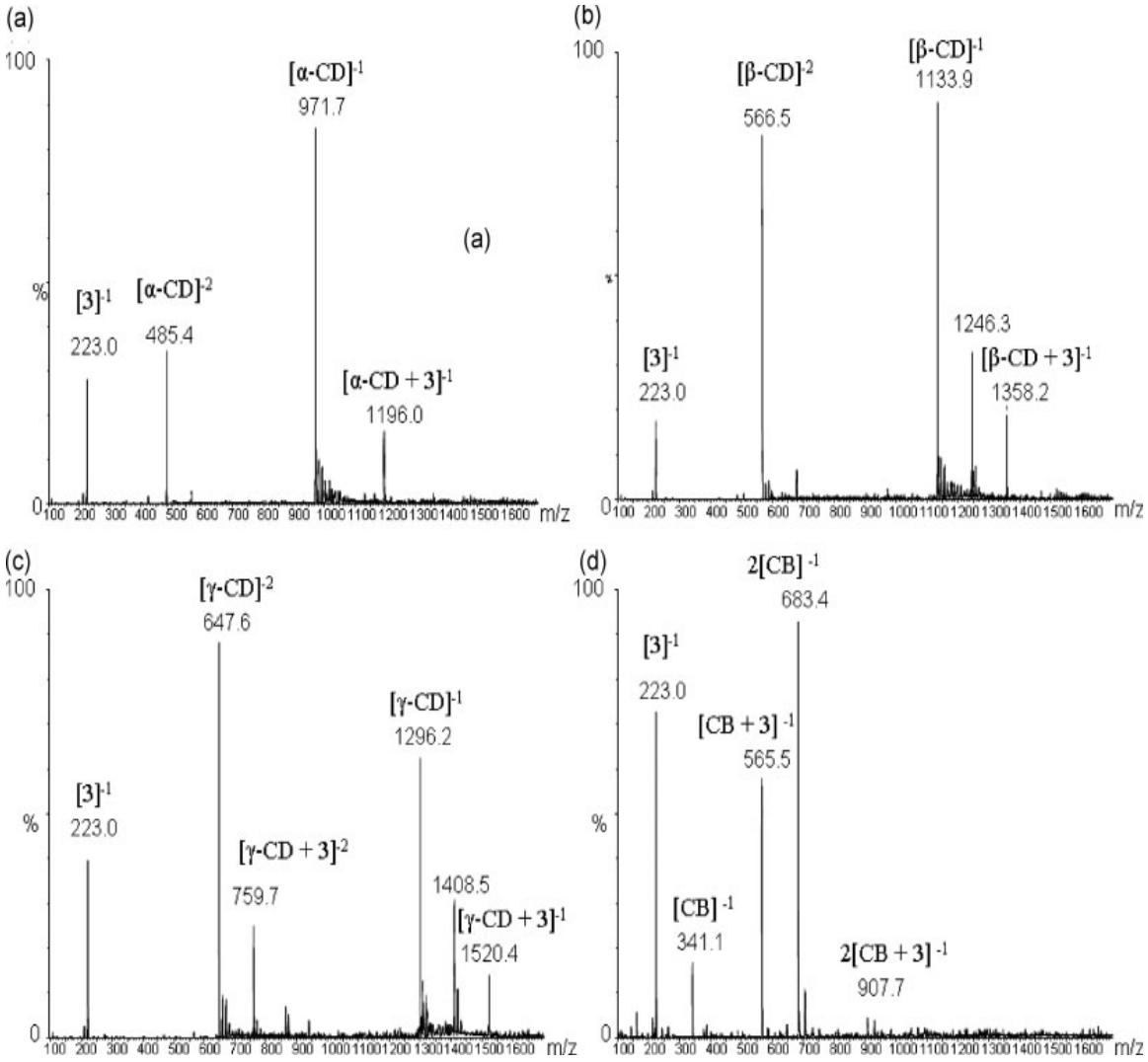

Figure 5.3. Electrospray ionization mass spectra of surrogate 3 (dicyclohexylacetic acid) in the presence of carbohydrate host molecules: a) α-CD, b) β-CD, c) γ-CD, and d) cellobiose at pH= 9.

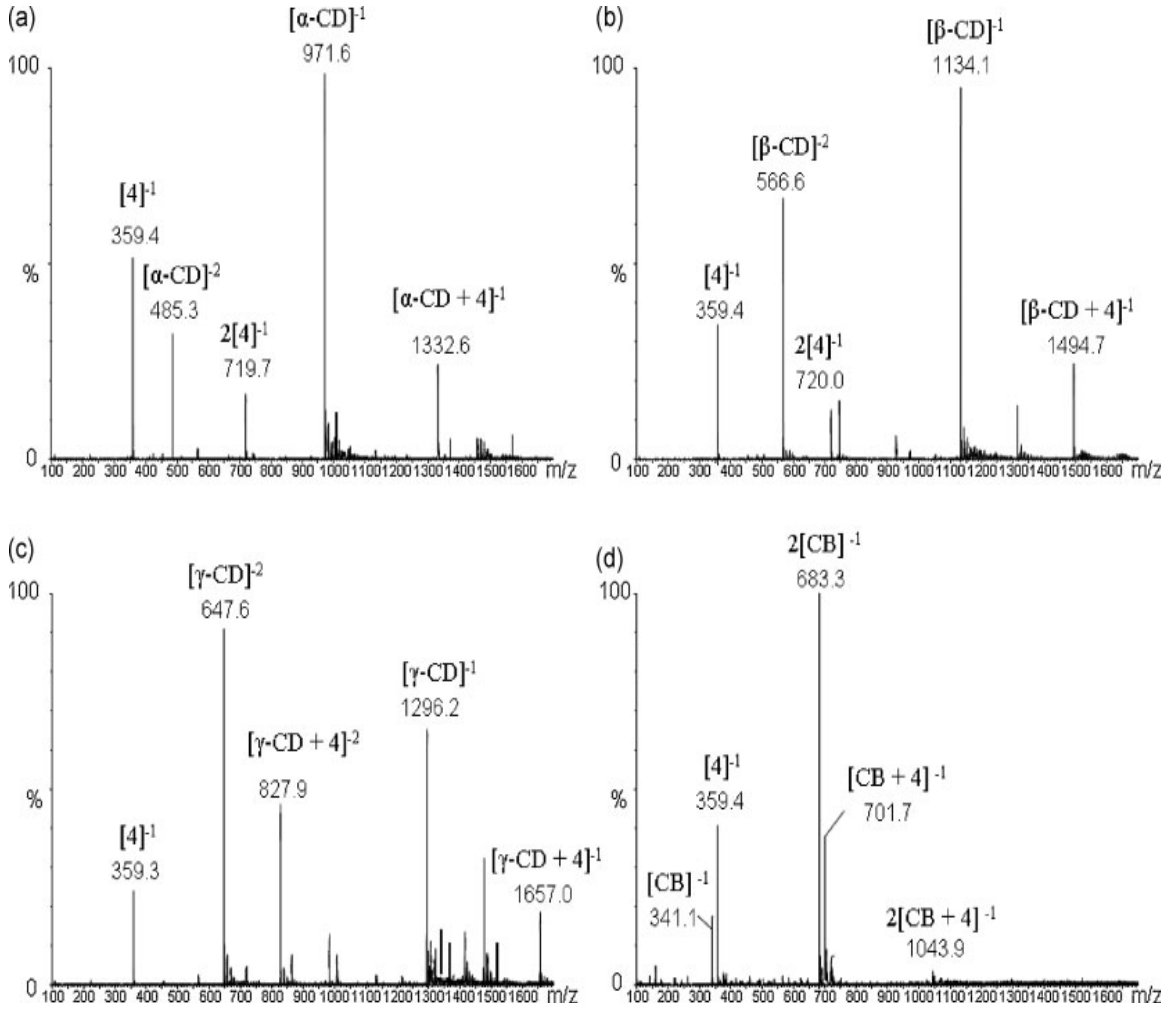

Figure 5.4. Electrospray ionization mass spectra of surrogate 4 (5β-cholanic acid) in the presence of carbohydrate host molecules: a) α-CD, b) β-CD, c) γ-CD, and d) cellobiose at pH= 9.

Figure 5.5 depicts the ESI-MS spectra for binary solutions containing each of the three CDs with Syncrude derived NAs,[38] respectively. In each case, the molecular ions corresponding to the free NAs, free CD, and 1:1 inclusion complex are observed. As seen in Figure 5.5, NAs are a complex mixture of alicyclic and aliphatic carboxylic acids with variable carbon number as evident by the distribution of molecular ions (m/z= 160-400). In the case of the 1:1 adducts, a similar range of m/z values are observed for the 1:1

complexes (m/z (CD + 160-400), however; the distribution of intensities for the individual cogeners as inclusion complexes differs from that pure stock solution of NAs, and indicates inclusion complex selectivity for 1:1 complexes. Given the range of molecular weights and structures of the cogeners of NAs, it is reasonable to assume that α-, β- and γ-CD would display some size-fit discrimination for cogeners possessing variable carbon number and Z-family, in accordance with the variable cavity diameter (α-CD=0.49nm, β-CD=0.62 nm, and γ-CD=0.79nm),[1] as observed for surrogates 1-4. Selective formation of inclusion complexes is most readily observed in three-coordinate plots of percentage abundance *vs*. carbon number (n) and Z-family. Previous studies have employed the use of similar 3-D graphs to evaluate evidence of sorption efficiency and selectivity.[15,35,45]

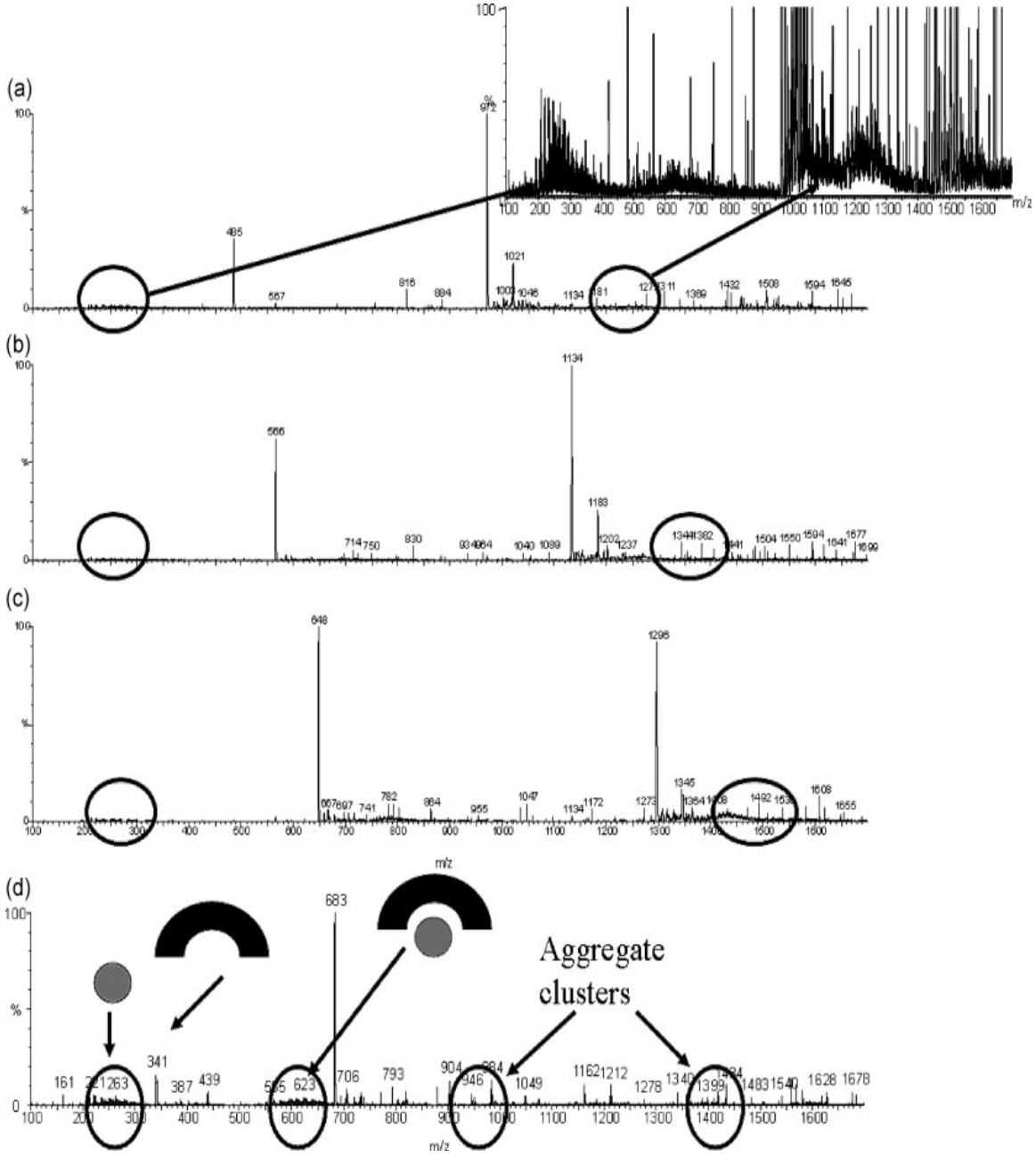

Figure 5.5. Electrospray ionization mass spectra of NAs in the presence of carbohydrate host molecules: a) α-CD, b) β-CD, c) γ-CD, and d) cellobiose at pH= 9. The first circle on the left of Figures 5.5 a, b, and c depicts the non-aggregated NAs, molecular weight typically 160 to 400. The circle to the right of Figures 5.5 a, b, and c depicts the aggregated NAs corresponding to α-CD.NAs centre ~ m/z 1021 (Figure 5.5a); β-CD.NAs centre ~m/z 1183 and β-CD.2NAs centre ~m/z 1250 (Figure 5.5b); and γ-CD.NAs centre ~m/z 1345 and γ-CD.2NAs centre ~m/z 1438 (Figure 5.5c) respectively.

Figure 5.6a depicts the abundance of molecular ions for NAs, according to Z-family (hydrogen deficiency) and carbon number (n) for a Syncrude obtained sample of NAs prior to treatment with host carbohydrate molecules and Figures 6b-f after equilibration with various carbohydrate compounds (e.g. α-, β-, and γ-CD and cellobiose). The 3-D graphs showing different profiles after sorption at pH=9. The profiles are shown for each carbon number and Z-family. A comparison of the stock solution of NAs with the extracts of CDs with NAs illustrates a key observation, i.e., the abundance of the cogeners of the NAs before and after equilibration vary according to the nature of the host molecules (α-, β- and γ-CD).

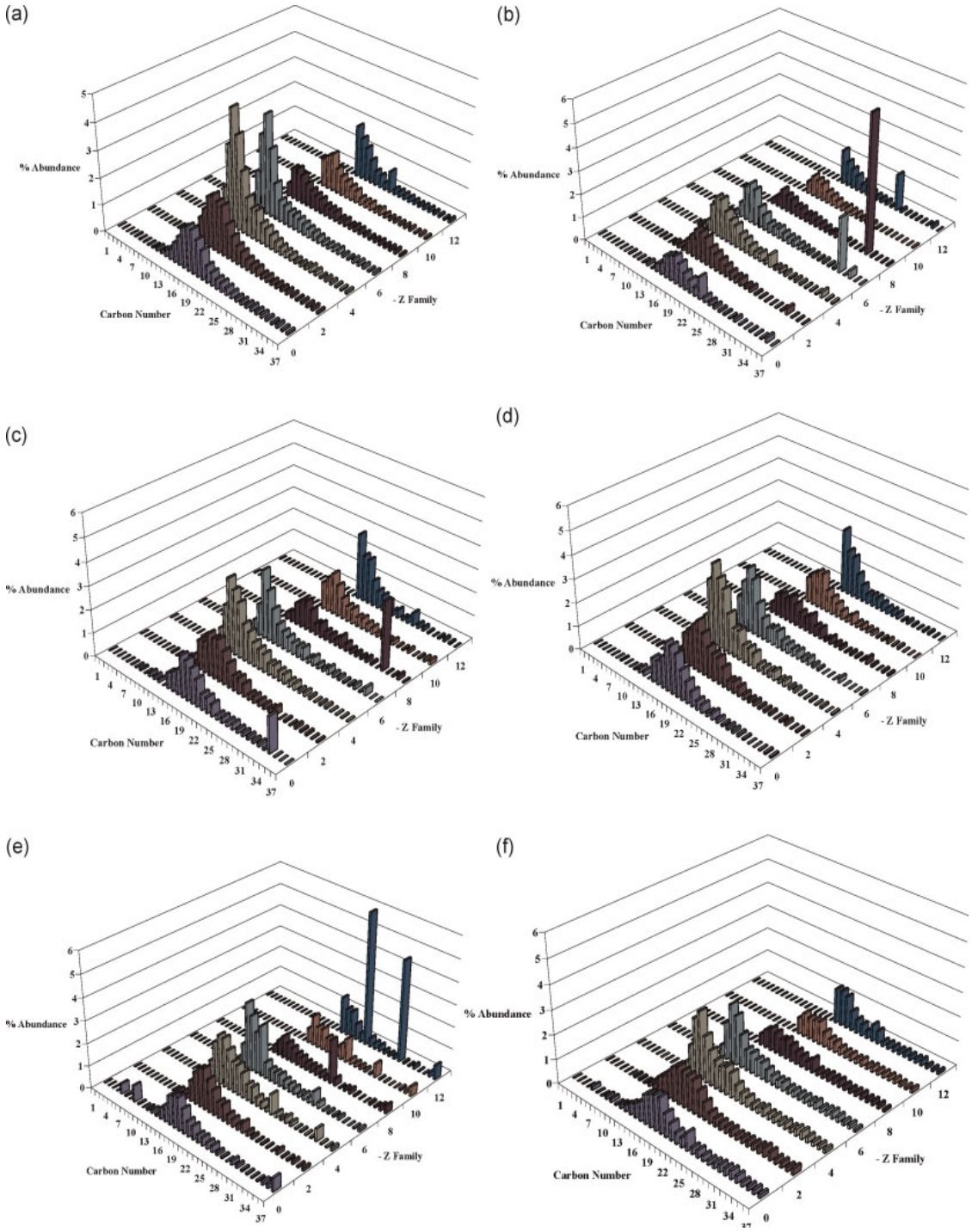

Figure 5.6. 3-D plots of ESI-MS data representing percent abundance of congeners with carbon number (n) and Z family for: a) Syncrude NAs, b) stock Syncrude NAs filtrate solution after sorption with α-CD, c) stock Syncrude NAs filtrate solution after sorption with β-CD, d) stock Syncrude NAs filtrate solution after sorption with γ-CD, e) stock Syncrude NAs filtrate solution after sorption with cellobiose, and f) stock Syncrude NAs filtrate solution after sorption with glucose.

Figure 5.6a shows the n- and Z-family distribution of cogeners for a stock solution of Syncrude NAs. In contrast, Figures 5.6b-e illustrates the composition and distribution of cogeners after equilibration with aqueous solutions containing excess CDs and cellobiose, respectively. In the case of Figure 5.6f, equilibration with glucose shows no apparent inclusion complexes formed and the distribution of cogeners is super imposable upon the results obtained in Figure 5.6a. There are clear difference in the size of cogeners that form complexes with α- and β-CD, whereas the distribution for γ-CD closely resembles that of the stock solution, however, it is noted that inclusion complexes are favoured for large carbon number and Z-family. The inclusion selectivity of NAs is consistent with the varying diameter of each CD cavity (α-CD=0.49nm, β-CD=0.62 nm, and γ-CD=0.79nm).[45] In a previous report,[22] evidence for selective sorption of commercial NAs was observed for β-CD based urethane polymers and granular activated carbon (GAC). Preferential sorption was observed for GAC with Fluka commercial grade NAs for the aliphatic NAs for n=10 and higher homologues (results not shown). As well, nearly complete sorption for the Fluka NA cogeners $Z \geq 2$ was observed. In the case of β-CD based urethane polymers, selective sorption is observed for cogeners Z = 0-4 as compared with cogeners $Z \geq 6$. These results are attributed to the molecular recognition properties (i.e. chemical nature and relative size of the diisocyanate linker unit) for such polymeric CD materials. The accompanying data in Table 1 highlights representative data for Z = –2 and –4 for NAs observed in ESI-MS spectra showing percent abundance of congeners with carbon number for Syncrude NAs and stock Syncrude NAs after sorption with a-cyclodextrin. The results in Table 1 provide clarity to the results and conclusions

in support of the evidence presented for the cyclodextrin/ naphthenic acid inclusion complexes.

Table 5.1. Representative data for Z = -2 and -4, NAs observed in ESI-MS showing percent abundance of congeners with carbon number for a) Syncrude NAs, and b) stock Syncrude NAs filtrate solution after sorption with α-CD.

	a		b	
Carbon #	**Z = -2 (RA%)**	**Z = -4 (RA%)**	**Z = -2 (RA%)**	**Z = -4 (RA%)**
7	0.024	N/A	0.023	N/A
8	0.033	N/A	0.027	N/A
9	0.068	N/A	0.046	N/A
10	0.273	0.182	0.000	0.078
11	0.205	0.439	0.100	0.174
12	0.466	1.359	0.145	0.501
13	0.930	3.038	0.135	1.285
14	1.354	4.437	0.648	1.741
15	1.900	3.540	0.956	1.757
16	2.056	2.320	1.307	1.339
17	1.906	1.441	1.307	1.082
18	1.846	1.137	1.185	0.963
19	1.278	1.141	0.872	0.694
20	0.927	0.773	0.747	0.589
21	0.681	0.688	0.598	0.435
22	0.567	0.541	0.460	0.310
23	0.401	0.394	0.332	0.348
24	0.317	0.298	0.258	0.191
25	0.288	0.229	0.292	0.544
26	0.175	0.201	0.135	0.115
27	0.186	0.118	0.170	0.156
28	0.127	0.102	0.077	0.128
29	0.124	0.122	0.052	0.071
30	0.111	0.193	0.029	0.097
31	0.118	0.152	0.013	0.088
32	0.097	0.067	0.038	0.053
33	0.067	0.093	0.052	0.048
34	0.094	0.093	0.272	0.054
35	0.093	0.070	0.027	0.249
36	0.105	0.058	0.038	0.063
37	0.078	0.088	0.022	0.060

In general, selective sorption of guest molecules such as carboxylic acids is consistent with the general concept of "size-fit" selectivity observed in many supramolecular host-guest systems.[6,43-44,46-47] The lipophilicity of carboxylic acid guest molecules generally increases as the molecular weight increases. In an independent study of inclusion complex stability of surrogate compounds and different NAs, it was concluded that cogeners/surrogate with greater molecular weights displayed greater binding affinity with β-CD in aqueous solution.[48] These results are anticipated to provide a further understanding of the sorption processes between cyclodextrin-based polymeric materials and carboxylic acid compounds in aqueous solution at various conditions.

5.5 Conclusions

ESI-MS was well suited for the study of a series of carbohydrate host molecules (cyclodextrins and cellobiose) and guest molecules (surrogates 1-4 and NAs) in aqueous solution. In the case of α-, β- and γ-CDs, inclusion complexes were formed with surrogates 1-4 with variable association constants and host-guest stoichiometry. The latter was inferred from the observed relative intensity and molecular ion adducts. Cellobiose was observed to predominantly form 1:1 non-inclusion complexes with the surrogate ions (except surrogate 2) and NAs in aqueous solution at pH=9. In contrast, α- and β-CD were observed to form stable 1:1 inclusion complexes with surrogates 1-3 whereas γ-CD formed stable 1:1 complexes with surrogate 4. Likewise, 1:1 inclusion complexes were formed between α-, β- and γ-CDs with NAs, however, γ-CD formed more stable inclusion complexes with larger molecular weight cogeners/surrogates.

Glucose did not form any apparent non-covalent complexes with surrogates 1-4 or NAs, respectively.

5.6 Acknowledgements

Financial assistance was provided by the Natural Sciences and Engineering Research Council and the Program of Energy Research and Development. M.H.M acknowledges the University of Saskatchewan for the award of a Graduate Teaching Fellowship and Environment Canada for the Science Horizons Program award.

5.7 References

1. Clarke, R. J.; Coates, J. H.; Lincoln, S. F. *Adv. Carbohydr. Chem. Biochem.* **1988**, *46*, 205-249.
2. Terekhova, I. V.; Kulikov, O. V. *Chem. Polysacch.* **2005**, 38-76.
3. Rekharsky, M. V.; Inoue, Y. *Chem. Rev.* **1998**, *98*, 1875-1918.
4. Schneider, H.-J.; Hacket, F.; Rudiger, V.; Ikeda, H. *Chem. Rev.* **1998**, *98*, 1755-1786.
5. Buvari, A. *J. Inclusion Phenom.* **1983**, *1*, 151-157.
6. Eftink, M. R.; Andy, M. L.; Bystrom, K.; Perlmutter, H. D.; Kristol, D. S. *J. Am. Chem. Soc.* **1989**, *111*, 6765-6772.
7. Gadre, A.; Rüdiger, V.; Schneider, H.-J.; Connors, K. A. *J. Pharm. Sci.* **1997**, *86*, 236-243.
8. Kralj, B.; Scaronmidovnik, A.; Jo; zcaron; Kobe, e. *Rapid Commun. Mass Spectrom.* **2009**, *23*, 171-180.
9. Szente, L.; Szejtli, J.; Szeman, J.; Kato, L. *J. Inclusion Phenom.* **1993**, *16*, 339-354.
10. Stoedeman, M.; Gomez-Orellana; Isabel; Hallen, D. *J. Inclusion Phenom. Macrocyclic Chem.* **2003**, *46*, 125-132.
11. Wilson, L. D.; Verrall, R. E. *J. Phys. Chem. B.* **2000**, *104*, 1880-1886.

12. Redenti, E.; Szente, L.; Szejtli, J. *J. Pharm. Sci.* **2001**, *90*, 979-986.
13. Lo, C. C.; Brownlee, B. G.; Bunce, N. J. *Anal. Chem.* **2003**, *75*, 6394-6400.
14. Clemente, J. S.; Fedorak, P. M. *Chemosphere* **2005**, *60*, 585-600.
15. Quagraine, E. K.; Peterson, H. G.; Headley, J. V. *J. Environ. Sci. Health, Part A: Toxic/Hazard. Subst. Environ. Eng.* **2005**, *40*, 685-722.
16. Headley, J. V.; Crosley, B.; Conly, F. M.; Quagraine, E. K. *J. Environ. Sci. Health, Part A: Toxic/Hazard. Subst. Environ. Eng.* **2005**, *40*, 1 - 27.
17. Mizobuchi, Y. *J. Chromatogr., A* **1981**, *208*, 35-40.
18. Crini, G. *Prog. Polym. Sci.* **2005**, *30*, 38-70.
19. Crini, G.; Bertini, S.; Torri, G.; Naggi, A.; Sforzini, D.; Vecchi, C.; Janus, L.; Lekchiri, Y.; Morcellet, M. *J. Appl. Polym. Sci.* **1998**, *68*, 1973-1978.
20. Ma, M.; Li, D. *Chem. Mater.* **1999**, *11*, 872-874.
21. Wenz, G. *Angew. Chem. Int. Ed. Engl* **1994**, *33*, 803-822.
22. Mohamed, M. H.; Wilson, L. D.; Headley, J. V.; Peru, K. M. *Process Saf. Environ. Prot.* **2008**, *86*, 237-243.
23. Wilson, L. D.; Verrall, R. E. *Can. J. Chem.* **1998**, *76*, 25-34.
24. Siimer, E.; Kurvits, M.; Kostner, A. *Thermochim. Acta* **1987**, *116*, 249-256.
25. Tanaka, K.; Mori, M.; Xu, Q.; Helaleh, M. I. H.; Ikedo, M.; Taoda, H.; Hu, W.; Hasebe, K.; Fritz, J. S.; Haddad, P. R. *J. Chromatogr., A* **2003**, *997*, 127-132.
26. Wilson, L. D.; Siddall, S. R.; Verrall, R. E. *Can. J. Chem.* **1997**, *75*, 927-933.
27. Ganem, B.; Li, Y. T.; Henion, J. D. *J. Am. Chem. Soc.* **1991**, *113*, 6294-6296.
28. Smith, R. D.; Light-Wahl, K. J. *Biol. Mass Spectrom.* **1993**, *22*, 493-501.
29. Cunniff, J. B.; Vouros, P. *J. Am. Soc. Mass Spectrom.* **1995**, *6*, 437-447.
30. Danikiewicz, W. *Mass spectrometry of CyDs and their complexes*; Wiley-VCH Verlag GmbH & Co. KGaA: Weinheim, Germany, 2008; Vol. 257.
31. Barbara, J. E.; Eyler, J. R.; Powell, D. H. *Rapid Commun. Mass Spectrom.* **2008**, *22*, 4121-4128.
32. Galaverna, G.; Corradini, R.; Dossena, A.; Marchelli, R. *Electrophoresis* **1999**, *20*, 2619-2629.
33. Cai, Y.; Tarr, M. A.; Xu, G.; Yalcin, T.; Cole, R. B. *J. Am. Soc. Mass Spectrom.* **2003**, *14*, 449-459.

34. Gabelica, V.; Galic, N.; Rosu, F.; Houssier, C.; Pauw, E. D. *J. Mass Spectrom.* **2003**, *38*, 491-501.
35. Headley, J. V.; Peru, K. M.; Barrow, M. P. *Mass Spectrom. Rev.* **2009**, *28*, 121-134.
36. Martin, J. W.; Han, X.; Peru, K. M.; Headley, J. V. *Rapid Commun. Mass Spectrom.* **2008**, *22*, 1919-1924.
37. Richardson, S. D. *Anal. Chem.* **2008**, *80*, 4373-4402.
38. Janfada, A.; Headley, J. V.; Peru, K. M.; Barbour, S. L. *J. Environ. Sci. Health, Part A: Toxic/Hazard. Subst. Environ. Eng.* **2006**, *41*, 985-997.
39. Purokoski, S.; Lajunen, K.; Hakkinen, P. *Finn. Chem. Lett.* **1987**, *14*, 1-5.
40. Kalenius, E.; Koivukorpi, J.; Kolehmainen, E.; Vainiotalo, P. *Eur. J. Org. Chem.* **2010**, *2010*, 1052-1058.
41. Paolantoni, M.; Gallina, M. E.; Sassi, P.; Morresi, A. *J. Chem. Phys.* **2009**, *130*, 164501/1-164501//8.
42. Yu, S.-C.; Bochot, A.; Bas, G. L.; Chéron, M.; Mahuteau, J.; Grossiord, J.-L.; Seiller, M.; Duchêne, D. *Int. J. Pharm.* **2003**, *261*, 1-8.
43. Song, L. X.; Wang, H. M.; Xu, P.; Zhang, Z. Q.; Liu, Q. Q. *Bull. Chem. Soc. Jap.* **2007**, *80*, 2313-2322.
44. Yang, B.; Yang, L.-J.; Lin, J.; Chen, Y.; Liu, Y. *J. Inclusion Phenom. Macrocyclic Chem.* **2009**, *64*, 149-155.
45. Schneider, H.-J. *Frontiers in Supramolecular Organic Chemistry and Photochemistry*; VCH: New York, 1991.
46. Harada, A.; Hashidzume, A.; Takashima, Y. *Cyclodextrin-based supramolecular polymers*; Springer, 2006; Vol. 201.
47. Tonelli, A. E. *Polymer* **2008**, *49*, 1725-1736.
48. Mohamed, M. H.; Wilson, L. D.; Headley, J. V.; Peru, K. M. *Can. J. Chem.* **2009**, *87*, 1747-1756.

CHAPTER 6

PUBLICATION 5

Description

The following is a verbatim copy of an article that was published in November of 2009 in the Canadian Journal of Chemistry journal (*Can. J. Chem.:* **2009**, *87(12)*, 1747-1756) and describes quantitative determination of the binding constant values for the inclusion complexes of β-CD/NAs and β-CD/NAs-surrogates using spectral displacement study.

Authors' Contribution

I conducted all the experimental work except for the ESI-MS which was done by Mr. Kerry Peru. This work was supervised by Dr. Wilson and Dr. Headley. I wrote the first draft of the manuscript with extensive editing by each supervisor prior to submission for publication. Written permission was obtained from all contributing authors and the publishers to include this material in this thesis.

Relation of Chapter 6 (Publication 5) to the Overall Objectives of this Project

As mentioned in the introduction, information on the binding affinity between β-CD and NAs is important for the application of such polymer materials in order to predict the formation of complex stability. The spectral displacement technique uses competitive equilibria with a chromophoric dye and the relative absorbance changes provide a measure of the concentration of NAs and its surrogates (non-chromophoric). This indirect

spectrophotometric measurement of the inclusate provides good accuracy for the determination of these binding affinities.

Graphical Abstract

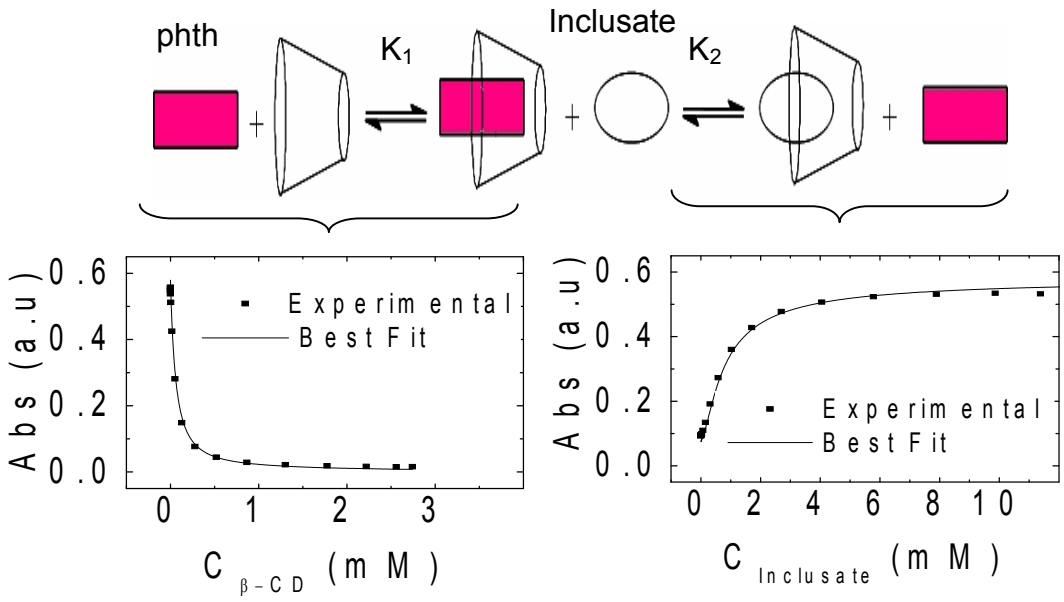

A dye based decolourization method is proposed for the indirect estimation of 1:1 β–cyclodextrin/inclusate equilibrium binding constants (K_2). The proposed method is suitable for spectroscopically transparent complex mixtures of naphthenic acids (NAs).

6. A Spectral Displacement Study of Cyclodextrin/Naphthenic Acids Inclusion Complexes

Mohamed H. Mohamed,[§] Lee D. Wilson, [§] John V. Headley[¥] Kerr M. Peru[¥]*

[§]Department of Chemistry, University of Saskatchewan, 110 Science Place, Saskatoon, Saskatchewan, S7N 5C9

[¥]Water Science and Technology Directorate, 11 Innovation Boulevard, Saskatoon, Saskatchewan, S7N 3H5

*Corresponding Author

Received 11 June 2009

6.1 Abstract

The spectral displacement technique has been used to obtain 1:1 β–cyclodextrin /carboxylate anion equilibrium binding constants (K_2) for some complex mixtures of naphthenic acids (NAs) and some examples of single component NAs in aqueous solution. Three specific examples of single component NAs were chosen with variable Z values as follows: 2-hexyldecanoic acid (Z = 0; surrogate 1), *trans*-4-pentylcyclohexanecarboxylic acid (Z = -2; surrogate 2) and dicyclohexylacetic acid (Z = -4; surrogate 3). The estimated K_2 values for surrogate 1, 2 and 3 are as follows: 1.42×10^3 M^{-1}, 52.2×10^4 M^{-1}, and 13.1×10^4 M^{-1}, respectively. The corresponding K_2 values are 2.34×10^4 M^{-1} and 1.27×10^4 M^{-1} for commercial (Fluka) and industrial (Syncrude) sourced NAs, respectively. The magnitude of K_2 for 1:1 complexes formed between β-CD and surrogate 1, 2 and 3 did not

correlate with the degree of hydrogen deficiency (Z-series) but there was a correlation with the size of the guest molecules (n) examined in this study. The correlation between complex stability and the relative size of the lipophilic fragments of the guest molecule are related to the importance of the hydrophobic effect for inclusion of such carboxylic acid guest molecules within β-CD.

6.2 Introduction

Naphthenic acids (NAs) are predominantly complex mixtures of saturated alicyclic and aliphatic carboxylic acids with the general formula $C_nH_{2n+Z}O_2$, where n is the number of carbon atoms and 2n+Z is number of hydrogen atoms where Z is the hydrogen deficiency; hydrogen loss due to ring structure. Generally, the carboxylic group is attached to a cyclopentane or cylcohexane ring through a methylene group or an alkyl chain containing five or more methylene groups as shown in Figure 1.1 in Chapter 1. The molecular structure, composition, and concentration of NAs are dependent on the source of crude oil.[1-5]

NAs are non-volatile, chemically stable, and possess surface activity. The acid dissociation constants range between 10^{-5} and 10^{-6} M^{-1} and are comparable to typical carboxylic acids (acetic acid = $10^{-4.8}$M, propionic acid = $10^{-4.9}$M, palmitic acid $10^{-4.9}$M).[5-7] The presence of NAs in petroleum has led to environmental, health and industrial concerns. NAs are known to be toxic to aquatic organisms, algae, and mammals. [5-8] NAs are suspected endocrine-disrupting substances; however, the toxicological implications of the various types of NAs are not well understood. Thus, there is a great need to develop improved methods to sequester NAs leachates from aquatic environments, such as oil

sands tailings ponds, and to alleviate concerns of their deleterious health and environmental effects.

Cylodextrins (CDs) are of interest, in part, because of their ability to form inclusion complexes in aqueous solution. In particular, they are well known to form relatively stable inclusion complexes with aliphatic and alicyclic carboxylic acids.[9-12] For the latter reason, CDs may display strong binding affinity to NA molecules.

Recently, cyclodextrin based polymeric materials were used to adsorb NAs from aqueous solutions with considerable success.[13] However, a detailed understanding of the sorption mechanism for polymeric materials requires an understanding of the types of inclusion complexes formed and the magnitude of the binding constants. Thus, this study outlines the use of the spectral displacement technique to study the interaction of β-cyclodextrin (β-CD) with NAs and single component examples of NAs in aqueous solution, respectively.

Various instrumental methods have been used to examine the nature of the CD/inclusate complexes formed between β-CD and carboxylic acid guest compounds. Among these techniques are ^{1}H NMR[14], sound velocity[15], conductivity[16], surface tension[17], electrochemical measurements[18], UV-VIS spectrophotometry[19] and fluorescence measurements[20]. The latter three methods involve direct measurement of bound or free concentrations of inclusates whereas the other methods involve the measurement of a bulk solution property (time averaged property consisting of two or more states) that is proportional to some aspect of the complexation process. The apparent discrepancies in the literature between the values of binding constants obtained from different techniques have been attributed to the relative accuracy of the measured variables. However, methods

which involve the measurement of free or bound inclusates concentrations are expected to yield a more accurate estimate of the binding constant.[21]

The spectral displacement technique[9,22-31] enables determination of the binding constants of spectroscopically transparent compounds such as NAs to β-CD. The determination of the binding constants for such complexes involves the measurement of the absorbance changes of a suitable chromophore in the presence of CD and a competing non-chromophoric inclusate. Some examples of the chromophores employed include phenolphthalein (phth)[9,22-29], methyl orange[30] and *p*-nitrophenol[31]. Scheme 1.6 in Chapter 1 illustrates the two competitive equilibria involved in the spectral displacement technique.

This technique involves certain assumptions and provide good accuracy for the determination of a CD-inclusate binding constant (K_2) values when the relative change in the absorbance of phth between bound and unbound states is large and is directly related to the amount of unbound inclusate. Non-spectroscopic techniques are sometimes susceptible to large errors when K_2 is large ($>10^4$ M^{-1}) because the fraction of unbound species is generally low for this condition and techniques which involve the measurement of macroscopic changes for a total solution property and do not reflect this contribution accurately. Consequently, there are greater uncertainties for the value of K_2 derived from such methods. A further complication arises due to implicit statistical bias in the analysis of the primary data using linearization methods; for example, the inherent assumptions in the Benesi-Hildebrand plots are generally not met for strongly bound host-guest systems.[22,32]

This paper presents the results of a determination of the binding constants between β-CD and different types NAs and some single component examples of NAs in aqueous

solutions at room temperature. The three components chosen to represent examples of NAs with variable Z values are 2-hexyldecanoic acid (Z = 0; surrogate 1), trans-4-pentylcyclohexanecarboxylic acid (Z = -2; surrogate 2) and dicyclohexylacetic acid (Z = -4; surrogate 3), respectively, as shown in Scheme 5.1 in Chapter 5.

6.3 Experimental

Absorption measurements were obtained with a double beam spectrophotometer (Varian CARY 100) at room temperature (295 ± 0.5 K) All solutions were prepared by volume in a 0.1 M sodium hydrogen carbonate buffer adjusted to pH 10.5 with 6M sodium hydroxide. The concentration of phth (C_{phth}) was maintained at ~ 2×10^{-5} M in all experiments. For the determination of the CD/inclusate binding constants, K_2, the concentration of β-CD ($C_{\beta\text{-CD}}$) was held constant at ~ 3×10^{-4} M and the concentration of NAs or single component NAs (surrogate 1-3) were varied to exceed the 1:1 mole ratio of the CD/inclusate. A stock solution of phth in ethanol was made and aliquots were utilized to prepare aqueous solutions of phth in buffer. The ethanol/water (0.04 %; v/v)[28] solution was used to increase the solubility of phth. All aqueous solutions were freshly prepared and run within 1.5 h to ensure that the absorbance changes due to any instability of phth at pH 10.5 did not contribute to experimental artefacts. The respective compositions of Fluka and Syncrude sourced NAs were determined using electrospray ionization mass spectrometry (ESI-MS) measurements with a Quattro Ultima mass spectrometer (Micromass, UK) equipped with an electrospray interface operating in the negative ion mode configuration, as described previously.[13]

β-CD (VWR) was used as received and the water content was determined using a thermogravimetric analyzer (Q5000, TA Instruments). The water contents were accounted for in the determination of $C_{\beta\text{-CD}}$ where the hydrate content varied from 10.98-11.53 (±0.3)% for different samples of β-CD hydrate. 2-hexyldecanoic acid (surrogate 1), *trans*-4-pentylcyclohexanecarboxylic acid (surrogate 2) and dicyclohexylacetic acid (surrogate 3) and Fluka NAs were obtained from Sigma-Aldrich. Syncrude-derived NAs were extracted in bulk from an Athabasca oil sands tailings pond using a published procedure.[33] Phth (Aldrich) was used as received since there was no difference in molar absorptivity between the purified and unpurified materials.[27]

A previously described[22] non-linear least squares (NLLS) fitting procedure was used to determine the 1:1 binding constants, K_1 and K_2, between β-CD and phth and the inclusate, respectively. The method utilizes the Beer-Lambert law and the assumption that the molar absorptivity of the β-CD/phth complex is zero.[23] The following equilibrium and mass-balance relations apply to the competitive equilibrium, as outlined in Scheme 6.1.

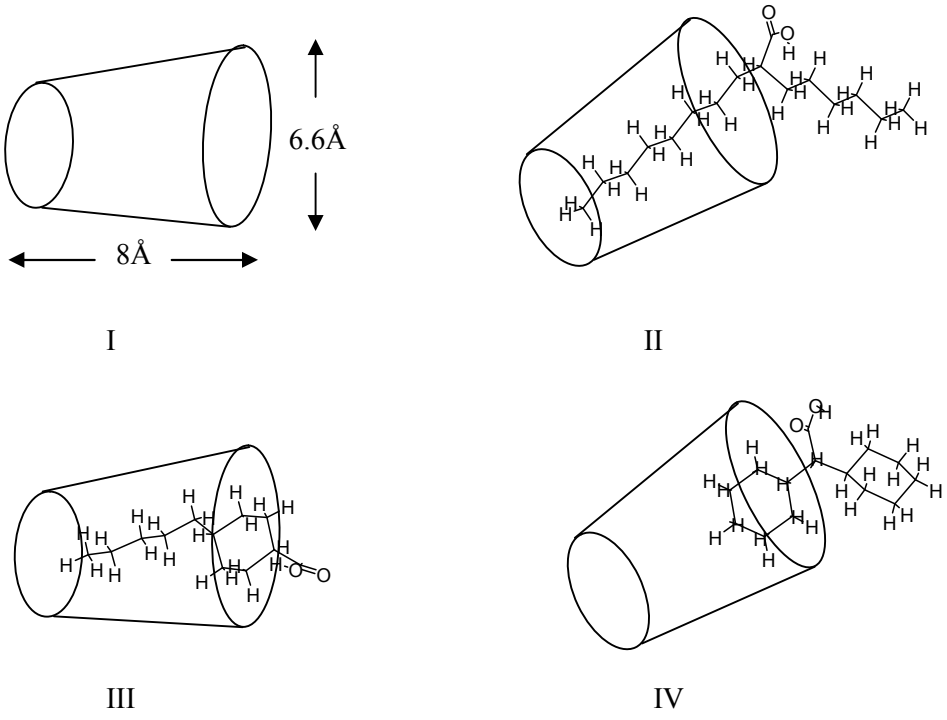

Scheme 6.1. Lipophilic fragments of the guest molecules that are included in β-CD. LSA values are derived from these included fragments. These molecular structures are; β-CD (I), β-CD/surrogate 1 (II), β-CD/surrogate 2 (III) and β-CD/surrogate 3 (IV), complex, respectively. Note: The relative size of the β-CD torus and the carboxylic acid are not be drawn to scale.

$$[S]_0 = [S] + [CD - S] = [S](1 + K_2[CD]) \qquad \text{Equation 6.1}$$

$$[phth]_0 = [[phth]] + [CD - [phth]] = [[phth]](1 + K_1[CD]) \qquad \text{Equation 6.2}$$

$$[CD]_0 = [CD] + [CD - S] + [CD - phth] \qquad \text{Equation 6.3}$$

The terms $[S]_0$, $[S]$, and $[CD\text{-}S]$ refer to the total, unbound, and 1:1 complexed forms of the inclusate, respectively. $[CD\text{-}S]$ and $[CD\text{-}phth]$ are related to $[S]_o$, $[phth]_o$, K_2, and K_1 as follows:

$$[CD - S] = [S]_o\left(1 + \frac{1}{K_2[CD]}\right)^{-1} \qquad \text{Equation 6.4}$$

$$[CD-phth]=[phth]_o\left(1+\frac{1}{K_1[CD]}\right)^{-1} \qquad \text{Equation 6.5}$$

Upon substitution into Equation 6.3 and rearrangement, the following cubic expression in terms of unbound β-CD ([CD]) is obtained in Equation 6.6.

$$[CD]^3+[CD]^2\left(\frac{K_2+K_1}{K_2K_1}+[phth]_o+[S]_o-[CD]_o\right)+[CD]\left(\frac{1}{K_2K_1}+\frac{[S]_o}{K_1}+\frac{[phth]_o}{K_2}-\frac{[CD]_o}{K_1}-\frac{[CD]_o}{K_2}\right)-\left(\frac{[CD]_o}{K_2K_1}\right)=0 \qquad \text{Equation 6.6}$$

The real solution to the cubic root of Equation 6.6 was obtained by application of the Newton-Raphson method[34-35] using appropriate boundary values of $[S]_o$, $[phth]_o$, K_2, and K_1. Values for [*CD-S*], [*CD-phth*] and [*phth*] were obtained using Beer-Lamber law for phth and Equation 6.1-6.3. The criterion utilized for the best fit in the NLLS procedure was the minimisation of the sums of the squares of the residuals (SSR) according to the relation, $SSR=\sum_i[(A_{calc})_i-(A_{expt})_i]^2$, where A_{calc} and A_{expt} are the calculated and experimental absorbance values, respectively.

The lipophilic surface area (LSA) of the apolar molecular fragments of the guest molecule included by β-CD was calculated using Spartan '06. The calculations were based on an equilibrium geometry optimization in the ground state with Hartree-Fock 3-21G in vacuum to obtain the minimized molecular structures.

6.4 Results and Discussion:

The low ethanol composition (0.04 % (v/v)) was chosen to eliminate possible interferences due to competitive binding by ethanol and undue solvent effects.[27,36-38] A pH of 10.5 was chosen in order to optimize ε_{phth}, to provide greater sensitivity for absorption

measurements, and to minimize the potential for deprotonation of the hydroxyl groups of β-CD ($pK_a \cong 12$). All absorption measurements were carried out at $\lambda = 552$ nm and no change in the shape of the visible absorption band with $C_{\beta\text{-CD}}$ was observed at this wavelength.

In order to obtain valid estimates of the 1:1 binding constant, the following conditions must be met when using the spectral displacement technique: (*i*) competing inclusate must not absorb in the wavelength region of interest or interact with the chromophore and (*ii*) inclusates must bind exclusively in a 1:1 stoichiometry. The first condition has been verified experimentally by measuring the absorbance change as a function of added NAs and the single component NAs (surrogate 1,2 or 3). *trans*-4-pentylcyclohexanecarboxylic acid and Fluka NAs showed a small increase in absorbance due an increased background absorbance attributed to weak interactions between unbound carboxylic anion guests and phth. Appropriate corrections were applied to absorbance data for these conditions. The formation of 1:1 inclusion complexes has been independently verified in these systems from a recent ESI-MS study of the same host-guest systems.[39] A further requirement is that the competing inclusate must fully displace the chromophore from the β-CD cavity and form a well-defined inclusion complex; not as a ternary outersphere complex, since the latter is known to affect the magnitude of K_2.[38] An additional practical consideration is that the value of K_1 for β-CD/phth is greater than or equal to the value of K_2 for β-CD/inclusate ($K_1 \geq K_2$).[22] Under these circumstances, it is possible to displace the phth over a suitable concentration range to obtain adequate absorbance changes.

Figure 6.1 illustrates a typical plot of absorbance vs $C_{\beta\text{-CD}}$ at a fixed concentration of phth. The line through the data points represents the calculated absorbance values obtained from the NLLS fitting procedure. The sharp falloff of absorbance as $C_{\beta\text{-CD}}$ increases represents the formation of the β-CD/phth complex since the molar absorptivity of the β-CD/phth complex is regarded as zero. Benesi- Hildebrand[40] plots were not utilized to determine values of K_1 since the assumption that the concentration of the complex is lower than the total concentration of β-CD is not usually valid for strongly bound inclusates. As well, such classical double reciprocal plots (1/abs vs 1/ $C_{\beta\text{-CD}}$) improperly weight the data at lower values of absorbance and higher values of $C_{\beta\text{-CD}}$. Consequently, a NLLS fitting procedure was employed to obtain values of K_1 and K_2. An average value of the 1:1 β-CD/phth binding constant ($K_1 = 2.6\pm0.3 \times 10^4$ M^{-1}) was estimated with good agreement with independent literature values.[9,23-24,26] The conditions employed in this study utilized a relatively low ethanol composition (0.04% v/v) as compared with Selvidge *et al*.[22] and the corresponding value of K_1 obtained is greater.

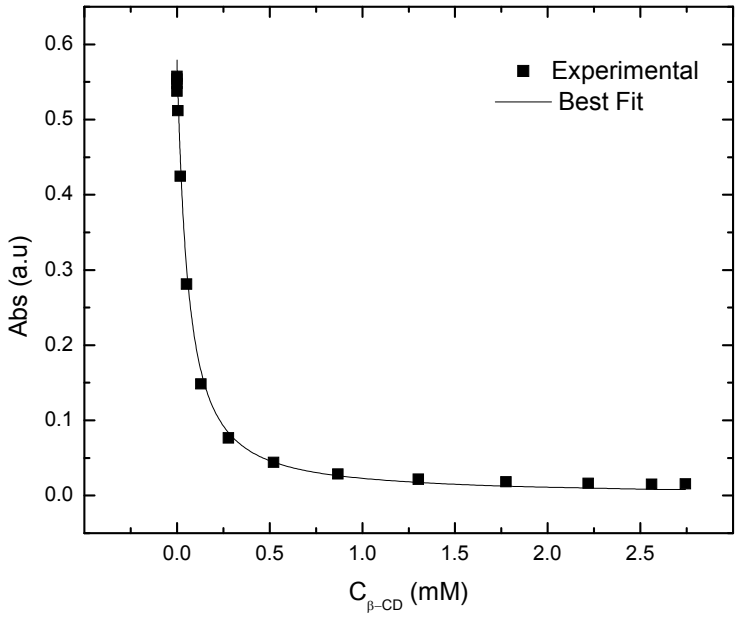

Figure 6.1. Absorbance (abs; λ = 552 nm) vs concentration of β-CD ($C_{\beta\text{-CD}}$) in 0.1M $NaHCO_3$ at pH 10.5, [phth] = 2×10^{-5} M and T = 295 K.

Figures 6.2a-c are representative plots of absorbance vs $C_{Inclusate}$ for binding of β-CD/inclusate of the single component NAs (i.e. surrogate 1-3). The absorbance values exhibit a smooth monotonic increase with increasing $C_{Inclusate}$ and corresponds to the displacement of phth from the β-CD cavity upon inclusion binding of the SENA molecules. Figure 6.2b represents an example of a strongly bound β-CD/inclusate system where the absorbance changes sharply for surrogate 2 and the shape of the isotherm becomes increasingly sigmoidal and the displacement of phth occurs over a narrower range of concentration of guest. surrogate 1 displays the weakest binding (*cf*. Figure 6.2a) amongst the three examples of single component NAs examined in Figure 6.2. Phth is displaced when $[\text{surrogate 1}]_o$ reaches ~25 mM whereas surrogate 2 and surrogate 3 reach saturation binding ~4 mM and 8 mM, respectively. In Figure 6.2c, surrogate 3 displays a prominent

sigmoidal shape as concentration increases but the absorbance changes are more gradual, as compared with surrogate 2. These observations indicate that there are differences in the binding affinity of β-CD/inclusate systems as follows: K_2 (surrogate 2) > K_2 (surrogate 3) > K_2 (surrogate 1). Table 6.1 lists the values of K_2 and ΔG^o for the formation of 1:1 complexes and estimates of lipophilic surface area (LSA) for the single component NAs. The values of K_2 range between 10^3 to 10^4 M^{-1} and Gibbs energy change values are negative indicating the complexation process of β-CD with the inclusates are favourable. There are several factors that govern the formation of CD inclusion complexes.[41] The hydrophobic effect is concluded as very important and is corroborated by the positive correlation between K_2 values and the LSA[42-43] values for the carboxylic acid guests molecules included in the β-CD cavity, as shown in Table 6.1. β-CD has an approximate cavity length[45] of 8 Å and a diameter of 6.6 Å, thus β-CD can include ~53 $Å^2$ of a inclusate's LSA. An illustration the latter is shown for the three single component NAs as outlined in Scheme 2. Moreover, the cavity volume of β-CD is ~262 $Å^3$ and may include relatively large apolar groups such as dodecyl alkyl chains[27] whereas it has been shown that α-CD (less in diameter than β-CD) may can include octyl chains.[43-44] Although the LSA of the inclusates were calculated as gas-phase optimized structures whereas the experiment was done in aqueous solution, the approach offers a semi-quantitative method of relating complex stability to the LSA parameter.[11] The use of LSA values is further corroborated by Connors *et.al.*[45] in their study of CDs with substituted carboxylic acids (*cf.* Table 1, reference 45). The binding constants increase as the LSA value increases for a series of cyclohexane carboxylic acids. These results support the role of the important role of the thermodynamics for hydration and dehydration of apolar compounds during complex

formation between β-CD and carboxylic acids guests.[27,46-48] The rearrangement of hydrate water includes desolvation of β-CD, dehydration of inclusates and reformation of hydration of shell for the complex. This is outlined by the following contributions to the overall Gibbs energy change of complexation (ΔG^o) for a typical 1:1 CD-inclusate complex.[49]

$$\Delta G^o = \Delta G^o{}_{H/W} + \Delta G^o{}_{I/W} + \Delta G^o{}_{H/I/W} + \Delta G^o{}_{W/W} \qquad \text{Equation 6.7}$$

where *I*, *H*, and *W* are inclusate, host, and solvent (water), respectively. The LSA has a large effect on the magnitude of solvent rearrangement, as anticipated for apolar guest compounds and associative processes governed by the hydrophobic effect.

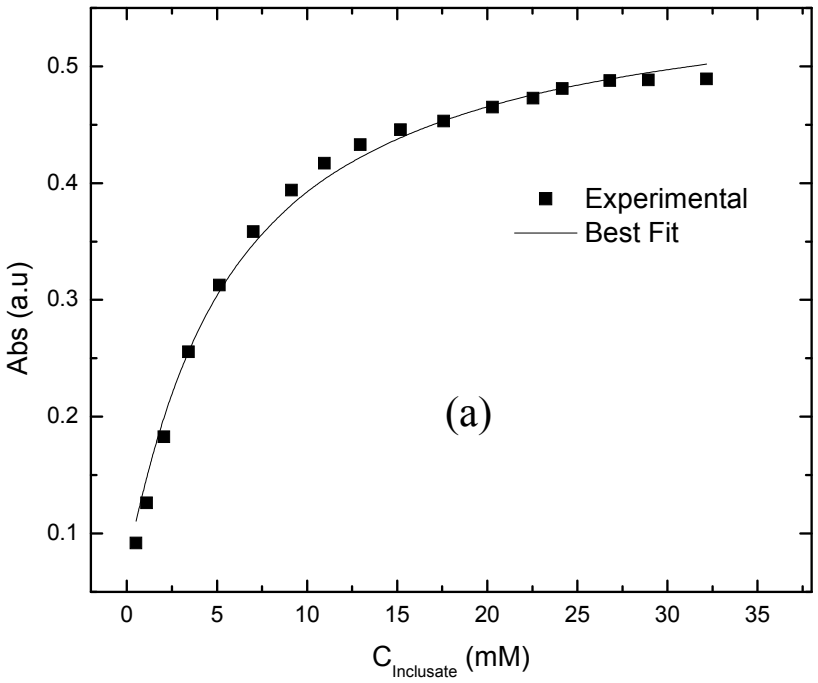

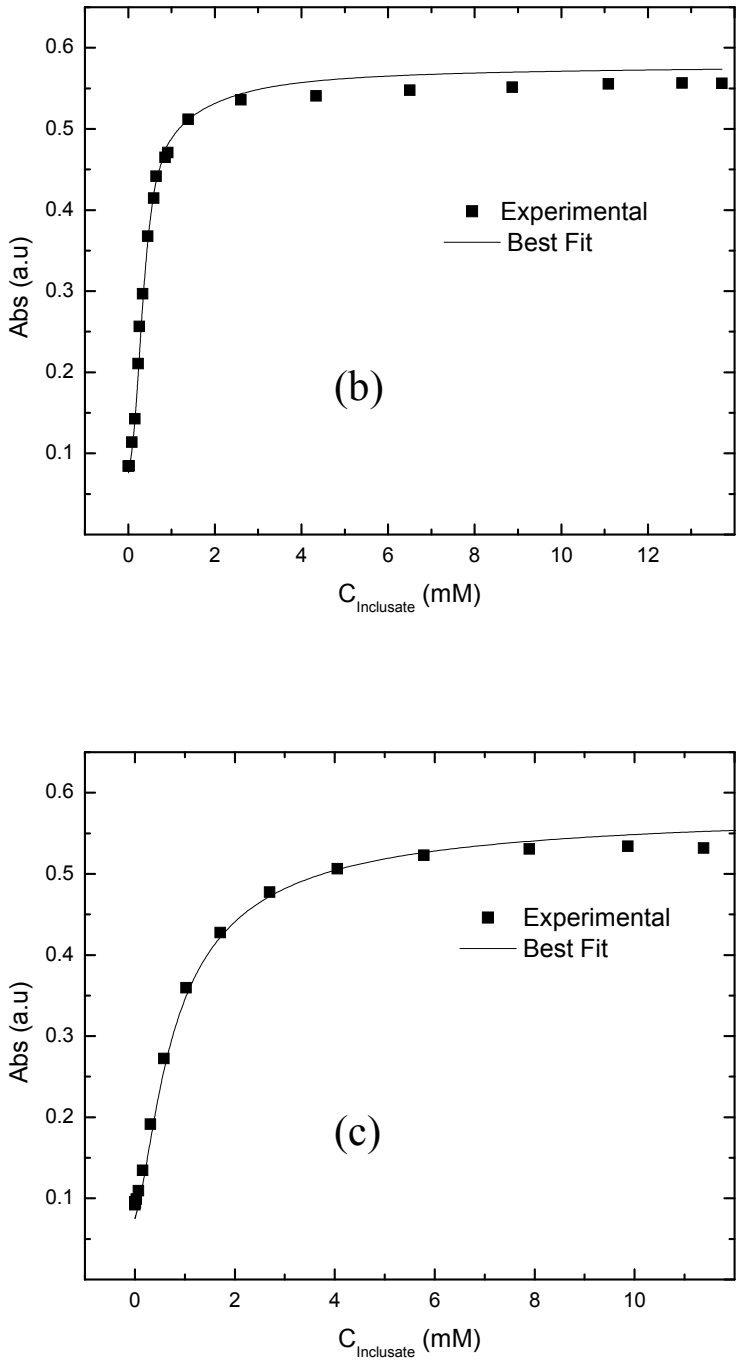

Figures 6.2a-c. Absorbance (abs; λ = 552 nm) vs concentration of specific examples of single component NAs in 0.1M $NaHCO_3$ at pH 10.5, [β-CD] = 2×10^{-4} M, [phth] = $2x10^{-5}$ M and T = 295 K; a) 2-hexyldecanoic acid (surrogate1), b) *trans*-4-pentylcyclohexanecarboxylic acid (surrogate2), and c) dicyclohexylacetic acid (surrogate3).

Table 6.1. 1:1 Binding constants and Gibbs free energy of complex formation for 1:1 CD-inclusate complexes using the spectral displacement method in 0.1 M $NaHCO_3$ buffer at pH 10.5 and T = 295 K.

Inclusate	K_2 (M^{-1})	[a]χ^2	[b]SEE	[c]ΔG (kJ/mol)	[d]LSA ($Å^2$)
Surrogate 1	$1.42(0.164) \times 10^3$	0.0103	0.0232	-17.9	17.2
Surrogate 2	$5.22(6.02) \times 10^4$	0.0140	0.0279	-26.8	45.4
Surrogate 3	$1.31(1.51) \times 10^4$	0.0319	0.0316	-23.3	21.3
Fluka NAs	$2.34(2.70) \times 10^{4f}$	0.00326	0.0117	-24.8	[e]NR
Syncrude NAs	$1.27(1.46) \times 10^{4f}$	0.0113	0.0232	-23.3	[e]NR

[a]χ^2 = Chi-square, [b]SEE = Standard Error of Estimate, [c]ΔG = -RT ln K_2 (K_2 is the 1:1 equilibrium binding constant), [d]Refer to Scheme 5.1 in Chapter 5 for molecular structures. Due to their distribution of variable molecular structures, the LSA values were not calculated for NAs and LSA values (surrogate 1-3) were estimated using Spartan '06, and [e]NR= Not Reported.
[f]Based on average molecular weight values; Fluka NAs (230 $gmol^{-1}$) and Syncrude NAs (362 $gmol^{-1}$), respectively.

Figures 6.3a-b are representative plots of absorbance vs $C_{Inclusate}$ for binding of β-CD/inclusate for Fluka and Syncrude NAs, respectively. Fluka NAs are more strongly bound than Syncrude NAs, as shown by the sigmoidal appearance of the absorbance profile in Figure 6.3a, as compared with Figure 6.3b. The former is more pronounced of the two curves, particularly the change in absorbance at the lower inclusate concentrations. The values of K_2 are shown in Table 6.1 and the observed differences may be related to structural variability of the NAs according to the Z-value and the carbon number of the respective samples. Fluka NAs have a narrower size distribution and lower average molecular weight, as shown in Figures 6.4a-b and 6.5a-b. The K_2 values represent an average binding constant since the NAs studied are mixtures of compounds with similar Z-values and carbon number. The molecular weight used in estimates of K_2 utilized the

average molecular weight of NAs since it is not known which specific cogeneners are included by β-CD. It is assumed that a random statistical distribution of the NA components are included; however, it is anticipated that high molecular weight components of NAs possessing greater LSA values will be bound more strongly than the lower molecular weight components. The average molecular weight may not represent the fraction of bound species but it is reasonable to report the K_2 values reported herein reflect the average binding constant for 1:1 complexes of β-CD/NAs. Recent developments in mass spectrometry have also indicated that the Athabasca oil sands acids may contain co-extractants containing S and N heteratoms along with aromatic and dicarboxylic acids.[50] The interactions of these species with β-CD are indirectly detected in the spectral displacement technique. However, the binding constants reported are representative of the oil sands acids in the wider context and not limited to the classical structures of NAs.

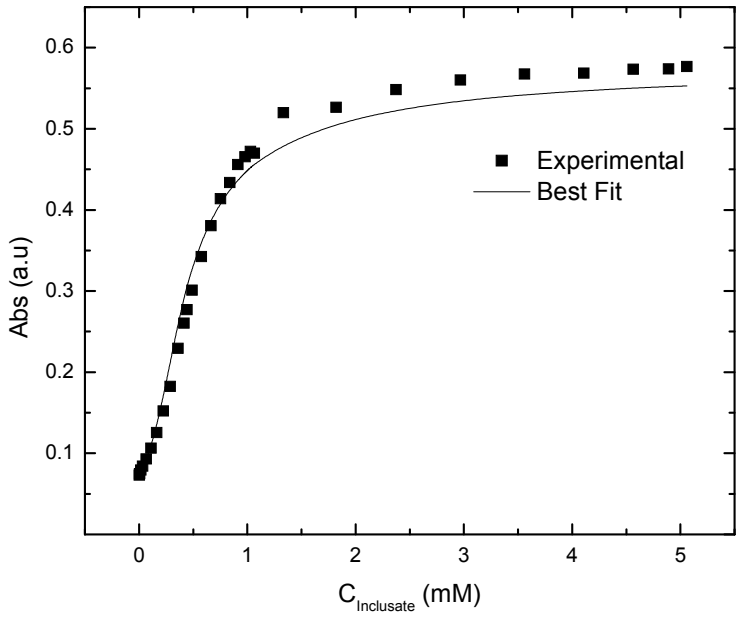

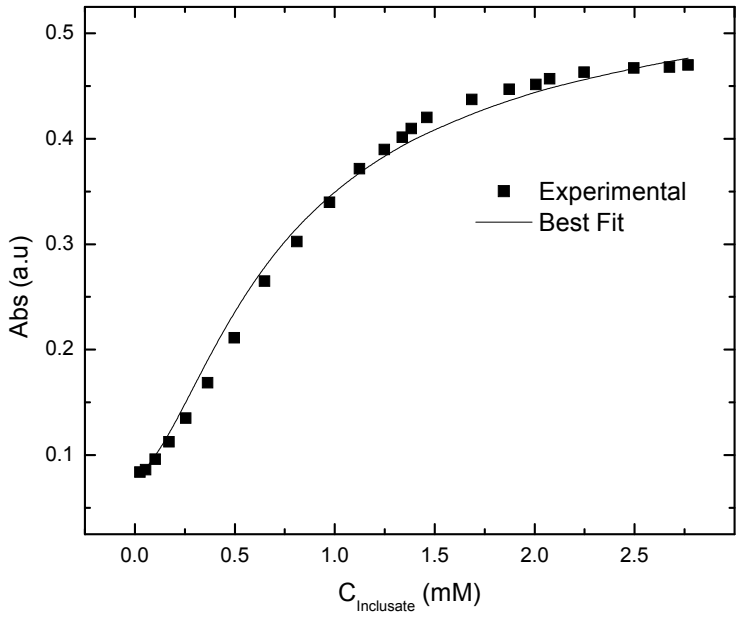

Figures 6.3a-b. Absorbance (abs; λ = 552 nm) vs concentration of inclusate (Fluka NAs) in 0.1M $NaHCO_3$ at pH 10.5, [β-CD] = 2×10^{-4} M, [Phth] = 2×10^{-5} M and T = 295 K; a) Fluka NAs, and b) Syncrude NAs.

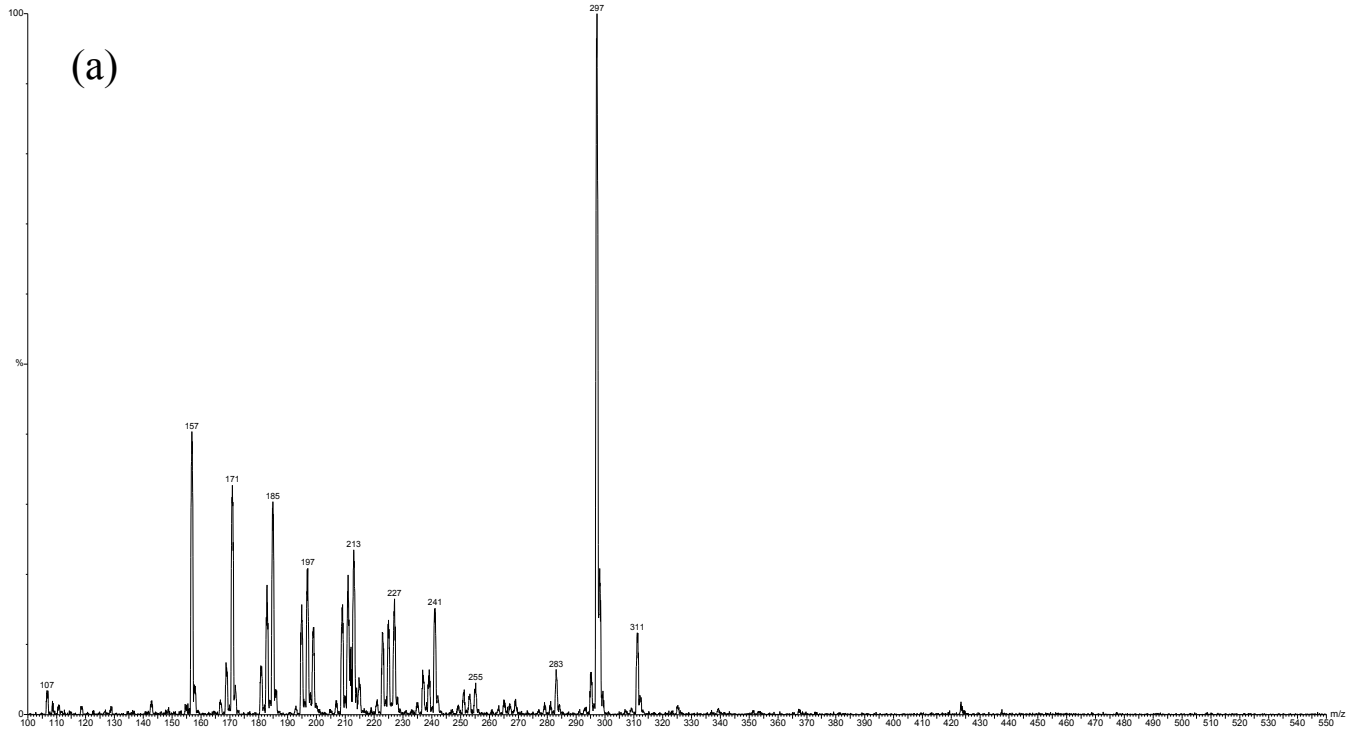

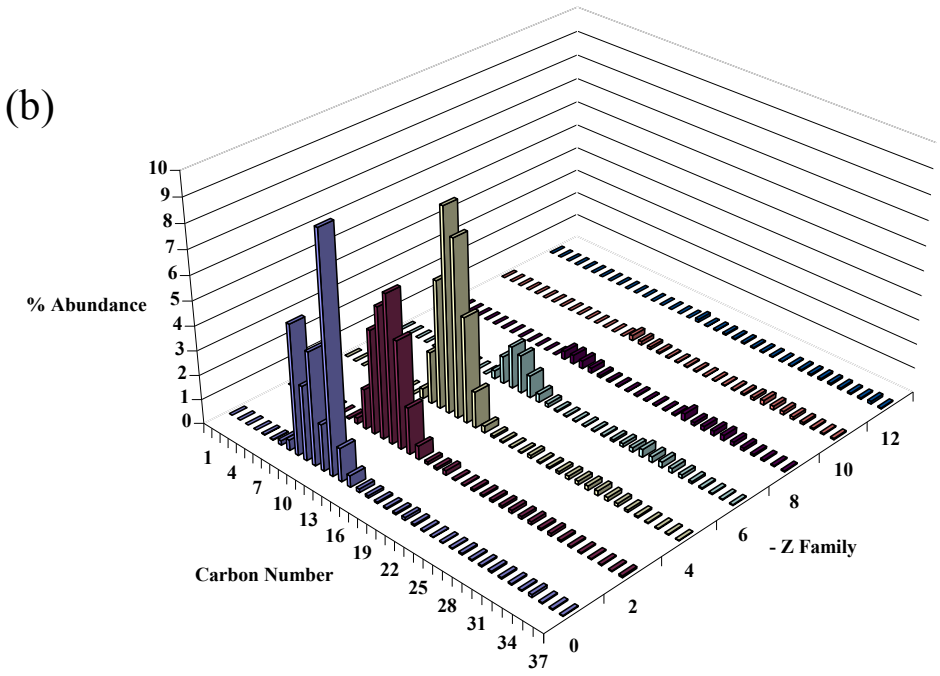

Figures 6.4a-b. a) ESI-MS spectrum of a 94.4 ppm sample of NAs (Fluka) at pH 6.30 illustrating the distribution of cogeners according to molecular weight, and b) 3-D plot of ESI-MS data representing percentage abundance of NAs with variable carbon number (n) and Z family series for a 94.4 ppm sample of NAs (Fluka) at pH 6.30.

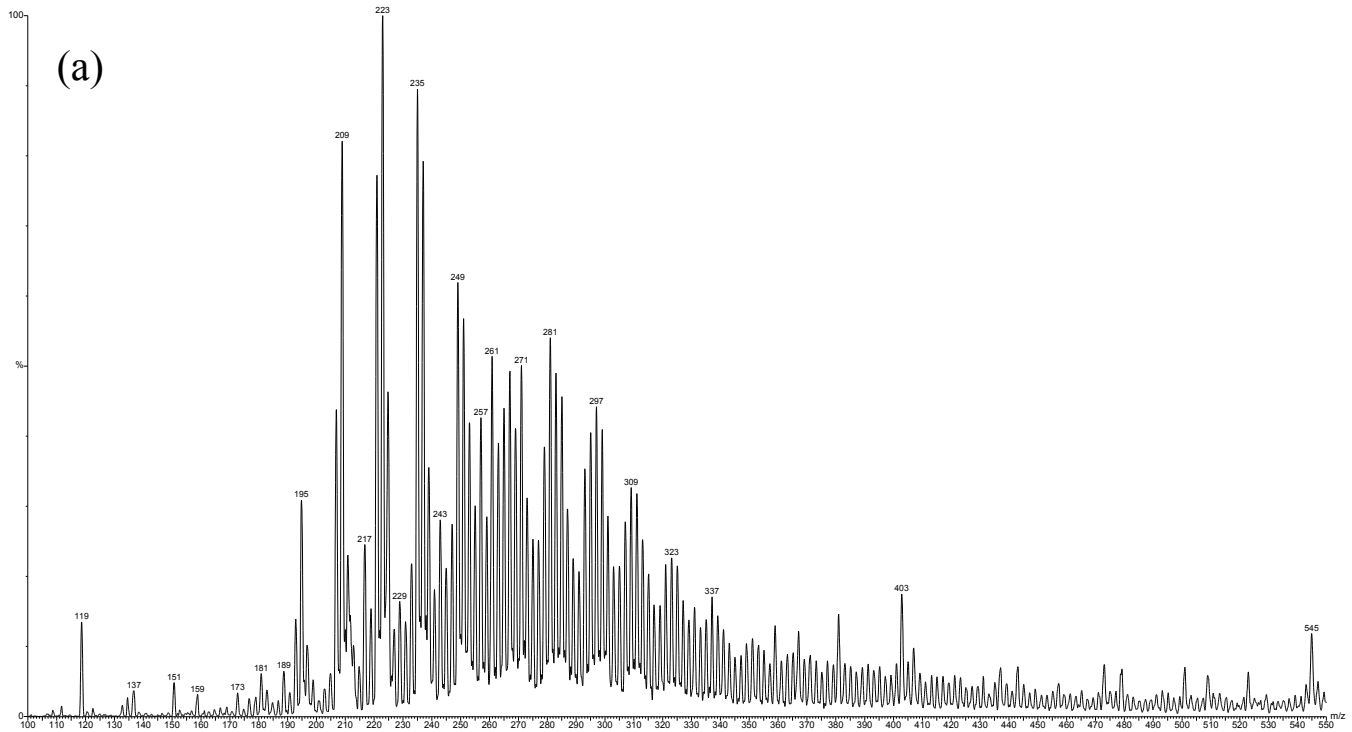

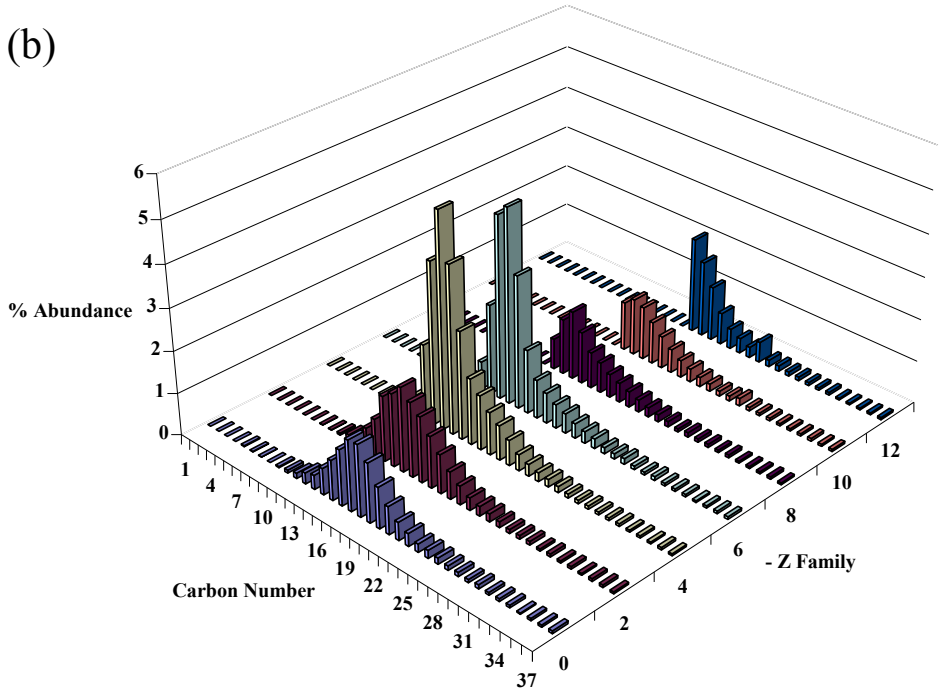

Figures 6.5a-b. a) ESI-MS spectrum of a 95.8 ppm sample of NAs (Syncrude) at pH 9.00 illustrating the distribution of cogeners according to molecular weight, and b) 3-D plot of ESI-MS data representing percentage abundance of NAs with variable carbon number (n) and Z family series for a 95.8 ppm sample of NAs (Syncrude) at pH 9.00.

6.5 Conclusions

The spectral displacement technique provides accurate estimates of the 1:1 binding constants (K_2) for a series of NAs and three examples of single component NAs (surrogate1-3). The values of K_2 for single components ranged from 10^3-10^4 M^{-1} and the NAs (i.e. Fluka and Syncrude) were ~ 10^4 M^{-1}. The K_2 values increased in accordance to their respective LSA values. Fluka NAs have greater K_2 values than syncrude NAs and the differences were attributed to the binding of corresponding greater molecular weight components in Fluka NAs vs Syncrude coextracted oil sands acids. Although the average

molecular weight of Syncrude NAs is higher than Fluka, the former contain impurities which do not appear to binding strongly to the β-CD.

The spectral displacement technique is a versatile method for obtaining accurate estimates of K_2 for carboxylate anions that possess strong binding affinities to β-CD and allows the indirect determination of the concentrations of inclusates in solution. To our knowledge this is the first quantitative study of the binding constants between NAs and β-CD reported to date. Further thermodynamic studies of complex formation are underway and should provide useful information regarding temperature effects on the stability for these CD/inclusate complexes. The results of this study will contribute toward a further understanding of the sorption mechanism between β-CD based polymeric materials and carboxylate ions in aqueous solution.

6.6 Acknowledgements

Financial assistance was provided by the Natural Sciences and Engineering Research Council and the Program of Energy Research and Development. M.H.M acknowledges the University of Saskatchewan for the award of a Graduate Teaching Fellowship and Environment Canada for the Science Horizons Program award.

6.7 References

1. Jolly, S. E. In *Kirk-Othmer Encyclopedia of Chemical Technology*; 2nd ed.; Kirk-Othmer, Ed.; Sun Oil Co.: Philadelphia, PA, 1967; Vol. 13, p 727-734.
2. Lo, C. C.; Brownlee, B. G.; Bunce, N. J. *Anal. Chem.* **2003**, *75*, 6394-6400.
3. Headley, J. V.; McMartin, D. W. *J. Environ. Sci. Health, Part A: Toxic/Hazard. Subst. Environ. Eng.* **2004**, *A39*, 1989-2010.

4. McMartin, D. W.; Headley, J. V.; Friesen, D. A.; Peru, K. M.; Gillies, J. A. *J. Environ. Sci. Health, Part A: Toxic/Hazard. Subst. Environ. Eng.* **2004**, *39*, 1361 - 1383.
5. Clemente, J. S.; Fedorak, P. M. *Chemosphere* **2005**, *60*, 585-600.
6. *Naphthenic acids in Kirk-Othmer Encyclopedia of Chemical Technology*; 4 ed.; Brient, J. A.; Wessner, P. J.; Doyle, M. N., Eds.; ohn Wiley & Sons: New York.
7. Kanicky, J. R.; Poniatowski, A. F.; Mehta, N. R.; Shah, D. O. *Langmuir* **1999**, *16*, 172-177.
8. Quagraine, E. K.; Peterson, H. G.; Headley, J. V. *J. Environ. Sci. Health, Part A: Toxic/Hazard. Subst. Environ. Eng.* **2005**, *40*, 685-722.
9. Buvari, A. *J. Inclusion Phenom.* **1983**, *1*, 151-157.
10. Eftink, M. R.; Andy, M. L.; Bystrom, K.; Perlmutter, H. D.; Kristol, D. S. *J. Am. Chem. Soc.* **1989**, *111*, 6765-6772.
11. Gadre, A.; Rüdiger, V.; Schneider, H.-J.; Connors, K. A. *J. Pharm. Sci.* **1997**, *86*, 236-243.
12. Gadre, A.; Connors, K. A. *J. Pharm. Sci.* **1997**, *86*, 1210-1214.
13. Mohamed, M. H.; Wilson, L. D.; Headley, J. V.; Peru, K. M. *Process Saf. Environ. Prot.* **2008**, *86*, 237-243.
14. Wood, D. J.; Hruska, F. E.; Saenger, W. *J. Am. Chem. Soc.* **1977**, *99*, 1735-1740.
15. Junquera, E.; Tardajos, G.; Aicart, E. *Langmuir* **1993**, *9*, 1213-1219.
16. Saint Aman, E.; Serve, D. *J. Colloid Interface Sci.* **1990**, *138*, 365-375.
17. Dharmawardana, U. R.; Christian, S. D.; Tucker, E. E.; Taylor, R. W.; Scamehorn, J. F. *Langmuir* **1993**, *9*, 2258-2263.
18. Wan Yunus, W. M. Z.; Taylor, J.; Bloor, D. M.; Hall, D. G.; Wyn-Jones, E. *J. Phys. Chem.* **1992**, *96*, 8979-8982.
19. Gelb, R. I.; Schwartz, L. M.; Cardelino, B.; Laufer, D. A. *Anal. Biochem.* **1980**, *103*, 362-368.
20. Fourmentin, S.; Surpateanu, G.; Blach, P.; Landy, D.; Decock, P.; Surpateanu, G. *J. Inclusion Phenom. Macrocyclic Chem.* **2006**, *55*, 263-269.
21. Mwakibete, H.; Cristantino, R.; Bloor, D. M.; Wyn-Jones, E.; Holzwarth, J. F. *Langmuir* **1995**, *11*, 57-60.

22. Selvidge, L.; Eftink, M. R. *Anal. Biochem.* **1986**, *154*, 400-408.
23. Buvari, A.; Barcza, L.; Kajtar, M. *J. Chem. Soc., Perkin Trans. 2* **1988**, *1972-1999*, 1687-1690.
24. Sasaki, K. J.; Christian, S. D.; Tucker, E. E. *Fluid Phase Equilib.* **1989**, *49*, 281-289.
25. Buvari, A.; Barcza, L. *Inorg. Chim. Acta* **1979**, *33*, L179-L180.
26. Gray, J. E.; MacLean, S. A.; Reinsborough, V. C. *Aust. J. Chem.* **1995**, *48*, 551-556.
27. Wilson, L. D.; Siddall, S. R.; Verrall, R. E. *Can. J. Chem.* **1997**, *75*, 927-933.
28. Meier, M. M.; Bordignon Luiz, M. T.; Farmer, P. J.; Szpoganicz, B. *J. Inclusion Phenom. Macrocyclic Chem.* **2001**, *40*, 291-295.
29. Tutaj, B.; Kasprzyk, A.; Czapkiewicz, J. *J. Inclusion Phenom. Macrocyclic Chem.* **2003**, *47*, 133-136.
30. Landy, D.; Fourmentin, S.; Salome, M.; Surpateanu, G. *J. Inclusion Phenom. Macrocyclic Chem.* **2000**, *38*, 187-198.
31. Suzuki, I.; Yamauchi, A. *J. Inclusion Phenom. Macrocyclic Chem.* **2006**, *54*, 193-200.
32. Funasaki, N.; Yodo, H.; Hada, S.; Neya, S. *Bull. Chem. Soc. Jap.* **1992**, *65*, 1323-1330.
33. Rogers, V. V.; Liber, K.; MacKinnon, M. D. *Chemosphere* **2002**, *48*, 519-527.
34. Mortimer, R. G. *Mathematics for Physical Chemistry*; 1st ed.; McMillan Publishing Co.: New York, 1981.
35. Parker, J.; L, B. G. *Spreadsheet Chemistry*; 1st ed.; Prentice-Hall Inc.: New Jersey, 1991.
36. Donze, C.; Chatjigakis, A.; Coleman, A. W. *J. Inclusion Phenom.* **1992**, *13*, 155-161.
37. Schuette, J. M.; Warner, I. M. *Anal. Lett.* **1994**, *27*, 1175 - 1182.
38. *Spectroscopic Studies in Cyclodextrin Solutions*; Warner, I. M.; Schuette, J. M., Eds.; JAI Press: Greenwich,CT, 1993; Vol. 2.
39. Mohamed, M. H.; Wilson, L. D.; Headley, J. V.; Peru, K. M. *Rapid Commun. Mass Spectrom.* **2009**, *23*, 3703-3712.

40. Benesi, H. A.; Hildebrand, J. H. *J. Am. Chem. Soc.* **1949**, *71*, 2703-2707.
41. Liu, L.; Guo, Q.-X. *J. Inclusion Phenom. Macrocyclic Chem.* **2002**, *42*, 1-14.
42. Cserháti, T. *Anal. Lett.* **1993**, *26*, 2687-2700.
43. Ishikawa, S.; Hada, S.; Neya, S.; Funasaki, N. *J. Phys. Chem. B.* **1999**, *103*, 1208-1215.
44. Funasaki, N.; Yamauchi, J.; Ishikawa, S.; Hirota, S. *Bull. Chem. Soc. Jap.* **2004**, *77*, 2165-2171.
45. Connors, K. A. *Chem. Rev.* **1997**, *97*, 1325-1358.
46. Merino, C.; Junquera, E.; Jiménez-Barbero, J.; Aicart, E. *Langmuir* **1999**, *16*, 1557-1565.
47. Castronuovo, G.; Niccoli, M. *J. Inclusion Phenom. Macrocyclic Chem.* **2005**, *53*, 69-76.
48. Todorova, N. A.; Schwarz, F. P. *J. Chem. Thermodyn.* **2007**, *39*, 1038-1048.
49. Wilson, L. D. Binding Studies of Cyclodextrin-Surfactant Complexes, University of Saskatchewan, 1998.
50. Headley, J. V.; Peru, K. M.; Barrow, M. P. *Mass Spectrom. Rev.* **2009**, *28*, 121-134.

CHAPTER 7

PUBLICATION 6

Description

The following is a verbatim copy of an article that was published in November of 2009 in the Process Safety and Environment Protection in IChemE journal (*Process Saf. Environ. Prot.:* **2009**, *86(4)*, 237-243) and describes sorption of NAs from aqueous solution using different types β-CD materials.

Authors' Contribution

I conducted all the experimental work except for the ESI-MS which was done by Mr. Kerry Peru. This work was supervised by Dr. Wilson and Dr. Headley. I wrote the first draft of the manuscript with extensive editing by each supervisor prior to submission for publication. Written permission was obtained from all contributing authors and the publishers to include this material in this thesis.

Relation of Chapter 7 (Publication 6) to the Overall Objectives of this Project

This chapter illustrates the application of the main objective of this thesis, which is sorption of NAs from aqueous solution using different types of β-CD materials. It offers comparison of another type of copolymers and a silica-based mesoporous material containing β-CD. A comparison of the different types of sorbent offers justification for the use of the β-CD PUs. The results are compared to the common sorbent with a relatively high surface area i.e. GAC.

7. Novel Materials for Environmental Remediation of Tailing Pond Waters Containing Naphthenic Acids

Mohamed H. Mohamed,[§] Lee D. Wilson, [§] John V. Headley[¥] Kerr M. Peru[¥]*

[§]Department of Chemistry, University of Saskatchewan, 110 Science Place, Saskatoon, Saskatchewan, S7N 5C9

[¥]Water Science and Technology Directorate, 11 Innovation Boulevard, Saskatoon, Saskatchewan, S7N 3H5

*Corresponding Author

Received 14 August 2007

7.1 Abstract

A nanofiltration strategy of tailing pond waters (TPWs) that utilizes cyclodextrin (CD)-based polymeric materials as supramolecular sorbents are proposed. Naphthenic acids (NAs) from the Athabasca TPWs are investigated as the target sorbate molecules.

The sorption properties of several supramolecular porous materials were characterized using equilibrium sorption isotherms in aqueous solution wherein electrospray ionization mass spectrometry was used to monitor the concentration of NAs in aqueous solution. The characterization of the supramolecular sorbents was performed using ^{13}C NMR and IR spectroscopy, while nitrogen porosimetry was used to estimate their surface area and pore structure properties. Independent estimates of surface area were obtained using a chromophore dye based adsorption method in aqueous solution.

The sorption results for NAs in solution were compared between a commercially available standard; granular activated carbon (GAC) with three types of synthetic materials. The sorption capacities for GAC ranged from 100-160 mg NAs/g of material whereas the polymeric materials ranged from 20-30 mg NAs/g of material over the experimental conditions investigated. In general, differences in the sorption properties between GAC and the CD-based sorbents were observed and were related to differences in the surface areas of the materials and the chemical nature of the sorbents. The CD-based supramolecular materials displayed different sorption capacities ranging from lower to higher (36.2-657 m^2/g) as compared to the value obtained for GAC (795 m^2/g).

7.2 Introduction

Naphthenic acids (NAs) are predominantly complex mixtures of saturated acyclic and aliphatic carboxylic acids with the general formula $C_nH_{2n+Z}O_2$, where n is the number of carbons and 2n+Z is number of hydrogen atoms where Z is the hydrogen deficiency; hydrogen loss due to ring structure. Generally, the carboxylic group is attached to a cyclopentane or cylcohexane ring through a $–CH_2-$ group or an alkyl chain containing five or more $–CH_2-$ groups. NAs are found in oilsands due to insufficient catagenesis of oilsands or as a biodegradation product by bacteria. Composition and concentration of NAs depend on the source of crude oil.[1-5]

The presence of NAs in oilsands tailings has led to environmental and industrial concerns. They are known to be toxic to aquatic organisms, algae, and mammals.[5-7] NAs are suspected endocrine-disrupting substances, however; the toxicology of all the various types of NAs are poorly understood. Consequently, the Government of Canada has issued

a zero discharge policy, due in part, to the presence of NAs in tailing pond waters (TPWs) as byproducts from the Athabasca oil sands steam extraction processes. Given the estimated crude oil reserves (*ca*. 174 billion barrels bitumen) in the Athabasca oil sands and the significant water consumption requirements (*ca*. 4 barrels water per 1 barrel bitumen) for the extraction processing, millions of litres of TPWs will be produced and may contain NAs as high as 110 ppm.[3,8-10] In addition, TPWs are not recyclable for the bitumen steam extraction process because the dissolved NAs are suspected to catalyze corrosion in steel alloys.[6,11-12]

The aforementioned problems and projected oil sands production activities in the Athabasca region has demonstrated an urgent need for the development of novel extraction strategies for the removal of NAs from TPWs.

Previous studies have examined different strategies for the removal of NAs from synthetic and industrial TPWs with limited success. Concentrated extracts of NAs that can be used as authentic standards for example, have employed liquid-liquid extraction methods using dichloromethane.[13] However, the potential formation of micro-emulsions and residual organic solvents remain a concern. A wide range of sorbents have been investigated with limited success, such as, granular activated carbons (GACs), soils, zeolites, clays, calcite, and mica.[14-19] As well, some examples of polymeric sorbents include poly(4-vinyl pyridine), polystyrene, and dimethylaminoethyl-cellulose.[14,20-21] Recent studies have investigated some commercially available nanofiltration (NF) membranes, characterized according to their rejection efficiency of magnesium sulfate from aqueous solution. Such types of NF membranes are anticipated to produce permeate

solutions with low concentrations (< 5 ppm) for NAs and calcium carbonate (< 40 ppm).[22]

Recently, cyclodextrin (CD)-based porous materials have been utilized for the sequestration of organic compounds from the gas and condensed phases.[23-25] Cyclodextrins (CDs) are cyclic compounds consisting of six, seven, and eight α-D-glucopyranoside units connected by α-(1, 4) linkages commonly referred to as α-, β-, and γ-cyclodextrins, respectively. CDs possess a characteristic toroidal shape with a well-defined lipophilic cavity and a hydrophilic exterior that is suitable for the inclusion of appropriate sized guest compounds (*cf*. Scheme 1.1 in Chapter 1). CDs are of interest, in part, because of their ability to form inclusion complexes in aqueous solution. In particular, they are also well known to form relatively stable inclusion complexes with aliphatic and alicyclic carboxylic acids.[26-28]

In addition, CDs can be incorporated into polymeric forms using a variety of synthetic strategies.[29-30] We anticipate that such polymeric materials would exhibit similar favourable binding affinity toward carboxylic acid compounds, such as NA molecules because of their lipophilic character and the presence of a carboxylic acid functional group. Polymeric materials that incorporate CD monomeric units are anticipated to exhibit strong binding affinity toward NAs due to cooperative binding and hydrophobic effects. In a previous study concluded that polymeric CDs exhibited enhanced binding towards p-nitrophenol (PNP).[25]

CD based porous materials of this type are anticipated to be superior to commercially available sorbents for the sorption of NAs from TPWs because of their molecular recognition potential to reduce concentrations from the part per million (ppm)

to part per trillion (ppt) concentration levels.[25] The objectives of this study are to compare the sorption properties of granular activated carbon (GAC) and three types of polymeric cyclodextrins (CD-EP, CD-PDI, and CD-ICS) toward naphthenic acids (NAs) in aqueous solution at different experimental conditions. The realization of this goal will address the utility of novel sorbents described in this study for the sequestration of NAs in aquatic environments and policy issues concerning the zero discharge policy for NAs in TPWs. The development of novel sorbents may offer a large scale method to effectively reduce NAs concentration in TPWs to suitable levels.[6-7]

To the best of our knowledge, this research study is the first example of the application of CD based materials as sorbents for the sorption of NAs. The development of the materials entails long term research to optimize sorption properties for NAs in aqueous solutions. The materials described herein are promising candidates for materials in NF membranes because they are non-leaching, recyclable, and exhibit good sorption properties for industrial remediation strategies of NAs in aquatic environments.

7.3 Experimental

7.31. Sorbents

Granular Activated Carbon (GAC)

GAC (Norit Rox 0.8) purchased from VWR was ground and sieved to a size 40 mesh particle size and then finally dried under vacuum.

β -CD cross linked with 1,4-Phenylene diisocyanate (CD-PDI)

A procedure for the synthesis of urethane based cyclodextrin materials was adopted from previous work.[25] The current method used for the synthesis of this polymer

used a new diisocyanate (1,4-phenylene diisocyanate, PDI) and a different solvent (dimethylacetamide, DMA). β-CD was purchased from VWR while DMA from Sigma-Aldrich. DMA was dried with molecular sieves (4 Å.beads, 8-12 mesh, Aldrich). ^{1}H NMR of DMA was recorded before and after addition of molecular sieves where the water content was estimated to be ~ 0.5%. 2.3g (2 mmol) of dried β-CD was weighed in a round bottom flask and dissolved in 10 mL of DMA followed by the slow addition of 0.96g (6 mmol) PDI dissolved in 30 mL of DMA. The mixture was stirred and heated at 68^{o}C for 24 hrs. Cold methanol was then added to the final reaction mixture upon cooling to room temperature to precipitate the polymeric product followed by filtration with a Buchner funnel. The isolated polymer was then Soxhlet-extracted with methanol for 24 hrs to remove the unreacted starting materials and low molecular weight impurities. The final product was dried in a pistol dryer for 24 hrs and subsequently ground and sieved to a size 40 mesh particle size.

β -CD cross linked with Epichlorohydrin (CD-EP)

The synthetic procedure of He and Zhao[23] was applied in this work for the synthesis of cross linked β-CD with epichlorohydrin (EP) with some modifications. 1 g of β-CD (0.9 mmol) was added to a round-bottom flask followed by the addition of 1.3 mL of 25% NaOH with stirring until all of the β-CD was dissolved. 1.04 mL (13 mmol) EP was added rapidly and heated to 50^{o}C while stirring for 65 hours. The product was then neutralized with 6M HCl followed by filtration and washing with millipore water and acetone. The product was dried in a vacuum oven for 24 hrs and subsequently ground and sieved to a size 40 mesh particle size.

β -CD functionalized mesoporous silica (CD-ICS)

The CD functionalized triethoxysilane (CD ICL) was synthesized by reacting dried β-CD with 3-isocyanatopropyltriethoxysilane in dry pyridine which was stirred at 70 °C under N_2 for 48 hrs, according to a previous method.[31-32] The solvent was removed under reduced pressure under N_2. The product CD ICL was obtained as a light yellow solid. CD ICL (X=1.81 mmol) was condensed with tetraethoxysilane (TEOS; 30.3X mmol) in the presence of hexadecylamine and a pore expander (e.g. 1, 3, 5- trimethyl benzene; 6.7 mmol) following a one pot direct synthesis in water at room temperature overnight.[33-34] The surfactant and pore expander were removed from the product mixture by Soxhlet extraction using ethanol as the solvent for 24 hrs. Finally after drying CD-ICS was isolated as a white powder which was subsequently ground and sieved to a 40 mesh particle size.

7.3.2 Characterization

Solid state ^{13}C NMR spectroscopy was performed using cross polarization (cp; ^{13}C $\{^1H\}$) with magic angle spinning (MAS). ^{13}C NMR spectra were run at 150.8 MHz on a Varian Inova-600 NMR spectrometer with rotor size 3.2 mm, spinning rate 16 kHz with a cp (^{13}C $\{^1H\}$) ramp pulse program. The chemical shifts were externally referenced to hexamethyl benzene at 16.9 ppm at ambient temperature. Data were processed with a 100 Hz line broadening with left shifting of the FID (1-2 data points) to correct the spectral baseline.

IR spectra were obtained with a Bio RAD FTS-40 spectrophotometer. Spectroscopic grade KBr was used as both the background and matrix over the range of 400-4000 cm^{-1}. Samples were prepared by mixing with pure spectroscopic grade KBr

approximately in appropriate amounts and ground in a small mortar and subsequently pressed into a pellet form for analysis. The spectra were recorded in Fourier Transform transmission mode at room temperature with a resolution of 4 cm^{-1} with multiple scans.

7.3.3 Sorption

Nitrogen porosimetry (Micromeritics ASAP 2010) was used to determine the surface area and pore structure characteristics of all supramolecular porous materials. An organic dye sorption method that utilized p-nitrophenol (PNP) was used to independently estimate the surface area of these materials according to a known method.[35]

Dye Sorption Method

In sorption experiments involving sorbents with p-nitrophenol (PNP; Aldrich), a 10^{-3} M stock solution of PNP was made at pH = 4.0 (buffered with potassium phosphate monobasic (KH_2PO_4), Aldrich). To a 10 mL glass bottle with teflon cap liners, fixed amounts of solid polymer were added to a fixed volume (7.00 mL) of PNP solution for different concentrations ranging from 10^{-3} to 10^{-4} M. The vials were further sealed with an aluminum foil liner between the cap and glass bottle and were placed at room temperature in a horizontal shaker to equilibrate for 24 hrs. An average of 10 data points were obtained for each sorption isotherm.

For analyses of PNP in solution, absorbance spectra were recorded for each filtrate and the equilibrium concentration was determined using the experimental determined molar absorptivity (ε_{PNP} = 9287 $Lmol^{-1}cm^{-1}$) with a λ_{max} = 317 nm, in agreement with a previous study.[36]

Sorption Isotherms with NAs

A similar procedure was applied for the sorption isotherms of NAs. Two separate stock solutions of NAs were made at different pH values (i.e. pH 9.00 and 5.00) from a 6.990 ppt aqueous stock solution extracted from Athabasca TPWs (pH 7.60). The stock solution was raised to pH 9.00 using 10^{-3} M ammonium hydroxide while the stock was lowered to pH = 5.00 using 10^{-3}M acetic acid. The two pH values were chosen for this study because industrial TPWs have a pH of ~ 8, hence, the NAs exist in their ionized forms. Thus, sorption experiments were performed at pH = 8.0 to understand the uptake of ionized NAs. At pH = 5.00, there is a need to understand how the sorption changes when the NAs exist in their non-ionized form.

The equilibrium concentrations of NAs were determined using negative ion mode electrospray mass spectrometry (ES-MS). Samples (5.0μL) were introduced into the eluent stream (200 μL/minute, 50:50 CH_3CN:H_2O containing 0.1% NH_4OH) using a Waters 2695 advanced separation system (Milford, MA). Mass spectrometry analysis was conducted using a Quattro Ultima mass spectrometer (Micromass, UK) equipped with an electrospray interface operating in the negative ion mode. MS conditions were as follows: source temperature 120 °C, desolvation temperature 220 °C, cone voltage setting -1 V, capillary voltage setting 0.03 kV, cone gas N_2 35 L/hr, desolvation gas N_2 170 L/hr. Both low and high mass resolutions were set at 14.0 and ion energy was 1.7. Entrance voltage was –1 V, collision energy -1 eV and exit voltage -1 V. The multiplier was set at 650 V. Full scan MS (m/z 100-550) was employed for extract mixtures. MassLynx version 4.1 software was utilized for all instrumental control and data acquisition/manipulation.

7.3.4 Data Analysis

The sorption results were studied using isotherms which are plots of equilibrium concentration NAs removed from solution per mass of sorbate used (Q_e) versus equilibrium concentration of NAs remaining in the solution (C_e). The Q_e value is calculated using Equation (7.1) below where C_o is initial sorbate concentration, V is volume of solution and m is the mass of sorbent.

$$Q_e = \frac{(C_o - C_e) \times V}{m} \qquad (7.1)$$

The linearised forms of the Langmuir and BET models can be applied to obtain estimates of the monolayer coverage (Q_m) of these materials by NAs (*cf.* Table 7.1). Table 7.1 lists the various models examined in this study to fit the experimental sorption data in aqueous solution. The criterion of the "best fit" for the two models used is defined by linear regression coefficients that most closely match a value of unity. K_L or K_{BET} represent the equilibrium constants for the sorption process for the Langmuir and B.E.T models, respectively. The surface area (SA; m^2/g) of the sorbents can be evaluated from the parameters obtained from the value of Q_m obtained from the best fit of the sorption isotherm data. A_m represents the cross-sectional area occupied by the adsorbate molecule on the surface area on a molar basis (m^2/mol), L is Avogadro's number (mol^{-1}), and N is the coverage factor.[35]

Table 7.1. Overview of the models for the equilibrium sorption isotherms in aqueous solution used in this work.

Model	Equation
Langmuir	$Q_e = \frac{K_L Q_m Ce}{1 + KC_e}$
BET	$Q_e = \frac{Q_m K_{BET} C_e}{(C_o - C_e)} + \frac{C_o Q_m K_{BET}}{(K_{BET} - 1)(C_o - C_e)}$
Surface Area	$SA = \frac{A_m Q_m L}{N}$

7.4 Results and Discussion

7.4.1 Characterization

IR Spectroscopy

IR spectroscopy was used to confirm the molecular identity of the polymeric materials synthesized in this study. Figure 7.1 shows representative FT-IR spectra observed for the CD-based urethane polymer (CD-PDI) and for the starting materials (β-CD and PDI). The spectra for CD-PDI confirm the identity of the polymer. The most noteworthy feature in the IR spectrum is the disappearance of the isocyanato group at around 2500-2080 cm^{-1} and the appearance of signals due to the formation of an amide vibrational bands (3376, 1696, and 1533 cm^{-1} corresponding to N-H, C=O, and C-N, respectively). These results support that the reaction was successful in the formation of a urethane linkage between β-CD and the isocyanate cross linking agent. CD-EPH and CD-ISC were similarly confirmed using this technique and the identity of both products were confirmed by IR results.

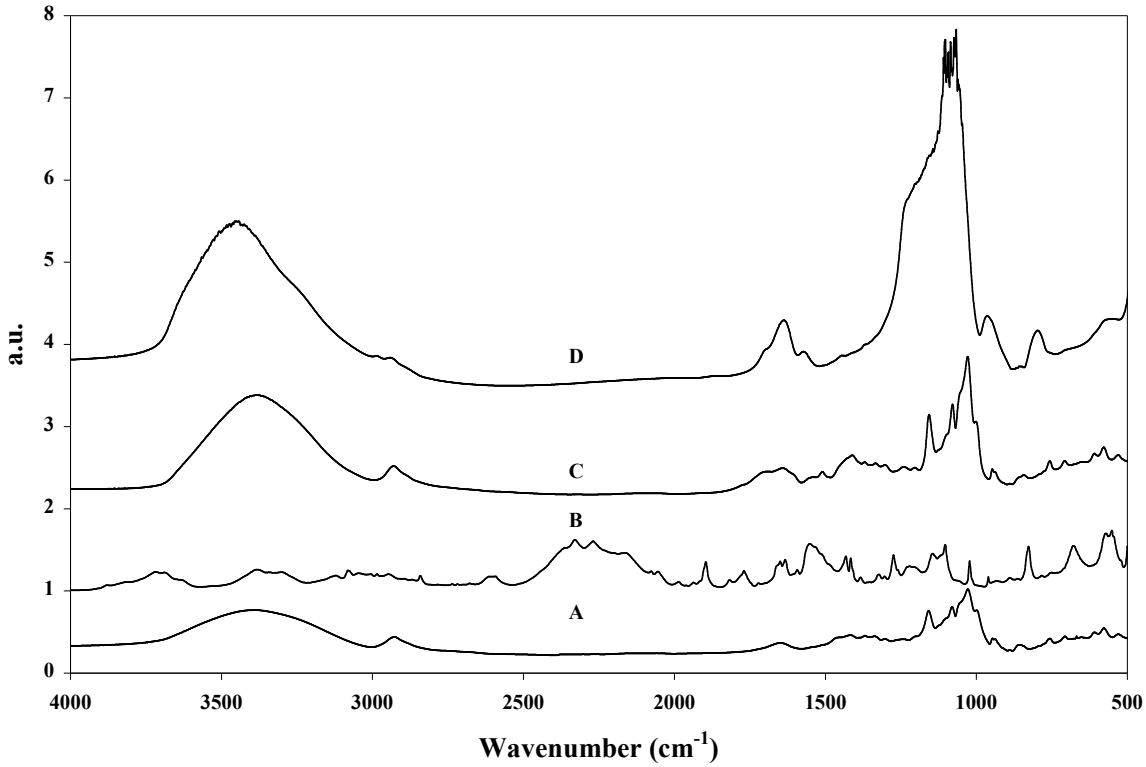

Figure 7.1. Infrared Spectra (KBr Pellets) of starting materials and polymeric products: a) β-CD, b) PDI, and c) CD-PDI, and d) CD-ICS recorded at ambient temperature; where a.u. represents arbitrary absorbance units.

^{13}C NMR Spectroscopy

Figure 7.2a-d show representative ^{13}C NMR spectra observed for the CD-based polymers (CD-PDI, CD-EP, and CD-ICS) synthesized in this work along with the β-CD starting material. Although each glucose unit of β-CD contains six unique C atoms, the spectrum for β-CD in Figure 2a reveals four ^{13}C NMR lines between 60-110 ppm due to overlap of some of the carbon resonance lines. The assignment and spectrum reported in Figure 2a for β-CD agrees with that previously reported.[31] Figures 7.2b-d show the ^{13}C NMR spectra for the CD-based polymers; CD-PDI, CD-EP, and CD-ICS, respectively. In all cases, the ^{13}C NMR signals of β-CD are observed in addition to the NMR signals due to the framework containing carbon atoms. In the case of CD-PDI, the ^{13}C signals

due to the phenyl ring are observed between 110-170 ppm. In Figure 7.2c, the ^{13}C signals for β-CD are observed in addition to some aliphatic carbon signals upfield that are attributed to the epichlorohydrin linkage. In contrast to Figure 7.2a, the signals for β-CD are attenuated and this is attributed to the different cross polarization dynamics of the highly cross linked CD-EP material relative to the crystalline β-CD. Figure 7.2d is a ^{13}C NMR spectrum for CD-ICS and the signals due to β-CD are seen as a broad envelop of lines from 60-110 ppm. The signals above 110 ppm are attributed to TMB occluded within the silica framework during the sol-gel process. Typically, these NMR signals are not observed because the silica materials are calcined to removed organic templates. However; the one pot method used in this study does not allow for calcination because it would remove the surface bound β-CD molecules that are covalently linked to the silica framework. The ^{13}C signals upfield from the β-CD signals are attributed to the ICL linker moiety within the silica framework. It should be noted that quantitative information from the ^{13}C line intensities are limited because the spectra were recorded using cross polarization and information about the cross polarization dynamics are required in order to obtain quantitative results. Overall, the ^{13}C NMR results in Figure 7.2 are in agreement with previously reported results[31-32,37-38] and the spectra in Figure 7.2 provide spectroscopic support of the molecular characterization of the products.

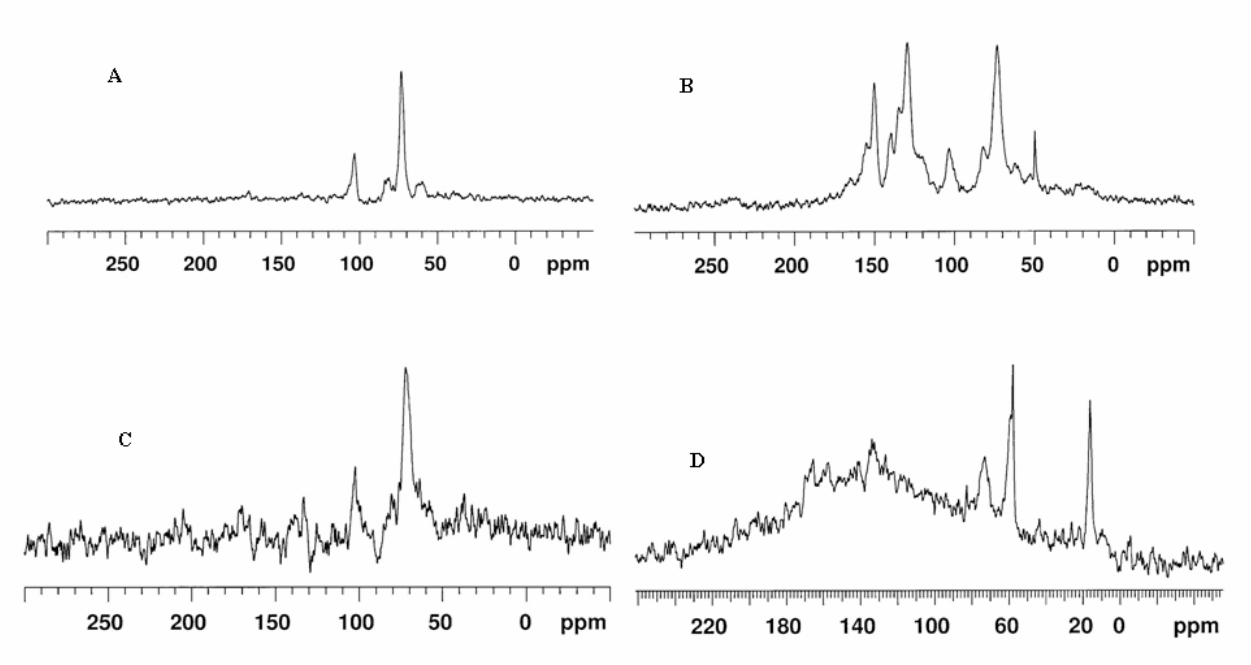

Figure 7.2. ^{13}C NMR spectra of polymeric products recorded at ambient temperature, 16 kHz spinning speed, and 150.8 MHz: a) β-CD hydrate, b) CD-PDI, and c) CD-PDI, and d) CD-ICS polymeric materials.

Surface Area Estimation

The results from dye (PNP) sorption method are given in Table 7.2 below according to the models presented in Table 7.1. It is observed that GAC adopts a monolayer adsorption (Langmuir) unlike the CD-based polymeric materials which appear to conform to multilayer adsorption (B.E.T).

Assuming PNP is adsorbed on the surface in a planar orientation parallel to the polymer surface structure; the surface area (SA) is estimated using the equation given in Table 7.1. The molecular surface for PNP (A_m) for this particular planar orientation is 5.25×10^{-19} m^2. The calculated surface areas are listed in Table 7.3. The estimates obtained from the dye based method are in reasonable agreement for GAC with those calculated from nitrogen porosimetry data. For CD based materials, the dye based method yields

lower SA estimates because the dye is primarily included within the CD macrocycle. Thus, lower SA estimates are predicted in accordance with the degree of surface attachment of CD molecules. [39-40]

Table 7.2. Sorption parameters for PNP* obtained from the Langmuir and B.E.T isotherms (pH 4.00 buffered with 10^{-3} M KH_2PO_4 and temperature of 25°C)

	GAC	CD-PDI	CD-EP	CD-ICS
Langmuir				
Q_m (mmol/g)	3.00	0.130	0.196	0.0571
K_L (L/mmol)	23.8	1.77	0.898	4.88
R^2	0.983	0.872	0.942	0.822
B.E.T				
Q_m (mmol/g)	2.51	0.114	0.184	0.298
K_{BET}(L.mmol/g^2)	$9.94x10^3$	196	86.7	22.2
R^2	0.955	0.983	0.991	0.915

*Using p-nitrophenol (PNP) as the chromophore dye at pH = 4.00 and a λ_{max} = 317 nm

Table 7.3. Surface area estimates of sorbent materials (pH 4.00 buffered with 10^{-3} M KH_2PO_4 and temperature of 25°C) obtained from porosimetry and the dye adsorption method*.

Polymeric Sorbent Material	Nitrogen Porosimetry (m^2/g)	Dye Sorption Method* (m^2/g)
GAC	993	795
CDPDI	30.3	36.2
CDEPH	101	59.1
CDICS	657	94.3

*Using p-nitrophenol (PNP) as the chromophore dye at pH = 4.00 and a λ_{max} = 317 nm

7.4.2 Sorption Characterization of Naphthenic Acids

Figures 7.3 and 7.4 represent the isotherms obtained from sorption of NAs at pH 9.00. The resulting parameters are listed in Tables 7.4 and 7.5 at pH conditions of 9.00 and 5.00, respectively. It is concluded that GAC and CD-PDI adopt a monolayer adsorption profile according to the "best fit" results for the Langmuir model. In contrast,

multilayer sorption behaviour is concluded for CD-EP and CD-ICS, as evidenced by the "s-shaped" curves that are typical of multilayer adsorption profiles.

Another interesting observation from the isotherm results are the differences in the sorption capacities between GAC, CDEPH and CD-PDI at pH = 5.00. The sorption capacities are listed in descending order as follows: GAC > CD-EP > CD-PDI. At pH = 9.00 (*cf.* Table 7.4), the sorption capacities are attenuated for GAC and CD-PDI except CD-EP shows a small increase. We attribute the latter to increased swelling of the polymer at these conditions. The reduction in sorption for the other materials is related to ionization of NAs which may result in changes to the orientation of the sorbate on the surface of the sorbent. The latter argument is consistent with previous results observed for sorption of PNP at different pH conditions for these sorbent materials.[40]

The binding constants for GAC and CD-EP decrease when the pH is lowered while that for CD-PDI increases. GAC is the sorbent with the highest binding constant at pH 9.00 while CD-PDI is the highest for pH 5.00.

The parameters for CD-ICS are less conclusive as they provide negative values for both sorption capacities and binding constants. This is a result of surface inaccessible CD on the surface of the CD-ICS material and the calculated errors that result because of the attentuated uptake of NAs. The CD-ICS material synthesized in this study contains 6% CD incorporation which may not be completely surface accessible because of occlusion within the silica framework during synthesis. Thus, we observe lower sorption capacities than predicted relative to CD grafted materials which are completely surface accessible. We have independently observed that mesoporous silica (MCM-type materials) without CD incorporation do not adsorb NAs or dyes, such as PNP, despite

their very high (~10^3 m^2/g) surface area.[39] Therefore, the low uptake of NAs in CD-ICS is attributed to the limited surface coverage of CD attachment. However, despite the relatively low surface area each of the polymeric sorbents, as compared with GAC, they all displayed a significant level of sorption towards NAs.

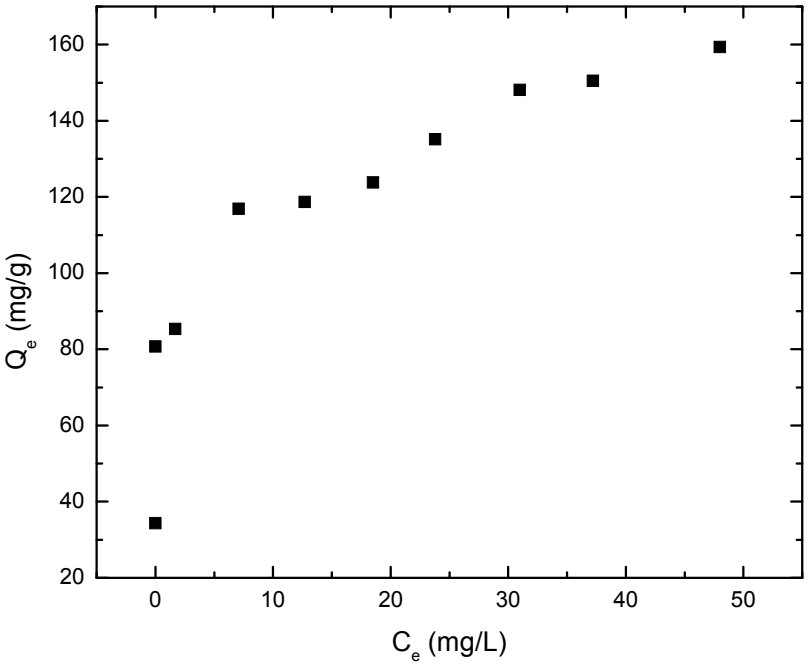

Figure 7.3. Sorption isotherm of fixed amounts (2.00 mg) of GAC with different concentration of NAs at pH 9.00 and temperature of 25^{o}C.

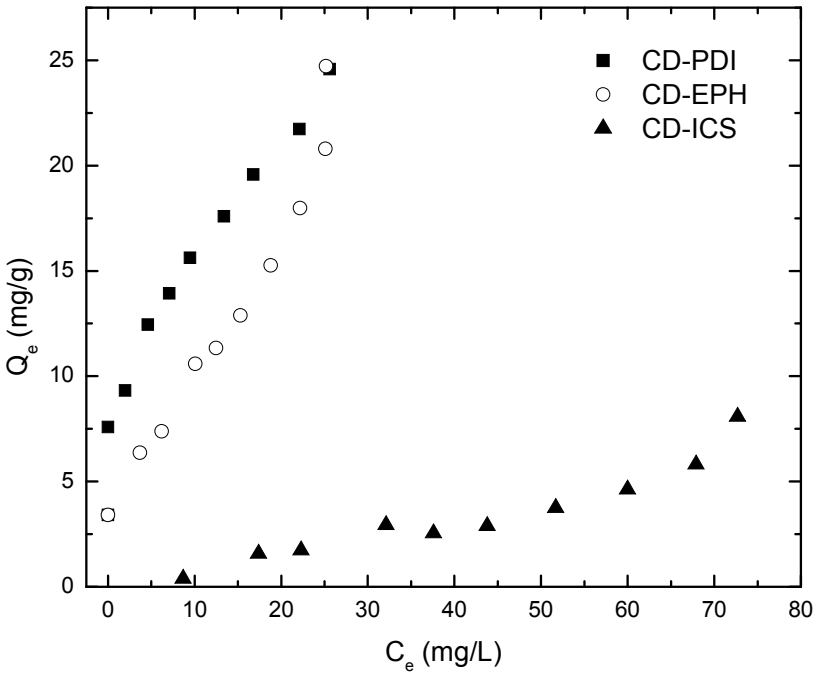

Figure 7.4. Sorption isotherm of fixed amounts (20.0 mg) of CD-based polymeric materials with different concentration of NAs at pH 9.00 and temperature of 25^{o}C.

Table 7.4. Langmuir and B.E.T Equilibrium sorption isotherm parameters for NAs at pH 9.00 (Unbuffered)* and 25^{o}C

	GAC	CD-PDI	CD-EP	CD-ICS
Langmuir				
Q_m (mg/g)	159	28.6	29.1	NR
K_L (L/mg)	0.377	0.152	0.0587	NR
R^2	0.987	0.962	0.871	0.301
B.E.T				
Q_m (mg/g)	143	22.2	21.1	NR
K_{BET}(L.mg/g^2)	7.00x10^3	2.25x10^3	790	NR
R^2	0.880	0.917	0.929	0.934

*Solutions were unbuffered and pH was adjusted using 10^{-3} M NH_4OH
NR indicates that the data was not reported due to negligible values

Table 7.5. Langmuir and B.E.T Equilibrium Sorption Isotherms Parameters for NAs at pH 5.00 (Unbuffered)* and Temperature of 25°C

	GAC	CD-PDI	CD-EP	CD-ICS
Langmuir				
Q_m (mg/g)	107	19.7	39.5	NR
K_L (L/mg)	0.245	0.317	0.0281	NR
R^2	0.989	0.962	0.738	0.628
B.E.T				
Q_m (mg/g)	101	13.5	28.7	NR
K_{BET}(L.mg/g^2)	2.47×10^3	1.86×10^4	348	NR
R^2	0.974	0.850	0.951	0.985

*Solutions were unbuffered and pH was adjusted using 10^{-3} M CH_3COOH
NR indicates that the data was not reported due to negligible values

7.5 Conclusions

The results of this work illustrate that CD-based polymeric materials can be used as novel sorbents in NF membranes for the remediation of NAs from TPWs. Although these materials possess low surface areas, they are suitable in the removal NAs, especially at lower pH for the case of CD-PDI. The current estimates indicate that CD-PDI has a higher binding constant with NAs, as compared to that of GAC despite its high sorption capacity. In general, the sorption capacity increases as the surface area of the material increases. This correlation between surface area and sorption capacity is observed for the materials developed in this research.

Ongoing efforts are underway in our research program to increase the surface area of polymeric materials in order to modify the sorption capacity of sorbents for various applications. In this regard, we anticipate that the sorption capacities of GAC can be surpassed with synthetic modification of such novel supramolecular porous materials. Future work is underway to optimize the sorption properties of these types of materials for the sequestration of NAs in aqueous solutions.

7.6 References

1. *Naphthenic acids in Kirk-Othmer Encyclopedia of Chemical Technology*; 4 ed.; Brient, J. A.; Wessner, P. J.; Doyle, M. N., Eds.; John Wiley & Sons: New York.
2. Lo, C. C.; Brownlee, B. G.; Bunce, N. J. *Anal. Chem.* **2003**, *75*, 6394-6400.
3. Headley, J. V.; McMartin, D. W. *J. Environ. Sci. Health, Part A: Toxic/Hazard. Subst. Environ. Eng.* **2004**, *A39*, 1989-2010.
4. McMartin, D. W.; Headley, J. V.; Friesen, D. A.; Peru, K. M.; Gillies, J. A. *J. Environ. Sci. Health, Part A: Toxic/Hazard. Subst. Environ. Eng.* **2004**, *39*, 1361 - 1383.
5. Clemente, J. S.; Fedorak, P. M. *Chemosphere* **2005**, *60*, 585-600.
6. Quagraine, E. K.; Peterson, H. G.; Headley, J. V. *J. Environ. Sci. Health, Part A: Toxic/Hazard. Subst. Environ. Eng.* **2005**, *40*, 685-722.
7. Headley, J. V.; Crosley, B.; Conly, F. M.; Quagraine, E. K. *J. Environ. Sci. Health, Part A: Toxic/Hazard. Subst. Environ. Eng.* **2005**, *40*, 1 - 27.
8. Department of Energy, G. o. A. Edmonton, AB, 2001; Vol. http://www.energy.gov.ab.ca/1876.asp
9. Schindler, D. W.; Donahue, W. F. *PNAS* **2006**, *103*, 7210-7216.
10. Headley, J. V.; Du, J.-L.; Peru, K. M.; McMartin, D. W. *J. Environ. Sci. Health, Part A: Toxic/Hazard. Subst. Environ. Eng.* **2009**, *44*, 591 - 597.
11. Slavcheva, E. *Brit. Corros. J.* **1999**, *34*, 125-131.
12. Turnbull, A.; Slavcheva, E.; Shone, B. *Corrosion* **1998**, *54*, 922-930.
13. Rogers, V. V.; Liber, K.; MacKinnon, M. D. *Chemosphere* **2002**, *48*, 519-527.
14. Gaikar, V. G.; Maiti, D. *React. Funct. Polym.* **1996**, *31*, 155-164.
15. Wong, D. C. L.; van Compernolle, R.; Nowlin, J. G.; O'Neal, D. L.; Johnson, G. M. *Chemosphere* **1996**, *32*, 1669-1679.
16. Rezaei Gomari, K. A.; Denoyel, R.; Hamouda, A. A. *J. Colloid Interface Sci.* **2006**, *297*, 470-479.
17. Zou, L.; Han, B.; Yan, H.; Kasperski, K. L.; Xu, Y.; Hepler, L. G. *J. Colloid Interface Sci.* **1997**, *190*, 472-475.
18. Janfada, A.; Headley, J. V.; Peru, K. M.; Barbour, S. L. *J. Environ. Sci. Health, Part A: Toxic/Hazard. Subst. Environ. Eng.* **2006**, *41*, 985-997.

19. Peng, J.; Headley, J. V.; Barbour, S. L. *Can. Geotech. J.* **2002**, *39*, 1419-1426.
20. Frank, R. A.; Kavanagh, R.; Burnison, B. K.; Headley, J. V.; Peru, K. M.; Der Kraak, G. V.; Solomon, K. R. *Chemosphere* **2006**, *64*, 1346-1352.
21. Saab, J.; Mokbel, I.; Razzouk, A. C.; Ainous, N.; Zydowicz, N.; Jose, J. *Energ. Fuel.* **2005**, *19*, 525-531.
22. Peng, H.; Volchek, K.; MacKinnon, M.; Wong, W. P.; Brown, C. E. *Desalination* **2004**, *170*, 137-150.
23. He, B.; Zhao, X. *React. Polym.* **1992**, *18*, 229-235.
24. Crini, G.; Bertini, S.; Torri, G.; Naggi, A.; Sforzini, D.; Vecchi, C.; Janus, L.; Lekchiri, Y.; Morcellet, M. *J. Appl. Polym. Sci.* **1998**, *68*, 1973-1978.
25. Ma, M.; Li, D. *Chem. Mater.* **1999**, *11*, 872-874.
26. Buvari, A. *J. Inclusion Phenom.* **1983**, *1*, 151-157.
27. Eftink, M. R.; Andy, M. L.; Bystrom, K.; Perlmutter, H. D.; Kristol, D. S. *J. Am. Chem. Soc.* **1989**, *111*, 6765-6772.
28. Gadre, A.; Connors, K. A. *J. Pharm. Sci.* **1997**, *86*, 1210-1214.
29. Wenz, G. *Angew. Chem. Int. Ed. Engl* **1994**, *33*, 803-822.
30. Harada, A.; Hashidzume, A.; Takashima, Y. *Cyclodextrin-based supramolecular polymers*; Springer, 2006; Vol. 201.
31. Liu, C.; Naismith, N.; Economy, J. *J. Chromatogr., A* **2004**, *1036*, 113-118.
32. Liu, C.; Lambert, J. B.; Fu, L. *J. Org. Chem.* **2004**, *69*, 2213-2216.
33. Richer, R. *Chemical Communications* **1998**, *16*, 1775-1777.
34. Richer, R.; Mercier, L. *Chem. Mater.* **2001**, *13*, 2999-3008.
35. Giles, C. H. *J. Appl. Chem.* **1970**, *20*, 37-41.
36. Dupuy, G.; Hilaire, G.; Aubry, C. *Clin Chem* **1987**, *33*, 524-528.
37. Ponchel, A.; Abramson, S.; Quartararo, J.; Bormann, D.; Barbaux, Y.; Monflier, E. *Micropor. Mesopor. Mat.* **2004**, *75*, 261-272.
38. Derouet, D.; Forgeard, S.; Brosse, J.-C.; Emery, J.; Buzare, J.-Y. *J. Polym. Sci. Part A: Polym. Chem.* **1998**, *36*, 437-453.
39. Mahmud, S. T. Research, University of Saskatchewan, 2007.
40. Kwon, J. H. Research-Based, University of Saskatchewan, 2007.

CHAPTER 8

PUBLICATION 7

Description

The following is a verbatim copy of an article that was published in November of 2010 in Physical Chemistry Chemical Physics journal (*Phys. Chem. Chem. Phys.*: **2011**, *13(3)*, 1112-1122). This paper describes the sorption of NAs from aqueous solution using the copolymers proposed for this project.

Authors' Contribution

I conducted all the experimental work except for the ESI-MS which was done by Mr. Kerry Peru. This work was supervised by Dr. Wilson and Dr. Headley. I wrote the first draft of the manuscript with extensive editing by each supervisor prior to submission for publication. Written permission was obtained from all contributing authors to include this material in this thesis.

Relation of Chapter 8 (Publication 7) to the Overall Objectives of this Project

This chapter is a follow up from the published study in Chapter 7 where it illustrates the use of the copolymers for the sequestration of NAs from aqueous solution. The study detailed herein is systematic because it shows the relative role of the β-CD macrocycle and the role of the linkers in the sorption of NAs.

Graphical Abstract

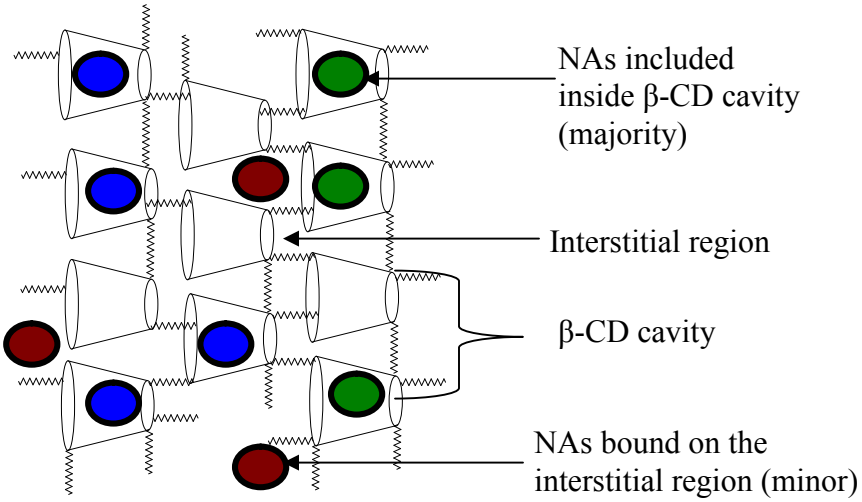

A novel series of β-cyclodextrin (β-CD) polyurethane copolymers display significant inclusion binding towards naphthenic acids (NAs) inside the β-CD cavities.

8. Sequestration of Naphthenic Acids from Aqueous Solution using β-Cyclodextrin-based Polyurethanes

Mohamed H. Mohamed,[§] Lee D. Wilson,[§] John V. Headley,[¥] Kerr M. Peru[¥]*

[§]Department of Chemistry, University of Saskatchewan, 110 Science Place, Saskatoon, Saskatchewan, S7N 5C9

[¥]Water Science and Technology Directorate, 11 Innovation Boulevard, Saskatoon, Saskatchewan, S7N 3H5

*Corresponding Author

Received 2 May 2010

8.1 Abstract

The sorption characteristics of naphthenic acids (NAs) in their anion form with β-cyclodextrin (β-CD) based polyurethanes, as sorbents, from aqueous solutions that simulate the conditions of oil sands process water (OSPW) are presented. The copolymer sorbents were synthesized at various β-CD:diisocyanate monomer mole ratios (e.g., 1:1, 1:2, and 1:3) with diisocyanates of variable molecular size and degree of unsaturation. The equilibrium sorption properties of the copolymer sorbents were characterized using sorption isotherms in aqueous solution at pH 9.00 with electrospray ionization mass spectrometry to monitor the equilibrium unbound fraction of anionic NAs in the aqueous phase. The copolymer sorbents were characterized in the solid state using ^{13}C CP-MAS NMR spectroscopy, IR spectroscopy and elemental analysis. The sorption results of the copolymer sorbents with anion forms of NAs in solution were compared with a

commercially available carbonaceous standard; granular activated carbon (GAC). The monolayer sorption capacities of the sorbents (Q_m) were obtained from either the Langmuir or the Sips isotherm models used to characterize the sorption characteristics of each copolymer sorbent. The estimated sorption capacity for GAC was 142 mg NAs per g sorbent whereas the polymeric materials ranged from 0-75 mg NAs per g sorbent over the experimental conditions investigated. In general, significant differences in the sorption capacities between GAC and the copolymer sorbents were related to the differences in the accessible surface areas and pore structure characteristics of the sorbents. The Sips parameter (K_{eq}) for GAC and the copolymer materials reveal differences in the relative binding affinity of NAs to the sorbent framework in accordance with the synthetic ratios and the value of Q_m. The diisocyanate linker plays a secondary role in sorption mechanism, whereas the β-CD macrocycle in the copolymer framework is the main sorption site of NAs because of the formation of inclusion complexes with β-CD.

8.2 Introduction

Canadian oil sands deposits are vast and represent the second largest source of crude oil after Saudi Arabia for the North American economy.[1] The oil sands industry in Northern Alberta, Canada uses a caustic warm water process to extract oils sands. The resulting oil sands process water (OSPW) is saline and contains a complex mixture of organic compounds dominated by a class of naturally occurring naphthenic acids (NAs). NAs are known to be toxic to aquatic organisms, algae, and mammals.[2-4] NAs are also

suspected to be endocrine-disrupting substances, however; the toxicology of the various components of NAs is poorly understood.

NAs (*cf.* Figure 1.1 in Chapter 1) are considered to be the principal toxic components in the OSPW. The structural formulae of NAs may be described by the traditional definition $C_nH_{2n+z}O_2$,[5-9] where "Z" is referred to as the "hydrogen deficiency" and is a negative, even integer. More than one isomer may exist for a given Z homolog, with variable molecular weight, and the carboxylic acid group is usually bonded or attached to a side chain, rather than directly to the alicyclic ring.[5-6] The molecular weights differ by 14 atomic mass units (CH_2) between n-series and by two atomic mass units (2H) between z-series.[10] However, more recently the term NAs has been widened to include more than the traditional NAs described above. For example, OSPW is known to contain other components containing, dicarboxylic and polycarboylic acids. Furthermore O_x (x=1-6) containing species along with heteroatom components such as S and N are also present in the OSPW acid extractable fractions.[11]

The oil sands industry operates with a zero discharge policy where the OSPW is retained in vast tailing ponds. Given the estimated crude oil reserves (*ca*. 174 billion barrels bitumen) in the Athabasca oil sands and the significant water consumption (*ca*. 2 to 4 barrels water per 1 barrel bitumen) for the extraction processing, there is growing interest to reclaim the OSPW.[1] The estimated levels of NAs in the OSPW can be as high as 110 mg/L and although the OSPW is recycled, residual levels of salts and NAs ultimately lead to corrosion problems.[3,12-14]

Strategies for the removal of NAs from synthetic and industrial OSPW have been met with limited success using various sorbents such as, granular activated carbons

(GACs), soils, zeolites, clays, calcite, and mica.[15-20] As well, some examples of conventional polymeric sorbents include poly(4-vinyl pyridine), polystyrene, and dimethylaminoethyl-cellulose.[15,21-22] Recent studies have investigated the utility of some commercially available nanofiltration (NF) membranes according to their rejection efficiency of magnesium sulfate from aqueous solution. These types of NF membranes are anticipated to produce permeate solutions with low concentrations (< 5 mg/L) for NAs and calcium carbonate (< 40 mg/L).[23] Another related filtration technique is micellar-enhanced ultra filtration (MEUF); this method is limited by the presence of residual colloidal materials along with the trace NAs.[24]

Cyclodextrins (CDs) are cyclic oligosaccharides consisting of six, seven, and eight α-D-(+) glucopyranoside units connected by α-(1, 4) linkages commonly referred to as α-, β-, and γ-CDs, respectively.[25] β-cyclodextrin (β-CD) possesses a characteristic toroidal shape with a well-defined lipophilic cavity and a hydrophilic exterior that is suitable for the inclusion of appropriate sized guest compounds. CDs are of interest, in part, because of their ability to form inclusion complexes in aqueous solution. In particular, they are also well known to form relatively stable inclusion complexes with aliphatic and alicyclic carboxylic acids.[26-31] CDs can be converted into insoluble polymeric materials using a variety of synthetic strategies.[32-34] Recently, β-CD has been incorporated into crosslinked copolymers with a variety of linker monomers (e.g. epichlorohydrin, glutaraldehyde, succinyl chloride, diisocyanates, diacid chlorides, dicarboxylic acids, cyanuric chloride).[32-37] These resulting copolymer materials have been utilized for the sequestration of organic compounds from the gas and condensed phases and exhibit similar binding affinity as compared with native β-CD. By analogy to β-CD

and its favorable affinity toward carboxylic acid compounds, copolymeric materials containing β-CD are hypothesized to have comparable binding affinity to NAs because of their suitable size-fit and amphiphilic character. As well, hydrophobic effects are anticipated to stabilize such host-guest complexes.

The use of synthetically engineered copolymer materials represents distinct advantages with respect to previous conventional approaches, and offers an innovative "green environmental remediation strategy". Previously, it was reported that polymeric β-CD materials may serve as novel sorbents for the remediation of NAs from OSPW, despite their lower sorption capacity, as compared with granular activated carbon (GAC).[34] The objectives of this study are to investigate the sorption properties of a range of structurally diverse synthetically engineered copolymer materials with NAs derived from OSPW at variable concentration at pH 9.00 and 298.15 K. This systematic study will contribute towards the development of improved solid phase copolymer materials with enhanced understanding of the sorption and molecular recognition properties towards NAs in aqueous solutions. The copolymer sorbents investigated in this work are a range of polyurethane based β-CD materials comprised of diisocyanates monomers that contain aliphatic and aromatic linker units which vary according to their molecular size (*cf*. Figure 1.3 in Chapter 1). An outcome of this research is the development of novel sorbents for the controlled sequestration of NAs in aquatic environments. The development of novel sorbents of the type described herein offers the potential for a large scale extraction method to sequester NAs from OSPW and contributing to a long term strategy for the reclamation of OSPW.[3-4]

8.3 Experimental

8.3.1 Materials

GAC (Norit Rox 0.8) and β-CD were purchased from VWR. 1,6-Hexamethylene diisocyanate (HDI), 4,4'-Discyclohexyl diisocyanate (CDI), 4,4'-Diphenylmethane diisocyanate (MDI), 1,4-Phenylene diisocyanate (PDI), 1,5-Naphthalene diisocyanate (NDI), dimethyl acetamide (DMA), anhydrous ethyl ether, potassium bromide, 4Å (8-12 mesh) molecular sieves, ammonium hydroxide and acetic acid were all purchased from Sigma Aldrich except for NDI which was from TCI America. Figure 1.3 shows the structures of the aforementioned linkers. NAs were obtained from OSPW at Syncrude Canada Ltd (Alberta, Canada) according to an established protocol.[19]

8.3.2 Methods

8.3.2.1 Synthesis of supramolecular sorbents

A procedure for the synthesis of urethane based cyclodextrin materials was adopted from previous work,[35] as outlined in the following procedure for a 1:3, β-CD:diisocyanate copolymer. DMA was dried with 4Å (8-12 mesh) molecular sieves, Aldrich). ^{1}H NMR of DMA was recorded before and after the addition of molecular sieves, and the water content was estimated to be ~ 0.5%. 3 mmol of dried β-CD was added to a round bottom flask with stirring until dissolved in 10 mL of DMA, followed by addition of a 9 mmol diisocyanate solution in 30 mL of DMA. The stirred mixture was heated at 68^{o}C for 24 h under Argon. The final reaction mixture was cooled to room temperature with addition of cold methanol to precipitate the copolymer product and subsequent filtration through a Whatman no. 2 filter. The product was thoroughly washed in a Soxhlet extractor with methanol for 24 h to remove any unreacted starting materials

and low molecular weight impurities. The final product was dried in a pistol dryer for 24 h and subsequently ground and passed through a 40 mesh sieve to ensure uniform particle sizes. A second cycle of washing in a Soxhlet extractor with anhydrous ethyl ether for 24 hrs was done to ensure the removal of residual solvents and reagents. The copolymer was repeatedly dried and ground, as outlined above. The nomenclature of the copolymers is described according to the type of the diisocyanate and the co-monomer mole ratio (β-CD:diisocyanate linker). For example, the 1:3 β-CD:HDI copolymer designation is referred to as HDI-X (X=3) where the molar quantity of β-CD is assumed to be unity relative to 3 moles of HDI.

8.3.2.2 Characterization of supramolecular sorbents

Solid state ^{13}C NMR spectroscopy was performed with cross polarization (cp; $^{13}C\{^{1}H\}$f and magic angle spinning. ^{13}C NMR spectra were run at 150.8 MHz on a Varian Inova-600 NMR spectrometer with 3.2 mm rotors, spinning rate 16 kHz with a CP ($^{13}C\{^{1}H\}$) ramp pulse program. The chemical shifts were externally referenced to hexamethyl benzene at 16.9 mg/L at ambient temperature. Data were processed with a 100 Hz line broadening with left shifting of the free induction decay, FID, (1-2 data points) to correct for any spectral baseline asymmetry.

IR spectra were obtained with a Bio-RAD FTS-40 spectrophotometer. Spectroscopic grade KBr was used as both the background and matrix over the range of 400-4000 cm^{-1}. Samples were prepared by mixing with pure spectroscopic grade KBr with grinding in a small mortar and subsequently pressed into a pelletized form for analysis. The spectra were recorded in Fourier Transform transmission mode at room temperature with a resolution of 4 cm^{-1} using multiple scans.

8.3.2.3 Sorption of NAs

Various solutions of NAs were prepared at pH 9.00 from a 6.990 g/L aqueous stock solution extracted from Athabasca OSPW (pH 7.60). The pH of the stock solution was raised to 9.00 using 10^{-3} M ammonium hydroxide. OSPW have a pH of ~ 8; hence, the NAs exist in their ionized forms, the acid dissociation constant range between 10^{-5} and 10^{-6} M.[2,38-39] Thus, sorption experiments were performed at pH 9.00 to ensure adequate solubility and to understand the uptake of the naphthenate ions. Hereafter, we refer to the ionized form of naphthenic acids as NAs.

To a 10 mL glass bottle with teflon lined caps, similar amounts of solid polymer were added to a fixed volume (7.00 mL) of an aqueous NAs solution at various concentrations ranging from ~ 10-100 mg/L. The concentration of NAs is ~110 mg/L in OSPW and is consistent with the choice of the maximum experimental concentration of 100 mg/L.[2-4,12] The vials were further sealed with parafilm seal between the cap and glass bottle and were placed at room temperature in a horizontal shaker to equilibrate for 24 hrs.

The equilibrium concentrations of NAs were determined using negative ion electrospray ionization mass spectrometry (ESI-MS). Samples (5.0 μL) were introduced into the eluent stream (200 μL/minute, 50:50 CH_3CN:H_2O containing 0.1% NH_4OH) using a Waters 2695 advanced separation system (Milford, MA). Mass spectrometry analysis was conducted using a Quattro Ultima mass spectrometer (Micromass, UK). MS conditions were as follows: source temperature 90 °C, desolvation temperature 220 °C, cone voltage setting 62 V, capillary voltage setting 2.63 kV, cone gas N_2 147 L/hr, desolvation gas N_2 474 L/hr. The low and high mass resolutions were set at 14.0

(arbitrary units) and ion energy was 1.7 eV. Entrance voltage was 96 V, collision energy 13 eV and exit voltage 56 V. The multiplier was set at 410 V. Full scan MS (m/z 100-550) was employed. MassLynx version 4.1 software was utilized for all instrumental control and data acquisition/manipulation.

8.3.2.4 Data analysis

The experimental sorption results were studied using equilibrium isotherms and are represented as plots of the amount of NAs removed from aqueous solution per mass of copolymer (Q_e) versus the unbound equilibrium concentration of NAs in the solution (C_e). Equation (8.1) defines the term Q_e in relation to experimental variables; where C_o is initial concentration (mg/L) of NAs, V is volume of solution (L), and m is the mass of sorbent (g).

$$Q_e = \frac{(C_o - C_e) \times V}{m} \qquad \text{Equation 8.1}$$

The Langmuir, Freundlich and Sips isotherm models were used to analyze the equilibrium sorption data.[40-42] The Langmuir model assumes that sorption is homogeneous within a monolayer, while the Freundlich and Sips models provide an assessment of the heterogeneity of the sorption process. The heterogeneity is estimated using the exponent terms (n_f and n_s) for the Freundlich and Sips models, respectively, where a value that deviates from unity indicates heterogeneity of a material. The Sips isotherm model is preferred because it represents a generalized isotherm which conforms to the Langmuir or Freundlich isotherms, in accordance with the adjustable parameters. The three isotherm models; Langmuir, Freundlich and Sips are defined in Equations 8.2-8.4, respectively. The monolayer coverage of NAs onto the copolymers is given by Q_m while the sorption process can be related to the equilibrium constant (K_i) appearing in

Equations 8.2-8.4. The criterion of the "best fit" for the three models used is defined by the correlation coefficient (R^2) and sum of square of errors (SSE) where values of R^2 near unity and values of SSE that approach zero, represent criteria for the "best fit". The data for each isotherm was fitted by minimization of the SSE as described by Equation 8.5. $Q_{e,i}$ is the experimental value, $Q_{f,i}$ is the simulated value according to the choice of isotherm model (*cf.* Equations 8.2-8.4) and N is the number of experimental data points.

$$Q_e = \frac{K_L Q_m C_e}{1 + K_L C_e} \qquad \text{Equation 8.2}$$

$$Q_e = K_F C_e^{1/n_f} \qquad \text{Equation 8.3}$$

$$Q_e = \frac{Q_m (K_s C_e)^{n_s}}{1 + (K_s C_e)^{n_s}} \qquad \text{Equation 8.4}$$

$$SSE = \sum \sqrt{\frac{(Q_{e,i} - Q_{f,i})^2}{N}} \qquad \text{Equation 8.5}$$

8.3.2.5 Molecular Polarizability Calculation

Molecular polarizability (α) was calculated using Spartan '08 V1.1.1. The quantity adopted for α is the atomic unit (au). The calculation was based on equilibrium geometry in the ground state with Hartree-Fock 3-21G(*) in vacuum. Total charge was set to zero and multiplicity was singlet. All the calculations were subjected to symmetry.

8.4 Results and Discussion

8.4.1 Characterization

The solid state ^{13}C CP-MAS NMR and IR spectra have been previously reported for some of the copolymer materials (e.g., CD-PDI copolymer at 1:3 ratio) and were fully characterized.[34] Additional results are reported in this work for the newly synthesized

urethane copolymer materials and the corresponding results are shown in Figure 8.1. Figure 8.1a-f illustrate typical ^{13}C solids NMR spectra observed for the CD-based polymers with the various types of diisocyanate linker units for the 1:3 β-CD:diisocyanate monomer mole ratio (*i.e.*, NDI, PDI, MDI, CDI and HDI) along with the native β-CD oligosaccharide for comparison. Although each glucose unit of β-CD contains six unique C atoms per glucose residue, the spectrum for β-CD hydrate in Figure 8.1a reveals four unique ^{13}C NMR lines between 55 and 110 ppm due to the overlap of some of the glucose signatures. The spectral assignment reported here agrees with other studies.[43-44] In particular, Gerbaud *et. al.*[44] observed similar chemical shifts for related copolymers formed between per(3,6-anhydro)-α-CD with diisocyanate linkers such as HDI and PDI, respectively (*cf*. Table/Figure in ref 44). In Figure 8.1b–f, ^{13}C signatures are observed for β-CD and the spectral lines for the various aliphatic (*cf*. 20-70 ppm) and aromatic (*cf*. 110-170 ppm) diisocyanate linker molecules, respectively. In comparison with the ^{13}C NMR spectra of native β-CD and the diisocyanate monomers (results not shown), the urethane copolymers exhibit broader line widths as is often observed for such amorphous materials. The appearance of a carbonyl signature (~170-180 ppm) provides additional structural support for the formation of copolymer products since the diisocyanate precursor is typically observed ~60 ppm upfield to that observed for urethane carbonyl signature. The decreased crystallinity apparent from the increased ^{13}C NMR line width is attributed to the random attachment of the diisocyanate linker molecules to the available hydroxyl group sites (C_2, C_3, and C_6) of β-CD and variable cross polarization dynamics of the copolymer materials, as compared with native β-CD hydrate. Scheme 1.4 in Chapter 1 depicts a generalized structure of a copolymer formed

between β-CD and a diisocyanate linker. The degree of substitution of the primary and secondary hydroxyl groups of β-CD is affected by the relative size of the diisocyanate crosslinker and its relative mole ratio. In a previous report, the structure of the copolymer varies in accordance with the relative mole ratio of β-CD and the diisocyanate (*cf*. 1.5 in Chapter 1).[46]

Elemental analyses provided estimates of the linker composition since the N content originates from the diisocyanate monomers and increases as its mole ratio increases (*cf*. Table 2.2 in Chapter 2). Corrections due to residual water and/or solvent mixtures within the copolymers after extensive drying under vacuum were not applied because the relative amounts of residual solvent in the products were not assessed. However, the total contribution of solvent overall varied from 0.3–2%, as indicated by thermogravimetric analysis (TGA), and is in agreement with the ^{1}H NMR spectra in solution where solvent (i.e. DMA and water) signatures were simultaneously observed (results not shown). The presence of residual solvent(s) was attributed to the occlusion of solvent within the polymer framework during formation of the copolymer. The calculated values for the elemental analyses in Table 2.2 for β-CD were corrected by accounting for the hydrate water content. Whilst the percentages of C and N increase as expected, H does not decrease as predicted. Applied corrections for the presence of hydrate water provide good agreement between the experimental and the calculated values.

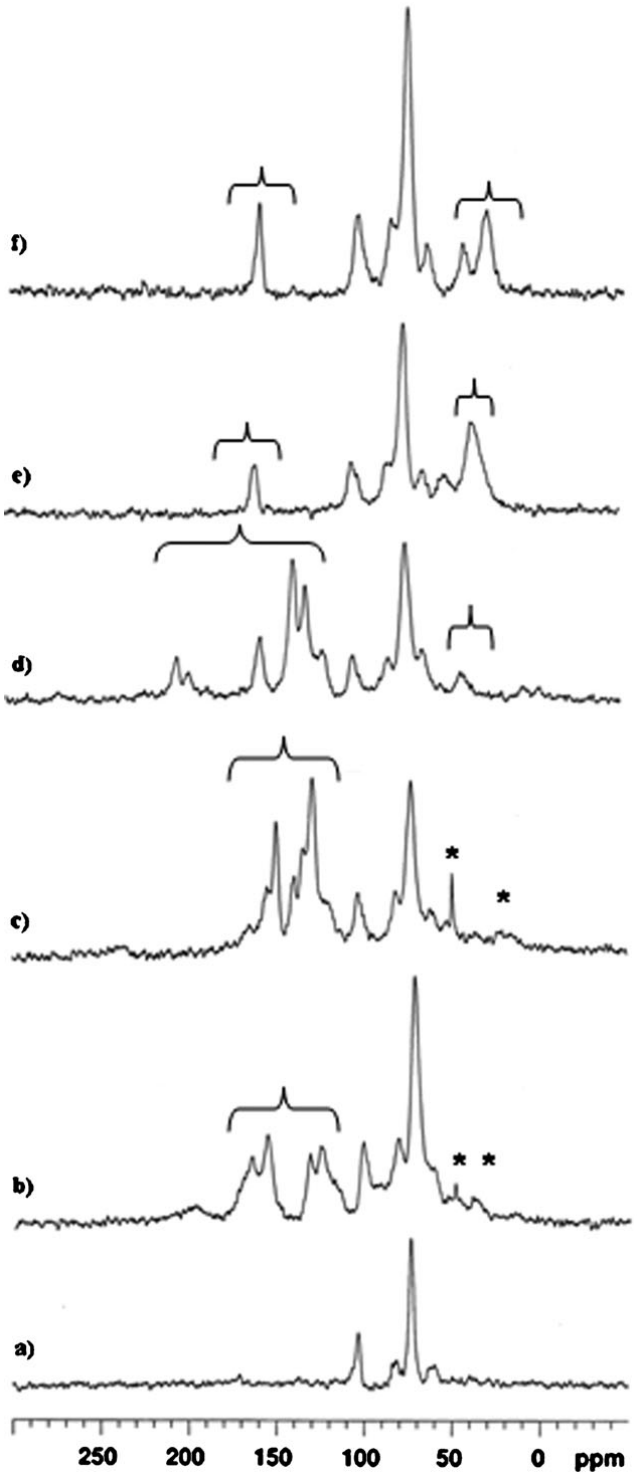

Figure 8.1. ^{13}C CP-MAS NMR spectra of β-CD copolymer materials recorded at ambient temperature, 16 kHz spinning speed, and 150.8 MHz: The spectra are listed as follows: (a) β-CD, (b) NDI-3, (c) PDI-3, (d) MDI-3, (e) CDI-3, and (f) HDI-3. The bracketed spectral signatures correspond to the diisocyanate linker unit and the signatures between 55-110 ppm correspond to β-CD. Spinning side bands are denoted with an asterisk.

8.4.2 Equilibrium Isotherm Models

Sorption isotherms provide a further understanding of the thermodynamics of sorption in a sorbent/sorbate system. The interpretation of experimental results is dependent on the suitable choice of an equilibrium isotherm model. The latter is represented as a plot of Q_e versus C_e at constant temperature and provides a physical interpretation of the concentration dependence and corresponding sorption parameters. Systematic comparisons of the sorption behavior for different sorbate/sorbent systems at variable experimental conditions provide some insight into the sorption mechanism. Therefore, it is important to establish reliable descriptions of equilibrium results and interpretation for a given sorbate/sorbent system. There are several isotherm models for analyzing experimental results; however, the Sips model serves as a good starting point to evaluate whether monolayer or multilayer processes are operative and whether the surface is homogenous or heterogeneous. As well, the Sips model provides an assessment of the sorption capacity and the binding affinity for a given sorbate/sorbent system.

In this work, the Langmuir, Freundlich and Sips models were systematically evaluated.[40-42] The Langmuir isotherm model assumes sorption onto a homogeneous monolayer and the sorbate does not affect neighboring sorption sites. The Freundlich isotherm assumes a heterogeneous sorbent surface with a non-uniform distribution of heats of adsorption. The parameter n_f in Equation 8.3 reflects the intensity of adsorption. In contrast, the Sips isotherm (*cf.* Equation 8.4) assumes a distribution of adsorption energies on the sorbent surface and may be considered as a hybrid form of the Langmuir and Freundlich isotherms depending on the experimental conditions. The use of Equation 8.4 when $n_s = 1$ reflects behavior of the Langmuir isotherm (*cf.* Equation 8.2); whereas

the conditions when $(K_s.C_e)^{ns} << 1$ describes the Freundlich isotherm (*cf.* Equation 8.3) behaviour. The parameter, n_s, (*cf.* Equation 8.4) provides an indication of the heterogeneity of the sorbent because values which deviate from unity resemble a highly heterogeneous sorbent; whereas $n_s = 1$, confers the properties of a homogenous sorbent.

8.4.3 Sorption of NAs

8.4.3.1 Choice of Isotherm Model

According to Equation 8.1, experimental isotherm results are plotted as Q_e versus C_e, as shown in Figure 8.2a-d for HDI-X, CDI-X, MDI-X, PDI-X, NDI-X and GAC, respectively. In general, there is a monotonic increase in Q_e vs. C_e as the total concentration of NAs increase. The relative magnitude of Q_e varies according to the nature of the sorbent and the synthetic ratio of the material (*i.e.* 1:1, 1:2, and 1:3). The sorption capacity of the sorbent and the relative binding affinity between NAs and sorbent material are important and were estimated from the "best-fit" parameters obtained from the various isotherm models (*cf.* Equations 8.2-8.4) listed in Tables 8.1 (*vide infra*).

In the case of the copolymer materials, the magnitude of Q_e vs. C_e is greatest for copolymers with unit mole ratios comprised of β-CD and linker monomer. The magnitude of Q_e decreases as the linker mole ratio increases (*i.e.* 1:1, 1:2 and 1:3). The magnitude of Q_e also varies according to the physicochemical properties of the linker molecule as illustrated by the variable sorption properties of the different copolymer materials. The isotherm parameters (Q_m, K and n) were estimated using a non-linear least squares (NLLS) fitting routine by minimizing the values of SSE (*cf.* Equation (8.5)). Overall, the Sips isotherm model provided the lowest SSE and the 'best fit" model

overall for the copolymers investigated in this study. In the case of GAC, the Freundlich isotherm provided the "best fit" results (*cf*. Tables 8.1).

To illustrate the relative difference amongst the three isotherm models, the sorption results for HDI-1 with NAs for the conditions described in Figure 8.2a are also shown in Figure 8.3. The Langmuir isotherm shows a poor fit; whereas, the Sips and Freundlich isotherms provide a better description of the observed sorption results. The Freundlich and Sips isotherms display a parameter (n_i) that deviates from unity. The latter result supports that the sorbent is heterogeneous and the goodness of each fit is shown in Figure 8.3. The Sips parameter ($n_s = 3.66$) that deviates from unity rules out the use of the Langmuir model since the latter result ($n_s \neq 1$) indicates a heterogeneous sorbent. The results shown in Figure 8.3 demonstrate the general utility and versatility of the Sips isotherm for describing the general nature of adsorption processes.

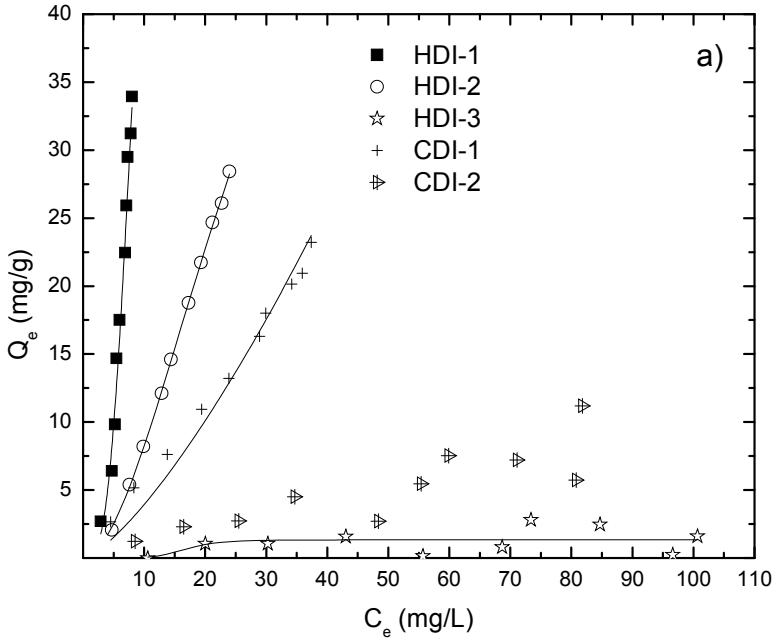

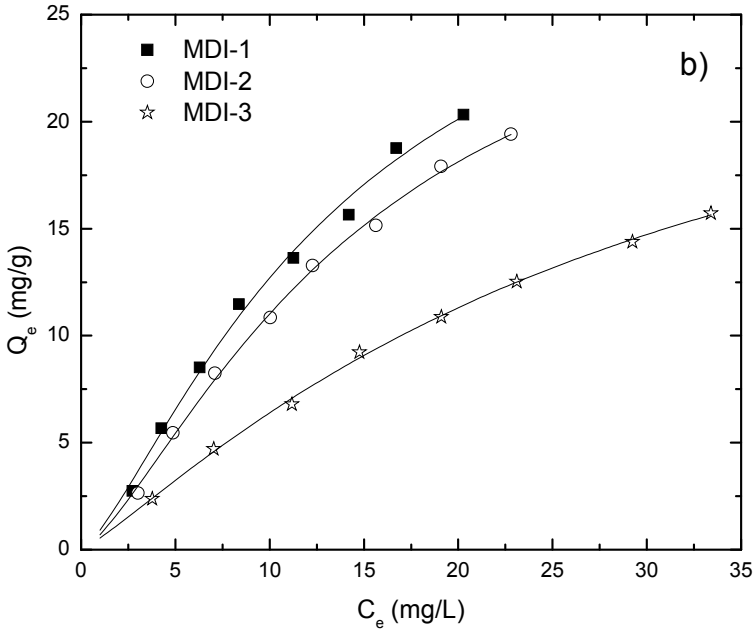
MDI-1
MDI-2
MDI-3
b)
Q_e (mg/g)
C_e (mg/L)
0
5
10
15
20
25
30
35

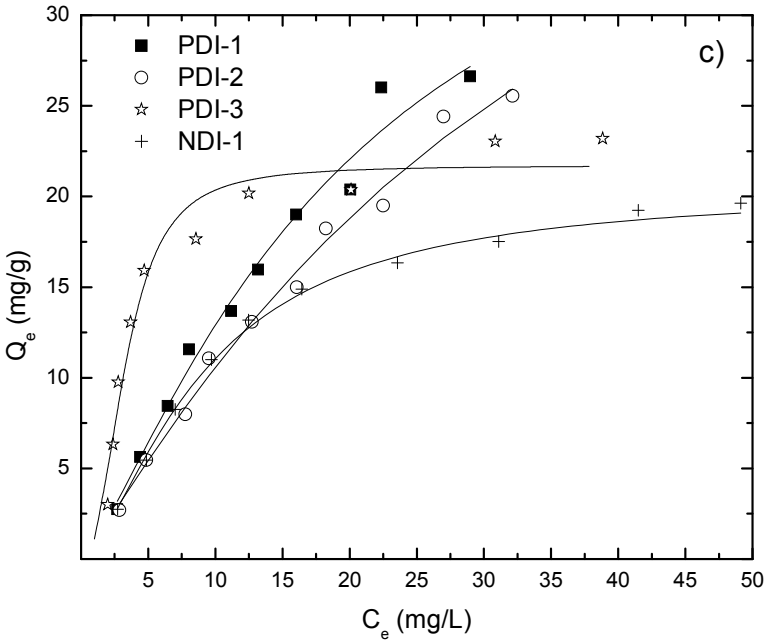
PDI-1
PDI-2
PDI-3
NDI-1
c)
Q_e (mg/g)
C_e (mg/L)
5
10
15
20
25
30
35
40
45
50

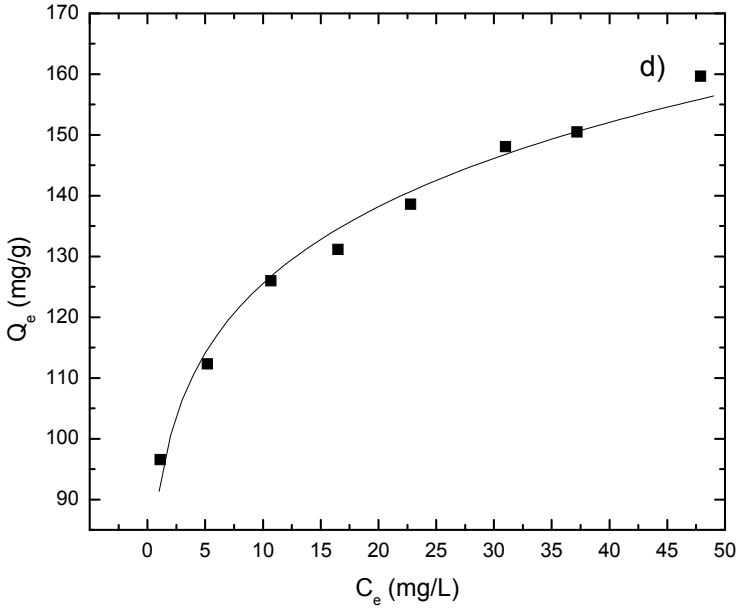

Figure 8.2a-d. Sorption isotherm for HDI, CDI, MDI, PDI, NDI and GAC respectively at pH 9.00 and 298 K. a) HDI-X,) CDI-X c) MDI-X d) PDI-X e) NDI-1 and f) GAC. X = 1, 2, 3 for 1:1, 1:2, and 1:3 β-CD:diisocyanate monomer mole ratios, respectively. The solid lines represent "best-fit" using Sips model.

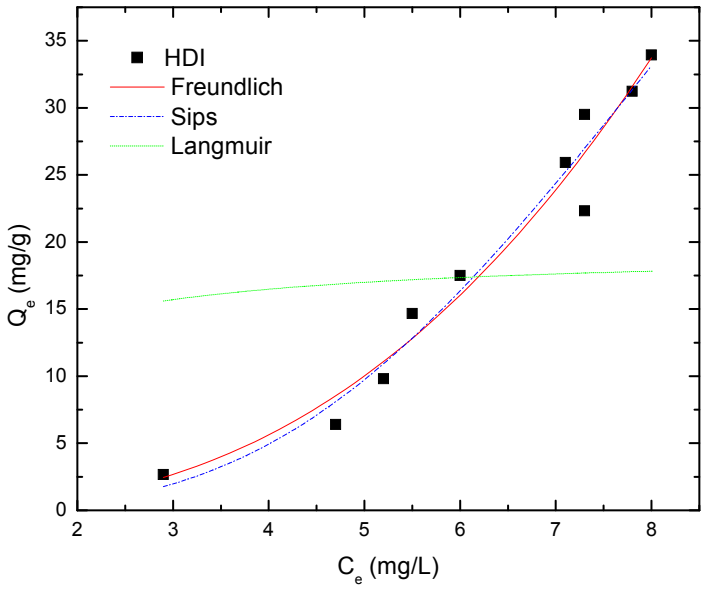

Figure 8.3. Experimental and "best-fit" results for the sorption isotherm of HDI-1 at pH 9.00 and 298K for the Freundlich, Sips and Langmuir models, respectively.

Table 8.1. Sorption parameters obtained from the Langmuir, Sips and Freundlich Isotherm models for the copolymers and GAC with NAs at 298 K and pH 9.00.

Isotherm Models	Parameters	Copolymer Sorbents										
		GAC	HDI-1	HDI-2	CDI-1	MDI-1	MDI-2	MDI-3	PDI-1	PDI-2	PDI-3	NDI-1
Langmuir	Q_m (mg/g)	147	-	-	-	61.4	59.1	41.6	72.3	77.1	26.9	25.5
	K_L (L/mg)	1.35	-	-	-	0.0251	0.0222	0.0184	0.0215	0.0160	0.195	0.0718
	R^2	0.954	-	-	-	0.989	0.992	0.998	0.979	0.990	0.908	0.975
	SSE	106	-	-	-	0.370	0.2486	0.04671	12.8	0.670	5.10	0.792
Sips	Q_m (mg/g)	-	75.5	73.0	70.4	32.2	30.1	29.4	44.1	56.6	21.7	20.5
	K_{Sips} (L/mg)	-	0.118	0.0324	0.0147	0.0729	0.0673	0.0334	0.0501	0.0268	0.304	0.111
	N	-	3.66	1.83	1.32	1.35	1.39	1.17	1.28	1.12	2.45	1.54
	R^2	-	0.986	0.999	0.989	0.994	0.998	0.999	0.982	0.991	0.962	0.991
	SSE	-	1.959	0.0520	0.628	0.216	0.0726	0.0242	10.6	0.629	2.07	0.146
Freundlich	K_F (L.mg/g)	91.4	0.146	0.234	0.460	2.13	1.65	1.11	2.09	1.68	7.13	3.55
	1/n	0.138	2.63	1.52	1.07	0.755	0.803	0.763	0.776	0.798	0.348	0.458
	R^2	0.997	0.982	0.993	0.994	0.983	0.984	0.991	0.969	0.986	0.807	0.916
	SSE	6.72	2.50	0.683	0.322	9.68	0.501	1.66	18.4	0.967	28.0	25.2

8.4.3.2 Copolymer-β-CD Sorbents with Aliphatic Linkers

The isotherm trends for HDI-X (X= -1, -2 and -3) copolymers are shown in Figure 8.2a where the HDI-1 copolymer displays representative behavior for a heterogeneous sorbent (n_s = 3.66) with high values of K_{eq} ($3.66x10^4$ M^{-1}). The HDI-2 polymer shows a similar trend as that for HDI-1 except for an increased slope in Q_e vs. C_e, indicating a reduced K_{eq} ($9.64x10^3$ M^{-1}) and lower heterogeneity (n_s = 1.83). The Q_m values for HDI-1 and HDI-2 are 75.5 and 73.0 mg NAs/g, respectively. As well, the results indicate that the sorption sites are approximately 50% occupied since the predicted Q_e values at saturation are ~ 35 and 30 mg NAs/g sorbent, respectively. The sorption affinity of the HDI-3 polymer is very low and the isotherm data illustrates a very weak dependence of Q_e vs. C_e. While the sorption capacity for HDI-1 and HDI-2 are similar, the value of Q_m for HDI-3 is evidenced by the reduced slope and apparent scatter in the data because of the low affinity toward NAs for this sorbent.

The CDI-based polymers (*cf.* Figure 8.2a) display a relatively high sorption affinity toward NAs by CDI-1; however, CDI-2 and CDI-3 sorbents exhibit attenuated uptake of NAs. Saturation of the copolymer sorption sites is not achieved over the range of C_e values examined for the CDI-1 polymer. The sorption capacity of CDI-1 is lower compared with HDI-1, as evidenced by a reduced value of K_{eq} ($4.36x10^3$ M^{-1}). The heterogeneity factor is also lower (n_s=1.32) indicating a more homogeneous adsorbent compared with the HDI-1 and HDI-2 copolymer materials.

8.4.3.3 Copolymer-β-CD Sorbents with Aromatic Linkers

The isotherm trends for MDI-based polymers are shown in Figure 8.2b where the isotherm depicts a gradual increase in Q_e vs. C_e for each copolymer. There is an incremental decrease in the sorption capacity (Q_m) with NAs with an increase in the crosslinking ratio. The relative ordering of the sorption capacity of MDI-X is as follows; MDI-1 (32.2 mg NAs/g sorbent) > MD1-2 (30.1 mg NAs/g sorbent) > MDI-3 (29.4 mg NAs/g sorbent). The magnitude of Q_e parallels the trend for the estimated values of K_{eq}. The value of K_{eq} decrease as the crosslinking ratio increases; $2.17x10^4$, $2.00x10^4$ and $9.93x10^3$ M^{-1}, respectively. The heterogeneity of MDI-1 and MDI-2 are similar but the MDI-3 copolymer is much less heterogeneous in nature.

PDI-based polymers (Figure 8.2c) show similar trends in sorption behavior to that of MDI-based copolymers at the 1:1 and 1:2 mole ratios. However, the 1:3 copolymer reaches saturation of the sorption sites at intermediate values of C_e. The sorption capacity for the PDI-1 and PDI-2 materials are correlated with the corresponding values of K_{eq} (M^{-1}); PDI-1 ($1.49x10^4$), PDI-2 ($7.98x10^3$) and PDI-3 ($9.03x10^4$). The trend in values for the estimated sorption capacity (Q_m) illustrates a similar pattern to that of the binding affinity. The values of Q_m (mg NAs/g sorbent) for PDI-1 (44.1), PDI-2 (56.6) and PDI-3 (21.7) and the heterogeneity factors display a similar pattern to that of K_{eq}. PDI-3 appears to be the most heterogeneous copolymer whereas PDI-2 has the least heterogeneity factor (n_s) as shown by the following results; PDI-3 (2.45), PDI-1 (1.28) and PDI-2 (1.12), respectively.

The NDI-1 copolymer (Figure 8.2c) shows a similar trend to that of the PDI-3 copolymer except that the isotherm for lower values of C_e exhibits greater concave behavior indicating a lower K_{eq} (i.e. $3.30x10^4$ M^{-1}). The value of Q_m and heterogeneity

factor is 20.5 mg NAs/g polymer and 1.54, respectively. NDI and PDI are both aromatic linkers but they differ in their molecular size; however, the value of K_{eq} is lower for PDI-1 as compared NDI-1. The opposite trend is observed in their sorption capacity.

8.4.3.4 Granular Activated Carbon

GAC has a relatively high sorption capacity and binding affinity toward NAs; it provides a well characterized sorbent for comparison with the copolymer CD-based materials. The Freundlich isotherm provides the "best-fit" results for the sorption of NAs, whereas, the Langmuir isotherm provides poor fitting results. However, the Langmuir isotherm can be used to provide a crude estimate of the sorption capacity, Q_m (146 mg NAs/g sorbent). The latter is approximately double as compared with the copolymer sorbents with the most favorable sorption properties (*i.e.* HDI-1). Since K_{eq} is model dependent, the K_{eq} from the Langmuir isotherm model can not be directly compared to the values obtained from the Sips model for the copolymer sorbents. Valid comparison of sorbent affinity must account for differences in values of n_s which deviate from unity. However, based on the trend for the GAC isotherm, one may expect a greater binding affinity with NAs due to the observed sharp rise of Q_e vs. C_e (*cf.* Figure 8.2d), as compared with the copolymer sorbents. The relative large sorption capacity is attributed to the greater surface area (~10^3 m^2/g) of GAC as compared with the lower surface area (~10^2 m^2/g) of the copolymer materials.[34]

8.4.3.5 Data Simulation using the Sips Isotherm Model

A detailed analysis of the sorption results using Sips model can be obtained through simulation of experimental results using assigned values of the "best-fit" parameters (*i.e.* K_s, n_s, and Q_m). The Sips model has up to three adjustable parameters but

for simplicity purposes, an isotherm quotient ratio of Q_e to Q_m (*cf*. Equation 8.4) are plotted against C_e. In this case, two parameters are varied, K_{eq} (K_s = Average Molecular Weight of NAs; L/mol) and n_s.[45] The value of K_{eq} derived from the Sips isotherm is model dependent and can not be directly compared to K values from the Langmuir or Freundlich models. The ratio of sorption parameters (Q_e/Q_m) is normalized across the data sets in Figure 8.3 to enable comparison of different results according to the adjustable parameters. The range of C_e values was based on the experimental ranges described above. Figure 8.4a-c illustrate the simulated curves for various K_{eq} and n_s for (*e.g.*, $K_{eq} = 3.0x10^2\ M^{-1}$, $3.0x10^3\ M^{-1}$, and $3.0x10^4\ M^{-1}$), respectively. The range of K_{eq} was based on previous work since $K_{eq} \approx 10^4$ described the approximate formation constant of complexes formed between native β-CD and NAs in aqueous solution.[30] For a particular value of K_{eq}, the simulations show that the isotherm displays greater curvature and deviation from a typical homogeneous ($n_s = 1$) sorbent. A sorbate/sorbent system with relatively high values of K_{eq} ($\sim 10^4$) and sorbent surface heterogeneity displays a sharp rise in Q_e before leveling off at higher values of C_e. However, the slope decreases as K_{eq} decreases for a given sorbent. On the other hand, a sorbate/sorbent system with a low K_{eq} ($\sim 10^2$) displays a linear trend when $n_s = 1$ (*i.e*. homogenous) whereas slight curvature is observed for heterogeneous ($n \neq 1$) sorbents. It is worth to note that, an increase in the concentration of NAs in bulk solution (higher C_e) will saturate the sorption sites even when the value of K_{eq} is low (less favorable sorption). The apparent lack of saturation of binding for the range of C_e values investigated in Figure 8.2 may be related to the relative magnitude of K_{eq}. In accordance with Le Chatelier's principle, the eventual saturation of binding sites is observed at relatively high values of C_e (~1400 mg/L) for n=1.5.

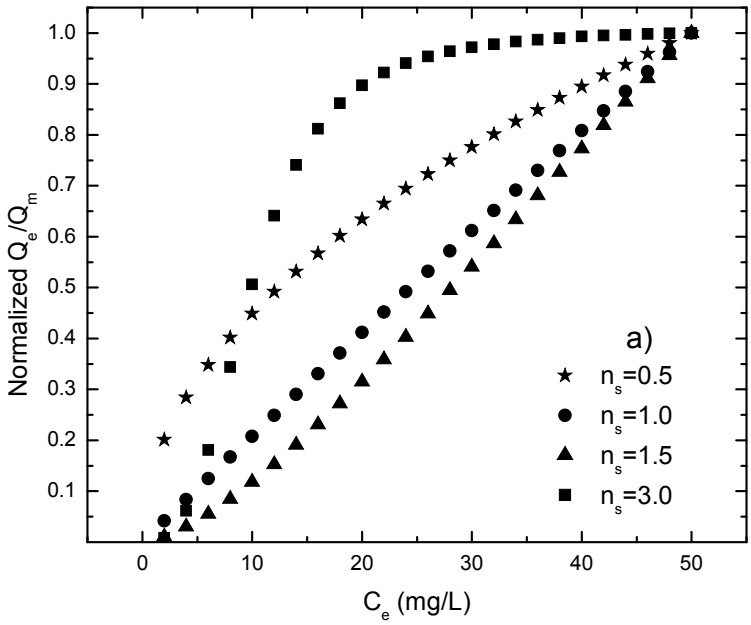
Normalized Q_e/Q_m
C_e (mg/L)
a)
n_s=0.5
n_s=1.0
n_s=1.5
n_s=3.0

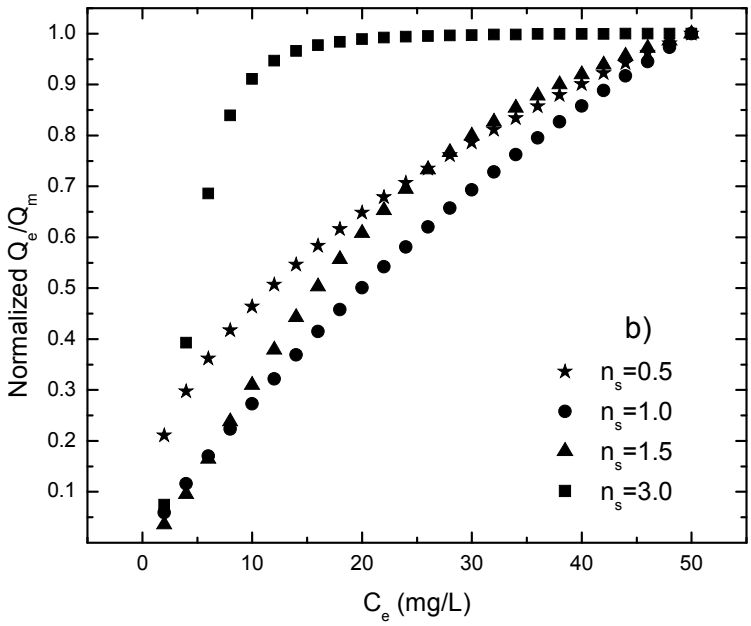
Normalized Q_e/Q_m
C_e (mg/L)
b)
n_s=0.5
n_s=1.0
n_s=1.5
n_s=3.0

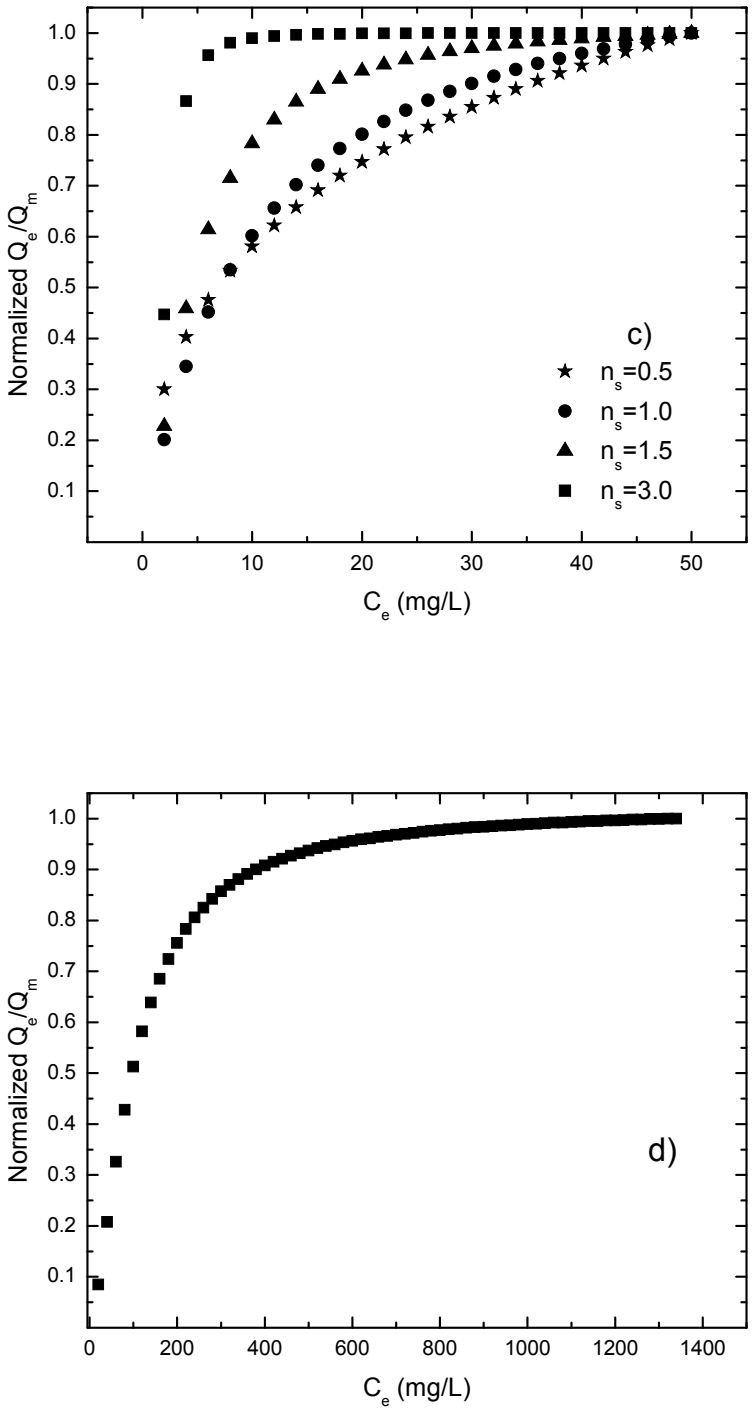

Figure 8.4. (a-c) Simulated sorption isotherms from Sips model using Equation 8.4 at different K_{eq} values; a) $3.0x10^2$ M^{-1}, b) $3.0x10^3$ M^{-1}, c) $3.0x10^4$ M^{-1}, and d) simulated sorption isotherm for K_{eq}=$3.0x10^2$ M^{-1} and n_s=1.5 from (a) over a range of C_e values, respectively.

8.4.3.6 Sorption Mechanism

Copolymer sorbent that contain β-CD have at least two potential sorption sites (*cf*. Scheme 1.2 in Chapter 1). The inclusion binding sites are located within the interior of the β-CD macrocycle and the non-inclusion sites are the interstitial regions adjacent to the linker domains of the copolymer. The linker monomers examined in this study vary according to their physicochemical properties (aliphatic *vs.* aromatic) and molecular size. The aliphatic-based linkers (HDI and CDI), show a more dramatic decrease in binding affinity and sorption capacity as the linker mole ratio is increased (*i.e*. decreasing CD content). In our previous work,[46] it was concluded that the relative accessibility of the inclusion binding sites of β-CD tend to decrease as the cross linker mole ratio increases because of steric effects. This is exemplified by the reduction in sorption capacity observed for HDI-3, CDI-2 and CDI-3 (*cf*. Table 2 in reference 46) where the relative accessibility of the β-CD interior was 4.78, 2.03 and 1.04%, respectively. Therefore, it is inferred that the β-CD inclusion sites plays a major role in the sorption of NAs from aqueous solution. Parallel trends are observed for the copolymer materials containing aromatic linkers because of their greater sorption capacity despite their lower binding affinity (i.e. K_{eq}). The reduced accessibility of β-CD is less pronounced for sterically bulky linker molecules (*e.g*., NDI, MDI, and CDI) as compared with smaller linkers (*e.g*., HDI , PDI), as outlined in Scheme 3 in a previous report.[46] The importance of host-guest interactions between β-CD and carboxylate anions are well documented, and the results reported herein support the conclusion that the intracavity sites of β-CD are the primary adsorption site for such copolymer sorbent materials.[30]

Copolymers containing aromatic crosslinker units display greater binding affinity toward NAs. For example, CDI (aliphatic) and MDI (aromatic) are of similar size, but the value of K_{eq} for MDI-X is greater than that of CDI-X sorbents despite the lower sorption capacity for the case of X=1. In addition, K_{eq} is further attenuated by the size and conformational motility of the linker monomer since the value of K_{eq} adopts the following order: NDI > MDI > PDI, for copolymers at the 1:1 crosslinking ratio. Evidence that the interstitial regions (cf. Scheme 1.2 in Chapter 1) may play a role in the binding of NAs is the variation of K_{eq} for different CD:linker mole ratios. In the case of MDI- and PDI-based copolymers, the value of K_{eq} for MDI-X decreases as X increases. In the case of PDI-X, K_{eq} decreases as follows; PDI-3 > PDI-1 > PDI-2. Moreover, the aliphatic-based copolymer (HDI-X and CDI-X) materials have greater sorption capacity than aromatic (*e.g.*, MDI, PDI and NDI) linkers. The latter indicates that the linker rigidity and electron density properties of the linker may contribute to the observed sorption affinity of the copolymer materials. The aforementioned observations indicate that the physicochemical characteristics of the interstitial regions play a secondary role in the sorption affinity of NAs (β-CD plays a primary role). Favorable dispersion interactions with NAs and the Gibbs free energy of solution are lowered upon sorption by the copolymers from aqueous solution. Favorable contributions to the adsorption enthalpy with NAs are anticipated for linker monomers with increasing size since the molecular polarizability (α) increases. This is particularly true in the case where accessibility of NAs is low where sorption occurs at the site of the linker domains. In cases where accessibility of inclusion sites of β-CD is relatively high, the effect of the linker polarizability is of secondary importance. Table 8.2 lists values of α for each of the

various linker monomers, the inclusion site accessibility[46] values, and relative binding affinity (K_{eq}; *cf*. Equation 8.4). According to Table 8.4, the values of α for aliphatic and aromatic monomers increase according to the increasing molecular weight; however, the magnitude of α values are similar for HDI and PDI or MDI and CDI. In general, the comparable binding affinity occurs irrespective of the change in values of α and these results provide further support that the interactions between NAs and the copolymer linker domains are secondary in nature. Inclusion binding of NAs with β-CD is the primary sorption site of the copolymer and it is highly dependent on the relative site accessibility, as described previously.[46] However, the monomer units affect the sorption accessibility at the β-CD inclusion sites according to monomer size and mole ratio because of steric effects. The secondary role of linker monomers in sorption with NAs is not expected to be uniform and some degree of molecular selectivity is expected for mixtures of NAs.

Table 8.2. Polarizability for linker monomers, K_{eq} and accessible percentage β-CD of 1:1 copolymer materials

Linker Monomer	Polarizability[a], α (au)^3	K_{eq}[b] (M^{-1}) x 10^4 for 1:1 copolymer	Accessible β-CD for 1:1 copolymer (%)[c]
HDI	87.1	3.50	100
CDI	149	0.436	33.2
MDI	151	2.17	38.0
PDI	87.9	1.49	68.3
NDI	126	3.30	77.6

[a] Calculated using Spartan `08 V1.1.1. The unit is atomic unit (au).
[b] Keq obtained from the Sips isotherm (equation 4) where $K_{eq}= K_{s.}$
c Values obtained from Table 2 of reference 46.

8.4.3.7 Molecular Selective Sorption

In order to further interpret the ESI-MS for the occurrence of sorption selectivity between NAs with either GAC or CD copolymer sorbents, respectively, the mass spectral data are plotted using a 3D-coordinate system of the percent abundance of unbound residual NAs according to the carbon number (n) and Z-family, as described in Figure 1.1 in Chapter 1. Previously we reported such 3D representations to evaluate the differences in sorption efficiency and NAs component selectivity with cyclodextrins.[31] A comparison of stock solutions of NAs (*cf.* Figure 8.5a) and the distribution of individual NAs components after sorption (Figure 8.5b-f) illustrates differences in the uptake selectivity. The abundance and distribution of residual NAs occur according to their size and degree of unsaturation, as compared with stock solutions of NAs, for a given copolymer sorbent system. In comparison to Figure 8.5a, the 3D plots in Figure 8.5b-f illustrate marked changes in the distribution of NAs before and after sorption. The selectivity results for the copolymer materials indicate that the degree of sorption is variable and the molecular discrimination between NAs according to size and Z-family are observed. According to the range of the C_e values of NAs remaining in solution after sorption, copolymers such as HDI-1 (Figure 8.5a) and CDI-1 (Figure 8.5b) have the greatest sorption amongst the copolymers investigated. Significant differences in molecular selectivity according to the size and hydrogen deficiency of NAs are evident. A comparison of MDI-1, PDI-1, and NDI-1 indicates that these copolymers affect the distribution of NAs components in a similar manner. This may be related to the comparable inclusion accessibility of the β-CD that contains aromatic linkers. According to previous work,[46] HDI-1 and CDI-1 have relatively high inclusion accessibility of the β-CD sites as observed in Figure 8.5b-c,

respectively. The decreased selectivity for the copolymer materials with aromatic linkers is observed in Figure 8.5d-f and is consistent with the reduced accessibility of the β-CD sites. The steric limitations to the β-CD inclusion sites attenuate the molecular selectivity in observed copolymers such as those containing aromatic linkers within the polymer structure. Overall, the results in Figure 8.5 illustrate that there is variable molecular selectivity toward NAs according to the nature of linker molecule and cross linking density in the copolymer material.

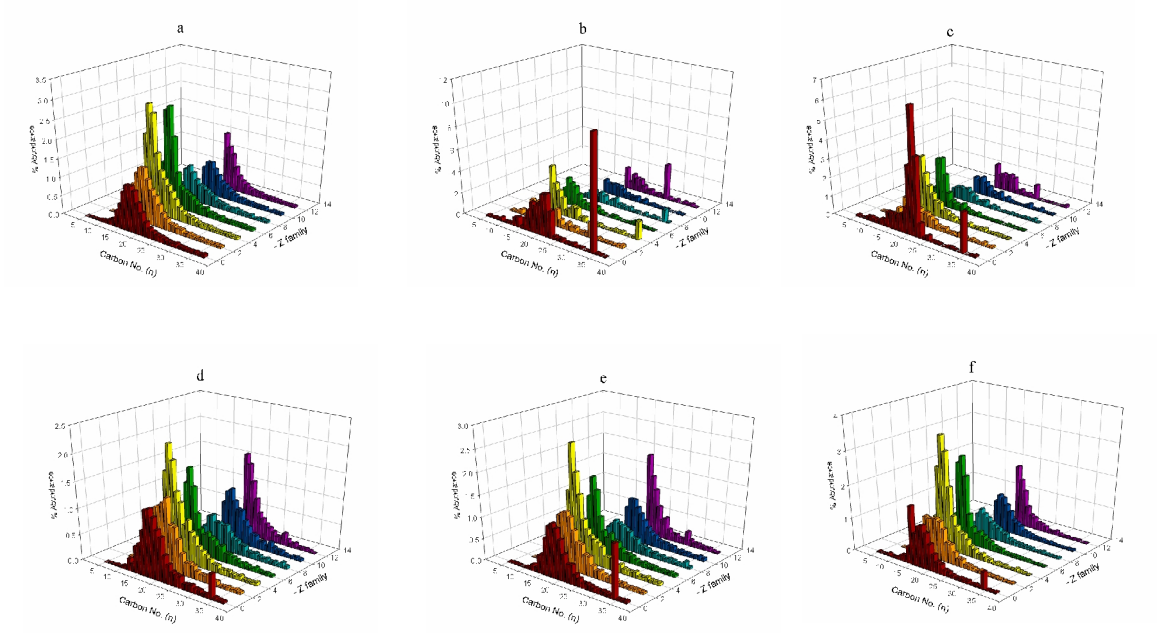

Figure 8.5a-f. 3D plots of; a) NAs stock solution before sorption, b) HDI-1, c) CDI-1, d) MDI-1, e) PDI-1 and f) NDI-1. The copolymer material mass ~ 20mg, C_o is 100 mg/L, pH 9.00 and 298 K

8.5 Conclusions

Copolymer sorbents containing β-CD display favourable sequestration of NAs from aqueous solution at alkaline conditions (pH = 9) that are considered similar to industrial OSPW environments. The sorption capacity and binding affinity varied for

each of the different copolymer materials according to the nature of the linker monomer and the synthetic mole ratios. Generally, copolymers crosslinked with aromatic monomers have higher binding affinity and reduced sorption capacity toward NAs while those with aliphatic linkers display opposite behaviour. The β-CD macrocycle in the copolymer sorbent plays a major role in the binding affinity of NAs while the linker monomer plays a secondary role in sorption of NAs in the absence of steric effects. Aromatic linker molecules enhance binding affinity toward NAs whereas aliphatic linkers increase the sorption capacity by increasing accessibility to the β-CD inclusion sites. The sorption properties of copolymers with NAs depend on the overall design of the sorbent in terms of the relative accessibility of the β-CD inclusion sites according to the linker type and crosslinking ratios. Molecular recognition of different components of NAs is observed according amongst the various copolymers studied. Further work on the development of copolymer sorbents with improved sorption capacity and selectivity is underway. Synthetically engineered copolymer materials with variable pore structure and physicochemical properties may provide sorbents with increased binding affinity, sorption capacity, and tunable molecular selectivity toward different NAs components found in OSPW.

8.6 Acknowledgements

Financial assistance was provided by the Natural Sciences and Engineering Research Council and the Program of Energy Research and Development. M.H.M acknowledges the University of Saskatchewan for the award of a Graduate Teaching Fellowship and Environment Canada for the Science Horizons Program award.

8.7 References

1. Nikiforuk, A. *Tar Sands: Dirty Oil And The Future Of A Continent*; Greystone Books: Vancouver, BC, 2008.
2. Clemente, J. S.; Fedorak, P. M. *Chemosphere* **2005**, *60*, 585-600.
3. Quagraine, E. K.; Headley, J. V.; Peterson, H. G. *J. Environ. Sci. Health, Part A: Toxic/Hazard. Subst. Environ. Eng.* **2005**, *40*, 671-684.
4. Headley, J. V.; Crosley, B.; Conly, F. M.; Quagraine, E. K. *J. Environ. Sci. Health, Part A: Toxic/Hazard. Subst. Environ. Eng.* **2005**, *40*, 1 - 27.
5. Dzidic, I.; Somerville, A. C.; Raia, J. C.; Hart, H. V. *Anal. Chem.* **1988**, *60*, 1318-1323.
6. Fan, T. P. *Energ. Fuel.* **1991**, *5*, 371-375.
7. Wong, D. C. L.; van Compernolle, R.; Nowlin, J. G.; O'Neal, D. L.; Johnson, G. M. *Chemosphere* **1996**, *32*, 1669-1679.
8. St. John, W. P.; Rughani, J.; Green, S. A.; McGinnis, G. D. *J. Chromatogr., A* **1998**, *807*, 241-251.
9. Hsu, C. S.; Dechert, G. J.; Robbins, W. K.; Fukuda, E. K. *Energ. Fuel.* **1999**, *14*, 217-223.
10. Herman, D. C.; Fedorak, P. M.; Costerton, J. W. *Can. J. Microbiol.* **1993**, *39*, 576-580.
11. Headley, J. V.; Peru, K. M.; Barrow, M. P. *Mass Spectrom. Rev.* **2009**, *28*, 121-134.
12. Headley, J. V.; McMartin, D. W. *J. Environ. Sci. Health, Part A: Toxic/Hazard. Subst. Environ. Eng.* **2004**, *A39*, 1989-2010.
13. Turnbull, A.; Slavcheva, E.; Shone, B. *Corrosion* **1998**, *54*, 922-930.
14. Slavcheva, E.; Shone, B.; Turnbull, A. *Brit. Corros. J.* **1999**, *34*, 125-131.
15. Gaikar, V. G.; Maiti, D. *React. Funct. Polym.* **1996**, *31*, 155-164.
16. Wong, D. C. L.; van Compernolle, R.; Nowlin, J. G.; O'Neal, D. L.; Johnson, G. M. *Chemosphere* **1996**, *32*, 1669-1679.
17. Rezaei Gomari, K. A.; Denoyel, R.; Hamouda, A. A. *J. Colloid Interface Sci.* **2006**, *297*, 470-479.

18. Zou, L.; Han, B.; Yan, H.; Kasperski, K. L.; Xu, Y.; Hepler, L. G. *J. Colloid Interface Sci.* **1997**, *190*, 472-475.
19. Janfada, A.; Headley, J. V.; Peru, K. M.; Barbour, S. L. *J. Environ. Sci. Health, Part A: Toxic/Hazard. Subst. Environ. Eng.* **2006**, *41*, 985-997.
20. Peng, J.; Headley, J. V.; Barbour, S. L. *Can. Geotech. J.* **2002**, *39*, 1419-1426.
21. Frank, R. A.; Kavanagh, R.; Burnison, B. K.; Headley, J. V.; Peru, K. M.; Der Kraak, G. V.; Solomon, K. R. *Chemosphere* **2006**, *64*, 1346-1352.
22. Saab, J.; Mokbel, I.; Razzouk, A. C.; Ainous, N.; Zydowicz, N.; Jose, J. *Energ. Fuel.* **2005**, *19*, 525-531.
23. Peng, H.; Volchek, K.; MacKinnon, M.; Wong, W. P.; Brown, C. E. *Desalination* **2004**, *170*, 137-150.
24. Deriszadeh, A.; Harding, T. G.; Husein, M. M. *J. Membr. Sci.* **2009**, *326*, 161-167.
25. *Cyclodextrin Chemistry*; Bender, M. L.; Komiyama, M., Eds.; Springer-Verlag: Berlin, Germany, 1978.
26. Buvari, A. *J. Inclusion Phenom.* **1983**, *1*, 151-157.
27. Eftink, M. R.; Andy, M. L.; Bystrom, K.; Perlmutter, H. D.; Kristol, D. S. *J. Am. Chem. Soc.* **1989**, *111*, 6765-6772.
28. Gadre, A.; Rüdiger, V.; Schneider, H.-J.; Connors, K. A. *J. Pharm. Sci.* **1997**, *86*, 236-243.
29. Mohamed, M. H.; Wilson, L. D.; Headley, J. V.; Peru, K. M. *Can. J. Chem.* **2009**, *87*, 1747-1756.
30. Mohamed, M. H.; Wilson, L. D.; Headley, J. V.; Peru, K. M. *Rapid Commun. Mass Spectrom.* **2009**, *23*, 3703-3712.
31. Gadre, A.; Connors, K. A. *J. Pharm. Sci.* **1997**, *86*, 1210-1214.
32. Wenz, G. *Angew. Chem. Int. Ed. Engl* **1994**, *33*, 803-822.
33. Harada, A.; Hashidzume, A.; Takashima, Y. *Cyclodextrin-based supramolecular polymers*; Springer, 2006; Vol. 201.
34. Mohamed, M. H.; Wilson, L. D.; Headley, J. V.; Peru, K. M. *Process Saf. Environ. Prot.* **2008**, *86*, 237-243.
35. Ma, M.; Li, D. *Chem. Mater.* **1999**, *11*, 872-874.

36. He, B.; Zhao, X. *React. Polym.* **1992**, *18*, 229-235.
37. Crini, G.; Bertini, S.; Torri, G.; Naggi, A.; Sforzini, D.; Vecchi, C.; Janus, L.; Lekchiri, Y.; Morcellet, M. *J. Appl. Polym. Sci.* **1998**, *68*, 1973-1978.
38. Brient, J. A.; Wessner, P. J.; Doly, M. N. In *Kirk-Othmer Encyclopedia of Chemical Technology*; 4th ed.; Kroschwitz, J. I., Ed.; John Wiley & Sons, Inc.: New York, NY, 1995; Vol. 16, p 1017-1029.
39. Kanicky, J. R.; Poniatowski, A. F.; Mehta, N. R.; Shah, D. O. *Langmuir* **1999**, *16*, 172-177.
40. Langmuir, I. *J. Am. Chem. Soc.* **1918**, *40*, 1361-1402.
41. Freundlich, H. M. F. *J. Phys. Chem.* **1906**, *57A*, 385-470.
42. Sips, R. *J. Chem. Phys.* **1948**, *16*, 490-495.
43. Liu, C.; Lambert, J. B.; Fu, L. *J. Org. Chem.* **2004**, *69*, 2213-2216.
44. Gerbaud, G.; Hediger, S.; Gadelle, A.; Bardet, M. *Carbohydr. Polym.* **2008**, 73, 64-73.
45. Yu, L.; Hui, X.; Joo-Hwa, T. *J. Environ. Eng.* **2005**, *131*, 1466-1468.
46. Mohamed, M. H.; Wilson, L. D.; Headley, J. V. *Carbohydr. Polym.* **2010**, *80*, 186-196.

CHAPTER 9

PUBLICATION 8

Description

The following is a verbatim copy of an article that was published in November of 2010 in the Journal of Colloid and Interface Science (*J. Colloid Interface Sci.*: **2011**, *356(1)*, 217-226). This paper describes the sorption mechanism of the copolymers using different adsorbents.

Authors' Contribution

I conducted all the experimental work except for the ESI-MS which was done by Mr. Kerry Peru. This work was supervised by Dr. Wilson and Dr. Headley. I wrote the first draft of the manuscript with extensive editing by each supervisor prior to submission for publication. Written permission was obtained from all contributing authors to include this material in this thesis.

Relation of Chapter 8 (Publication 7) to the Overall Objectives of this Project

This chapter exploits the dye sorption studies for PNP and phth and NAs conducted in Chapter 2, 3, and 8 respectively. It outlines the generalized sorption mechanism of the copolymers using adsorbents of different size and at different pH conditions. It illustrates the role of the sorption sites (β-CD cavity and the linker framework domains) in sorption and the applicapibility of the copolymers in different pH conditions.

Graphical Abstract

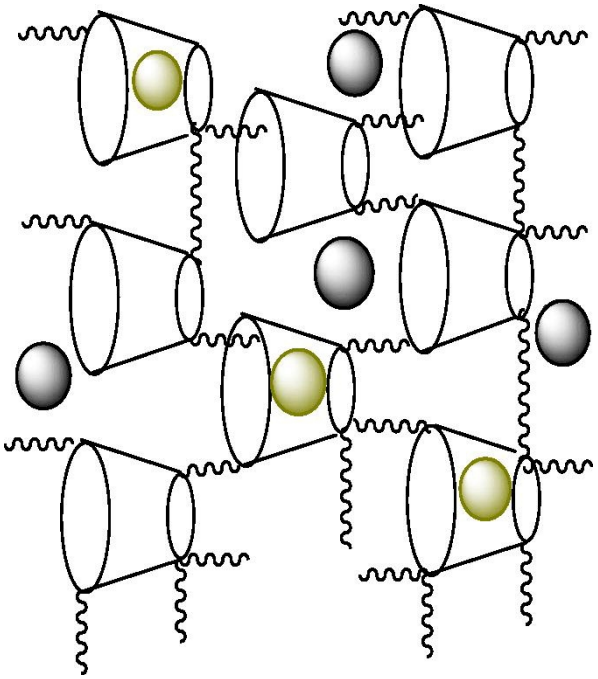

Research Highlights

β-cyclodextrin (β-CD) based polyurethane sorbents exhibit tunable sorption properties according to the co-monomer composition. Inclusion and non-inclusion binding observed for p-nitrophenol (PNP), phenolphthalein (phth) and naphthenates (NAs). Tunable sorption capacity and binding affinity are observed according to the nature of the adsorbate, copolymer sorbent, and experimental (i.e. concentration and pH) conditions.

9. Investigation of the Sorption Properties of β-Cyclodextrin-based Polyurethanes with Phenolic Dyes and Naphthenates

Mohamed H. Mohamed,[§] Lee D. Wilson,[§] John V. Headley,[¥] Kerr M. Peru[¥]*

[§]Department of Chemistry, University of Saskatchewan, 110 Science Place, Saskatoon, Saskatchewan, S7N 5C9

[¥]Water Science and Technology Directorate, 11 Innovation Boulevard, Saskatoon, Saskatchewan, S7N 3H5

*Corresponding Author

Received 26 August 2010

9.1 Abstract

The sorption of p-nitrophenol (PNP), phenolphthalein (phth) and naphthenates (NAs) with β-cyclodextrin (β-CD) based polyurethane sorbents from aqueous solutions are reported. The copolymer sorbents were synthesized at various β-CD/diisocyanate monomer mole ratios (e.g., 1:1, 1:2, and 1:3) with diisocyanates of variable molecular size and hydrogen deficiency. The copolymer sorbents were characterized in the solid state using ^{13}C CP-MAS NMR spectroscopy, IR spectroscopy and elemental (C,H,N) analysis. The equilibrium sorption properties of the copolymer sorbents in aqueous solution were characterized using isotherm models at pH 4.6 and 9.0 for PNP, pH 9.0 for naphthenates and pH 10.5 for phth. UV-Vis spectroscopy was used to monitor the unbound fraction of the phenolic dyes in the aqueous phase, whereas, electrospray

ionization mass spectrometry was used to monitor the unbound fraction of naphthenates. The sorption results of the copolymer sorbents were compared with a commercially available carbonaceous standard; granular activated carbon (GAC). The sorption properties and capacities of the copolymer sorbents (Q_m) were estimated using the Sips isotherm. The sorption capacity for GAC was 2.15 mmol PNP/g, 0.0698 mmol phth/g, and 142 mg NAs/g, respectively, whereas the polymeric materials ranged from 0.471-1.60 mmol/g (PNP), 0.114-0.937 mmol/g (phth), and 0-75.5 mg/g (naphthenates), respectively, for the experimental conditions investigated. The observed differences in the sorption properties were attributed to the accessible surface areas and pore structure characteristics of the copolymer sorbents. The binding constant, K_{eq}, for copolymer materials for each sorbate is of similar magnitude to the binding affinity observed for native β-CD. PNP showed significant binding onto the copolymer framework containing diisocyanate domains, whereas, negligible sorption to the sites was observed for phth and naphthenates. The β-CD inclusion sites in the copolymer framework are concluded to be the main sorption site for phth and naphthenates through the formation of well-defined inclusion complexes.

9.2 Introduction

Supramolecular porous materials with remarkable sorption properties are afforded through the incorporation of macrocyclic porogen monomers, such as β-cyclodextrin, in the copolymer framework.[1-10] Examples of such novel copolymer materials for sorption-based applications range from recognition of biomolecules to the controlled release of pharmaceuticals.[11-12] Ongoing efforts are directed towards the development of improved

solid phase extraction (SPE) materials with enhanced sorption and molecular recognition properties.[13-16]

Cyclodextrin-based copolymer materials have a wide range of industrial applications because of their unique sorption properties.[17] The sustained interest in the research and application of cyclodextrin-based copolymer materials is attributed, in part, to the ability of such copolymer materials to sequester guest molecules in the gas phase and condensed states.[3,6,18] Technological applications that rely on the formation of inclusion complexes are wide ranging and include for example; chemical separations, catalysis, molecular sieves, food processing, pharmaceutical excipients and cosmetics.[1,4,17,19-24] In particular, the ability to maintain the inclusion properties of the cyclodextrin moiety[25] in such copolymers is of primary importance in materials research and design.

Previous reports indicate that polymeric β-CD materials[6,26-31] may serve as novel sorbents for the inclusion of organic molecules from aqueous solutions and may possess binding affinity comparable to native β-CD.[31-33] A recent report[31] concluded that the systematic variation of the copolymer structure enables tuning of the inclusion site accessibility; a property that is critical in cases where the copolymer sorption and molecular recognition involves the formation of CD/guest inclusion complexes. CD-based copolymer materials with variable cross link density and linker size were shown to have tunable inclusion site accessibility according to the steric effect of the primary and secondary hydroxyl groups in the annular region of β-CD.[31] The degree of substitution at the primary and/or secondary hydroxyl sites affects the physicochemical properties of the copolymers, i.e., intrinsic and framework pore structure. Key factors that affect the

sorption of adsorbates in copolymer sorbent materials are: *i*) linker composition and their physicochemical properties, *ii*) inclusion site accessibility, *iii*) physicochemical properties of the adsorbate, and *iv*) pore structure properties of the adsorbent.[29,31]

In this study, we report the sorption of a series of novel β-CD-based polyurethane copolymers with phenolic dyes and naphthenic acids (NAs), respectively, in aqueous solutions. The phenolic dyes studied herein are p-nitrophenol (PNP) and phenolphthalein (phth) which have been used previously for the estimation of surface area of sorbent materials[34-35] and molecular recognition by β-CD domains[31,36-38], respectively. NAs have been extensively described in previous work.[29,39-40] The copolymer materials are comprised of β-CD and diisocyanate co-monomers with variable aliphatic and aromatic molecular structure features according to their relative molecular size and conformational flexibility (*cf*. Figure 1.2 in Chapter 1). The results of this study are intended to provide an improved understanding of the relative role of the linker and macrocycle domains of the copolymer in the sorption process. This study is anticipated to contribute to the further development of improved SPE materials with enhanced sorption and molecular recognition properties; owing to the presence of a macrocyclic porogen (*i.e*. β-CD).

9.3 Experimental

9.3.1 Materials

β-CD, Phenolphthalein (phth), granular activated carbon (GAC); (Norit Rox 0.8), potassium bromide (FTIR Grade), sodium hydroxide, sodium hydrogen carbonate, was purchased from VWR. 1,6-hexamethylene diisocyanate (HDI), 4,4'-dicyclohexylmethane

diisocyanate (CDI), 4,4'-diphenylmethane diisocyanate (MDI), 1,4-phenylene diisocyanate (PDI), 1,5-naphthalene diisocyanate (NDI), dimethyl acetamide (DMA), cellobiose (CL), p-nitrophenol (PNP), ethanol, anhydrous ethyl ether, ammonium hydroxide, 4 Å (8-12 mesh) molecular sieves, were purchased from Sigma Aldrich, except for NDI, which was obtained from TCI America. Potassium phosphate monobasic and D(+)-glucose monohydrate (GL) were purchased from EMD Chemicals. Athabasca oil sands process water (OSPW) derived NAs were obtained according to an established protocol.[41]

9.3.2 Methods

9.3.2.1 Synthesis and Characterization of Supramolecular Sorbents

CD-based polyurethane materials were synthesized as described previously. [29,31] The copolymer materials were characterized using solid state ^{13}C CP-MAS NMR spectroscopy, FT-IR, TGA, and elemental analyses (CHN), as described previously[31]. The nomenclature of the copolymers is described in accordance to the linker type, the synthetic mole ratio of the β-CD macrocycle and the diisocyanate linker. For example, in the case of 1:3 β-CD:HDI, the copolymer designation will be referred to as HDI-3. The molar quantity of β-CD is assumed to be unity in all cases.

9.3.2.2 Sorption of Phenolic Dyes (PNP and phth)

Various concentrations of PNP (0.1-20 mM) were prepared at pH 4.60 in 0.01 M potassium phosphate monobasic buffer solution and pH 9.00 in 0.01 M $NaHCO_3$ buffer, respectively. Phth was prepared at a fixed concentration (0.03 mM) in 0.01 M $NaHCO_3$ buffer. The molar absorptivity of phenolic dyes were estimated as 10, 026 L mol^{-1} cm^{-1} (pH 4.60) and 17, 596 L mol^{-1} cm^{-1} (pH 9.00) for PNP, and 28, 308 (pH 10.50) for phth,

respectively. The experimental values are in good agreement with previous reports.[40,42-47] To a 10 mL glass bottle with teflon cap liners, constant amounts of solid polymer (~ 20 mg) were added to a fixed volume (7.00 mL) of an aqueous PNP solution. In the case of phth sorption, variable masses of sorbent ranging from 1-20 mg were added to a fixed volume (7 mL) of 0.03 mM phth. The vials were further sealed with parafilm between the cap and glass bottle and were placed at room temperature in a horizontal shaker to equilibrate for 24 hrs. The equilibrium concentrations of PNP and phth were determined using a double beam spectrophotometer (Varian CARY 100) at room temperature (295 ± 0.5 K) by monitoring the absorbance changes at λ_{max} = 317 nm (pH 4.60) and λ_{max} = 400 nm (pH 9.00) for PNP, and , λ_{max} = 552 nm (pH 10.50) for phth, respectively.

9.3.2.3 Sorption of Naphthenic Acids

Various concentrations of NAs were prepared at pH 9.00 from a 6990 mg/L aqueous stock solution extracted from Athabasca OSPW (pH 7.60). The pH of the stock solution was raised to 9.00 using 10^{-3} M ammonium hydroxide. OSPW have a pH of ~ 8, therefore, the NAs exist predominantly in their ionized forms since the acid dissociation constant ranges between 10^{-5} to 10^{-6} M^{-1}. [48-50] The sorption experiments for NAs were performed at pH 9.00 to ensure adequate solubility [pH > pK_a (NAs)] and to understand the uptake of NAs at these industrially relevant conditions. To a 10 mL glass bottle with teflon cap liners, constant amounts of solid polymer (~ 20 mg) were added to a fixed volume (7.00 mL) containing NAs at various concentrations ranging from ~ 10-100 mg/L. The concentration of NAs can be found up to ~110 mg/L in OSPW therefore the conditions used herein were chosen such that the upper experimental concentration reflect that of the OSPW concentrations[51-52]. The vials were further sealed with parafilm,

as described above for the sorption of phenolic dyes. The equilibrium concentrations of NAs were determined using negative ion electrospray ionization mass spectrometry (ESI-MS). The instrumental conditions for the analyses of NAs have been described previously.[39]

9.3.2.4 Data Analysis

The equilibrium sorption isotherms represented as plots of the amount of NAs adsorbed per mass of copolymer (Q_e) versus the unbound equilibrium concentration of NAs in the aqueous solution (C_e). Equation 9.1 defines how Q_e is obtained where C_o is the initial concentration (mmol/L or mg/L) of NAs, V is volume of solution (L), and m is the mass of sorbent (g).

$$Q_e = \frac{(C_o - C_e) \times V}{m} \qquad \text{Equation 9.1}$$

The Langmuir, Freundlich and Sips isotherm models were used to analyze the experimental equilibrium sorption data.[53-55] The Langmuir model assumes that sorption is homogeneous within the monolayer; whereas, the Freundlich and Sips models provide an assessment of the heterogeneity of the sorption process. The Sips isotherm model is preferred because it represents a generalized isotherm model which can be interpreted in the context of monolayer or multi-layer adsorption isotherms, in accordance with the adjustable parameters (n_s; *cf.* Equation 9.4). The three isotherm models; Langmuir, Freundlich and Sips are shown in Equations 9.2-9.4, respectively. The binding affinity between the NAs and the sorbent can be related to the equilibrium constants (K_i) appearing in Equations 9.2-9.4. The criterion of the "best fit" for the three models is determined by the correlation coefficient (R^2) and sum of square of errors (SSE). Values of R^2 near unity and values of SSE that approach zero, represent the criteria for the "best

fit". The experimental data for each isotherm was fitted by minimization of the SSE, described by Equation 9.5. $Q_{e,i}$ is the experimental value, $Q_{f,i}$ is the simulated value according to the chosen isotherm model (*cf.* Equations 9.2-9.4), and N is the number of experimentally obtained data points.

$$Q_e = \frac{K_L Q_m C_e}{1 + K_L C_e} \qquad \text{Equation 9.2}$$

$$Q_e = K_F C_e^{1/n_f} \qquad \text{Equation 9.3}$$

$$Q_e = \frac{Q_m (K_s C_e)^{n_s}}{1 + (K_s C_e)^{n_s}} \qquad \text{Equation 9.4}$$

$$SSE = \sum \sqrt{\frac{\left(Q_{e,i} - Q_{f,i}\right)^2}{N}} \qquad \text{Equation 9.5}$$

9.4 Results and Discussion

9.4.1 Equilibrium Isotherm Models

Sorption isotherms provide a detailed understanding of the thermodynamics of sorption in a sorbent/sorbate system and may be represented as a plot of Q_e versus C_e at constant temperature. The interpretation of the experimental results is dependent on the choice of a suitable isotherm model to obtain an accurate physical interpretation of the concentration dependence of Q_e and for the reliable calculation of the corresponding sorption parameters.

The Langmuir, Freundlich and Sips models were used to evaluate experimental sorption isotherms of GAC and copolymer materials.[53-55] The Langmuir isotherm model assumes that sorption occurs onto a homogeneous monolayer and the sorbate does not

affect adsorption of neighboring sites. The Freundlich isotherm assumes a heterogeneous sorbent surface with non-uniform distribution of heats of adsorption. The parameter n_f in Equation 9.3 is related to the intensity of adsorption. In contrast, the Sips isotherm (*cf.* Equation 9.4) assumes a distribution of adsorption energies onto the sorbent surface and may be considered a composite model of the Langmuir and Freundlich isotherms. The use of eq 4 for n_s = 1 resembles the Langmuir isotherm (*cf.* Equation 9.2) and when $(K_s \times C_e)^{n_s}$ is <<<1 describes the Freundlich isotherm (*cf.* Equation 9.3). The parameter n_s (*cf.* Equation 9.4) is an indicator of the heterogeneity of the sorbent since values of n_s that deviate from unity infer a highly heterogeneous sorbent, whereas, a value of unity confers a homogenous sorbent (*cf.* Equation 9.2).

9.4.2 Binding Constant of β-CD/Sorbate

The 1:1 equilibrium binding constant, K_{eq}(β-CD/PNP between native β-CD and PNP was determined experimentally at pH 4.60 using the Benesi-Hildebrand plot where the K_{eq} was determined to be 197 M^{-1}, and is in agreement with previous estimates.[56-58] At higher pH, Eftink and Harrison,[56] found that both α- and β-CD had a 10-fold higher binding affinity towards the deprotonated form of PNP (high pH) as compared to that of the protonated form. They argued that the improved binding is due to the added involvement of London dispersion interactions between the CD cavity and the delocalized charge of the anionic guest. Recently, this observation was observed in a CD bonded silica sorbent where the percentage recovery of PNP increased as the pH increased.[59] Also, Bergeron *et al*.[60] illustrated the differential binding affinity between β-CD and carboxylic acids at different pH. The values of K_{eq} for the 1:1 β-CD/phth (2.66×10^4 M^{-1}) and β-CD/naphthenates (1.27×10^4 M^{-1}) at pH 10.5 were determined

previously with UV-Vis spectrophotometryr.[40] The enhanced binding affinity observed for NAs and phth with β-CD is largely attributed to favourable hydrophobic effects and ion-dipole interactions.

9.4.3 Sorption of P-nitrophenol

According to Equation 9.1, the experimental isotherms results are plotted as Q_e versus C_e, as shown in Figure 9.1a-f for HDI-X, CDI-X, MDI-X, PDI-X, CL-CDI (1:3) and GL-CDI (1:3), and GAC, respectively. In general, there is a monotonic increase in Q_e vs. C_e as the total concentration of PNP increases. The relative magnitude of Q_e varies according to the chemical nature of the sorbent and the composition of the copolymer (i.e. 1:1, 1:2, and 1:3). The sorption capacity and the relative binding affinity of the sorbent with PNP are important parameters derived from the "best-fit" of the isotherm models (*cf.* Equation 9.2-9.4). The fitting parameters (Q_m, K_i and n_i) were obtained using a non-linear least squares (NLLS) fitting routine by minimizing the SSE (Equation 9.5). Overall, the Sips isotherm model provided the lowest SSE with the most uniform "best fit". The corresponding parameters are listed in Table 9.1.

In the case of the copolymer materials, the magnitude of Q_e vs. C_e is greatest for copolymers with monomer mole ratios (β-CD/linker) that exceed unity. The magnitude of Q_e increases as the linker content increases (i.e. 1:1, 1:2 and 1:3). This may infer that PNP is adsorbed within the pores of the copolymer framework at the linker rich domains.[61] PNP is a relatively small molecule and can be adsorbed within the inclusion and non-inclusion pore domains of the copolymer framework. Moreover, the overall lipophilicity of the copolymers increases as the crosslinking density increases. Favorable hydrophobic interactions may occur between PNP and the copolymers since the

diisocyanate linkers are relatively apolar in nature. The magnitude of Q_e also varies according to the physicochemical properties of the linker molecule as illustrated by the sorption properties of the different copolymer materials (*cf.* Table 9.1).

The isotherm trends for HDI-based copolymers are shown in Figure 9.1a where the HDI-1 copolymer displays a non-uniform increase in Q_e and indicates a low affinity towards PNP. Since HDI-1 is relatively water soluble, it may be regarded as somewhat hydrophilic in nature due to the presence of many accessible OH groups of β-CD results in attenuated sorption with PNP. At greater co-monomer ratios (>1:1), the lipophilicity and the sorption capacity of the copolymer markedly increases. HDI-2 displays representative behavior for a heterogeneous sorbent (n_s = 0.915) with a lower K_{eq} value (62.4 M^{-1}) than that of native β-CD/PNP (197 M^{-1}). However, the K_{eq} derived from the Sips isotherm, is model dependent and can not be directly compared to the K_{eq} value derived from the Benesi-Hildebrand plot. A similar trend is observed for HDI-3 as compared with HDI-2, except there is an increased slope observed for Q_e vs C_e. These results indicate an increased value of for K_{eq} (103 M^{-1}) and greater heterogeneity (n_s = 0.977) as the linker content increases. The Q_m values for HDI-2 and HDI-3 are similar (i.e. ~ 1.15 mmol PNP/g sorbent).

The CDI-based copolymers (*cf.* Figure 9.1b) displays a greater sorption toward PNP for CDI-3; whereas, CDI-2 and CDI-1 exhibit reduced sorption with PNP. The relative ordering of the sorption capacity (mmol PNP/g sorbent) of CDI-X is as follows; CDI-3 (1.96) > CD1-2 (1.89) > CDI-1(0.492). Saturation of the sorption sites is achieved for the CDI-1 copolymer ~ 16 mM, whereas, saturation for CDI-2 and CDI-3 is achieved ~ 13 and 6 mM, respectively. The positive increase for Q_e parallels the increasing

crosslink density of the copolymer where the amount of PNP adsorbed increases as linker content (–X) increases. This trend can be rationalized in terms of an incremental change in the lipophilic character of the copolymer as the content of the linker (-X) domains increase, as described above. The relative ordering of the values of K_{eq} are observed as follows: CDI-1 (308 M^{-1}) > CDI-3 (127 M^{-1}) > CDI-2 (78.6 M^{-1}). Overall, it can be argued that the binding affinity decreases as the β-CD content decreases in the copolymer material. Although the β-CD inclusion sites are considered to be the primary binding site, PNP preferentially adsorbs onto the linker framework of the copolymer at pH values < pKa (PNP). The binding affinity to the linker domains appears to be greater than that of the β-CD inclusion sites. The estimated heterogeneity factor (n_s) for the CDI-based copolymers also indicates there is an increase of heterogeneity when the linker content of the copolymer increases.

The isotherms for the aromatic-based (i.e. MDI and PDI) copolymers are shown in Figure 9.1c-d, respectively. A similar trend is observed compared to that of CDI-based copolymers, except for PDI-3, where the sorbent displays a continual uptake of PNP over the entire concentration range. The Sips model provides "best fit" results as compared with the Freundlich model; hence, the copolymer is regarded as heterogeneous. The relative ordering of the sorption capacities (mmol PNP/g sorbent) of MDI-X and PDI-X is as follows; MDI-3 (1.42) > PDI-2 (1.25) > MD1-2 (0.950) > MDI-1(0.568) > PDI-1 (0.471).

In order to confirm whether the linker framework plays a significant role in the sorption of PNP, Q_e values were estimated from the isotherms at X=1, where the mole ratio of β-CD in the copolymers:PNP (1:1). Q_e values were found to be 0.610, 0.521,

0.531, and 0.619 mmol/g for HDI-3, CDI-3, MDI-3 and PDI-3, respectively. These values are lower than their respective Q_m values, hence, PNP is interpreted to associate preferentially with the linker framework. Moreover, a GL-CDI (1:3) (glucose:CDI (1:3)) copolymer was prepared to examine the sorption properties of a non-porogenic carbohydrate monomer. This copolymer is non-porogenic in nature compared with the various β-CD copolymers. Figure 9.1e shows the sorption isotherm of GL-CDI (1:3) where the saturation is achieved at relatively low concentrations, and the value of Q_m is 0.091 mmol PNP/g sorbent. The role of the porogen was further tested using a CL-CDI (1:3) (cellobiose:CDI (1:3)) copolymer. CL is amphiphilic in nature due to its concave shape and may form complexes with apolar organic molecules, as shown in previous work.[39] The isotherm generated from the sorption of PNP with CL-CDI (1:3) is shown in Figure 9.1e with a Q_m of 1.10 mmol PNP/g sorbent. The K_{eq} values of GL-CDI (1:3) and CL-CDI (1:3) are 5.72×10^3 and 626 M^{-1}, respectively. The differential binding of PNP toward GL- and CL-based copolymer materials is attributed to the favourable hydrogen bonding interactions between PNP and the hydroxyl groups of the carbohydrate moiety. GAC is a commonly used sorbent for many sorption-based applications, in part, because it is readily available and has favourable sorption capacity toward organic compounds such as phenolic dyes.[62] Figure 9.1f shows a sorption isotherm for GAC with PNP and these sorption results provide a useful standard material for comparison with the copolymer materials designed in this study. As expected, both Q_m (2.03 mmol PNP/g sorbent) and K_{eq} (6.42×10^3 M^{-1}) exceed the values of K_{eq} for the copolymers, however, copolymers such CDI-2, CDI-3, MDI-3 and PDI-3 have comparable sorption capacity to GAC as shown in Table 9.1.

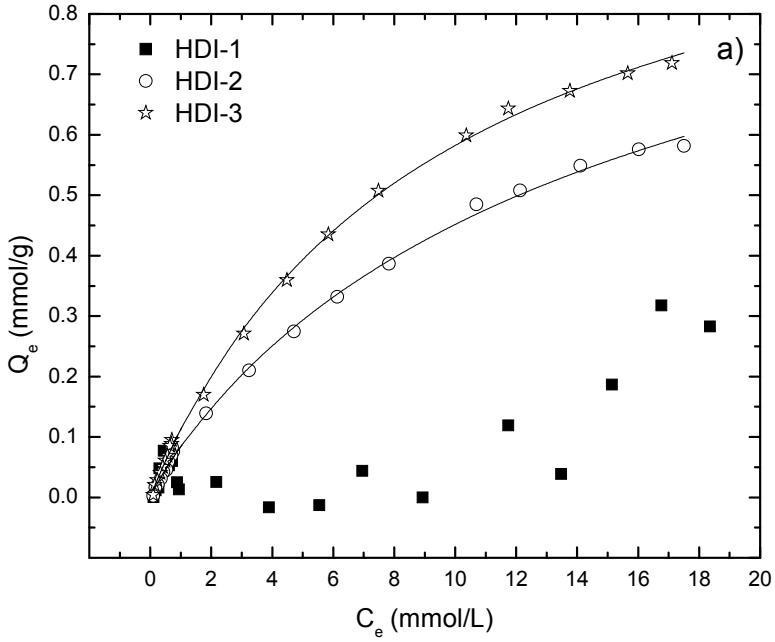
HDI-1
HDI-2
HDI-3
a)
Q_e (mmol/g)
C_e (mmol/L)

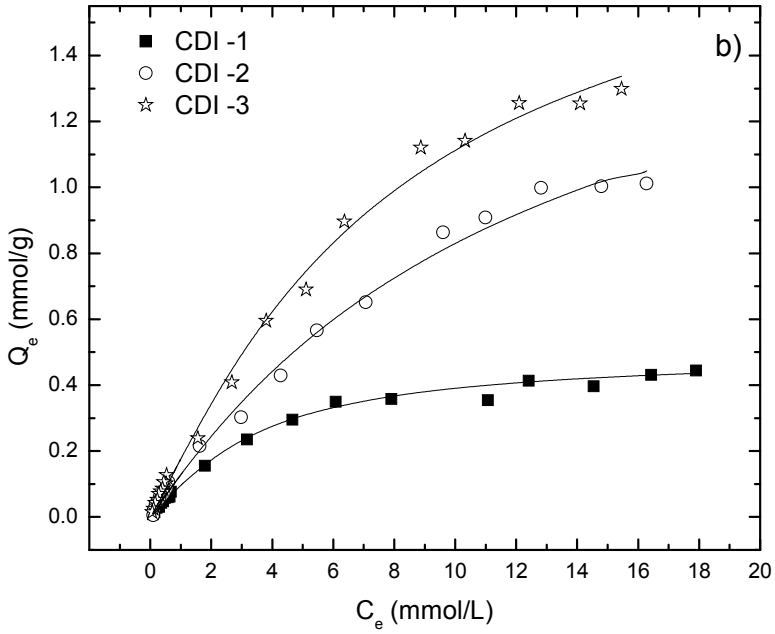
CDI -1
CDI -2
CDI -3
b)
Q_e (mmol/g)
C_e (mmol/L)

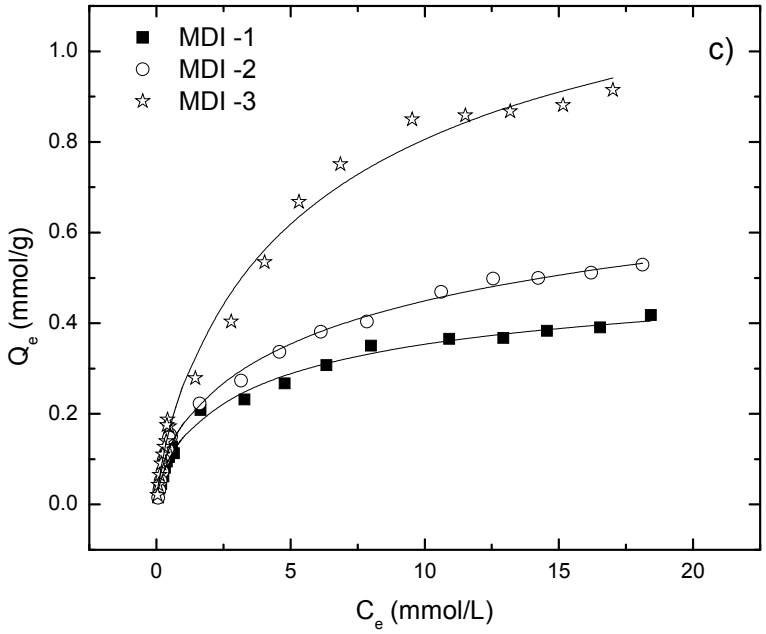
MDI -1
MDI -2
MDI -3
c)
1.0
0.8
0.6
0.4
0.2
0.0
Q_e (mmol/g)
0
5
10
15
20
C_e (mmol/L)

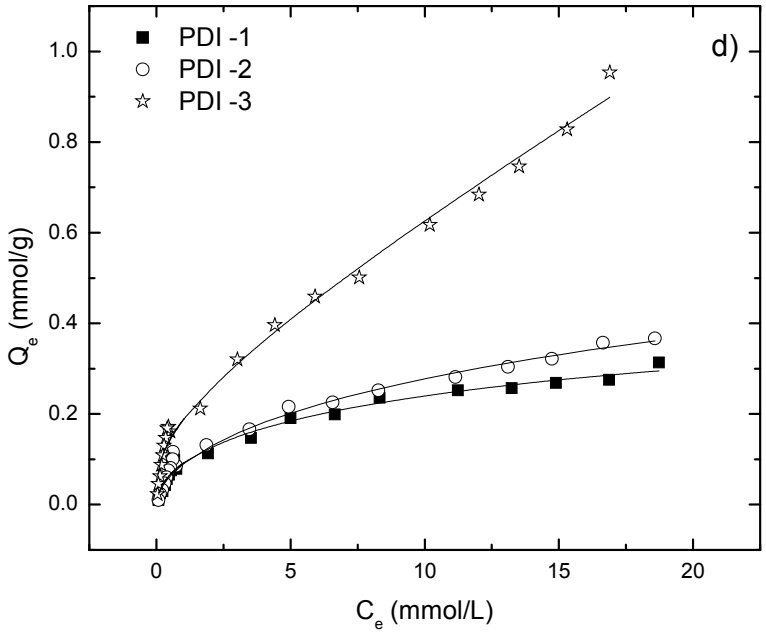
PDI -1
PDI -2
PDI -3
d)
1.0
0.8
0.6
0.4
0.2
0.0
Q_e (mmol/g)
0
5
10
15
20
C_e (mmol/L)

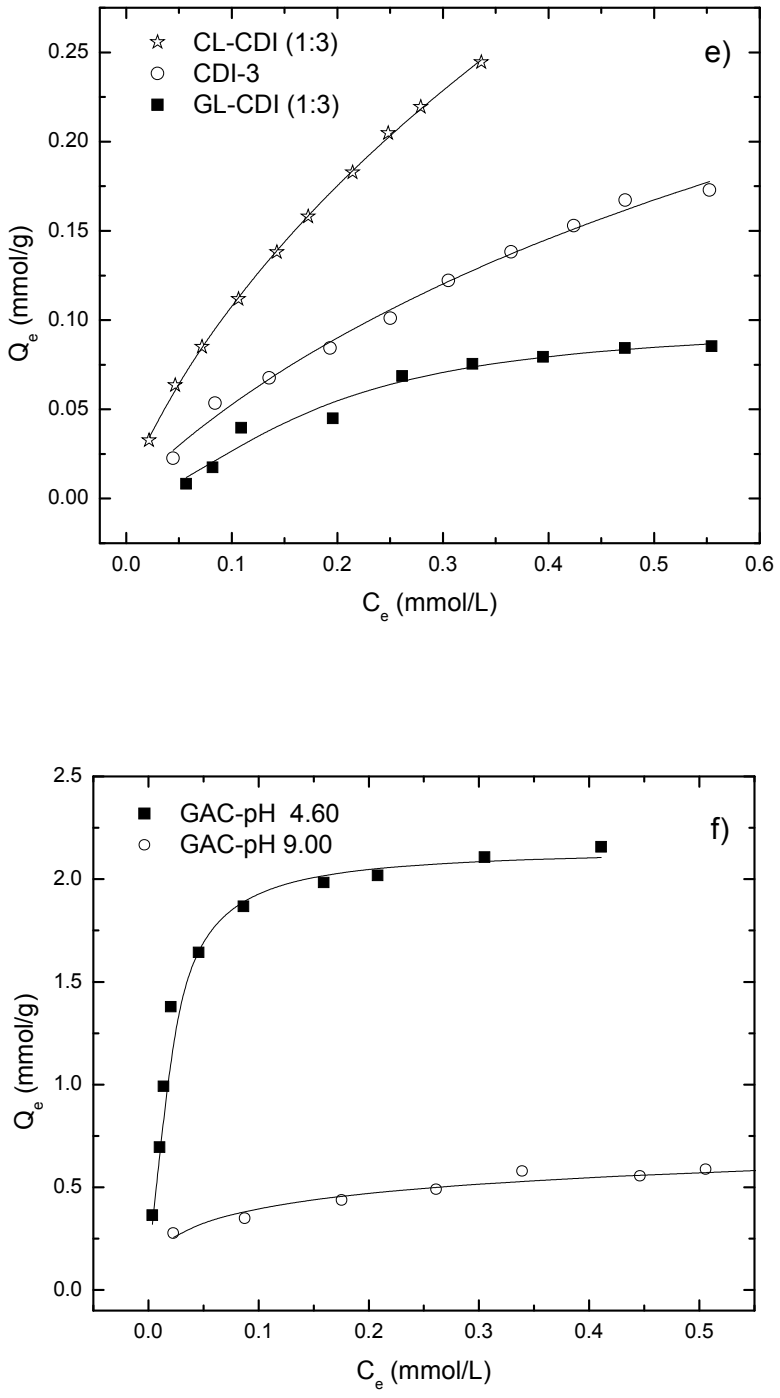

Figure 9.1a-f. Sorption isotherms for copolymers and GAC with PNP in aqueous solution, respectively at pH 4.60 and 295 K with PNP. a) HDI-X, b) CDI-X, c) MDI-X, d) PDI-X, e) [CL-CDI (1:3)/CDI-3/GL-CDI (1:3)], f) GAC; pH 4.60 and 9.00. X = 1, 2, 3 for 1:1, 1:2, and 1:3 β-CD:diisocyanate co-monomer mole ratios, respectively. The solid lines represent "best-fit" using the Sips isotherm model.

Table 9.1. "Best-fit" sorption parameters obtained from the Sips Isotherm model for HDI-X, CDI-X, MDI-X, PDI-X, CL-CDI (1:3), GL-CDI (1:3) and GAC. X = 1, 2, 3 for 1:1, 1:2, and 1:3 β-CD:diisocyanate monomer mole ratios, respectively. The isotherm conditions were temperature of 295 K and pH 4.60 in aqueous solution.

Sorbent[a]	Q_m (mmol/g)	K_{Sips} (mM)[b]	K_{eq} (M^{-1})	n	R^2
HDI-2	1.15	0.0624	62.4	0.915	0.999
HDI-3	1.15	0.103	103	0.977	0.999
CDI-1	0.492	0.308	308	1.20	0.985
CDI-2	1.89	0.0786	78.6	1.02	0.995
CDI-3	1.96	0.127	127	1.12	0.995
MDI-1	0.568	0.211	211	0.669	0.992
MDI-2	0.950	0.0833	83.3	0.590	0.992
MDI-3	1.42	0.143	143	0.760	0.990
PDI-1	0.471	0.107	107	0.745	0.989
PDI-2	1.25	0.0110	11.0	0.569	0.992
GAC	2.03	6.42	6.42×10^3	0.366	0.994
GL-CDI (1:3)	0.0981	5.72	5.72×10^3	1.76	0.969
CL-CDI (1:3)	1.10	0.626	626	0.801	0.999

[a] The SSE < 0.02 for all "best-fit" using Sips isotherm.
[b] $K_{eq} = K_{Sips}$

Figure 9.2 illustrates the sorption results for PNP at pH 9.00 for selected copolymers. The copolymers generally show a decreased uptake of PNP at pH 9.00 compared to sorption conditions at pH 4.60, as shown in Figure 9.2. This observation has been observed recently[45] and is attributed to the fact that deprotonated PNP is negatively charged and more water soluble due to deprotonation of the phenolic proton. Hence, the electrostatic repulsion between deprotonated PNP, causes the adsorbates to adsorb at a reduced surface coverage to minimize unfavorable repulsions. This infers that the possible causes for the PNP adsorption are hydrophobic effects, H-bonding, and van der Waals interactions. This is confirmed by the GAC sorption data (*cf.* Figure 9.1f) where there is both a reduction in Q_m (1.05 mmol PNP/g sorbent) and K_{eq} (3.10×10^3 M^{-1}), compared to the parameters at pH 4.60 (*cf.* Table 9.1). In addition, the aromatic-based

copolymers (MDI and PDI) had the greatest attenuation in their sorption capacities, as compared to the aliphatic-based copolymers (HDI and CDI). This may be due to the changes in the orientation of PNP during adsorption on to the linker framework. At pH 9.00, an orthogonal orientation between PNP and aromatic linkers reduces the favourable π-π stacking interactions for a coplanar arrangement of PNP predicted at pH 4.60.

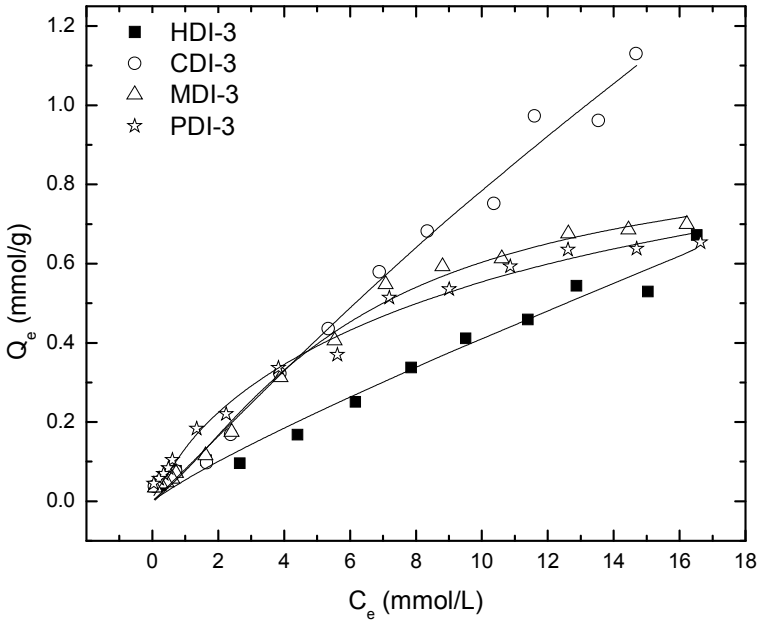

Figure 9.2 Sorption isotherm for HDI-3, CDI-3, MDI-3, and PDI-3 with PNP, respectively, at pH 9.00 and 295 K in aqueous solution. The solid lines represent "Best-fit" curves obtained from the Sips model.

9.4.4 Sorption of Phenolphthalein

Figure 9.3a-e illustrate the isotherm data for phth with HDI-X, CDI-X, MDI-X, PDI-X (X=1-3) copolymers at the 1:1, 1:2 and 1:3 mole ratios, and GAC, respectively. Visually, the decolourization of phth increases as the relative amount of β-CD in the copolymer increased as X decreased from 3 to 1 (i.e 1:3 to 1:1). The attenuated

decolourization of phth as X increases is attributed to the increasing steric effect in the annular hydroxyl region of β-CD because efficient decolourization of this dye requires inclusion binding of the phth dianion with H-bonding. This inclusion mode becomes inhibited as –X increases, and this is consistent with the concomitant steric effects, and the greater size of phth compared with PNP.

The isotherm trends for HDI-X (X=-1, -2 and -3) copolymers are shown in Figure 9.3a where the HDI-1 material displays representative behavior for a heterogeneous sorbent (n_s = 1.89) with a relatively high value of K_{eq} ($1.78x10^5$ M^{-1}). The HDI-2 copolymer shows a similar trend as that for HDI-1 except the former displays an attenuated isotherm, indicating a reduced K_{eq} ($1.22x10^5$ M^{-1}) and lower heterogeneity (n_s = 1.80). The Q_m values (mmol phth/g sorbent) for HDI-1 (0.231) and HDI-2 (0.230) are similar. The sorption affinity of the HDI-3 copolymer is relatively low and the isotherm data illustrates a very weak concentration dependence of Q_e. While the sorption capacity for HDI-1 and HDI-2 are similar, the value of Q_m for HDI-3 is almost negligible, and the apparent scatter in the isotherm data for HDI-3 is a consequence of the reduced binding affinity with phth. Similar to HDI-3, CDI-2 and CDI-3 show a similar reduced binding affinity with phth. In contrast, CDI-1 (*cf.* Figure 9.3b) had a moderate Q_m of 0.155 mmol phth/g sorbent and K_{eq} of $6.07x10^4$ M^{-1}.

The isotherm trends for MDI-based polymers are shown in Fig. 4c where the isotherms depict a gradual increase of Q_e vs. C_e for each copolymer. There is monotonic decrease in the sorption capacity (Q_m) with phth as the cross linking density increases. The relative ordering of the sorption capacity (mmol phth/g sorbent) of MDI-X sorbents are as follows; MDI-1 (0.130) > MD1-2 (0.116) > MDI-3 (0.114). The magnitude of Q_e

and Q_m parallels the trend in magnitude for the estimated values of K_{eq}, as follows: MDI-1 ($1.11x10^5$ M^{-1}) > MDI-2 ($1.02x10^5$ M^{-1}) > MDI-3 ($4.16x10^4$ M^{-1}), respectively. The heterogeneity factor decreases as the cross linking ratio increases, and may be understood in terms of the reduced ability of phth to partition into the sorbent material as X increases due to steric constraints of the inclusion sites.

PDI-based polymers (Figure 9.3d) show a continual linear increase in sorption behavior over the entire concentration range, without any sign of saturation. The relative ordering of the sorption capacity (mmol phth/g sorbent) of PDI-X is as follows; PDI-1 (0.222) > PD1-2 (0.139) > PDI-3 (0.0521). The heterogeneity factor and K_{eq} (M^{-1}) values are comparatively similar for each copolymer; PDI-1 ($9.90x10^4$), PDI-2 ($1.31x10^5$) and PDI-3 ($9.41x10^4$). The copolymers are considered heterogeneous since the value of n_s ranges between 1.6-1.8 for the PDI-X copolymer materials.

NDI-X copolymers (Figure 9.3e) display an initial linear increase in Q_e and show some indication of saturation at higher concentration of phth. The saturation of the isotherm is more pronounced as the β-CD content of the copolymer increases. The relative ordering of the sorption capacity (mmol phth/g sorbent) of NDI-X is as follows; NDI-1 (0.262) > ND1-2 (0.218) > NDI-3 (0.0851). The values of K_{eq} (M^{-1}) are as follows; NDI-1 ($1.09x10^5$), NDI-2 ($5.34x10^4$), and NDI-3 ($9.51x10^4$), while the heterogeneity (n_s) values are as follows; NDI-1 (1.89), NDI-2 (1.32) and NDI-3 (1.47), and parallel a similar trend as that for K_{eq}. These results are consistent with the relatively high inclusion site accessibility and heterogeneity of the copolymer framework.

In general, the sorption trend is opposite to that for PNP because the sorption capacity for phth decreases as X increases. Increasing the cross link density may reduce

the sorption properties of the copolymer materials for two possible reasons; (*i*) steric crowding of the hydroxyl annular region of β-CD attenuates the formation of inclusion complexes, and (*ii*) copolymers with greater linker content (increasing X) result in the formation of non-inclusion domains with variable pore structure that provide in secondary binding sites for adsorbates as X increases. Thus, the anticipated steric effects are consistent with the reduced decolourization observed for phth in such highly cross linked materials, as observed in Figure 9.3a-e. Copolymers with greater crosslink density provide limited accessibility to include phth because of steric restrictions to the β-CD inclusion sites. This limited accessibility is indirectly supported by the isotherm for GAC in Figure 9.3f because the value of Q_m is ~ 5% the magnitude compared to the copolymers except for PDI-3, as observed in Table 9.2.

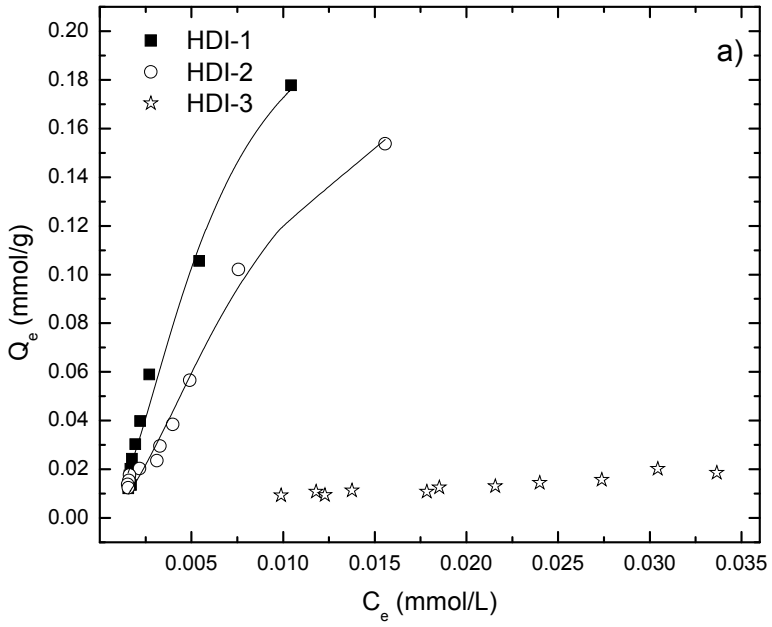

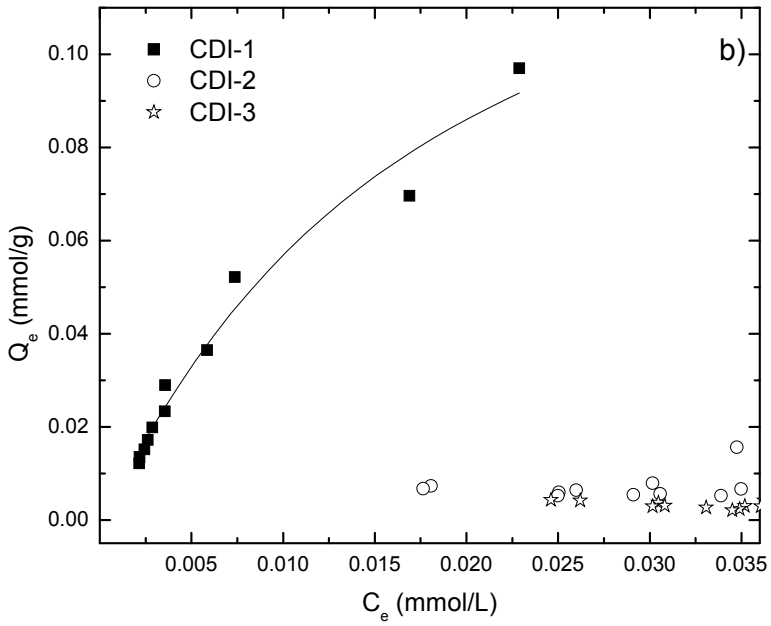
b)
CDI-1
CDI-2
CDI-3
0.10
0.08
0.06
0.04
0.02
0.00
Qe (mmol/g)
0.005
0.010
0.015
0.020
0.025
0.030
0.035
Ce (mmol/L)

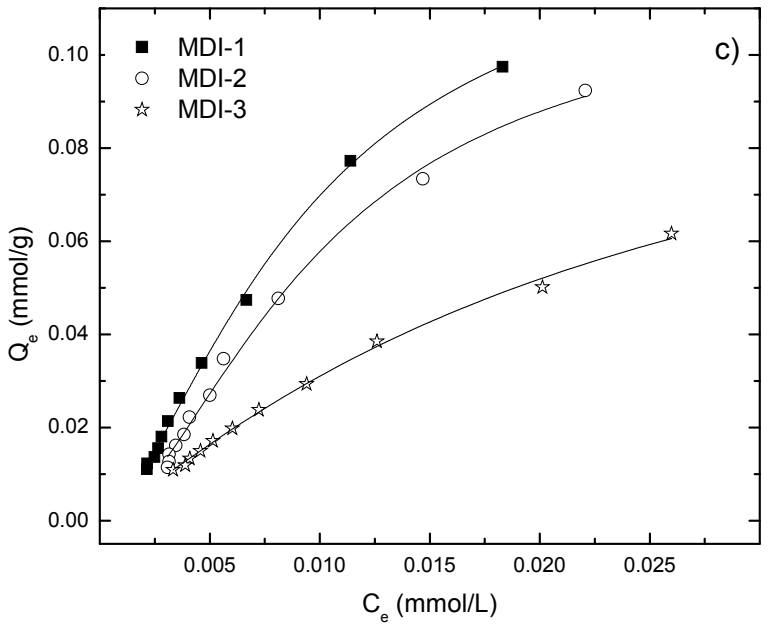
c)
MDI-1
MDI-2
MDI-3
0.10
0.08
0.06
0.04
0.02
0.00
Qe (mmol/g)
0.005
0.010
0.015
0.020
0.025
Ce (mmol/L)

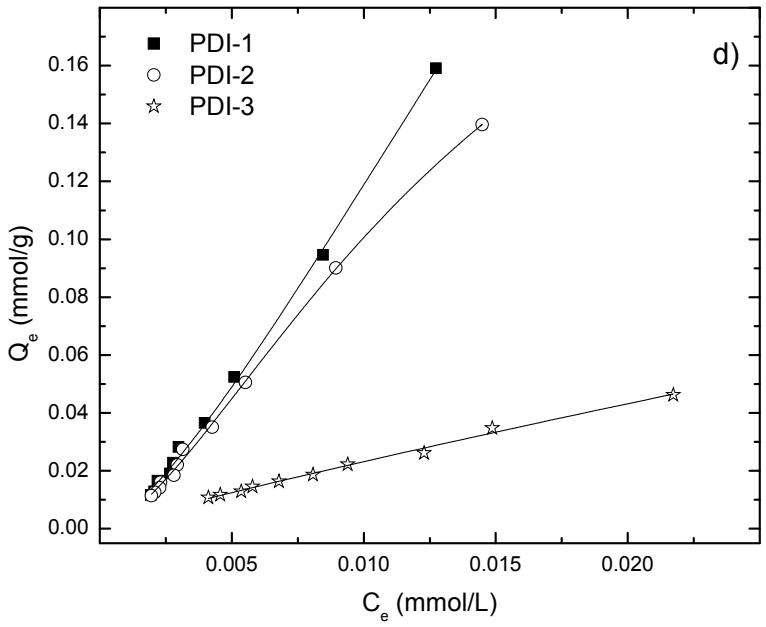
PDI-1
PDI-2
PDI-3
d)
0.16
0.14
0.12
0.10
0.08
0.06
0.04
0.02
0.00
Qe (mmol/g)
0.005
0.010
0.015
0.020
Ce (mmol/L)

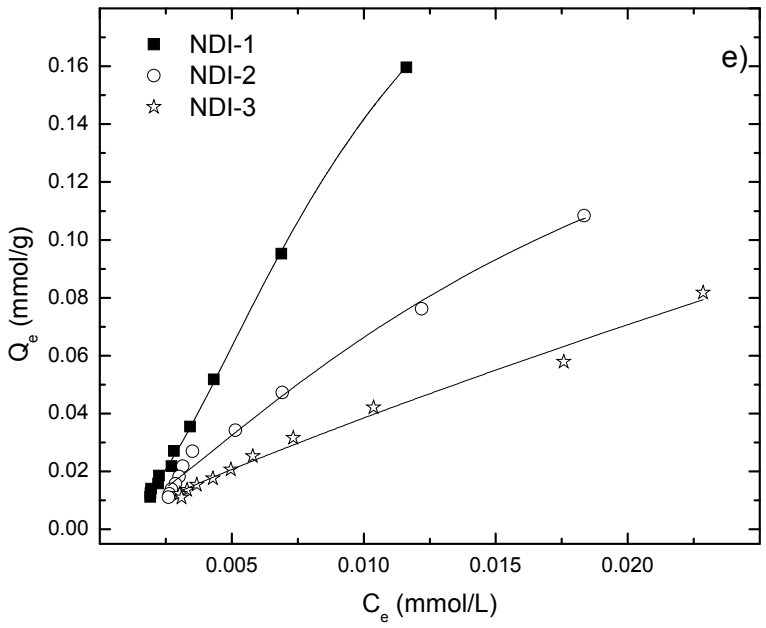
NDI-1
NDI-2
NDI-3
e)
0.16
0.14
0.12
0.10
0.08
0.06
0.04
0.02
0.00
Qe (mmol/g)
0.005
0.010
0.015
0.020
Ce (mmol/L)

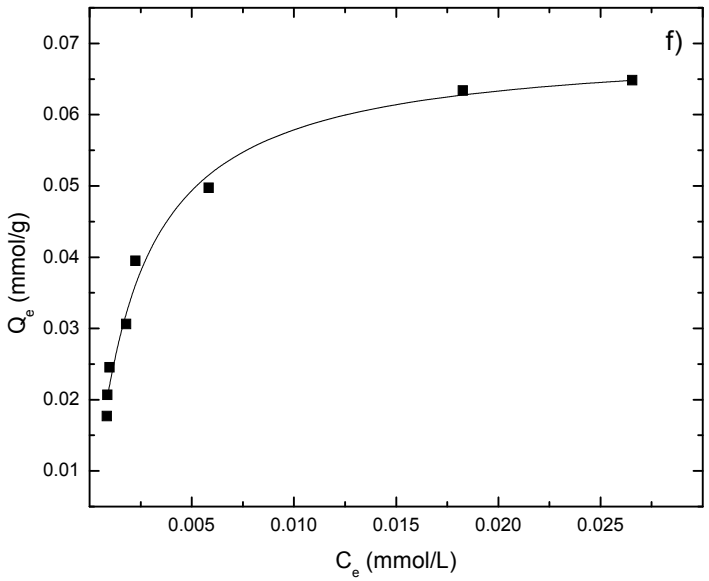

Figure 9.3. Sorption isotherm for HDI, CDI, MDI, PDI, and GAC with phth in aqueous solution, respectively, at pH 10.50 and 295 K. a) HDI-X, b) CDI-X, c) MDI-X, d) PDI-X, e) GAC. X = 1, 2, 3 for 1:1, 1:2, and 1:3 β-CD:diisocyanate co-monomer mole ratios, respectively. Solid lines represent fittings from the Sips isotherm model.

Table 9.2. "Best-fit" sorption parameters obtained from Sips isotherm model for HDI-X, CDI-X, MDI-X, PDI-X, NDI-X and GAC. X = 1, 2, 3 for 1:1, 1:2, and 1:3 β-CD:diisocyanate monomer mole ratios, respectively. The isotherm conditions were 295 K and pH 10.50 in aqueous solution.

Sorbent[a]	Q_m (mmol/g)	K_{Sips} (mM)	K_{eq} (M^{-1})	n	R^2
HDI-1	0.231	178	$178x10^3$	1.89	0.985
HDI-2	0.205	122	$122x10^3$	1.80	0.987
CDI-1	0.155	60.7	$60.7x10^3$	1.10	0.973
MDI-1	0.130	110	$110x10^3$	1.71	0.999
MDI-2	0.116	102	$102x10^3$	1.58	0.996
MDI-3	0.114	41.6	$41.6x10^3$	1.15	0.997
PDI-1	0.222	99.0	$99.0x10^3$	1.71	0.997
PDI-2	0.139	131	$131x10^3$	1.75	0.985
PDI-3	0.0521	94.1	$94.1x10^3$	1.63	0.943
NDI-1	0.262	109	$109x10^3$	1.89	0.999
NDI-2	0.218	53.4	$53.4x10^3$	1.32	0.992
NDI-3	0.0851	95.1	$95.1x10^3$	1.47	0.989
GAC	0.0698	481	$481 x10^3$	1.01	0.989

[a] The SSE < $3.9 x10^{-4}$ for all "best-fit" using the Sips isotherm model.

9.4.5 Sorption of Naphthenic Acids

The sorption behaviour of NAs at pH 9.00 is comparable to the results for phth, as shown by Figure 8.2a-d in Chapter 8 and Table 9.3. The isotherm trends for HDI-X (X=1, 2 and 3) copolymers are shown in Figure 8.2a where the HDI-1 material displays representative behavior of a heterogeneous sorbent (n=3.66) with relatively high values of K_{eq} ($3.66x10^4$ M^{-1}). The HDI-2 polymer shows a similar trend, as observed for HDI-1, with a greater slope in Q_e vs C_e, indicating a reduced value of K_{eq} ($9.64x10^3$ M^{-1}) with reduced heterogeneity (n_s=1.83). The Q_m values for HDI-1 and HDI-2 are 75.5 and 73.0 mg NAs/g, respectively and the sorption results in Figure 8.2a indicate that the sorption sites are ~ 50% saturated since the corresponding Q_e values are ~ 35 and 30 mg NAs/g sorbent, respectively. The sorption affinity of the HDI-3 polymer is relatively low and the isotherm data illustrates a very weak concentration dependence of Q_e. While the sorption capacity for HDI-1 and HDI-2 are similar, the value of Q_m for HDI-3 is low. The apparent scatter in the data for HDI-3 is a consequence of the low binding affinity toward NAs. The latter is consistent with the low inclusion site accessibility of β-CD, according to the phth decolourization results outlined in a previous study[31].

The CDI-based polymers (*cf.* Figure 8.2b) display a relatively high sorption toward NAs for CDI-1; however, CDI-2 and CDI-3 sorbents display a reduced uptake of NAs, as described above for HDI-3. The saturation of the sorption sites is not achieved for CDI-1 over the range of C_e values despite its lower sorption capacity, as compared with HDI-1. The difference in Q_m for CDI-1 is further evidenced by a reduced value of K_{eq} ($4.36x10^3$ M^{-1}) and a lower heterogeneity factor (n_s=1.32). CDI-1 is concluded to be a less heterogeneous copolymer, as compared with HDI-1 and HDI-2 copolymer materials.

The isotherm trends for MDI-based polymers are shown in Figure 8.2c where a gradual increase is observed in Q_e vs C_e for this copolymer. There is an incremental decrease in the sorption capacity (Q_m) with NAs as X increases. The relative ordering of the sorption capacity (NAs/g sorbent) for MDI-X is as follows; MDI-1 (32.2) > MD1-2 (30.1) > MDI-3 (29.4). The magnitude of Q_m parallels the trend in values of K_{eq} (M^{-1}) as follows: MDI-1 ($2.17x10^4$) > MDI-2 ($2.00x10^4$) > MDI-3 ($9.93x10^3$), respectively. The heterogeneity of MDI-1 and MDI-2 are similar, whereas, MDI-3 is somewhat less heterogeneous in nature.

The PDI-based polymers (Figure 8.2d) show similar trends in adsorption behavior to that of MDI-based copolymers at X = 1 and 2. However, the 1:3 copolymer reaches saturation of the sorption sites at intermediate C_e values. The PDI-3 material may have a more closed framework structure, and is consistent with its reduced inclusion site accessibility. In Figure 8.2d, the sorption of PDI-3 is severely attenuated whereas PDI-1 and -2 have a more open framework. The relative binding affinity, K_{eq}, values (M^{-1}) are as follows; PDI-1 ($1.49x10^4$), PDI-2 ($7.98x10^3$) and PDI-3 ($9.03x10^4$). The sorption capacity (Q_m) for these copolymers show a similar trend to that of the binding affinity. The Q_m values (mg NAs/ g sorbent) for PDI-X are comparable as follows: PDI-1 (44.1), PDI-2 (56.6) and PDI-3 (21.7). The heterogeneity factors display similar trends to that of K_{eq}. PDI-3 appears to be the most heterogeneous sorbent; whereas, PDI-1 and -2 have the lowest heterogeneity factors (n_s); PDI-3 (2.45), PDI-1 (1.28) and PDI-2 (1.12).

The NDI-1 copolymer (Figure 8.2e) shows a similar trend to that of the PDI-3 copolymer; however, the isotherm at lower C_e values indicates that the binding sites are approaching saturation conditions. This is supported by a lower value of K_{eq} ($3.30x10^4$

M^{-1}), and the values for Q_m and the heterogeneity factor are 20.5 mg NAs/g polymer and 1.54, respectively. NDI and PDI are both aromatic linkers that differ in size and lipophilicity, NDI-1 vs PDI-1. The value of K_{eq} is lower for PDI-1 as compared NDI-1, and the opposite trend is observed for their sorption capacity. This may be related to the amount of accessible β-CD sites since PDI-1 had more accessible β-CD inclusion sites than NDI-1, as shown in previous work.[31]

The relatively high sorption capacity and binding affinity of GAC towards NAs provides a standard material for comparison with the polymeric CD materials. In Figure 8.2f, the greater Q_m observed for GAC is attributed to the relatively large surface area of GAC (~1000 m^2/g); whereas the copolymers have much lower surface area (~10^1-10^2 m^2/g).[29] The Freundlich isotherm provides the "best-fit" model for GAC sorption with NAs. The Langmuir isotherm provides less favourable fitting results; however, the value of Q_m (146 mg NAs/g sorbent) provides a crude estimate of its sorption capacity. The sorption capacity of GAC is approximately double that compared with the copolymers exhibiting the most favorable sorption properties (i.e HDI-1). Since K_{eq} is model dependent, the K_{eq} derived from the Langmuir isotherm model does not directly compare to the estimates obtained from the Sips isotherm for the copolymer sorbents, unless the heterogeneity factor (n_s) is unity. However, the general features of the GAC isotherm (Figure 8.2f), support an apparently greater sorption capacity as a consequence of its greater surface area and binding affinity (K_{eq}) with phenolic adsorbates. The sharp concentration dependence of Q_e for GAC with NAs is shown in Figure 8.2f and supports the foregoing comments regarding surface area and K_{eq} as compared with the copolymer materials.

Scheme 1.2 in Chapter 1 illustrates a generalized scheme of the types of adsorption that may occur for the various types of phenolic adsorbates (*i.e*. PNP, phth, and NAs) investigated in this work. According to Figure 6, there are two main binding sites identified as inclusion and non-inclusion sites, respectively. In general, adsorbates with greater lipophilic character are bound within the inclusion sites provided that the copolymer materials have sufficient site accessibility.[31] In contrast, adsorbates with greater hydrophilic character or those which have limited site accessibility to the inclusion sites are preferentially bound in the non-inclusion domains. The foregoing results are consistent with a comprehensive sorption study of NAs and the relative importance of the hydrophobic effect in the formation of cyclodextrin inclusion complexes.[63] It is important to recognize that the Sips isotherm implicitly accounts for all potential adsorption sites (*i.e.* inclusion and non-inclusion) since the K_{Sips} parameter (*cf*. Equation 9.4) represents all equilibria which contribute to the overall sorption process.

9.5 Conclusions

Copolymer-based β-CD sorbents display tunable heterogeneous sorption properties towards phenolic dyes and NAs in aqueous solution according to the nature of the experimental conditions. The sorption capacity and binding affinity varies because of the difference in the type of linker monomer, co-monomer mole ratios, and adsorbate species. Generally, small hydrophilic molecules like PNP may bind at the inclusion sites or onto the linker framework domains; whereas, large lipophilic molecules like phth and NAs bind mainly within the β-CD inclusion sites provided that there is access to these

inclusion sites. In the case of the anionic form of PNP, its greater hydrophilicity and electrostatic create repulsions within an adsorbed monolayer resulting in reduced sorption, as observed for GAC. In general, aliphatic-based copolymers (HDI and CDI) exhibit better sorption towards PNP, especially at pH 4.6. NAs and phth showed decreased sorption toward copolymers with greater linker content. This infers that the reduced accessibility of the β-CD inclusion sites in the copolymer framework are reduced as the degree of cross linking increases. As well, the inclusion sites play a major role in the binding affinity of lipophilic adsorbates (i.e. NAs and phth) at alkaline pH conditions since the magnitude of binding affinity of the copolymers is similar for NAs and phth, respectively, as is similarly observed for native β-CD. While the sorption of phth is primarily driven by the availability of β-CD inclusion sites, the sorption of NAs was enhanced for aliphatic-based copolymers. The aromatic-based copolymers have higher binding affinity toward NAs while those with aliphatic linkers have greater sorption capacity. This difference in sorption assumes that, apart from the β-CD macrocycle playing a major role in the binding affinity, the nature of the linker monomers play a secondary role when steric effects are minimized. The improved understanding of the sorption mechanism for such adsorbates described in this work (*cf*. Scheme 1.2 in Chapter 1) is expected to aide in the design of copolymer materials with improved physicochemical properties for sorption-based applications.

9.6 Acknowledgements

Financial assistance was provided by the Natural Sciences and Engineering Research Council and the Program of Energy Research and Development. M.H.M

acknowledges the University of Saskatchewan for the award of a Graduate Teaching Fellowship and Environment Canada for the Science Horizons Program award.

9.7 References

1. Mizobuchi, Y. *J. Chromatogr., A* **1980**, *194*, 153-161.
2. Koradecki, D.; Kutner, W. *J. Inclusion Phenom.* **1991**, *10*, 79-96.
3. He, B.; Zhao, X. *React. Polym.* **1992**, *18*, 229-235.
4. Sreenivasan, K. *Polym. Int.* **1994**, *34*, 221-223.
5. Shao, Y.; Martel, B.; Morcellet, M.; Weltrowski, M.; Crini, G. *J. Inclusion Phenom.* **1996**, *25*, 209-212.
6. Crini, G.; Bertini, S.; Torri, G.; Naggi, A.; Sforzini, D.; Vecchi, C.; Janus, L.; Lekchiri, Y.; Morcellet, M. *J. Appl. Polym. Sci.* **1998**, *68*, 1973-1978.
7. Janus, L.; Crini, G.; El-Rezzi, V.; Morcellet, M.; Cambiaghi, A.; Torri, G.; Naggi, A.; Vecchi, C. *React. Funct. Polym.* **1999**, *42*, 173-180.
8. Baille, W. E.; Huang, W. Q.; Nichifor, M.; Zhu, X. X. *J. Macromol. Sci., Pure Appl. Chem.* **2000**, *A37*, 677-690.
9. Phan, T. N. T.; Bacquet, M.; Morcellet, M. *J. Inclusion Phenom. Macrocyclic Chem.* **2000**, *38*, 345-359.
10. Crini, G. *Bioresour. Technol.* **2003**, *90*, 193-198.
11. Moya-Ortega, M. D.; Alvarez-Lorenzo, C.; Sigurdsson, H. H.; Concheiro, A.; Loftsson, T. *Carbohydr. Polym.* **2010**, *80*, 900-907.
12. Tian, W.; Fan, X.; Kong, J.; Liu, Y.; Liu, T.; Huang, Y. *Polymer* **2010**, *51*, 2556-25 64.
13. Schneiderman, E.; Stalcup, A. M. *J. Chromatogr., B: Biomed. Sci. Appl.* **2000**, *745*, 83-102.
14. Yu, J. C.; Jiang, Z.-T.; Liu, H.-Y.; Yu, J.; Zhang, L. *Anal. Chim. Acta* **2003**, *477*, 93-101.
15. Bhaskar, M.; Aruna, P.; Ganesh Jeevan, R. J.; Radhakrishnan, G. *Anal. Chim. Acta* **2004**, *509*, 39-45.
16. Zhu, X.; Wu, M.; Gu, Y. *Talanta* **2009**, *78*, 565-569.
17. Szejtli, J. *Chem. Rev.* **1998**, *98*, 1743-1754.

18. Ma, M.; Li, D. *Chem. Mater.* **1999**, *11*, 872-874.
19. Wiedenhof, N. *Staerke* **1969**, *21*, 119-123.
20. Hoffman, J. L. *J. Macromol. Sci., Part A* **1973**, *7*, 1147-1157.
21. Buschmann, H.-J. *J. Cosmet. Sci.* **2002**, *53*, 185-191.
22. Del Valle, E. M. M. *Process Biochem.* **2004**, *39*, 1033-1046.
23. Szejtli, J. *Pure Appl. Chem.* **2004**, *76*, 1825-1845.
24. Astray, G.; Gonzalez-Barreiro, C.; Mejuto, J. C.; Rial-Otero, R.; Simal-Gándara, J. *Food Hydrocolloids* **2009**, *23*, 1631-1640.
25. *Cyclodextrin Chemistry*; Bender, M. L.; Komiyama, M., Eds.; Springer-Verlag: Berlin, Germany, 1998.
26. Kutner, W. *J. Inclusion Phenom.* **1992**, *13*, 257-265.
27. Asanuma, H.; Kakazu, M.; Shibata, M.; Hishiya, T.; Komiyama, M. *Chem. Commun. (Cambridge, U.K.)* **1997**, *20*, 1971-1972.
28. Asanuma, H.; Kakazu, M.; Shibata, M.; Hishiya, T.; Komiyama, M. *Supramol. Sci.* **1998**, *5*, 417-421.
29. Mohamed, M. H.; Wilson, L. D.; Headley, J. V.; Peru, K. M. *Process Saf. Environ. Prot.* **2008**, *86*, 237-243.
30. Wenz, G. *Recognition of Monomers and Polymers by Cyclodextrins*; Springer: Berlin, Germany, 2009; Vol. 222.
31. Mohamed, M. H.; Wilson, L. D.; Headley, J. V. *Carbohydr. Polym.* **2010**, *80*, 186-196.
32. Nielsen, T.; Wintgens, V.; Larsen, K.; Amiel, C. *J. Inclusion Phenom. Macrocyclic Chem.* **2009**, *65*, 341-348.
33. Nielsen, T. T.; Wintgens, V. r.; Amiel, C.; Wimmer, R.; Larsen, K. L. *Biomacromolecules* **2010**, In Print.
34. Giles, C. H. *J. Appl. Chem.* **1970**, *20*, 37-41.
35. Giles, C. H. *Text. Res. J.* **1977**, *47*, 347-350.
36. Buvari, A.; Barcza, L.; Kajtar, M. *J. Chem. Soc., Perkin Trans. 2* **1988**, *1972-1999*, 1687-1690.
37. Georgiou, M. E.; Georgiou, C. A.; Koupparis, M. A. *Anal. Chem.* **1995**, *67*, 114-123.

38. Taguchi, K. *J. Am. Chem. Soc.* **1986**, *108*, 2705-2709.
39. Mohamed, M. H.; Wilson, L. D.; Headley, J. V.; Peru, K. M. *Rapid Commun. Mass Spectrom.* **2009**, *23*, 3703-3712.
40. Mohamed, M. H.; Wilson, L. D.; Headley, J. V.; Peru, K. M. *Can. J. Chem.* **2009**, *87*, 1747-1756.
41. Janfada, A.; Headley, J. V.; Peru, K. M.; Barbour, S. L. *J. Environ. Sci. Health, Part A: Toxic/Hazard. Subst. Environ. Eng.* **2006**, *41*, 985-997.
42. Bowers, G. N., Jr; McComb, R. B.; Christensen, R. G.; Schaffer, R. *Clin. Chem.* **1980**, *26*, 724-729.
43. Lynam, M. M.; Kilduff, J. E.; Weber, W. J. *Journal of Chemical Education* **1995**, *72*, 80-84.
44. Zhu, L.; Chen, B.; Tao, S.; Chiou, C. T. *Environ. Sci. Technol.* **2003**, *37*, 4001-4006.
45. Li, J.-M.; Meng, X.-G.; Hu, C.-W.; Du, J. *Bioresour. Technol.* **2009**, *100*, 1168-1173.
46. Szasz, G. *Clin. Chem.* **1967**, *13*, 752-759.
47. Wilson, L. D.; Siddall, S. R.; Verrall, R. E. *Can. J. Chem.* **1997**, *75*, 927-933.
48. Clemente, J. S.; Fedorak, P. M. *Chemosphere* **2005**, *60*, 585-600.
49. *Naphthenic acids in Kirk-Othmer Encyclopedia of Chemical Technology*; 4 ed.; Brient, J. A.; Wessner, P. J.; Doyle, M. N., Eds.; ohn Wiley & Sons: New York.
50. Kanicky, J. R.; Poniatowski, A. F.; Mehta, N. R.; Shah, D. O. *Langmuir* **1999**, *16*, 172-177.
51. Quagraine, E. K.; Headley, J. V.; Peterson, H. G. *J. Environ. Sci. Health, Part A: Toxic/Hazard. Subst. Environ. Eng.* **2005**, *40*, 671-684.
52. Headley, J. V.; McMartin, D. W. *J. Environ. Sci. Health, Part A: Toxic/Hazard. Subst. Environ. Eng.* **2004**, *A39*, 1989-2010.
53. Langmuir, I. *J. Am. Chem. Soc.* **1918**, *40*, 1361-1402.
54. Freundlich, H. M. F. *J. Phys. Chem.* **1906**, *57A*, 385-470.
55. Sips, R. *J. Chem. Phys.* **1948**, *16*, 490-495.
56. Eftink, M. R.; Harrison, J. C. *Bioorg. Chem.* **1981**, *10*, 388-398.
57. Le Saux, T.; Hisamoto, H.; Terabe, S. *J. Chromatogr., A* **2006**, *1104*, 352-358.

58. Bezsoudnova, K.; Yatsimirsky, A. *React. Kinet. Catal. Lett.* **1997**, *62*, 63-69.
59. Fan, Y.; Feng, Y.-Q.; Da, S.-L.; Feng, P.-Y. *Anal. Sci.* **2003**, *19*, 709-714.
60. Bergeron, R. J.; Channing, M. A.; McGovern, K. A.; Roberts, W. P. *Bioorg. Chem.* **1979**, *8*, 263-281.
61. Crini, G. *Prog. Polym. Sci.* **2005**, *30*, 38-70.
62. Dabrowski, A.; Podkoscielny, P.; Hubicki, Z.; Barczak, M. *Chemosphere* **2005**, *58*, 1049-1070.
63. Mohamed, M. H.; Wilson, L. D.; Headley, J. V.; Peru, K. M. *Phys. Chem. Chem. Phys*. **2010**, DOI: 10.1039/c0cp00421a.

CHAPTER 10

PUBLICATION 9

Description

The following is a verbatim copy of an article that was published in December of 2008 in the Journal of Environmental Science and Health, Part A; Toxic/Hazardous Substances Environmental Engineering (*J. Environ. Sci. Health, Part A:* **2008**, *43(14)*, 1700-1705) and describes the fluorescence of NAs and the potential use of UV-Vis absorption and fluorescence emission spectrophotometry for the screening of NAs in aqueous solution.

Authors' Contribution

I performed all the experimental work with the exception of the ESI-MS measurements done by Mr. Peru. This work was supervised by Dr. Wilson and Dr. Headley. I wrote the first draft of the manuscript with extensive editing by each supervisor prior to submission for publication. Written permission was obtained from all contributing authors and the publishers to include this material in this thesis.

Relation of Chapter 10 (Publication 9) to the Overall Objectives of this Project

This research work is directly related the overall objectives of this project because it contributes to a further understanding of the way NAs are defined. Furthermore, this work contributes to a potentially new analytical method of quantifying NAs using UV-

Vis/Fluorescence spectrophotometry. This method opens the potential of developing tool for *in-situ* screening NAs in OSPW.

10. Screening of Oil Sands Naphthenic Acids by UV-Vis Absorption and Fluorescence Emission Spectrophotometry

Mohamed H. Mohamed,[§] Lee D. Wilson,[§] John V. Headley,[¥] Kerry M. Peru[¥]*

[§]Department of Chemistry, University of Saskatchewan, 110 Science Place, Saskatoon, Saskatchewan, S7N 5C9

[¥]Water Science and Technology Directorate, 11 Innovation Boulevard, Saskatoon, Saskatchewan, S7N 3H5

*Corresponding Author

Received 21 April 2008

10.1 Abstract

Oil sands extracted naphthenic acids fractions are known to contain impurities with various levels of unsaturation and aromaticity. These constituents contain functional groups that absorb ultraviolet-visible wavelength (UV-Vis) and give intense florescence emission in contrast to the fully saturated alicyclic naphthenic acids. UV-Vis absorption and fluorescence emission spectrophotometry are presented here as inexpensive and quick screening methods which use the detection of chromophoric surrogate compounds that serve as an internal standard for the indirect analysis of oil sands naphthenic acids. The method detection limit for the screening techniques was approximately 1 mg/L with an observed linear range of 1- 100 mg/L. The precision of measurements was generally within 10% r.s.d. There was generally good agreement (within 20% r.s.d) for isotherm

parameters from non-linear fitting of Langmuir, BET and Freundlich models for sorption of Athabasca oil sands naphthenic acid mixtures to activated carbon samples determined by UV-Vis absorption, fluorescence emission spectroscopy, and conventional direct injection electrospray ionization mass spectrometry.

10.2 Introduction

The oil sands industry in Northern Alberta, Canada uses caustic warm water to recover oil-laden bitumen from the sand and clay components. The resulting oil sands process water (OSPW) is highly saline and contains a complex mixture of organic compounds dominated by a class of naturally occurring naphthenic acids (NAs). The NAs are known to be among the principal toxic components in the OSPW. The structural formulae of NAs may be described by $C_nH_{2n+z}O_2$, where "z" is referred to as the "hydrogen deficiency" and is a negative, even integer.[1-5] More than one isomer will exist for a given z homolog, and the carboxylic acid group is usually covalently bonded or attached to an alkyl side chain, rather than directly to the alicyclic ring.[1-2] The molecular weights differ by 14 mass units (CH_2) between n-series and by two mass units (H_2) between z-series.[6] NAs are known to be weakly biodegradable, and are therefore well–suited for use in identification of oil source maturation.[7-8]

There is a need to better characterize NAs along with other organic acids and constituents within crude oils and aquatic environments.[9-12] Early methods such as FT-IR spectroscopy of the carbonyl functional group have played a key role in the measurement of NAs. Currently, mass spectrometry is the method of choice for study the environmental distribution or fate of NAs in OSPW. MS methods include applications of

GC-MS[13-14], electrospray[15] and atmospheric pressure chemical ionization-MS[16], and high-resolution MS (HRMS) methods with[17] or without[10] HPLC separation.

Recent developments in mass spectrometry of NAs have revealed a number of other components that do not fit the fully saturated and typical empirical structure $C_nH_{2n+z}O_2$ shown in Figure 1.3 in Chapter 1. The above classical definition of NAs has therefore become more loosely used to describe the range of organic acids found within crude oil. For example, crude oil acids contain NAs along with significant levels of other organic acids with N and/or S atoms. These constituents have various levels of unsaturation and aromaticity. Collectively, more than 3000 chemically different heteroatom compositions that contain O_2, O_3, O_4, O_2S, O_3S, and O_4S were determined in a sample of South American heavy crude.[18]

In view of the significant levels of organic constituents reported for oil sands derived NAs, along with independent mass spectral evidence of various levels of unsaturation and aromaticity, the objective of the current work was to explore the utility of UV-Vis absorption and fluorescence emission spectroscopy as a screening technique for the quantification of oil sands acids. Here we compare the characterization and quantification of Athabasca oil sands NA mixtures by conventional direct injection ESI-MS with UV-Vis absorption and fluorescence emission spectrophotometric detection. The latter methods are presented as rapid and inexpensive instrumental methods for a quantitative screening method which utilizes the detection of chromophoric constituents as internal standard surrogates for the analysis of oil sands NAs.

10.3 Experimental

Chemicals and materials

Unless otherwise noted, all other chemicals and materials were obtained from Fisher Scientific (Edmonton, AB, Canada). Granulated activated carbon (GAC) (Norit Rox 0.8) was obtained from VWR and used as received.

Naphthenic acid analysis by ESI-MS

Samples were analyzed for NAs using a Quattro Ultima (Waters Corp. Milford, MA, USA) triple quadrupole mass spectrometer equipped with an electrospray ionization (ESI) interface operating in the negative ion mode. Instrument operating parameters are reported elsewhere.[19]

UV-Vis instrumental conditions

Experiments were conducted using a Cary 100 Scan UV-Vis spectrophotometer (Varian). Scan controls were: average time (s) = 0.1; data interval (nm) = 1.00 and scan rate (nm/min) = 600. A double beam monochromator and quartz cells were utilized for solution absorption measurements. Absorbance calibrations were measured at a wavelength of 263 nm with sample pH adjusted to either 9 or 5, respectively. For NAs at pH = 9, the linear calibration curve had an R^2 value of 0.997 with an extinction coefficient of 0.005 $L.mg^{-1}.cm^{-1}$. Calibration curves for NAs at pH = 5 had an R^2 value of 0.997 with an extinction coefficient of 0.0063 $L.mg^{-1}.cm^{-1}$.

A representative series of absorbance spectra and the corresponding calibration curve for measurements at pH 9 are shown in Figures 10.1 and 10.2. Similar results were

obtained for measurements obtained at pH = 5, and to conserve space, the corresponding plots are not shown.

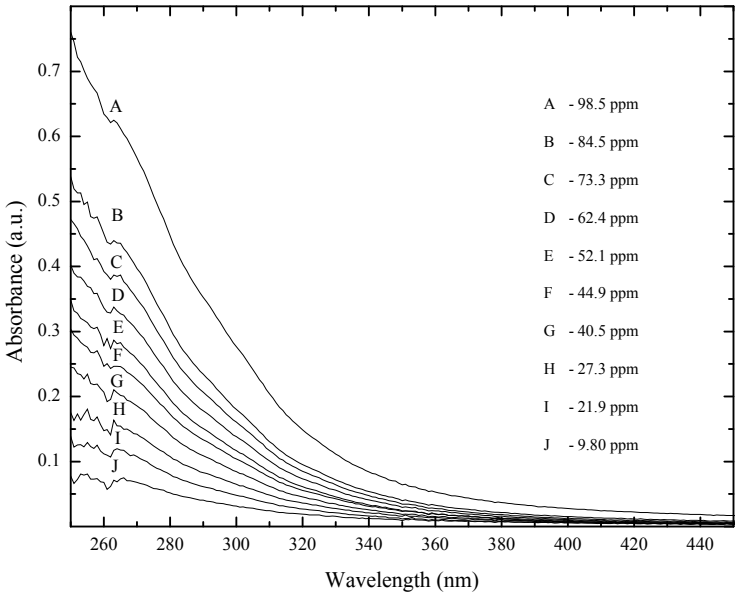

Figure 10.1. UV-Visible Absorbance Spectra of NAs at pH 9 and variable concentrations (A-J, see inset).

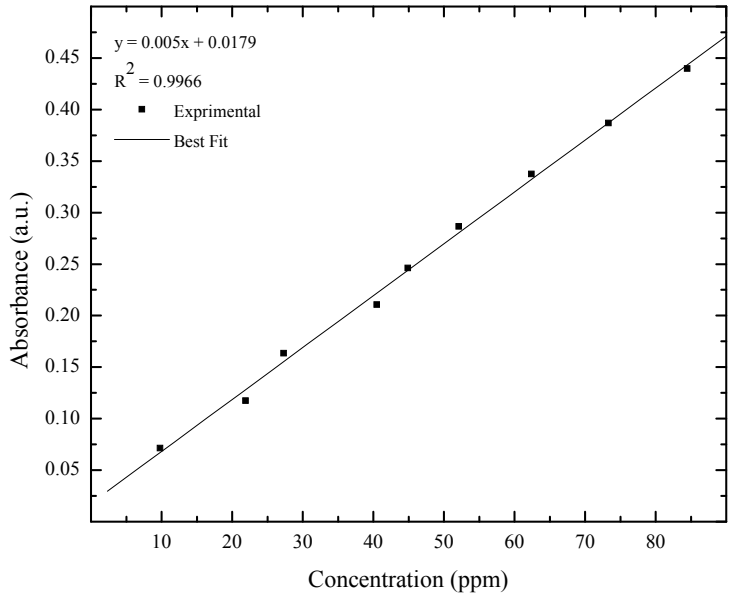

Figure 10.2. Linear calibration curve of NAs at pH 9 using UV-Vis absorbance data at λ=263 nm.

For fluorescence measurements, a PTI (Photon Technology International) Fluorescence Master Systems was used with Felix32 software for data collection and analysis. Instrumental parameters were: slit width of 2.00 nm; hardware configuration set to digital-double-double for both excitation and emission scans; integration time 3 seconds; data collection time 1 second; average set to 1 (number of times the experiment will be repeated); number of points for one average set to 5; and step size set to 1 nm. Thus, the overall scan rate was 1nm/3sec. Other instrumental parameters were: lamp power supply set at 70 watts; and photonmultiplier at 1101 V. Data was collected as a voltage signal which was then Fourier Transformed to quantum intensity (number of photons per second).

10.4 Results and Discussion

As illustrated in Figures 10.1 and 10.2, the Athabasca oil sands derived NAs contain components which are amenable to quantitative detection using UV-Vis absorbance at 263 nm. Further evidence of the absorbance of NAs is given by the observed excitation-emission spectra. For brevity, examples are illustrated at pH 9 in Figures 10.3-10.7, although corresponding data (not shown) was obtained at pH 5. As shown in Figures 10.3-10.7, the intensity of the maxima for the emission spectra was observed to be variable with different excitation wavelengths. These observations indicate that there are multiple fluorescent components in the NAs containing mixture.

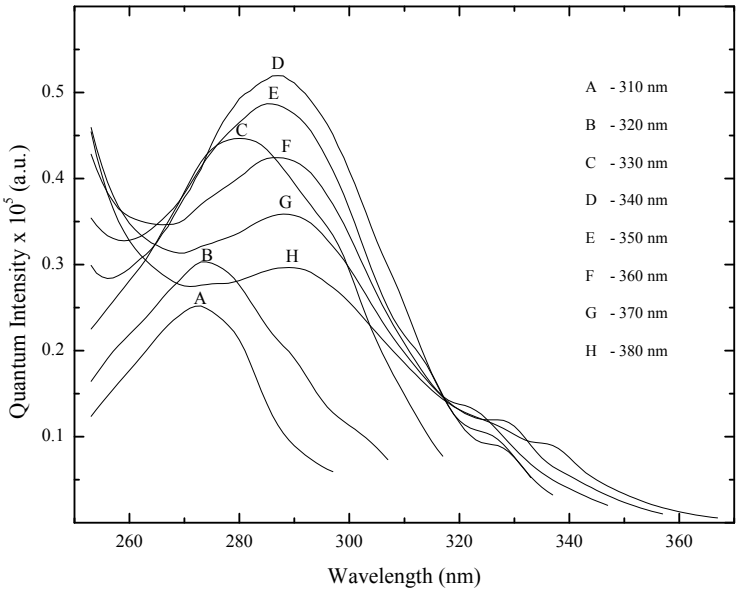

Figure 10.3. Excitation-Emission spectra of NAs at pH 9 at a fixed concentration (9.8 ppm).

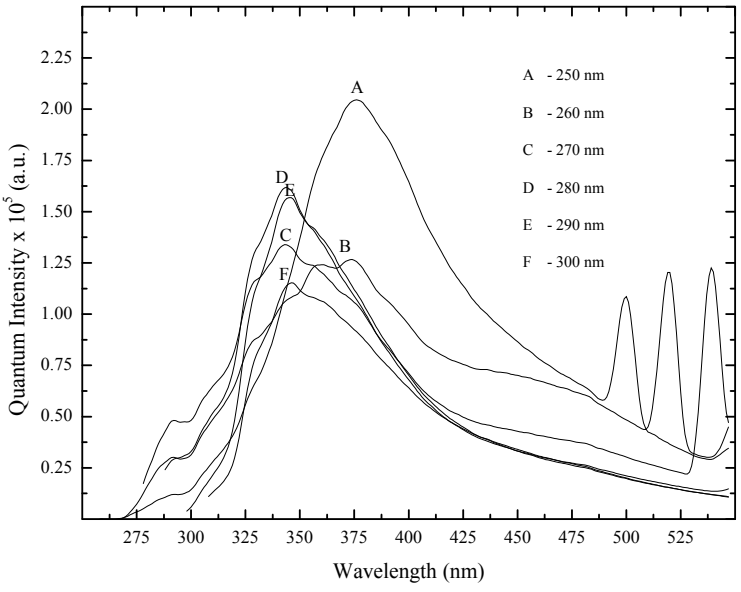

Figure 10.4. Emission spectra of NAs at pH 9 and a concentration of 98.5 ppm. The observed emission bands between 500-550nm are attributed to Raman vibrational bands of the solvent (water).

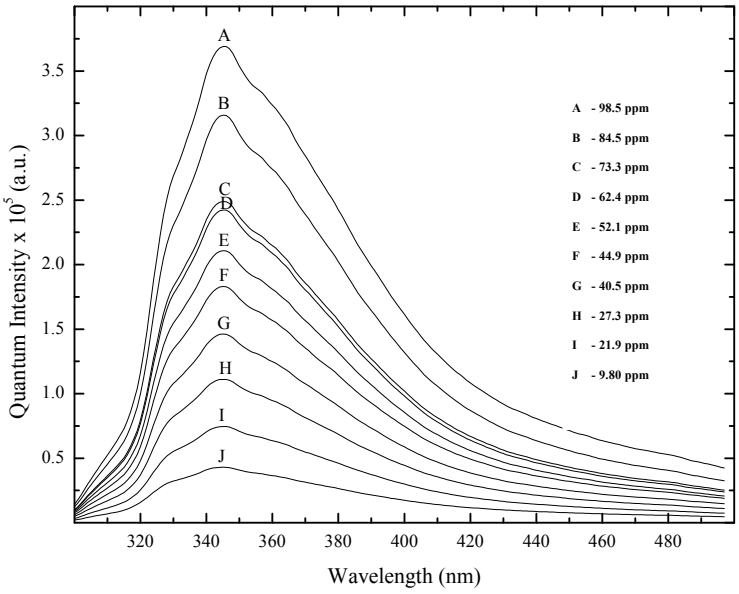

Figure10.5. Emission Spectra of NAs at pH 9 at variable concentration of NAs.

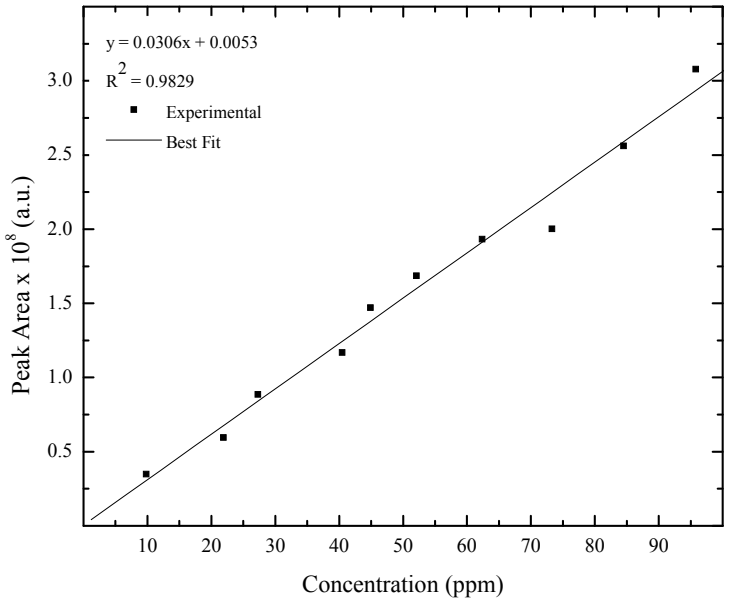

Figure 10.6. Calibration curve of NAs at pH 9 obtained using the total integrated peak area of the fluorescence emission spectra between 300-500 nm.

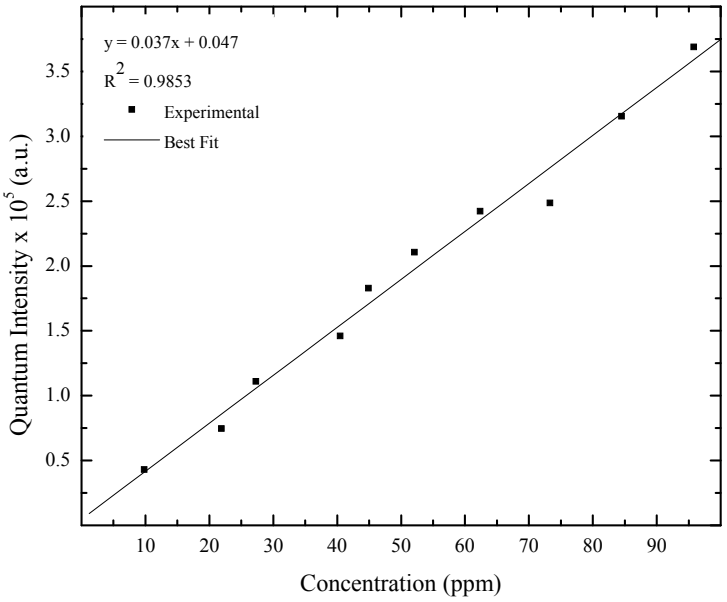

Figure 10.7. Calibration curve of NAs at pH 9 using maximum quantum emission intensity of fluorescence at λ_{em} = 346 nm.

In Figure 10.3, the fluorescence emission spectra obtained at different excitation wavelengths are shown. One observes that there are similar variations in fluorescence intensity for a given excitation wavelength. Moreover, the fluorescence emission spectra exhibit shoulders near the emission maxima indicating the presence of additional emission bands supporting the presence of fluorophore components at the 260 nm excitation wavelength. The identification of the chromophoric constituents that give rise to the emission spectra is beyond the scope of the present study and will be the subject of a forthcoming publication. The purpose of the current study is to determine the utility of UV-Vis absorbance and fluorescence emission spectrophotometry as potential screening methods for the detection of chromophoric surrogates present within oil sands derived NAs extracts. Thus, quantitative calibration curves were obtained for fluorescence

emission using the excitation wavelength of 290 nm to monitor chromophoric surrogates at variable concentrations and pH conditions.

For the case of NAs at pH 9, the calibration curve of fluorescence emission peak area vs. concentration had an R^2 value of 0.983 and an R^2 of 0.985 from a plot of maximum quantum intensity at 346 nm against concentration. While for NAs at pH 5, the corresponding values were 0.991 and 0.990 for peak area and quantum intensity, respectively.

In view of the goodness of fit of the calibration curves for the respective absorbance and fluorescence data, we anticipate that either approach has potential as a new screening technique for estimation of levels of NAs in water samples. The calibration curves are linear in the range of 1- 100 mg/L (typical of OSPW), with a precision generally less than 10% r.s.d. based on triplicate analyses. The detection limit of this method was approximately 1 mg/L.

The application of the UV-Vis absorbance and fluorescence spectrophotometry was extended to the analysis of the sorption of oil sands NAs in water samples. The spectrophotometric quantification was applied to the measurement of the sorption of NAs (pH = 9) with granular activated carbon (GAC)- Norit Rox 0.8. The latter was used as received without crushing the sample. Surface area estimates obtained from nitrogen porosimetry of *as-received* and powdered samples were found to be similar (~ 9×10^2 m^2/g).[20-21] Likewise, for comparison of the results, the samples were independently analyzed by conventional electrospray ionization mass spectrometry.

The results of this comparison are summarized in Table 10.1-10.2 and illustrated in Figure 10.8. There was good general agreement between the quantitative estimates

obtained using the MS and spectrophotometric methods. For example, the "best fit" of the Langmuir isotherm and the estimated Q_m (monolayer coverage) were 91.7 mg of NAs per g of GAC and 98.0 mg of NAs per g of GAC according to estimates from absorbance and fluorescence methods, respectively. The Langmuir model was observed to be the "best-fit" for UV-Vis and ESI-MS while the Freundlich model provided a better fit to the fluorescence emission data. The observed differences can be related to the differences in the sensitivity of fluorescence spectrophotometry and mass spectrometry, particularly at low equilibrium concentrations of NAs in aqueous solution. Overall, the estimate for Q_m using the Langmuir model was similar for all three methods investigated. The observed differences in the "goodness of fit" for the various models may reflect differences in the sensitivity, accuracy and precision of the respective measurements. As well, it should be noted that the assumption that the concentration of the chromophoric surrogates estimated by spectrophotometric methods parallels that of the non-chromophoric NAs. The origins of such differences arising from the oil sands acids measured by the respective methods are a topic of on-going research in our group.

Table 10.1. Quantitative estimates (mg/L) of NAs after sorption with GAC with NAs at pH 9 and 25^{o}C.

Vial #	UV	Fluorescence (Peak Area)	Fluorescence (Quantum Intensity)	ESI-MS
9	65.1	53.7	51.5	61.2
8	55.6	47.7	46.0	54.0
7	42.7	36.5	33.4	43.0
6	35.3	27.7	25.7	35.0
5	28.7	20.1	17.3	27.6
4	28.1	24.6	23.7	24.7
3	19.5	18.2	17.6	18.8
2	7.00	2.44	1.28	8.75
1	5.99	1.40	1.16	5.95

Table 10.2. Isotherm Parameters from Non-linear Fitting of Langmuir, BET and Freundlich Models Using the three analytical technique

Isotherm Models	Parameters	Analytical Method			
		UV-Vis	Fluorescence (Peak Area)	Fluorescence (Quantum Intensity)	ESI-MS
Langmuir	Q_m (mg/g)	100	110	113	117
	K_L (L/mg)	0.028	0.084	0.108	0.025
	R^2	0.957	0.909	0.893	0.935
	SSE	18.2	43.5	49.8	13.4
B.E.T	Q_m (mg/g)	67.3	97.8	106	65.0
	K_{BET} (L.mg/g^2)	130	919	101	970
	R^2	0.940	0.912	0.894	0.912
	SSE	27.9	42.9	49.5	22.0
Freundlich	K_F (L^n.mg^{1-n}/g)	26.6	26.9	43.0	9.61
	1/n	0.213	0.307	0.205	0.485
	R^2	0.941	0.943	0.927	0.938
	SSE	28.0	31.6	38.7	13.7

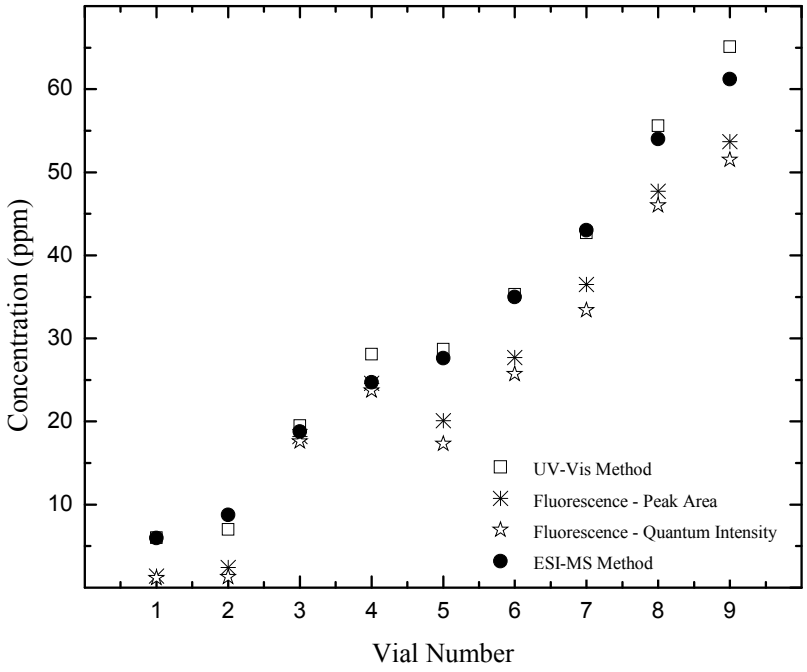

Figure 10.8. Concentration of NAs estimated using different methods.

Therefore, the spectrophotometric screening techniques described herein appear to be well suited for application to the quantitative analysis of oil sands NAs in aqueous solution. The methods are non-destructive, rapid, and amenable to field applications. In view of these attractive features, the screening techniques may be ideal for future applications to *in-situ* quantification of NAs in industrial OSPWs.

10.5 Conclusions

UV-Vis absorption and fluorescence emission spectrophotometric detection of chromophoric constituents in oil sands derived NAs was demonstrated to be a relatively inexpensive technique for quantification of oil sands derived NAs. There was good

agreement (within 20% r.s.d) between analyses of Athabasca oil sands NA mixtures by conventional direct injection ESI-MS and spectrophotometric techniques. The lower detection limit of 1 mg/L is well suited for the screening of levels in OSPW. The use of UV-Vis absorbance and fluorescence emission spectrophotometric methods are potentially useful methods for semi-quantitative *in-situ* estimates of concentrations of NAs in OSPW.

10.6 References

1. Dzidic, I.; Somerville, A. C.; Raia, J. C.; Hart, H. V. *Anal. Chem.* **1988**, *60*, 1318-1323.
2. Fan, T. P. *Energ. Fuel.* **1991**, *5*, 371-375.
3. Wong, D. C. L.; van Compernolle, R.; Nowlin, J. G.; O'Neal, D. L.; Johnson, G. M. *Chemosphere* **1996**, *32*, 1669-1679.
4. St. John, W. P.; Rughani, J.; Green, S. A.; McGinnis, G. D. *J. Chromatogr., A* **1998**, *807*, 241-251.
5. Hsu, C. S.; Dechert, G. J.; Robbins, W. K.; Fukuda, E. K. *Energ. Fuel.* **1999**, *14*, 217-223.
6. Herman, D. C.; Fedorak, P. M.; Costerton, J. W. *Can. J. Microbiol.* **1993**, *39*, 576-580.
7. Meredith, W.; Kelland, S. J.; Jones, D. M. *Org. Geochem.* **2000**, *31*, 1059-1073.
8. Headley, J. V.; Tanapat, S.; Putz, G.; Peru, K. M. *Can. Water Res.* **2002**, *J27*, 25-42.
9. Barrow, M. P.; McDonnell, L. A.; Feng, X.; Walker, J.; Derrick, P. J. *Anal. Chem.* **2003**, *75*, 860-866.
10. Barrow, M. P.; Headley, J. V.; Peru, K. M.; Derrick, P. J. *J. Chromatogr., A* **2004**, *1058*, 51-59.
11. Clemente, J. S.; Fedorak, P. M. *Chemosphere* **2005**, *60*, 585-600.

12. Quagraine, E. K.; Peterson, H. G.; Headley, J. V. *J. Environ. Sci. Health, Part A: Toxic/Hazard. Subst. Environ. Eng.* **2005**, *40*, 685-722.
13. Clemente, J. S.; MacKinnon, M. D.; Fedorak, P. M. *Environ. Sci. Technol.* **2004**, *38*, 1009-1016.
14. Scott, A. C.; Mackinnon, M. D.; Fedorak, P. M. *Environ. Sci. Technol.* **2005**, *39*, 8388-8394.
15. Lo, C. C.; Brownlee, B. G.; Bunce, N. J. *Anal. Chem.* **2003**, *75*, 6394-6400.
16. Lo, C. C.; Brownlee, B. G.; Bunce, N. J. *Water Res.* **2006**, *40*, 655-664.
17. Bataineh, M.; Scott, A. C.; Fedorak, P. M.; Martin, J. W. *Anal. Chem.* **2006**, *78*, 8354-8361.
18. Headley, J. V.; Peru, K. M.; Barrow, M. P. *Mass Spectrom. Rev.* **2009**, *28*, 121-134.
19. Martin, J. W.; Han, X.; Peru, K. M.; Headley, J. V. *Rapid Commun. Mass Spectrom.* **2008**, *22*, 1919-1924.
20. Kwon, J. H. Research-Based, University of Saskatchewan, 2007.
21. Mohamed, M. H.; Wilson, L. D.; Headley, J. V.; Peru, K. M. *Process Saf. Environ. Prot.* **2008**, *86*, 237-243.

CHAPTER 11

11. Summary, Conclusions and Proposed Future work

11.1 Summary and Conclusions

The objectives of the research have been achieved through the successful development and synthesis of engineered copolymers with remarkable and tunable physicochemical (i.e. textural and sorption) properties. Such materials have high potential in sorption-based applications such as the remediation of naphthenic acids (NAs). The overall success of this research is supported by eight published articles in peer reviewed journals that represent seminal contributions in the scientific literature. Chapters 2-9 describe the various sub-projects and Scheme 11.1 illustrates the organization of the thesis and how it relates to the overall research objective. Chapters 2-9 are verbatim copies of published peer review articles that detail the various sub-projects and their connectivity to the overall objectives of the thesis, as outlined below.

Chapter 2 outlines the synthesis and characterization of the β-cyclodextrin polyurethanes (β-CD PUs). This study improved the understanding of the relationship between copolymer design and the development of optimal sorbent materials.*The highlights of the materials characterization are as follows: (i) a measured practical upper limit of the β-CD/linker co-monomer ratio (~1:7) for the urethane copolymer materials investigated, and (ii) optimal co-monomer mole ratios in the range 1:1 to 1:3 for sorption based applications that involve the formation of β-CD inclusion complexes. An additional highlight of this chapter is the use of thermogravimetric analysis (TGA) as a materials characterization technique (first example in the literature) which provides semi-quantitative to quantitative analysis of the copolymer composition. This published*

work represents one of the first examples of a comprehensive and systematic study of β-CD PUs in the literature. The results illustrate the importance of a guided materials design strategy and the relationship to the accessibility of β-CD sites at variable crosslinking density. The results of this study led to the publication described in Chapter 4.

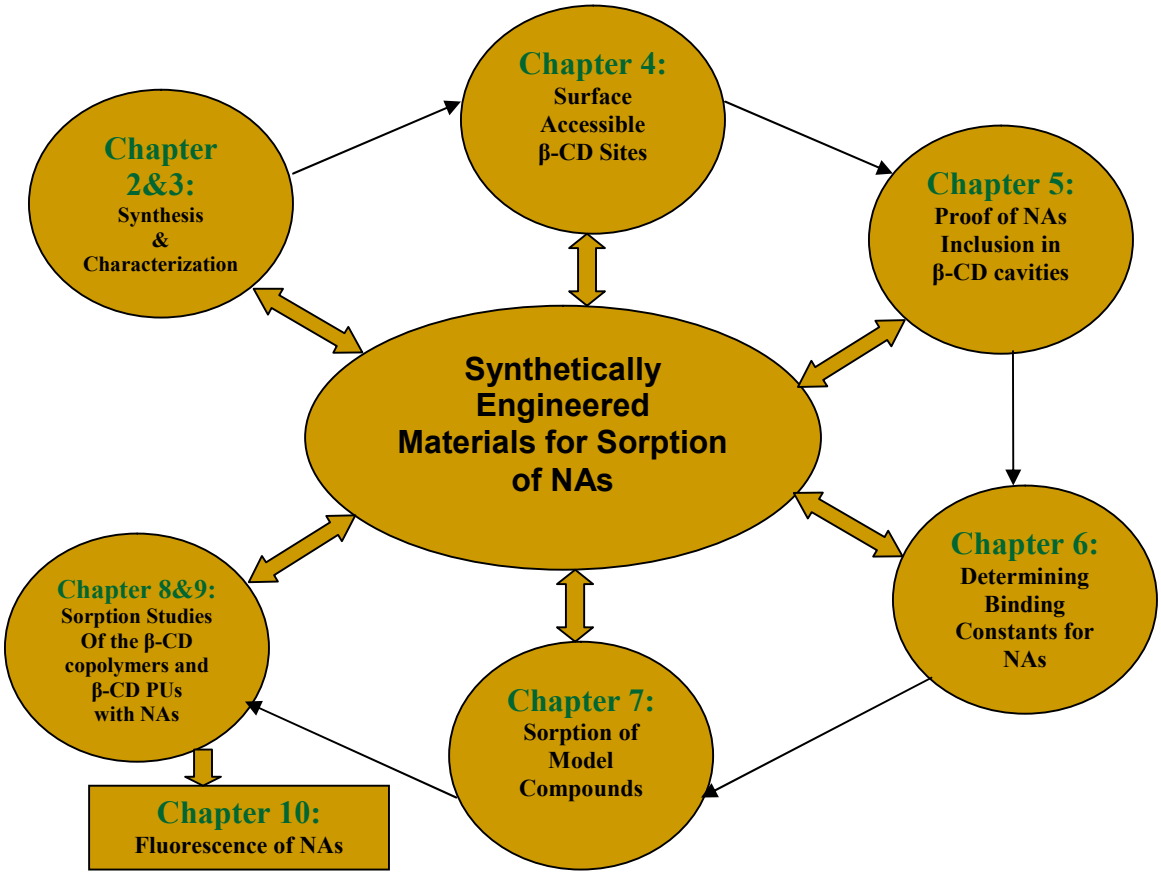

Scheme 11.1. A flowchart of the various projects and their relationship to the overall thesis research objectives.

Chapter 3 describes a systematic study of the surface area and pore structure properties of the copolymers using nitrogen porosimetry and dye-based (p-nitrophenol) sorption method. It was concluded that the textural properties exhibit a significant

dependency on the hydration state of the copolymer due to the swelling of the material framework in aqueous solution. Nitrogen adsorption results for copolymers in their anhydrous states indicate that the copolymers are mesoporous with relatively low surface areas (~10^1 m^2/g) while estimates from the dye-based sorption method had greater surface areas (~10^2 m^2/g) by an order of magnitude. The surface area and pore structure (i.e. textural) properties of the copolymers vary according to the type of diisocyanate crosslinker, co-monomer mole ratios, and the relative hydration state of framework morphology. In general, the discrepancy of SA values between the solid-gas and solid-solution adsorption techniques are evident for these types of "soft" carbohydrate-based materials. In contrast, the parity of agreement for SA values is evidenced for rigid frameworks such as zeolites and graphene-based carbon materials. The results obtained in this study and in Chapter 2 have contributed to the systematic design of copolymer sorbents with improved sorption capacity and molecular recognition properties for a range of target guest molecules. *The highlight of this work was the recognition of the variability of the textural properties for these types of copolymers in their anhydrous and hydrated states. This study is one of the first examples in the literature to show PU copolymers exhibit morphology dependence on hydration that affects the swelling and the framework structure of the sorbents according to the respective diisocyanate co-monomer.*

Chapter 4 demonstrated that the surface accessibilities of the β-CD inclusion sites in copolymer frameworks range between 1-100%, as evidenced by the decolourization of phenolphthalein (phth). The method relies on the formation of 1:1 β-CD/phth inclusion complexes. The specific molecular recognition between β-CD and phth provides useful

results about the sorption properties of β-CD based sorbent materials. In contrast to other design strategies that employ relatively high β-CD:linker reactant ratios, the copolymers in this study were prepared at relatively low co-monomer mole ratios (1:1 to 1:3), and yet, the surface accessibility was remarkably different for the five sets of copolymer sorbent materials investigated. The differences were attributed to steric effects of the inclusion sites due to linker size. This dye method embodies a simplistic and relatively low cost analytical technique for β-CD based copolymer materials. *The highlight of this work is the proposed use of phth as an inclusion selective guest and its use as a versatile optical probe for β-CD based copolymer sorbent materials. The molecular selectivity of this dye-based method will contribute to the design of novel types of β-CD copolymer materials for sorption-based applications that involve inclusion binding of adsorbates from solution and gas phase media, respectively. The systematic quantitative study of this probe for these types of copolymers is a first example of such a study in the scientific literature.*

Since the synthetically engineered copolymers were intended for capturing NAs from aqueous solution, there was a need to show evidence that cyclodextrins (CDs) can form stable inclusion complexes with NAs in its cavity. Chapter 5 demonstrated the formation of inclusion complexes with NAs and three examples of single component NAs (surrogates1-4) for the three most-researched types of α-, β-, and γ- CDs. It was found that α- and β-CD formed stable 1:1 inclusion complexes with surrogates 1-3; whereas, γ-CD formed stable 1:1 complexes with surrogate 4. Likewise, 1:1 inclusion complexes were formed between α-, β- and γ-CDs with NAs, however, γ-CD formed more stable inclusion complexes with larger molecular weight congeners/surrogates. The relative

importance of the inclusion binding sites was evident by comparing the reduced binding affinity of glucose with NAs since it does not form any measurable non-covalent complexes with surrogates 1-4 and NAs, respectively. However, an amphiphilic disaccharide (cellobiose) was observed to form 1:1 aggregate complexes with the surrogate ions (except surrogate 2) and NAs. *The highlight of this work is the unequivocal evidence that NAs form inclusion complexes within the CD cavities, and represents the first example in the literature.*

The ESI-MS results illustrated that inclusion complexes were formed between NAs and CDs as outlined in Chapter 5. However, there was a need determine the binding affinity of the complexes formed with β-CD to understand the equilibria of such noncovalent complexes. Thus Chapter 6 is a direct follow up from Chapter 5 where the 1:1 binding constant (K) of NAs with β-CD was determined using the spectral displacement technique. This method provided accurate estimates of the 1:1 K values between β-CD and a series of NAs and its surrogates. The K values for the surrogates ranged from 10^3-10^4 M^{-1} and the NAs (i.e. Fluka and Alberta-drived NAs) were ~ 10^4 M^{-1}. The K values increased in accordance to their respective lipophilic surface area (LSA) values. Fluka NAs have greater K values than Alberta-derived NAs and the observed differences in complex stability were attributed to the binding of higher molecular weight components in Fluka NAs vs Alberta-derived coextracted oil sands NAs. Although the average molecular weight of Alberta-derived NAs is higher than Fluka, the former contain impurities which do not appear to bind strongly to β-CD. *The highlight of this work illustrates the application of the spectral displacement technique to provide accurate*

estimates of the 1:1 binding constants of inclusion complexes formed between NAs andβ-CD.

Chapter 7 highlighted preliminary sorption experiments for NAs with three different types of β-CD sorbent materials. The results of this work illustrated that CD-based polymeric materials can be used as novel sorbents for sequestering NAs from aqueous media. The results showed that β-CD PU copolymer had greater binding affinity for NAs overall. In general, the sorption capacity increases as the surface area of the material increases. This correlation between surface area and sorption capacity was observed for the materials investigated. *The highlight of this work is that β-CD PU copolymers can be used to capture NAs from aqueous solution and this work was the first example in the literature showing that β-CD-based materials have application as efficient sorbent materials.*

Chapter 8 was a continuation from Chapter 7 after showing that β-CD PU copolymer display good overall sorption towards NAs. A systematic study was conducted using the synthetically engineered copolymers from Chapter 2. This study concluded that β-CD PU copolymers are excellent sorbents for sequestering NAs from aqueous solution at alkaline conditions, similar to the conditions found in oil sands process water (OSPW). The sorption capacity and binding affinity of the different copolymer materials were dependent on the crosslinker type and its relative co-monomer mole ratio. In general, copolymers comprised of aromatic monomers have a greater binding affinity toward NAs while those containing aliphatic-based linkers have a greater sorption capacity. The β-CD macrocycle in the copolymer framework plays a key role in the binding affinity of NAs while the linker monomers are of secondary importance; provided that guest molecules

can access the β-CD inclusion sites. Aromatic linkers enhance the binding affinity by increasing the LSA, whereas, the aliphatic linkers enhance the sorption capacity by altering their morphology through swelling in aqueous solution. The latter is argued on the basis of the swellability and gellation properties of certain aliphatic-based copolymers, as demonsrated in Chapter 3. The sorption properties of the copolymers with NAs depend on the structure of the porous framework. The sorbent properties are affected by the relative accessibility of the β-CD inclusion sites, the type of crosslinker, and the relative crosslinking ratios. The porous copolymers display selective uptake towards individual components of NAs, according to their molecular size and hydrogen deficiency, in aqueous solutions. *The highlight of this work is that engineered synthetic copolymer materials with variable pore structure and physicochemical properties afford sorbents with variable binding affinity, sorption capacity, and tunable molecular selectivity toward different NAs components found in OSPW. Furthermore, this was a first example in the literature reporting an extensive study of the potential use of β-CD PUs in sequestrating NAs from aqueous media.*

The results of Chapter 9 provided a more detailed understanding of the sorption properties of engineered β-CD PUs towards phenolic dyes and NAs in aqueous solutions. In general, the copolymers display tunable sorption properties and applicability over a range of pH conditions. The sorption capacity and the relative binding affinity of the copolymers were shown to vary according to the difference in the type of linker monomer, co-monomer mole ratio, and nature of the adsorbate species. Generally, small amphiphilic molecules like PNP may bind at the inclusion sites or onto the linker framework domains; depending on the pH conditions. Adsorbates with greater lipophilic

character like phth and NAs bind favorably within the β-CD inclusion sites at alkaline pH conditions. Moreover, aliphatic-based copolymers (HDI and CDI) at moderate co-monomer ratios exhibit favourable sorption affinity towards PNP at low pH. NAs and phth display similar sorption behaviour where it is observed that Q_m decreased with increasing crosslink density while the HDI-1 copolymer had the lowest sorption affinity overall. Thus, the relative accessibility of the β-CD inclusion sites of the copolymer framework plays a key role in the overall binding affinity towards NAs and phth at alkaline pH conditions. This is confirmed by the similar binding affinity for each adsorbate, as compared with their respective binding constants with native β-CD. The sorption behaviour of the copolymers towards NAs indicates that the linker domains play a secondary role provided that inclusion complexes are formed with the β-CD sites. *The highlight of this work is the detailed understanding of the sorption mechanism of these copolymers towards phenolic dyes and NAs. This work is a first example in the literature in providing a systematic study towards understanding the sorption behavior of β-CD PUs towards organic compounds.*

Chapter 10 was a side project which showed that Alberta-derived NAs display UV-Vis and fluorescence optical properties. The recognition of the potential fluorescence behaviour of NAs challenges the classical definition of such compounds. This work provides experimental support on the recent progress in mass spectrometry of NAs where additional components in the mixture have revealed components that do not fit the criteria according to the classical structure ($C_nH_{2n+Z}O_2$) shown in Figure 1.3 in Chapter 1. On the other hand, the discovery of the favourable UV-Vis absorption and fluorescence emission characteristics offer a potential quantitative analytical method for the estimation

of *in-situ* concentration of NAs in OSPW. *The highlights of this work includes the recognition of the limits of classical definition of NAs and the adsorption of the published method by the Oil Sand Tailings Research Facility (OSTRF) for the development of a miniature fluorescence sensor for the detection and characterization of NAs in OSPW.*[1]

Overall, the objectives of the thesis were met successfully. This research work has contributed to the development of a new class of sorbent materials for sorption-based applications that will aid in the reclamation of the OSPW containing NAs. A deeper understanding of the physicochemical and sorption properties of the β-CD PUs has led to the development of a diverse range of sorbent materials with tunable physicochemical properties.

11.2 Proposed Future Work

Further studies detailing the morphology and swelling properties of the copolymers is required at various hydration levels. Compressibility measurements may offer additional support on the swelling of these materials in their anhydrous and hydrated states. This would involve the measurement of the volume change of the copolymers at various pressure conditions, as shown in Equation 11.1 where β is the isothermal compressibility (1/Pascal), V is volume (L) and p is the applied pressure (Pascal). A Piezometer can be used to obtain these measurements where the pressure range is from bar to megabar.[2-5]

$$\beta = -\frac{1}{V}\frac{\partial V}{\partial p} \quad \text{Equation 11.1}$$

To further understand the sorption mechanism, a better understanding of the thermodynamic parameters (K, ΔH^o, ΔS^o, etc.) of the inclusion process is required in both

the native and polymerized β-CD (PU). This can be achieved by obtaining equilibrium sorption isotherms at different temperatures[6] and the determination of the equilibrium binding constants at variable temperature using the spectral displacement method outlined in Chapter 6. By studying the temperature (T) dependence of the association constant (K) with the van't Hoff relation, ΔH^o and ΔS^o values can be obtained. The resulting linear plots of ln K vs 1/T will yield a slope which is related to $-\Delta H^o/R$ and a y-intercept of $\Delta S^o/R$, as shown in Equation 11.2. ΔH^o ($J.mol^{-1}.K^{-1}$) and ΔS^o ($J.K^{-1}$) are the standard enthalpy and entropy change for the sorption process, respectively. R is the gas constant ($J.mol^{-1}.K^{-1}$). A comparison of the thermodynamic parameters with glucose- and cellobiose-based copolymers may be helpful in the understanding of the thermodynamics of inclusion and non-inclusion binding. Furthermore, the determination of isosteric heats of adsorption is valuable for the study of heterogeneous sorbents of the type investigated in this study. The isosteric adsorption enthalpy (ΔH_θ)[7-9] can be determined using the Clausius-Clapeyron (Equation 11.3) for a given equilibrium isotherm at a given surface coverage (θ) from the slope of the plot of ln C_e versus T^{-1}, where C_e is the concentration of free solute at equilibrium. Where θ is defined as a ratio between Q_e and Q_m. The values of ΔH_θ are obtained from these plots for each equilibrium uptake or θ, which is proportional to Q_e. The values of $-\Delta H_\theta$ are referred to as $Q_{isosteric}$ and plotted against θ. These plots will provide information on the concentration dependent switching between the various sorption sites, assuming there are two or more sites possessing different K_i values. If $K_1 >> K_2$, then site 1 is filled first followed by site 2 (*cf.* Scheme 11.2).

$$\ln(K) = -\frac{\Delta H^o}{RT} + \frac{\Delta S^o}{R} \qquad \text{Equation 11.2}$$

$$\Delta H_{isost,\theta} = R\frac{d\ln Ce}{d\left(\frac{1}{T}\right)} \quad \text{Equation 11.3}$$

$$\text{Sorbate + Site1} \xrightleftharpoons{K_1} \text{Sorbate-Site 1}$$

$$\text{Sorbate + Site 1} \xrightleftharpoons{K_2} \text{Sorbate-Site 2}$$

Scheme 11.2. Sorption equilibria between a sorbate with two sorption sites in the β-CD PUs; where Site 1 represents an inclusion site and Site 2 represents a linker domain in the copolymer material.

Furthermore kinetic studies at ambient and variable temperatures are required to further understand the overall sorption mechanism of NAs with the copolymers. Kinetics parameters (rates) will confirm the conclusion regarding the mechanism of the sorption process (i.e. sorption being heterogeneous) and also offer information on the rates of adsorption. Rate data are valuable for the design of flow systems in packed bed columns, etc. through an understanding of the mass transfer effects and its variability on the materials design.

3D-plots (*cf*. Figure 8.5 in Chapter 8) of mixtures of NAs remaining after sorption with different copolymers exhibit variable size/shape selectivity amongst components in mixtures of NAs, as shown in Figure 8.5 of Chapter 8. Therefore, there is a need to further study the thermodynamics of the individual components. Investigation of the isotherms for each congener (i.e. according to carbon number and hydrogen deficiency) will provide thermodynamic parameters (i.e. Q_m and K_i) which are anticipated to provide

a detailed understanding of the molecular recognition properties of such sorbent materials.

Previously, theoretical calculations of the docking of CDs with different organic species have been explored for determining the free energy of binding.[10-12] Therefore, the docking of NAs and its surrogates with β-CD and the copolymers are of interest because it may reveal the underlying factors that govern the differential stability among the complexes according to the optimal "binding geometry". Structural evidence of this type (i.e. inclusion and non-inclusion binding) will aid in providing support for dual mode sorption sites as concluded in Chapter 9. Similarly, docking studies should examine the stability of complexes formed with variable guest types such as PNP and phth, respectively. The foregoing assumes that solvent effects can be adequately accounted for in the calculations. Minimally, gas phase calculations would show relative size-fit relations for the sorbent-sorbate systems.

A spectroscopic study (IR/Raman/NMR) of the solid sorbent phase with variable loadings of adsorbate would provide direct structural insight regarding the nature of the sorption sites (i.e. inclusion vs. non-inclusion). Results of this type would complement thermodynamic, kinetic and computational modeling studies outlined above. Work of this type of research is planned and currently underway.

11.3 References

1. OSTRF; Oil Sands Tailing Research Facility Edmonton, AB, 2009; Vol. 2010.
2. Dayantis, J. *Makromol. Chem.* **1969**, *129*, 89-108.
3. Janssen, S.; Schwahn, D.; Springer, T.; Mortensen, K. *Macromolecules* **1995**, *28*, 2555-2560.
4. Jones Parry, E.; Tabor, D. *J. Mater. Sci.* **1973**, *8*, 1510-1516.
5. Richards, T. W.; Palitzsch, S. *J. Am. Chem. Soc.* **1919**, *41*, 59-69.

6. Srivastava, V. C.; Mall, I. D.; Mishra, I. M. *Chem. Eng. J.* **2007**, *132*, 267-278.
7. Gazpio, C.; Sánchez, M.; Isasi, J. R.; Vélaz, I.; Martín, C.; Martínez-Ohárriz, C.; Zornoza, A. *Carbohydr. Polym.* **2008**, *71*, 140-146.
8. Li, H.; Jiao, Y.; Xu, M.; Shi, Z.; He, B. *Polymer* **2004**, *45*, 181-188.
9. Li, H.; Xu, M.; Shi, Z.; He, B. *J. Colloid Interface Sci.* **2004**, *271*, 47-54.
10. Cai, W.; Xia, B.; Shao, X.; Guo, Q.; Maigret, B.; Pan, Z. *Chem. Phys. Lett.* **2001**, *342*, 387-396.
11. Mayer, B.; Marconi, G.; Klein, C.; hler, G.; Wolschann, P. *J. Inclusion Phenom. Macrocyclic Chem.* **1997**, *29*, 79-93.
12. Funasaki, N.; Ishikawa, S.; Neya, S. *Langmuir* **2002**, *18*, 1786-1790.